**Austin M. Ramsey**

**curriculum vitae**

austin.ramsey@som.umaryland.edu

## CAREER GOAL

(i) To understand molecular mechanisms underlying basal glutamatergic synapse organization and function, (ii) the interplay of these synaptic mechanisms in pathologically relevant circuits, (iii) and designing approaches to restore key features of pathological circuit function.

## EDUCATION

Duquesne University: Fall 2011-Fall 2014
Pittsburgh, PA

- Bachelor of Arts, *cum laude*
  - Major: Psychology; Minor: Biology
- Irene and Eric Simon Brain Research Foundation Summer Fellow

University of Maryland School of Medicine: Fall 2015 – Fall 2021
Baltimore, MD

- PhD candidate in the Program in Neuroscience
- Ruth L Kirschstein National Research Service Award (F31)

### Relevant coursework

| | |
|---|---|
| Cognitive and systems neuroscience (A) | 3 cr., Carnegie Mellon University |
| Mechanisms in biomedical science (B+) | 8 cr., University of Maryland |
| Molecular neuroscience biophysics (A) | 1 cr., University of Maryland |
| Synaptic physiology and pharmacology (A) | 4 cr., University of Maryland |
| Special topics in applied math (A) | 3 cr., University of Maryland, Baltimore County |
| Fundamentals of biostatistics (A-) | 3 cr., University of Maryland |
| Proseminar in experimental design (A-) | 3 cr., University of Maryland |
| Special readings: history of neuroscience journal club (A) | 1 cr., University of Maryland |
| Fundamentals of microscopy (A) | 1 cr., University of Maryland |

## PUBLICATIONS

"Subsynaptic positioning of AMPARs by LRRTM2 controls synaptic strength."
*Science Advances.* 2021. *doi: 10.1126/sciadv.abf3126*
*bioRxiv.* 2021. *doi: 10.1101/2021.04.30.441835.*
**Ramsey AM***, Tang AH*, LeGates TA, Guo XZ, Carbone BE, Thompson SM, Biederer T, Blanpied TA.

"Synapse assembly in the absence of presynaptic $Ca^{2+}$ channels and $Ca^{2+}$ entry."
*Neuron*. 2020. *doi: 10.1016/j.neuron.2020.05.032.*
Held RG*, Liu C*, Ma K*, **Ramsey AM**, Tarr TB, De Nola G, Wang SSH, Wang J, van den Maagdenberg AMJM, Schneider T, Sun J, Blanpied TA, Kaeser PS.

"Mapping the proteome of the synaptic cleft through proximity labeling reveals new cleft proteins."
*Proteomes*. 2018. *doi: 10.3390/proteomes6040048.*
Cijsouw T, **Ramsey AM**, Lam TT, Carbone BE, Blanpied TA, Biederer T.

"The dosing of aerobic exercise therapy on experimentally-induced pain in healthy female participants."
*Scientific Reports*. 2019. *doi: 10.1038/s41598-019-51247-0.*
Polaski AM, Phelps AL, Szucs KA, **Ramsey AM**, Kostek MC, Kolber BJ.

## EXTRAMURAL TALKS

**Ramsey AM**, Tang AH, LeGates TA, XZ Guo, Carbone BE, Thompson SM, Biederer T, Blanpied TA.
"Subsynaptic positioning of AMPARs by LRRTM2 controls synaptic strength."
- Vanderbilt University. Nashville, TN. 8/2021

**Ramsey AM**, Tang AH, LeGates TA, XZ Guo, Carbone BE, Thompson SM, Biederer T, Blanpied TA.
"Subsynaptic positioning of AMPARs by LRRTM2 controls synaptic strength."
- University of Colorado. Denver, CO. Virtual. 7/2021

**Ramsey AM**, Tang AH, LeGates TA, Thompson SM, Biederer T, Blanpied TA.
"LRRTM2 maintains synaptic strength through the subsynaptic positioning of AMPARs."
- Cold Spring Harbor Laboratory: Molecular Mechanisms of Neuronal Connectivity. Virtual. 09/2020

- Future Trends in Synapse and Circuit Plasticity. Gotemba, Shizuoka Prefecture, Japan. 9/2019

## CONFERENCE ABSTRACTS

**Ramsey AM**, Tang AH, LeGates TA, Thompson SM, Biederer T, Blanpied TA. "LRRTM2 maintains synaptic strength through the subsynaptic positioning of AMPARs."

- Future Trends in Synapse and Circuit Plasticity. Gotemba, Shizuoka Prefecture, Japan. 9/2019
- Cell Biology of the Neuron II. Janelia Farms, Ashburn, VA. 9/2019
- Program in Neuroscience Annual Retreat. University of Maryland, Baltimore, MD. 6/2019

**Ramsey AM**, Tang AH, Biederer T, Blanpied TA. "Dynamic control of synaptic substructure and function by adhesion molecules."

- Society for Neuroscience. San Diego, CA. 11/2018
- Gordon Research Seminar/Conference: Synaptic Transmission. Waterville Valley, NH. 8/2018
- Program in Neuroscience Annual Retreat. University of Maryland, Baltimore, MD. 6/2018

**Ramsey AM,** Tang AH, Blanpied TA. "LRRTM2 controls synapse structure and function." Program in Neuroscience Annual Retreat. University of Maryland, Baltimore, MD. 7/2017

**Ramsey AM*,** Dharmasri PA*, Blanpied TA. "Optical labeling of structurally potentiated spines in dissociated hippocampal cultures." Program in Neuroscience Rotation Talks. University of Maryland, Baltimore, MD. 5/2016

**Ramsey AM**, Kolber BJ. "Effects of exercise and social defeat stress on anxiety, depression and pain sensitivity." 10th Anniversary Dinner for the Irene and Eric Simon Brain Research Foundation. Parsippany, NJ. 11/2014

**Ramsey AM**, Kolber BJ. "Behavioral indices of anxiety and depression in the chronic variable stress paradigm." Summer Undergraduate Research Program. Duquesne University, Pittsburgh, PA. 7/2014

**Ramsey AM**, Eaton B, Lawrence R, Pisarcik H, Kranjec A. "Matching spatial relationships between schemas, pictures, and words." Undergraduate Research and Scholarship Symposium. Duquesne University. Pittsburgh, PA. 4/2014

**Ramsey AM**, Holdaway M, Markarian L, Vaishnav S, Kranjec A. "Eye-tracking decision-making during soccer refereeing." Duquesne University, Pittsburgh, PA.

- Duquesne Undergraduate Research and Scholarship Symposium. 4/2014
- Duquesne Undergraduate Psychology Conference. 4/2014

**Ramsey AM**, Kranjec A. "Does language influence thought? The perception of spatial relations in mild aphasics." Wimmer Family Foundation. Duquesne University, Pittsburgh, PA. 12/2013

## HONORS & AWARDS

| | |
|---|---|
| 11/2020 | The Glaser Prize for Excellence in Imaging, Department of Physiology, University of Maryland School of Medicine, Baltimore, MD |
| 09/2019 | Poster Award, Future Trends in Synapse and Circuit Plasticity, Gotemba, Shizuoka Prefecture, Japan |
| 09/2018 | Ruth L. Kirschstein National Research Service Award F31MH116583, National Institute of Mental Health, Bethesda, MD |
| 09/2018 | Trainee Professional Development Award, Society for Neuroscience, San Diego, CA |
| 06/2018 | Best Poster Award (*1st Place*), Program in Neuroscience Annual Retreat, University of Maryland, Baltimore, MD |
| 11/2017 | Image feature – *Interstellate, Vol. 2* |
| 10/2017 | The Glaser Prize for Excellence in Imaging, Department of Physiology, University of Maryland School of Medicine, Baltimore, |

| | |
|---|---|
| | MD |
| 06/2017 | Best Poster Award (*4th place*), Program in Neuroscience Annual Retreat, University of Maryland, Baltimore, MD |
| 11/2016 | Image feature – *Interstellate, Vol. 1* |
| | Additional feature in *L'ADN Magazine* (9/2019) |
| 04/2014 | Best Poster, Undergraduate Research and Scholarship Symposium, Duquesne University, Pittsburgh, PA |
| 04/2014 | Duquesne Undergraduate Research Program Summer Scholarship, Duquesne University, Pittsburgh, PA – *declined* |
| 04/2014 | Irene and Eric Simon Brain Research Foundation Summer Fellow, Sparta, NJ |
| 12/2013 | Faculty-Student Research Award, Wimmer Family Foundation, Pittsburgh, PA |
| 04/2013 | Outstanding Scholarship (Honorable Mention), Undergraduate Research and Scholarship Symposium, Duquesne University, Pittsburgh, PA |
| 08/2011- | *cum laude*, Dean's List, Duquesne |
| 12/2014 | University, Pittsburgh, PA |

**ABSTRACT**

Title of dissertation:

Subsynaptic positioning of AMPARs by LRRTM2 controls synaptic strength

Austin M. Ramsey, Doctor of Philosophy, 2021

Dissertation Directed by Thomas A. Blanpied, PhD, Department of Physiology

Recent evidence suggests that the nanoscale organization of proteins within synapses may control the strength of communication between neurons in the brain. The unique subsynaptic distribution of glutamate receptors, which cluster in nano-alignment with presynaptic sites of glutamate release, supports this idea. However, testing it has been difficult because mechanisms controlling this subsynaptic organization remain unknown. Reasoning that transcellular interactions could influence AMPAR positioning, we targeted a key transsynaptic adhesion molecule implicated in controlling AMPAR number at synapses, LRRTM2, using engineered, rapid proteolysis. Severing the LRRTM2 extracellular domain led quickly to nanoscale de-clustering of AMPARs away from release sites, not prompting their escape from synapses until much later. This rapid remodeling of AMPAR position produced significant deficits in evoked, but not spontaneous, postsynaptic receptor activation. These results dissociate receptor number within synapses from their nano-positioning in determination of synaptic function and support the novel concept that adhesion molecules acutely position AMPA receptors to dynamically control synaptic strength.

# Subsynaptic positioning of AMPARs by LRRTM2 controls synaptic strength

by
Austin M. Ramsey

Dissertation submitted to the Faculty of the Graduate School of the
University of Maryland, Baltimore in partial fulfillment
of the requirements for the degree of
Doctor of Philosophy
2021.

**TABLE OF CONTENTS**

**LIST OF FIGURES**

## LIST OF ABBREVIATIONS

| | |
|---|---|
| ∑[peak p(o)] | Summed peak open probability |
| 3D | Three dimensional |
| aCSF | Artificial cerebrospinal fluid |
| ADAM22 | A disintegrin and metalloprotease domain 22 |
| AKAP | A-kinase anchor protein |
| AMPAR | α-amino-3-hydroxy-5-methyl-4-isoxazolepropionic acid receptor |
| AP | Action potential |
| AZ | Active zone |
| BRS | α-bungarotoxin recognition sequence |
| BTX | α-bungarotoxin |
| C1q | Complement component 1q |
| CA1 | Cornu Ammonis-1 |
| $Ca^{2+}$ | Calcium |
| CA3 | Cornu-Ammonis-3 |
| CAM | Cell adhesion molecule |
| CAST | CAZ-associated structural protein |
| $Ca_v$ | Voltage-gated calcium channel |
| CAZ | Cytomatrix at the active zone |
| cdKO | Conditional double knockout |
| Cer3 | Cerulean 3 |
| CMOS | Complementary metal oxide semiconductor |

| | |
|---|---|
| cryo-ET | Cryogenic electron tomography |
| CV | Coefficient of variation |
| DG | Dentate gyrus |
| DIV | Days in vitro |
| dSTORM | Direct stochastic optical reconstruction microscopy |
| DV2 | Dual view 2 |
| ECD | Extracellular domain |
| ECR | Extracellular region |
| EAAT1,2 | Excitatory amino acid transporter 1,2 |
| EM | Electron microscopy |
| EPSC | Excitatory postsynaptic current |
| ER | Endoplasmic reticulum |
| ERES | Endoplasmic reticulum exit sites |
| FBS | Fetal bovine serum |
| FLRT | Family of leucine-rich repeat transmembrane proteins |
| $GABA_AR$ | Gamma-Aminobutyric Acid Type A Receptor |
| GCaMP3 | Genetically-encoded calmodulin-based indicator |
| GEF | Guanine nucleotide exchange factor |
| GFP | Green fluorescent protein |
| GKAP | GUK-associated protein |
| GluA1/2 | Protein subunits transcribed from Gria1/2 |
| GluA1-4 | Protein subunits transcribed from Gria1-4 |
| GluA2/3 | Protein subunits transcribed from Gria2/3 |

| | |
|---|---|
| Gly | Glycine |
| GlyR | Glycine receptor |
| GPI | Glycosylphosphatidylinositol |
| GRIA1-4 | Glutamate Receptor Ionotropic AMPA 1-4 |
| GRIP-1 | Glutamate receptor-interacting protein |
| GTP | Guanosine-5'-triphosphate |
| HEK | Human embryonic kidney |
| hLRRTM | Human leucine-rich repeat transmembrane |
| HSPG | Heparan sulfate proteoglycan |
| IgG | Immunoglobulin G |
| KDR | Knockdown replacement |
| LBD | Ligand-binding domain |
| LGI1 | Leucine rich glioma inactivated 1 |
| LNS | Laminin-alpha, Neurexin and Sex hormone-binding globulin |
| LRR | Leucine-rich repeat |
| LRRTM1-4 | Leucine-rich repeat transmembrane protein 1-4 |
| LTD | Long-term depression |
| LTP | Long-term potentiation |
| MAGUK | Membrane-associated guanylate kinase |
| mEos | Monomeric eos |
| mEPSC | Miniature excitatory postsynaptic current |
| miRNA | Micro ribonucleic acid |

| | |
|---|---|
| MNND | Mean nearest neighbor distance |
| Munc13 | Mammalian unc13 |
| MVR | Multi-vesicular release |
| NCAM180 | Neural cell adhesion molecule 180 |
| ND | Nanodomain |
| NGL | Netrin G ligand |
| NL-1 | Neuroligin-1 |
| NL-1 ΔC | Neuroligin-1 C-terminal deletion |
| NMDAR | N-methyl D-Aspartate receptor |
| NMJ | Neuromuscular junction |
| NND | Nearest neighbor distance |
| nNOS | n-nitric oxide synthase |
| Nrxn1-3 | Neurexin1-3 |
| NSF | N-ethylmaleimide sensitive factor |
| NTD | N-terminal domain |
| OE | Overexpression |
| PAINT | Point accumulation in nanoscale topography |
| PALM | Photo-activatable light microscopy |
| PAR | Protease-activated receptor |
| PBS | Phosphate buffered saline |
| PDZ | Postsynaptic density protein (PSD-95), drosophila disc large tumor suppressor (Dlg1), zonula occludens-1 protein (zo-1) |

| | |
|---|---|
| PFA | Paraformaldehyde |
| PSD | Postsynaptic density |
| PSD-95 | Postsynaptic density protein 95 |
| PTPσ | Receptor-type tyrosine-protein phosphatase sigma |
| RBP | Rim binding protein |
| RIM | Rab3-interacting molecule |
| ROI | Region of interest |
| SALMs | Synaptic adhesion-like molecule |
| SEP | Super ecliptic phluorin |
| SEP-TM | Super ecliptic phluorin transmembrane protein |
| shRNA | Short hairpin ribonucleic acid |
| SlitRKs | Slit- and Trk-like protein |
| SNAP | Soluble NSF attachment protein |
| SNAP-25 | Soluble NSF attachment protein 25 |
| SNARE | SNAP receptor proteins |
| $Sr^{2+}$ | Strontium |
| SS4- | Splice site 4 lacking |
| SS4+ | Splice site 4 containing |
| STED | Stimulated emission depletion microscopy |
| STORM | Stochastic optical reconstruction microscopy |
| SV | Synaptic vesicle |
| SynCAM1 | Synaptic cell adhesion molecule 1 |
| SynGAP-1 | Synaptic ras GTPase-activating protein 1 |

| | |
|---|---|
| TARP | Transmembrane AMPA receptor regulatory protein |
| TGN | Trans-golgi network |
| THR | Thrombin |
| TIRF | Total internal reflection microscopy |
| TMD | Transmembrane domain |
| VAMP | Vesicle-associated membrane protein |
| VGCC | Voltage-gated calcium channel |
| VGLUT1-3 | Vesicular glutamate transporter 1-3 |
| vSNARE | Vesicular SNARE |
| ZDC2 | Z drift compensator 2 |
| α2δ | Alpha 2 delta subunit of calcium channels |

# CHAPTER 1: Introduction

## Section 1. The synapse is a critical point of regulation in learning and memory

### 1.1 The synapse is a transcellular signaling junction for complex molecular compartments

Brain function underlies our everyday behaviors and internal states. Individual regions of the brain, which consist of many cell types, serve specialized functions. Importantly, specific cell types in these key brain areas communicate through a collection of cell-cell junctions, known as synapses, where signals propagate from one cell to the other, known as synaptic transmission. Synapses in a general sense are diverse in terms of their geometry, composition, and function. Glutamatergic synaptic transmission generally acts to increase the probability that a downstream neuron will also undergo an action potential. For glutamatergic transmission to occur, these synapses require the coordination of three unique compartments of the synapse: the active zone (AZ), the synaptic cleft, and the postsynaptic density (PSD).

The AZ is a specialized site of neurotransmitter exocytosis and is responsive to depolarization. Action potentials in the presynaptic neuron elicit a series of voltage-dependent channel opening and closing events which produces depolarization of the axon. As the action potential propagates down the axon, away from the cell body, it reaches a series of sites locally enriched with a diverse set of molecules arranged into nanometer-scale structures. The AZ is responsible for facilitating the exocytosis of the neurotransmitter glutamate at excitatory terminals. As the depolarizing signal invades the presynaptic AZ, local voltage-dependent processes begin to unfold. Voltage-gated calcium channels (VGCCs) anchored within the active zone by key scaffolding molecules like Rab3 interacting molecule (RIM), which helps to closely couple VGCCs to neurotransmitter-

containing vesicles, undergo channel opening allowing a brief elevation of local intracellular calcium. Nearby vesicle fusion machinery, such as the SNARE complex, is triggered by this elevation in calcium and undergoes changes in their conformation. An intricate series of these calcium-dependent conformational changes in many AZ molecules leads to the fusion of the glutamate-containing vesicle with the presynaptic membrane, emptying its contents into the synaptic cleft. This conversion of voltage changes into chemical signaling acts to propagate the signal received at the AZ across the cleft to be received by another neuron. However, glutamate exocytosis does not always require induction by an action potential, but instead occurs spontaneously through a separate set of regulatory mechanisms. Through at least these two distinct modes, glutamate is released into the synaptic cleft, and it has been thought that these two forms of synaptic transmission serve unique purposes.

Once the synaptic vesicle fuses with the presynaptic membrane, glutamate quickly escapes through the fusion pore and enters the synaptic cleft. The cleft is the extracellular region between the PSD and AZ, and is densely packed with proteins (Lucic et al., 2005). Though a variety of proteins reside within the cleft, postsynaptic glutamate receptors help to transduce the signal from the AZ at the surface of the postsynaptic cell. Once exocytosed, a small fraction of glutamate molecules will become bound to nearby receptors within the postsynaptic density. The most abundant synaptic glutamate receptors are the α-amino-3-hydroxy-5-methyl-4-isoxazolepropionic acid receptors (AMPARs), which are responsible for the majority of fast synaptic transmission. These AMPARs are held in place by postsynaptic scaffolding molecules, one example being the abundant PSD-95. AMPAR activation by the binding of two to four glutamate molecules results in robust channel

opening, influx of cations, and the depolarization of the postsynaptic compartment. When this depolarization of the postsynaptic compartment is strong enough, it leads to the opening of the N-methyl D-Aspartate Receptors (NMDARs), and an influx of calcium into the calcium-scarce environment of the PSD. This complex sequence of events leads to the action of many downstream glutamate-dependent, calcium-dependent, and voltage-dependent processes, which can produce ongoing changes in the composition, organization, and function of the synapse, known as synaptic plasticity. The degree to which AMPARs can depolarize the postsynaptic neuron, often considered as the strength of the response, is a key parameter since the depolarization of the downstream neuron will be integrated with all the other inputs received concurrently and may in turn elicit its own action potential.

The coordinated actions within the AZ, synaptic cleft, and postsynaptic density produce an electrochemical signal which is propagated from one neuron to another. As the predominant form of synaptic transmission in the brain, glutamatergic transmission is known to influence many circuits, which permit communication within and between brain regions, and that are responsible for many of our everyday behaviors and internal states. Investigation into the mechanisms underlying glutamatergic function has far-reaching implications for a variety of fundamental human and animal behaviors, including those which are disrupted in many diseases and disorders.

1.2 Why do we use behavior as a means to understand the brain?

Many model organisms exhibit behaviors that can be leveraged as natural benchmarks for the performance of synapse and circuit function (Maren, 2005; Kim & Jung, 2006; Smith & Graybiel, 2016; Dexter et al., 2012; Nilsen et al., 2004; Miklosi & Andrew, 2006). A common hypothesis is that if a circuit is functioning properly, behaviors occur as expected. However, if for instance a particular set of neurons in a circuit are forced to behave differently in terms of their patterned activity or if particular synaptic functions are impaired, then we can observe how functional circuit changes, mediated by synapses, relate to the changes in behavior (Johansen et al., 2012). The challenge lies in relating these phenomena to make inferences about whether the behavior of the animal is impacted due to changes in circuit function. Importantly, though, the manipulation itself can even inform us as to how individual molecules instruct synaptic properties within specific circuits in particular contexts (Guo et al., 2010; Lüthi & Lüscher, 2014; Wolff & Ölveczky, 2018; Friedrich et al., 2010). Deducing how molecules lead to changes in behavior must be done carefully, both in experimental design and how conclusions are arrived at, because these phenomena exist at such different scales and exhibit their own complex systems.

A variety of approaches allow us to manipulate features of synaptic and circuit function and measure the resultant changes in protein content and organization as well as functional synaptic properties. These measurements include many informative parameters to estimate the organization and functional capabilities of the synapse. However, without a higher order benchmark to assess “proper” circuit function, it remains unclear how a manipulation of synaptic features is consequential. For instance, there may be a deficit in some form of short-term plasticity, but whether this form of short-term plasticity is

important in the behavior of interest cannot be known unless the behavior is specifically assayed. Otherwise, I predict that deficits in synaptic function affect behavior because the neuron exists within a circuit suspected to be involved in that behavior. Without the explicit test of the hypothesis at a higher order of function, the consequence of a synaptic manipulation remains a prediction. The power of using behavior as a tool to assess synapse function arises when this form of short-term plasticity may be a well-described phenotype in a separate behavior, confirming that the synaptic or circuit-level changes that have occurred indeed have consequences. Behavioral assays can recruit diverse patterns of activity and put specific biological demands on the array of synapses contained within a circuit. This provides us with clues to deficits in synaptic function we may not have previously understood, specifically, how individual synapses need to operate in order to uphold behavioral performance.

Circuit efficacy is thought to underlie behavioral performance. What defines circuit efficacy is unclear (Hembrook-Short et al., 2019). Even so, the cumulative impact of changes in circuit efficacy would appear only to be important as it relates to the performance of the circuit in serving an observable role in behavior. This way of thinking helps to operationalize behavioral performance as a natural benchmark for efficacy of lower-order systems like circuits and synapses. And relatedly, synaptic efficacy may be considered as an individual synapse's capability to maintain proper circuit function. These synapses may exist in an individual neuron potentially involved in many different circuits to ultimately produce a range of behaviors or internal states. The efficacy of synaptic transmission is commonly referred to as simple increases in the consistency or strength of transmission (López, 2002). However, it is interesting to consider whether changes in

synaptic composition and function, that still yield desirable circuit or behavioral functions, are simply the result of a synapse operating effectively.

Many unique behavioral benchmarks exist which allows for experimental tests of how unique synaptic properties influence behaviors. And paramount to the study of basic synaptic function and behavior, is that truly fundamental mechanisms of synaptic function can often generalize between circuits. These circuits may be involved in vastly different behaviors, with at times only modest nuances in their particular molecular composition, organization, or function. This greatly motivates and reinforces the idea that investigating fundamental mechanisms of synapse function are critical to furthering our understanding of circuit and brain function in various diseases and disorders. The discovery of fundamental synaptic mechanisms provides us with a great deal to gain in our understanding of basic circuit function which is likely applicable in a wide variety of behaviors, including those implicated in diseases and disorders. Identifying how synapses *can* operate gives us a set of principles by which we can build hypotheses in the future that help to find explanations for pathological circuit function and behavior.

## 1.3 The molecular correlates of a memory: stable changes in circuit function

Synaptic plasticity can provide an excellent opportunity to explore how molecular changes at individual synapses influence circuit function and behavior (Citri & Malenka, 2008). Patterned activity from upstream neurons can lead to alterations of individual synapses resulting in lasting changes in circuit function important for behavioral performance in a number of tasks. However, exactly how synapses can undergo changes

in their organization and function is not well understood. This dearth leaves our understanding of the physiological mechanisms that allow for changes in circuit function incomplete. Disruptions of synapse-level features, such as the presence or absence of particular molecules or their ability to bind other molecules, are also known to influence behavioral performance related to learning and memory. For example, disruption of the association between PSD-95 and neuronal nitric oxide synthase (nNOS) leads to impaired NMDAR activation at a subset of synapses (Li et al., 2018). The disruption to this interaction leads to impaired long-term potentiation (LTP) which underlies performance in a conditioned freezing response in rats. This is just a singular example of how molecular changes at synapses (decreased association of PSD-95 and nNOS) correspond to certain behaviors (decreased freezing), and their underlying circuit function (decreased input strength, perhaps even at a particular synapses).

LTP is a process through which synaptic transmission is strengthened for sustained periods (Malenka & Bear, 2004). The induction of LTP is NMDAR-dependent and leads to postsynaptic signaling cascades, many of which are calcium-dependent. The expression of LTP leads to changes in the molecular composition and organization of synapses, which is stably maintained. Most notably, additional AMPARs are stably recruited to synapses that underwent LTP. These lasting molecular changes lead to increases in synaptic strength. LTP has been a phenomenological window through which we can learn more about the capability of synapses to undergo molecular changes in response to activity changes. These molecular changes are what is thought to give rise to new or altered function of the synapse, and in the case of LTP to increase synaptic strength. As discussed previously, understanding how these mechanisms may generalize to other activity-dependent

phenomena or synapses in other circuits is of great interest. Importantly, LTP as a paradigm may potentially even relate to processes under more physiological conditions, e.g., firing rates known to exist within certain brain circuits.

One example of the benefits of the study of LTP and the molecular changes at synapses is the use of mathematical estimates of quantal transmission to better understand the physical locus of changes following LTP. Three parameters are typically used to describe synaptic transmission: the number of functional neurotransmitter release sites (*n*), the probability of release from a single release site (*p*), and the postsynaptic response to a single-vesicle release event (*q*). Interestingly, many labs were studying LTP at a variety of different synapses with various biological preparations. Consequently, it was discovered that the synaptic locus where changes occurred could vary between these different synapse types and even the type of LTP-inducing stimuli used. This provided an opportunity to explore how certain types of patterned activity were able to induce changes at synapses of specific properties, and which molecules were responsible for facilitating these changes. Efforts to understand the underlying synaptic mechanisms of LTP revealed much about the fundamental molecular actions of synapses. An excellent example is the discovery of "silent synapses" (Durand et al., 1996; Isaac et al., 1995; Liao et al., 1995). There were early observations that changes to the quantal parameter *p*, inconsistent with the notion of a postsynaptic change in AMPAR content following LTP. Stimulation of presynaptic terminals that fail to elicit detectable postsynaptic signals are expected to be failures in neurotransmitter release. It was observed that following LTP that there were fewer synaptic failures, perhaps meaning that measures of *p* were increased. However, this lack of failures was later found to be due to the increased trafficking and stabilization of AMPARs at

synapses which previously lacked them, and no change to presynaptic function. Because of this "unsilencing" of synapses, vesicle release less frequently resulted in the failure to provoke a response, which was previously mistaken as a property a release probability. Investigations into the synaptic mechanisms of LTP has forced neuroscientists to more carefully consider the synaptic mechanisms underlying the phenomenon (Malenka, 2003). Additionally important, though, was the discovery that strengthening of synapses through induction of LTP revealed how strongly some neuronal circuits can control particular aspects of animal behavior.

In hippocampal Schaeffer collateral synapses, following the induction of LTP, the number of AMPARs present in synapses increases. In which case, given the same quantum of glutamate, more receptors are available and within close proximity to neurotransmitter release meaning that more receptors could be activated. Whole-cell patch clamp recordings show increases in estimations of $q$, suggesting that the response to single vesicle release is enhanced in LTP (Foster & McNaughton, 1991; Benke et al., 1998). Evidence from fluorescence imaging of tagged AMPARs quite directly demonstrates that following the induction of LTP one could observe the trafficking of more AMPARs into synapses (Matsuzaki et al., 2004). Interestingly, there were some observations in changes to $p$, inconsistent with the notion of a postsynaptic change in AMPAR content after LTP. This arose from the finding of a decrease in the number of failures to elicit neurotransmitter release following LTP induction. However, this was later found to be due to the increased trafficking and stabilization of AMPARs at synapses which previously lacked them. Because of this unsilencing of synapses, vesicle release less frequently resulted in the failure to provoke a response, which was previously mistaken as a property a release

probability. It was eventually agreed upon that at the hippocampal CA3-CA1 Schaeffer collateral synapses there is an increase in the number of AMPARs trafficked and incorporated into synapses following LTP, independent of changes in release probability.

LTP provides an excellent example of a framework through which we can induce robust changes in the activity of connected neurons. These regimented changes in activity allow us the opportunity to test hypotheses about how synapses are able to undergo changes, which may inform us of general rules of how synapses are built and maintained. For example, the realization that the unsilencing of synapses could lead to changes in experimental measures of release probability, when in fact there were changes at the molecular level in the synaptic incorporation of AMPARs into previously AMPAR-lacking synapses. Molecular mechanisms governing synapse organization and function during robust changes in response to LTP induction, can potentially inform us about how synapses may operate under basal physiological conditions. Importantly, fundamental mechanisms of synapse function will similarly inform our predictions about how physiological cases of synaptic plasticity are executed. Determining whether novel fundamental synaptic mechanisms have real consequences in circuit function or behavior is a valiant goal. Independent of any specific role in circuit function or behavior, phenomena such as LTP help to contextualize these fundamental mechanisms which are likely widely applicable to many types of synapses, circuits, and behaviors. The investigation of fundamental mechanisms of synaptic transmission are equally as important as identifying the circuit functions or behaviors that they are involved in, because the contexts in which they are applicable are not yet understood.

## Section 2. AMPA-type glutamate receptor number impacts responsiveness to neurotransmitter release

### 2.1 Structure, synthesis, and trafficking of AMPA-type glutamate receptors

The number of AMPARs within a single synapse is a key property determining the amplitude of the excitatory postsynaptic current (EPSC). AMPAR synthesis, trafficking, and incorporation into synapses contribute to controlling the number of AMPARs at synapses. These mechanisms are important to consider in our understanding of fundamental mechanisms of synaptic transmission. While these processes are still being investigated, especially in the context of plasticity, there is much already understood about the regulation of AMPAR content within synapses.

AMPARs are ionotropic glutamate receptors. In mammals, there are four unique genes (GRIA1-4) responsible for the expression of the AMPAR subunits (GluA1-4). All four subunits contain an extracellular region (ECR) with two bilobate domains, which make up the majority of the receptors bulk. The N-terminal domain (NTD) is involved in receptor assembly (Herguedas et al., 2013) and trafficking (Watson et al., 2017). The ligand binding domain (LBD) is important for channel gating of the receptor. The transmembrane domain (TMD) of these subunits is principally involved in pore formation and can undergo modifications that alter its selectivity for $Ca^{2+}$ (Greger et al., 2017). Many auxiliary subunits make a direct and stable interface with the TMD and LBD to influence AMPAR trafficking, mobility, and channel kinetics (Yan & Tomita, 2011). GluA1-4 are assembled into hetero-oligomeric receptors containing four individual subunits. The two most abundant populations of these tetrameric receptors are GluA1/2 heterodimers and GluA2/3 heterodimers, with GluA1/2 being the predominant dimer-of-dimers (Wenthold et al.,

1996, Lu et al., 2009, Schwenk et al., 2012, 2014, Zhao et al., 2019). In contrast, it is possible for the GluA1 subunit alone to assemble into a homomeric tetramer, which imparts differences in channel selectivity for calcium ions. The expression of each of these receptor subunits, and their complement at the cell surface, has distinct implications for neuronal development and signaling.

AMPAR biosynthesis is a major point in the regulation of neuronal signaling. AMPARs go through extensive processing in the ER during their biosynthesis, where complex mechanisms aid in the assembly of these multimeric structures. AMPAR biogenesis provides a pool of available receptors able to be secreted and trafficked to synapses, though this process does appear to be rate-limited by the availability of their auxiliary subunits (Kessels et al., 2009; Bissen et al., 2019). Properly assembling receptors is important for basic synapse function. There are several key features that their assembly can influence, such as, which dimers are paired (Boulter et al., 1990; Keinanen et al., 1990; Herguedas et al., 2019; Zhao et al., 2019; Schwenk et al., 2021), which isoforms or edited subunits are included, and proper auxiliary subunit association. These features influence both single-channel properties, but also importantly the AMPAR complexes trafficking and lateral diffusion. Ultimately, exactly how these AMPAR complexes are assembled is important for how they become incorporated into synapses as well as their function once incorporated. AMPAR biogenesis involves a series of checkpoints to effectively assemble single monomers into dimers. Once these dimers are formed into tetramers, auxiliary subunits are integrated into what is then a hetero-octameric complex. Then, ER export is enabled by ERES, which entails the induction of transport vesicles in the ER membrane, which can be trafficked as an intracellular vesicle, capable of traveling further down the

secretory pathway (Hollman et al., 1991; Mosbacher et al., 1994; Bowie & Mayer, 1995; Koh et al., 1995; Sobolevsky et al., 2009; Schwenk et al., 2012; Greger et al., 2017; Twomey & Sobolevsky, 2018; Schwenk et al., 2021).

Once AMPARs have been trafficked into these vesicles in the ER, these receptors are then directed to the surface of the cell. However, the mechanisms involved in appropriately trafficking these receptors to the surface are complex, but are known to be activity dependent, and the mechanisms involved in directing these newly delivered receptors are of great interest in the strengthening of synaptic connections. Considering any given intracellular transport vesicle could have AMPARs with different single-channel properties, it is interesting to consider how these complexes navigate to specific subcellular sites in order to deliver receptor complexes endowed with particular features in the ER (Kennedy & Ehlers, 2006). This is thought to be achieved in part through the Golgi apparatus and the *trans*-Golgi network (TGN), where further modifications of these receptor complexes can occur. And, there is growing evidence that Golgi-independent pathways and local translation for the delivery of AMPARs which diverge from classical trafficking pathways.

## 2.2 Lateral diffusion and synaptic incorporation of AMPA-type glutamate receptors

Once exocytosed, AMPARs diffuse laterally within the plasma membrane (Borgdoff & Choquet, 2002). The lateral mobility of AMPARs is an important step in their synaptic trafficking and incorporation, both under basal conditions (Heine et al., 2008; Heine et al., 2009; Czöndör et al., 2012) and plasticity (Petrini et al., 2009; Penn et al.,

2017; Pandya et al., 2018). AMPARs are found predominantly at synapses. However, the majority of their exocytosis occurs at extrasynaptic sites (Chen et al., 2000; Nicoll et al., 2006; but see Kennedy et al., 2010). Thus, AMPARs must often travel by lateral diffusion from extrasynaptic sites to synaptic sites in order to be incorporated in synapses by a number of different mechanisms able to counteract their diffusion, which will be discussed later. Notably, their lateral mobility is known to be impacted by channel subunit composition, perhaps implicating subunit-specific protein-protein interactions (Kropf et al., 2008). This includes intracellular interactions with abundant scaffolding molecules, such as PSD-95 (Bats et al., 2007), or synaptic cell adhesion molecules important for the recruitment of scaffolds (Mondin et al., 2011). AMPARs must traverse the cell surface to get from extrasynaptic sites of exocytosis to synaptic sites, where they can influence synaptic transmission.

AMPARs are also found to be mobile within individual synapses (Tardin et al., 2003). Previous to this discovery, it was well understood that AMPAR exo- and endocytosis was important for synaptic transmission and plasticity (Nishimune et al., 1999; Lüscher et al., 1999; Passafaro et al., 2001; Ehlers, 2000), since synaptic AMPAR number was understood to be a determinant of postsynaptic strength (DiAntonio et al., 1999; Bellingham et al., 1998; O'Brien et al., 1998). Despite the number of AMPARs accumulated at a synapse, once activated, AMPARs quickly desensitize, which contributes to decreases in synaptic channel conductance, and it was found that the mobility of AMPARs aided in the exchange of desensitized AMPARs for other, non-desensitized AMPARs (Heine et al., 2008). This suggests that repeated vesicle fusion events would more consistently activate a greater number of receptors when receptors were able to

exchange in and out of synapses between release events. AMPAR mobility at synapses is suspected to be controlled by the cytoskeleton (Kerr et al., 2012), scaffolding molecules (Ehrlich et al., 2004; Bats et al., 2007; MacGillavry et al., 2013; Constals et al., 2015; Klaassen et al., 2016), the extracellular matrix (Frischknecht et al., 2009; but see Klueva et al., 2014), secreted factors (Pandya et al., 2018), steric hindrance (Li et al., 2016; Lee et al., 2017), and synaptic activity (Groc et al., 2004; Ehlers et al., 2007). The mobile fraction of synaptic AMPARs (Kerr et al., 2012; Li et al., 2016), or the percentage of molecules that are free to diffuse (Petazzi et al., 2020), has been estimated to be between 20% to 60% (Ashby et al., 2006; Bats et al., 2007; Heine et al., 2008; Frischknecht et al., 2009; Martin et al., 2009; Arendt et al., 2010). More recent estimates *in vivo* suggest a number closer to 70%, where 50% of the mobile receptor population are mobile within the synapse and the other half move between synaptic and extrasynaptic areas (Chen et al., 2021). Taken together, many molecular mechanisms influence AMPAR lateral mobility and contribute to their availability at synapses, which has consequences for synaptic transmission and synaptic plasticity.

## Section 3. The biophysical constraints surrounding AMPAR activation within a single synapse

From the information above, it is clear that the number of AMPARs at synapses is important for the strength of the postsynaptic response. Even still, several constraints appear to limit AMPAR activation following glutamate release, suggesting factors beyond receptor number additionally control synapse strength. Among the most critical is that a variety of modeling approaches suggests that AMPARs even ~90 nm from the site of glutamate release open with only about half the likelihood of those close to the site of vesicle fusion, due to the low affinity and rapid desensitization of receptors. This greatly diminishes the expected EPSC, a prediction in line with experimental results suggesting that glutamate release from a single vesicle is not sufficient to maximize postsynaptic receptor activation. Unfortunately, it has been difficult to test whether such distance-dependence plays a physiological role in neurons because the mechanisms that determine the precise positioning of receptors across from sites of release are not known.

### 3.1 Glutamate packaging into vesicles can influence receptor activation

Vesicular glutamate concentrations can influence the activation of postsynaptic AMPARs. Glutamate is a negatively charged amino acid that is responsible for the majority of excitatory synaptic transmission in the mammalian brain (Zhou et al., 2014). Glutamate is stored in intracellular vesicles that cluster within axonal boutons, where active zones are known to be positioned. When a glutamate-containing vesicle fuses with the surface plasma membrane within the active zone, glutamate spills into the extracellular space until reaching equilibrium as it diffuses throughout the cleft. High enough local concentrations

of glutamate in the cleft will bind to postsynaptic glutamate receptors. The activation of these receptors leads to channel permeability which is understood to drive the majority of excitatory transmission.

Glutamate-containing vesicles (~40 nm) begin as precursor vesicles in the secretory pathway. These precursors are trafficked into the axon and later mature into vesicles compatible for synaptic transmission. Glutamate-containing vesicles likely share a lot of common machinery with other types of synaptic vesicles (Takamori et al., 2006). These common features involve general aspects of vesicle fusion, recycling, and degradation. Vesicles involved in glutamate release contain vesicular glutamate transporters (VGLUT1-3) which help to fill the vesicle with approximately ~2000 molecules of the abundant neurotransmitter (Santos et al., 2009; Burger et al., 1989). VGLUT1 is the most abundant protein family member in hippocampus and is associated with synapses that display a relatively low release probability (Fremeau et al., 2001). Interestingly, the amount of VGLUT expression has been found to influence the amount of glutamate that can be stored and released from vesicles upon fusion (Liu et al., 1999). In hippocampus, increasing vesicular glutamate through VGLUT overexpression increases postsynaptic responses to the release of single vesicles, which may act by increasing the likelihood of activating postsynaptic AMPARs (Daniels et al., 2004, Wojcik et al., 2004, Wilson et al., 2005). Importantly, this suggests that in their native state, typical glutamate-containing vesicles aren't capable of saturating the postsynaptic complement of AMPARs. But, it is possible that this is not the case at all synapses, where expression levels of proteins that regulate the proton- and chloride-dependent mechanisms for glutamate transport into the vesicle (Winter et al., 2005). Curiously, the mechanisms surrounding the regulation of the

equilibrium setpoint for the concentration of glutamate in a given vesicle is unclear, probably due to how basic these cellular components are, but is driven by intracellular glutamate and chloride concentrations, proton availability, and the number of available transporters (Eriksen et al., 2020). Although potential mechanisms exist to achieve postsynaptic receptor saturation, vesicular glutamate concentrations do not typically saturate postsynaptic receptors.

### 3.2 Diffusion of the neurotransmitter glutamate in the synaptic cleft

The majority of glutamate only escapes the vesicle when it fuses with the surface plasma membrane (Sudhof et al., 2013). This results in the rapid diffusion of ~2,000 molecules of glutamate in the cleft at ~0.4 $\mu m^2$/ms (when adjusted for the slower tortuosity in the dense cleft environment; Raghavachari & Lisman, 2004; Rusakov & Kullman, 1998; Longsworth, 1958) as the volume of the vesicle is joined with that of the extracellular space. Glutamate diffusion is an extremely stochastic process which is sculpted by the local architecture of this trans-cellular junction and has been the focus of many numerical models (Rusakov & Kullmann, 1998; Barbour & Hausser, 1997; Holmes, 1995, Raghavachari & Lisman, 2004; Ventriglia & Maio, 2000; Kullman & Asztely, 1998; Holcman & Schuss, 2014; Maio et al., 2017; Franks et al., 2002, 2003; Holcman & Yuste, 2015; Kinney et al., 2013; Rusakov & Stewart, 2021). Using "ground truth" parameters obtained from high resolution electron microscopy as geometrical constants and estimations of a variety of synaptic object copy numbers, these models often aim to understand how the local environment or properties of these glutamate-containing vesicles change glutamate diffusion and the activation of a variety of postsynaptic receptors. Importantly, even within

the small volume in the cleft, glutamate concentrations following fusion drop off steeply away from the site of release (Raghavachari & Lisman, 2004) and decline very quickly (Clements et al., 1996; Diamond & Jahr, 1997; Rusakov et al., 1998). Because of these features, only a very small volume directly closest to the site of vesicle fusion in the extracellular space experiences the high concentrations of glutamate that most efficiently activate AMPARs, which I will explore in more detail below. As the glutamate in the cleft equilibrates it indeed undergoes reuptake into cells through glutamate transporters, mainly EAAT1,2 (Tzingounis et al., 2007), but this process is much slower than the rate at which glutamate diffuses into the much larger extracellular volume, and even additional escape routes or increased density of transporters do not significantly impact the rapid drop-off in the local glutamate concentration during the first 500 ms (Kessler, 2013). Thus, glutamate in the cleft from the release of a single vesicle is brief and spatially restricted.

### 3.3 Glutamate binding to AMPARs

There are a number of postsynaptic receptors for the neurotransmitter glutamate, both metabotropic and ionotropic (Traynelis et al., 2010). A considerable number of unique glutamate receptors present an array of potential binding sites for glutamate once it has been exocytosed, all with varying affinities for the ligand glutamate. AMPARs, constituting the majority of glutamatergic transmission in the brain, exhibit a surprisingly low affinity for glutamate at around 200-500 μM (Weston et al., 2006; Matsui & Jahr, 2004; Nielson et al., 2004; Barbour et al., 2001; Franks et al., 2002; Volodymyr & Remy, 1999; Kejzar, 2020; Voronin et al., 2004; Savtchenko & Rusakov, 2005; Choquet & Hosy, 2020; Kullman et al., 1996). Glutamate binds to AMPARs at four interlobe clefts of the

individual subunits within the ligand-binding domain (LBD) of the biolobate hetero-octameric receptor complex (Armstrong & Gouaux, 2000; Greger et al., 2017).

The binding of glutamate quickly leads to the desensitization of the receptor with a time constant of ~5 ms (Stern-Bach et al., 1998; Mayer & Westbrook, 1987; Trussell & Fischbach, 1989; Jonas & Spruston, 1994; Otis et al., 1994). The receptor's apparent affinity for glutamate is dependent upon the number of glutamate molecules bound to the four available binding sites of a tetrameric complex. AMPARs occupied by a single glutamate molecule display a low apparent affinity and increasing the occupancy of the receptor increases the receptor's apparent affinity for glutamate (Prieto & Wollmuth, 2010). Importantly, increased occupancy also influences the conductance of the channel, both in terms of the severity of the conformational change in the channel (i.e. more open) and the channels ability to remain stably open before it ultimately desensitizes (Greger et al., 2017). Therefore, AMPARs that bind to one molecule of glutamate may partially flicker open infrequently passing minimal current, but AMPARs that bind two to four molecules of glutamate will exhibit a higher, more stable conductance that increases with occupancy before being desensitized. Thus, exposing AMPARs very quickly to very high concentrations of glutamate maximizes the likelihood that they 1) open rather than desensitize after binding glutamate, and 2) open with the highest conductance at the highest occupancy state.

Given these biophysical characteristics of AMPARs, the fact that glutamate in the cleft is transient and scarce takes on potentially strong physiological impact. The local cleft glutamate concentration in proximity to a receptor greatly impacts its occupancy, which mediates receptor conductance and desensitization, determining the strength of

transmission. This situation raises many possibilities for how AMPAR activation can be regulated by the organization of the synapse, namely the distribution of glutamate release sites and receptors down to the nanoscale. In the next sections, I discuss what is known about these critical features of synaptic organization.

## Section 4. Molecular constituents of neurotransmitter release sites

### 4.1 Vesicles, $Ca^{2+}$ channels, scaffolds, and fusion-competence

In order to successfully release glutamate into the cleft a number of complex molecular processes must unfold (Sudhof et al., 2013). As discussed previously, vesicles are continuously cycled and filled with neurotransmitter (Heuser & Reese, 1973; Sudhof, 2004; Hori & Takahashi, 2012; Martineau et al., 2017). Many of these vesicles will await translocation, priming, and eventual fusion with the surface plasma membrane in the reserve pool, where they are thought to sequester key cytosolic factors related to the vesicle recycling process (Denker et al., 2011). The readily releasable pool is a collection of vesicles that are to a degree ready to fuse quickly upon the influx of calcium. Release of vesicles in the RRP is driven by action-potential-dependent opening of voltage-gated calcium channels (Kaeser & Regehr, 2017). Distal vesicles will eventually translocate as far as 100 nm (Zenisek et al., 2000) and dock at the active zone, with the help of active zone scaffolding molecules such as RIM and ELKS, where vesicles undergo priming, making them fusion-competent (Sudhof., 2004).

It remains incompletely understood precisely which properties differentiate a cluster of active zone molecules from a functional release site, or where these specialized sites are located within the active zone. High on the list for these release-requisite molecules is the SNARE fusion machinery (synaptobrevin/VAMP, SNAP-25, and syntaxin; Jahn & Scheller, 2006), which orchestrates the fusion of the vesicular membrane with the plasma membrane in and energy- and calcium-dependent manner. Much is understood regarding which molecules are necessary for various forms of neurotransmitter exocytosis, and release of synaptic vesicles only requires two SNARE complexes to

achieve fusion, and even a single SNARE complex *in vitro* permits vesicle fusion (van den Bogaart et al., 2010; Sinha et al., 2011; Chang et al., 2015). SNARE fusion machinery and calcium channels undergo lateral diffusion in the membrane and are stabilized by their protein interactions to permit neurotransmitter exocytosis (Ribrault et al., 2011; Heck et al., 2019).

## 4.2 Scaffolds bring $Ca^{2+}$ channels and vesicles together

There are a number of active zone molecules that act to stabilize vesicles and $Ca^{2+}$ channels within close proximity to one another (Rosendmund et al., 2003; Sudhof, 2013; Kaeser et al., 2011). This set includes vesicle-associated proteins, integral membrane proteins in the plasma membrane, and several cytosolic factors. Anchored to the vesicle in a GTP-dependent manner are a family of Ras-related small GTPases important for vesicle priming, of which Rab3 is the most prominently expressed in the brain (Schluter et al., 2006). Rab3/27 binds two key molecules, namely Rab3-interacting molecule (RIM) which is important for docking (Wang et al., 1997), and Munc13, which is important for vesicle priming (Augustin et al., 1999; Richmond et al., 2001; Varoqueaux et al., 2012; Ma et al., 2013). In addition to this, RIM binding protein (RBP) also aids in the docking of synaptic vesicles through binding interactions with RIM and calcium channels (Wang et al., 2000; Hibino et al., 2002). Furthermore, these molecular complexes are linked to the cytoskeleton via the cytoskeletal matrix of the active zone (CAZ)-associated structural protein (CAST), where CAZ has been observed to contact vesicle membranes and CAST has been identified to bind to RIM (Harlow et al., 2001; Ohtsuka et al., 2002; Wang et al., 2002). Additional scaffolding for vesicles is provided by Bassoon which binds to the cytoskeleton and

occupies the space between vesicles (Dieck et al., 1998). Similar in structure to Bassoon, the protein Piccolo also has links to the cytoskeleton, but additionally binds to Rab3 and SNARE fusion machinery and is thought to be important for trafficking of vesicles at the active zone (Fenster et al., 2000). Thus, a number of scaffolds with different combinations of binding interactions all contribute to the fidelity of neurotransmitter release. Importantly, though, many of these proteins contain C2 domains, making calcium availability likely central to their function, and intracellular [$Ca^{2+}$] is tightly regulated in neurons.

4.3 Calcium influx through VGCCs activate fusion machinery

Calcium permeability in active zones is predominantly mediated through voltage-gated calcium channels. There are three main families of $Ca_v$ channels, but in the hippocampus, P/Q- (Cav2.2) and N-type (Cav2.1) calcium channels are predominantly responsible for the influx of calcium observed in response to an action potential and co-exist at single active zones (Wu et al., 1994; Wheeler et al., 1994; Catterall, 2011). However, depending on the frequency of stimulation, Cav2.1 (N-Type), Cav2.2 (P/Q-Type), and Cav2.3 (R-Type) can have varied contributions to calcium permeability (Dolphin & Lee, 2020). Additionally, kinase-dependent phosphorylation can influence the association between N-type channels and the synprint region of RIM (Coppola et al., 2001). The association between P/Q-type channels and RIM is mediated by the beta auxiliary subunit (Kiyonaka et al., 2007) and influences channel function by suppressing inactivation.

These calcium channels are directly in complex with scaffolds as well as the SNARE fusion complex (Brunger et al., 2009). The SNARE fusion complex consists of

synaptobrevin/VAMP located in the vesicular membrane, the cytosolic component SNAP-25 and associated molecules NSF and SNAP, syntaxin located on the surface plasma membrane, and the critical calcium-sensitive fusion-trigger, synaptotagmin (Söllner & Rothman, 1994; Jahn & Schneller, 2006). Importantly, the presence of RIM in the active zone facilitates synchronous neurotransmitter release by binding to the a1 auxiliary subunit, helping to bring vesicles within close proximity to both N- and P/Q-type, but not L-type channels, through a PDZ-domain-mediated interaction (Kaeser et al., 2011; Han et al., 2011). Thus, RIM is a critical scaffold that localizes calcium channels within close proximity to calcium sources, which is critical for SNARE-mediated vesicle fusion. However, other scaffolding molecules in this super-complex, such as Munc13, are also important for a myriad of molecular events that enable stable transmission (Augustin et al., 1999; Varoqueaux et al., 2002; Calloway et al., 2015; Sakamoto et al., 2018). Generally, RIM is considered a physical tether for calcium channels and vesicles, while Munc13 also acts a physical tether, it has also been shown that it modulates channel activity directly (Kaeser et al., 2012). Both Munc13 and RIM are non-homogenously distributed throughout the active zone, and this has been suggested to influence vesicle release kinetics (Kaeser et al., 2011; Han et al., 2011; Zhou et al., 2013; Hu et al., 2013), and even the nanometer-scale location of vesicle fusion within the active zone (Tang et al., 2016; Sakamoto et al., 2018).

## Section 5. Nanoscale distribution of neurotransmitter release sites

### 5.1 Advancements permitting visualization at the nanoscale

Within the presynaptic active zone, molecules critical for vesicle priming and Ca2+ channel recruitment such as the Rab3 interacting molecule (RIM) and Munc13 are clustered into ~100 nm nanodomains (Zhou et al., 2013, Tang et al., 2016; Haas et al., 2018; Sakamoto et al., 2018; Bohme et al., 2018). These AZ nanodomains are widely conserved across many synapse types and are thought to govern vesicle positioning and establish sites in the AZ where action potentials drive synaptic vesicle exocytosis with highest probability.

Electron microscopy can also be used to visualize the spatial distribution of vesicle fusion in the active zone (Torri-Tarreli et al., 1985; Richmond et al., 1999). This approach gives the highest available resolution images of vesicle fusion with the plasma membrane, but only captures a single snapshot following stimulation. Recently, it was found that synaptic vesicles are correlated with specific molecular complexes identified by de novo generation and classification of cryo-ET structures in the synaptic cleft and PSD (Lucic et al., 2021). Notably, electron microscopy can be combined with optogenetics and rapid cryofixation to capture the ultrastructure of synapses only milliseconds following stimulation (Watanabe et al., 2013; Watanabe, 2016; Borges-Merjane et al., 2020). Depending on the interval between the optogenetic stimulation and cryofixation, different types of neurotransmitter release can be observed. Synchronous vesicle fusion occurs within 1 millisecond after stimulation, and asynchronous release happens several milliseconds later (Li et al., 2021). Recently, this flash and freeze approach was coupled with immunogold labeling of synaptic proteins (Li et al., 2021). It was found that

asynchronous and synchronous neurotransmitter release occurred in different lateral positions within the active zone. Computer simulations suggested that this organization indeed was important for optimizing NMDAR activation during asynchronous release (Li et al., 2021). These data helped to demonstrate that different modes of release may take place at unique locations within the active zone and may play roles in optimizing receptor activation.

The diffraction limit of light renders conventional imaging approaches incapable of discriminating individual molecules within 250-300 nm of one another (Weiss, 2000). Developments in light microscopy has led to diffraction unlimited resolution imaging of labeled proteins at nanometer resolution (Huang et al., 2008; Betzig et al., 2006; Rust et al., 2006; van de Linde et al., 2009; reviewed in Maglione & Sigrist, 2013). These novel super-resolution imaging modalities involve the activation of fluorescently-tagged molecules, either by genetic approaches or immunolabeling. However, this excitation is performed in a way that permits the estimation of the position of single-molecule emitters using statistical approaches. At any given point in time, no two molecules are emitting light within the same synapse, which would obscure the estimation of their position. Individual molecule positions are collected sequentially over many frames, building a map of molecular positions one-by-one to yield 10-100 nm resolution images of protein distributions. These high-resolution images of synaptic protein distributions have revealed much about the internal organization of synapses.

Recently, our lab developed a novel approach to map the nanoscale positions of individual release events. This was achieved by fusion of a super-ecliptic pHluorin to VGluT1, and when a single vesicle would fuse with the surface plasma membrane, single

vesicle fluorescence could be detected and localized using similar approaches to other statistical single molecule localization approaches (Tang et al., 2016). Additionally, these release site positions were mapped over the distribution of RIM1. This was achieved by expression of RIM1-mEos3.2, which allowed for sparse 405 nm photoconversion and single molecule detection using PALM. This revealed that the local density of the molecule RIM1 in the active zone was predictive of where evoked vesicle fusion events occurred. Because evoked release preferentially took place nearby the highest density of RIM molecules, it suggests that molecularly defined sub-regions of the active zone may control the lateral subsynaptic position of evoked neurotransmitter release. Notably, spontaneous release occurred over a much larger area of the active zone (Tang et al., 2016). The differences in the areas over which evoked and spontaneous release took place, suggest that they may fuse at unique sites in the active zone. Thus, it appears that specialized sites forming nanodomains of tens of nanometers in the active zone, such as the scaffolding molecule RIM1, may represent sites where evoked neurotransmitter release preferentially takes place. What these sites of release are comprised of and where they are located is not known, but likely constitutes a number of molecules with specific roles in neurotransmitter release and mapping active zone proteins may help to reveal their molecular composition.

## 5.2 Unique spatial distributions of neurotransmitter release

The molecular composition and active zone distribution of neurotransmitter release sites may determine presynaptic properties of transmission. It is possible that neurotransmitter release can be served by a small number of molecules, and whether they form nanoclusters could be inconsequential for release (van de Bogaart et al., 2010).

However, the alignment of sites of evoked neurotransmitter release with nanoclusters of active zone scaffolds suggest that the concentration of these scaffolds facilitates evoked release (Tang et al., 2016). Beyond our lab's work demonstrating the spatial instruction of evoked neurotransmitter release sites by RIM1, others have investigated the priming factor Munc13, which has a critical role in neurotransmitter release. It was found that Munc13 is partitioned into several sub active zone supramolecular assemblies, where it was able to recruit synataxin-1 (Sakamoto et al., 2018). They found that the number of these Munc13 nanoclusters was related to the number of readily releasable vesicles, which was consistent with glutamate release at those synapses (Sakamoto et al., 2018). Interestingly, the number of Munc13 nanoclusters matched their statistical estimations of the number of single synaptic release sites, perhaps suggesting that each Munc13 nanocluster itself represents a neurotransmitter release site (Sakamoto et al., 2018).

Additional work has also been done to investigate the variability of Munc13 in synapses and how this relates to release probability. The study combined paired recordings and correlative single-molecule imaging and high-resolution freeze fracture replica imaging of immunogold-labeled Munc13 (Karlocai et al., 2021). It was independently observed that Munc13 segregates into sub-active zone structures, consistent with prior work (Karlocai et al., 2021; Sakamoto et al., 2018; Tang et al., 2016). Additionally, the authors suggest that the amount of Munc13 correlates with the number of release sites per active zone, using rough estimates of the number of contacts and electrophysiologically-derived fluctuation analysis to estimate *n* (Karlocai et al., 2021). While these experiments fell short in some respects, namely low experimental power due to the difficult nature of the experiments, the ambition of these experiments hopefully inspires similarly detailed

investigations. Pairing physiological recordings with single-molecule imaging of single synapses will be important for the field to gain new understanding of how the spatial distribution of molecules imparts unique properties to neurotransmitter release sites.

The nanoscale organization of calcium channels regulates neurotransmitter release, but how calcium channel mobility impacts their nanoscale organization is not well understood. The nanometer scale distance of calcium channels from vesicles can greatly impact single-vesicle release probability. Recently, it was found that calcium channels themselves are mobile, partition into nanoscale domains, and can be controlled by splicing at exon 47 (Heck et al., 2019) which controls their mobility and influences release probability. Surprisingly, calcium channels inside the nanodomains displayed the highest mobility. This increased mobility was suggested to induce clustering of VGCCs with the splice insert at exon 47, and acted to increased vesicle release probability, perhaps suggesting the importance of the splice insert for proper coupling with synaptic vesicles. If the molecular constituents of release sites are mobile, similar to what was reported for calcium channels, it remains possible that certain types of neurotransmitter release sites themselves may be mobile, and that release site positions within active zones are dynamic.

Nanostructural organization of active zones has been described in other model organisms as well. In drosophila NMJs, it was discovered that Unc13, the drosophila homolog of Munc13, was segregated into modular sites, and the number of these sites was able to be rapidly remodeled following the induction of homeostatic plasticity (Bohme et al., 2019). This remodeling was not observed to be important for the initial potentiation induced by homeostatic plasticity, but rather was important as a structural element that sustained the potentiated AZ after prolonged periods (Bohme et al., 2019). Thus, the

consolidation of homeostatic plasticity in the drosophila NMJ requires the incorporation of new Unc13 modular release sites. Not only are these release site positions dynamic under basal conditions, but they can be added or removed during plasticity, raising questions about the structural stability of individual release sites.

Neurotransmitter release sites appear to be guided by nanoclusters of key AZ molecules. Mapping the nanoscale lateral distributions of release-relevant molecules and functional release sites will be important for dissecting the spatial configurations of neurotransmitter release in active zones. RIM and Munc13 seem to mark defined sites of neurotransmitter release and determining their colocalization with other active zone machinery may help to establish additional molecular constituents of release sites. In particular, whether additional molecules also need to form nanoclusters to allow for neurotransmitter fusion at defined sites within the active zone. These neurotransmitter release sites are smaller than the typical active zone and will require high resolution imaging to determine which molecules are colocalized with one another at the nanoscale. Defining the molecular constituents of neurotransmitter release may inform us about what differentiates evoked release sites from other types of neurotransmitter release, such as spontaneous or asynchronous release. Furthermore, these release sites can be altered by activity and even re-arrange within active zones. It will be important to understand how release site distributions and their molecular composition ultimately contribute to the formation of a functional release site, which subcompartments of the active zone these release sites are located, and additionally how they are modulated in response to certain types of activity.

## Section 6. The subsynaptic organization of AMPARs and their associated scaffolds

### 6.1 The lateral subsynaptic distribution of AMPARs

As previously discussed, the subsynaptic distribution of AMPARs within the PSD may be involved in controlling synaptic strength. AMPAR number within the PSD strongly influences synaptic strength, but not all AMPARs present in the PSD undergo activation after glutamate release. This suggests that the postsynaptic response to release is not always optimal. Additional factors that control receptor activation beyond number may be involved. Neurotransmitter release sites are non-homogenously distributed within the active zone, controlling which subcompartments in the cleft will experience the highest concentrations of glutamate. Because of the biophysical constraints surrounding AMPAR activation, the lateral distribution of receptors within individual synapses may impact AMPAR activation and synaptic transmission.

The organization of AMPARs likely depends on their number within synapses. Both larger spines (Nusser et al., 1998; Matsuzaki et al., 2001) and larger PSDs (Ehrlich & Malinow, 2004; Tanaka et al., 2005) are known to contain a greater number of AMPARs. From patch clamp recordings, the number of functional AMPARs in a spine can range from 0 to 140, and on average a spine may contain ~93 functional receptor complexes (Matsuzaki et al., 2001). This number is consistent with estimations from EM tomography and EM immunogold labeling (Chen et al., 2008; Nusser et al., 1998). Roughly ~80% of AMPARs are located within a dendritic spine are concentrated into the postsynaptic density, rather than extrasynaptic sites (Tanaka et al., 2005; Goodman et al., 2017). However, the reserve pool of extrasynaptic AMPARs is important for the expression of

LTP and may be increased following induction changing this proportion (Makino & Malinow, 2009; Granger et al., 2013).

AMPARs located within the PSD exhibit a heterogeneous distribution, i.e. in most synapses they are not uniformly or randomly distributed, but instead form subsynaptic clusters (Nair et al., 2013; MacGillavry et al., 2013; Tang et al., 2016; Grunwald et a., 2011; Jacob & Weinberg, 2015; Szepesi et al., 2014; Watson et al., 2021). These subsynaptic clusters of AMPARs were identified using many imaging approaches, including EM, PALM, STORM, PAINT, and STED. (Nair et al., 2013; MacGillavry et al., 2013). The details of the modalities are not important now, but each depends upon a different set of principles, and the observation of AMPAR nanodomains was robust across all approaches. AMPAR nanodomains exhibit on average an ~80 nm diameter, where their local density is elevated above the average synaptic AMPAR density. New analysis approaches have even been developed to help more finely discriminate between AMPARs in and out of nanodomains (Levet et al., 2015). Identification of single molecules suggest that roughly ~27 AMPARs are located within nanodomains on average (Nair et al., 2013). On average, there are ~1.2 nanodomains per synapse, and scales with PSD and spine size (Nair et al., 2013; Tang et al., 2016). Notably, there are AMPARs that exist outside of these nanoscale domains throughout the rest of the PSD. The mechanisms that determine AMPAR incorporation into nanodomains versus generally in the PSD are important to understand, because these nanodomains are expected to be involved in synapse function (MacGillavry et al., 2013; Nair et al., 2013).

There are many different mechanisms that counteract AMPAR diffusion within the PSD. The most well-described mechanisms act intracellularly through AMPAR auxiliary

subunits. AMPAR auxiliary subunits often bind to PDZ domains, a common motif among intracellular scaffolds, influencing their mobility in synapses (Bats et al., 2007; Sumioka et al., 2010). EM tomography demonstrates that AMPARs are accompanied by intracellular PSD-95 and vertical filaments that reach into the cleft (Chen et al., 2008). Many other non-PDZ protein interactions have been observed (Bissen et al., 2019), and likely also influence AMPAR mobility, but will be discussed in detail in the next section. The specific criteria which establish a molecule as an AMPAR anchor can be ambiguous and will be discussed in detail later. Both protein interactions and steric hindrance are expected to immobilize AMPARs within the PSD, but the molecular mechanisms that determine the subsynaptic positioning of AMPARs within synapses are not well understood.

## 6.2 A network of heterogeneously distributed scaffolds may instruct AMPAR position

Protein interactions immobilize AMPARs, and this is often achieved through their auxiliary subunits. TARPs and cornichons are the major auxiliary subunits of AMPARs (Shi et al., 2010; Yan et al., 2012), exhibiting the highest degree of association with AMPAR subunits (Schwenk et al., 2012). Although cornichons are important for AMPAR subunit assembly during trafficking, few cornichons are actually found at the cell surface, whereas TARPs are thought to play a critical role controlling AMPAR mobility in the plasma membrane (Shi et al., 2010). TARPs were originally discovered as calcium channel auxiliary subunits in drosophila (Tomita et al., 2003). These auxiliary subunits were then identified in mammalian brain and particularly enriched in hippocampus where they control surface expression of AMPARs (Tomita et al., 2003; Tomita et al., 2004).

Though AMPAR auxiliary subunits help to counteract AMPAR diffusion in hippocampal PSDs, these auxiliary subunits do not achieve immobilization without other protein interactions. TARP-AMPAR complexes are most efficiently immobilized by proteins concentrated within immobilized synaptic protein clusters. These are typically membrane-proximal scaffolds which can be directly attached to the intracellular face of the surface plasma membrane through post-translational modifications (Topinka et al., 1998; Craven et al., 1999). PSD-95 is a prominent example of an AMPAR scaffold, and in mature synapses is highly abundant. There are several families of scaffolds that possess many of the same motifs known as MAGUKs (Elias & Nicoll, 2007; Oliva et al., 2012; Zhu et al., 2016). Many of these MAGUKs have been found to act as scaffolds, helping to stabilize several molecules within the PSD (Chen et al., 2015). Immobilized scaffolding molecules exist within the PSD and help stabilize AMPARs as they enter the PSD (Bats et al., 2007; Barrera-Ocampo & Chater, 2013). Notable scaffolds such as PSD-95, GKAP, AKAP, Shank3, and Homer1 also exhibit varied subsynaptic distributions within the PSD, forming nanometer scale subdomains (MacGillavry et al., 2013; Nair et al., 2013; Fukata et al., 2013; Tang et al., 2016; Purkey et al., 2018). It remains unknown exactly how many abundant scaffolding molecules are organized laterally within synapses especially relative to other scaffolds, or their exact affinities for the TARP-AMPAR complex (Deng et al., 2006; Sainlos et al., 2010; Mastro et al., 2017; Zeng et al., 2019). The combination of scaffolding molecules' lateral distribution and relative affinities for the TARP-AMPAR complex likely influences how AMPARs traverse the PSD, where they become immobilized, and how long the receptors dwell at those subsynaptic positions. The

determination of this positioning in relationship to sites of neurotransmitter release may control receptor activation and influence basal transmission or plasticity.

Beyond the lateral organization of specific scaffolding molecules, scaffold organization further from the plasma membrane may inform us about their ability to influence AMPAR mobility or stable positioning, even if indirectly through the control of other scaffolds. Proteins like PSD-95 which bind to the TARP-AMPAR complex and are associated with the membrane directly through myristoylation will most directly influence AMPAR lateral mobility. Alternatively, cytosolic Homer1, which associates with Shank much deeper in the PSD (Hayashi et al., 2009; Dani et al., 2010), is less likely to directly influence the mobility of receptors but may be important for organizing other synaptic scaffolds that can more directly influence receptor mobility. These direct protein interactors that are deeper axially also exhibit similar heterogenous distribution to that of AMPARs, and other membrane-associated scaffolds, creating axial columns of protein-rich substructures (Tang et al., 2016).

Scaffolding molecules within the postsynaptic density exhibit heterogenous distributions similar to those of AMPAR nanodomains (MacGillavry et al., 2013). These molecules are known to help immobilize AMPARs (Bats et al., 2007). It has been suggested that the lateral organization of these scaffolding molecules instruct the subsynaptic positioning of AMPARs by acting to immobilize them (MacGillavry et al., 2013), and that this nanoscale organization is important for synaptic function. The subsynaptic organization of many postsynaptic scaffolding molecules that can interface with the TARP-AMPAR complex may be important for AMPAR positioning. However, it is not well understood how their relative affinities influence immobilization of AMPARs.

Thus, the mechanisms which control the postsynaptic distribution of AMPARs are not well understood. Factors beyond postsynaptic scaffolding molecules' nano-organization and intracellular affinity for TARP-AMPAR complexes may be responsible for the subsynaptic positioning of AMPARs.

## Section 7. The trans-synaptic arrangement of neurotransmitter release sites and postsynaptic receptors

In mammalian brain, presynaptic sites of glutamate exocytosis as marked by RIM nanoclusters are in fact aligned with postsynaptic nanoclusters of AMPARs across the cleft in an organization referred to as a nanocolumn (Tang et al., 2016). If receptor distance to the site of neurotransmitter exocytosis regulates receptor activation, then this aligned organization likely enhances basal excitatory synaptic transmission, and its disruption would reduce synaptic strength. This is important to determine, since modulation of transsynaptic alignment then would open a number of different mechanisms of synaptic plasticity. It remains unclear how subsynaptic alignment of receptor clusters with release sites is created or maintained. In Section 7, I will first discuss the evidence for the nanoscale alignment of neurotransmitter receptors to sites of neurotransmitter release (Section 7.1), the functional consequences of this organization for synaptic transmission (Section 7.2), and the potential molecular mechanisms of trans-synaptic nano-alignment (Section 7.3). Once established, I will discuss my hypothesis and experimental approach (Section 7.4).

### 7.1 Evidence for the alignment of neurotransmitter receptors to sites of release

Using single molecule imaging and new analyses of protein distributions, Tang et al. (2016) were able to quantify how the subsynaptic distribution of proteins were related in 3D space. This analysis revealed for the first time that nanoclusters of scaffolds in the AZ and PSD, RIM and PSD-95, respectively, were trans-synaptically aligned across the cleft. Importantly, the local density of RIM was found to be predictive of sites of evoked

neurotransmitter exocytosis (Tang et al., 2016), and these postsynaptic scaffolds, especially PSD-95 are known to immobilize AMPARs (Bats et al., 2007). Tang et al. quantified whether AMPARs were also enriched within this trans-synaptic nanocolumn, and indeed the local density of RIM within the AZ was predictive of the density of AMPARs across the cleft. Thus, AMPARs are concentrated directly across from preferential sites of evoked release (Tang et al., 2016). Not only do the AZ and PSD exhibit patterned distributions of molecules, but these molecules are enriched with one another across the cleft. Studies using flash-and-freeze electron microscopy, Li et al. (2021) independently found AMPARs were aligned across from sites of release. Flash-and-freeze allows for cryo-fixation milliseconds after optogenetic stimulation of terminals allowing ultrastructural analysis of synapses during different modes of transmission (Watanabe et al., 2013). Li et al. discovered that distinct modes of neurotransmitter synchronous and asynchronous release occurred with different lateral patterns the active zone. Using a new method to visualize AMPARs by EM, they were able to combine this flash-and-freeze approach and relate vesicle release positions to the postsynaptic distribution of AMPARs. Li et al. found that AMPARs were trans-synaptically aligned to sites of synchronous vesicle fusion (Li et al., 2021).

Quantifications of synaptic nanostructure using cryogenic electron microscopy (cryo-ET) has further established that the trans-synaptic arrangement of synaptic vesicles relates to cleft and postsynaptic protein distributions (Martinez-Sanchez et al., 2021). Martinez-Sanchez et al. found that synaptic AMPARs and “tethers” in the cleft are aligned with synaptic vesicles within individual synapses in a tri-partite complex. The molecules that establish this tripartite trans-synaptic complex were not known, other than they may be mediated by the “tethers” in the cleft (Martinez-Sanchez et al., 2021). Evidence for cleft

proteins acting as tethers in controlling AMPAR cluster position relative to RIM clusters has been reported (Haas et al., 2018). It was suggested that NL-1 controls the pre-to-postsynaptic alignment of AMPARs to RIM clusters at submicron distances. Similarly, disruption of the LGI1-ADAM22-MAGUK complex in the synaptic cleft led to increased distances between RIM and PSD-95 at submicron scales (Fukata et al., 2021).

Inhibitory synapses also exhibit the nanoscale trans-synaptic alignment of receptors to RIM nanodomains (Crosby et al., 2019; Yang et al., 2021). Using structured illumination microscopy, Crosby et al. identified subsynaptic domains of $GABA_A$Rs aligned across from RIM nanodomains. In response to elevated activity, the number of these inhibitory subsynaptic domains increased, and maintained alignment across the cleft. Gephyrin was also found to be enriched in this trans-synaptic organization and stabilized $GABA_A$Rs clusters within this trans-synaptic organization (Crosby et al., 2019). It was discovered that glycinergic (GlyRs) and GABAergic receptors ($GABA_A$Rs) at mixed inhibitory PSDs were trans-synaptically aligned with RIM nanodomains and could even occupy non-overlapping subsynaptic domains (Yang et al., 2021). Elevated activity levels led to reduced clustering of $GABA_A$Rs, while the clustering of GlyRs was unaffected (Yang et al., 2021). Several receptor types are capable of being aligned at the nanoscale with sites of neurotransmitter release as marked by RIM.

Many types of neurotransmitter receptors form subsynaptic clusters. Neurotransmitter release preferentially occurs over RIM nanodomains. These receptor nanodomains and RIM nanodomains are aligned across the cleft, aligning receptors at the nanoscale to sites of release. Changes to nanodomain properties and nano-alignment alter synaptic function, as suggested from the examples above. However, functional tests of the

distance-dependence of AMPARs at intact synapses has not been performed, making conclusions regarding the sensitivity of synaptic transmission to this nanostructural organization unclear.

## 7.2 Numerical models predict that nano-alignment impacts synaptic strength

Prior numerical models suggest that the density of glutamate receptors relative to sites of release influences receptor activation (Raghavachari & Lisman et al., 2004). Whether the postsynaptic distribution of AMPARs across from sites of evoked neurotransmitter release impacts transmission in synapses is not known. Importantly, the mechanisms which establish and maintain this trans-synaptic organization are also not well understood, limiting our ability to make causal conclusions about whether AMPAR nano-organization impacts postsynaptic receptor activation. However, many models suggest that the distance of AMPARs to sites of glutamate exocytosis influence the likelihood of their activation.

As discussed in Section 3, Glutamate release in the cleft is brief and the highest local concentration experienced by receptors only activates a fraction of total synaptic glutamate receptors (Holmes et al., 1995; Ishikawa et al., 1999; Liu et al., 1999; McAllister & Stevens, 2000; Raghavachari & Lisman, 2004). Receptor clusters displaced from sites of neurotransmitter exocytosis are expected to open with a distance-dependent probability, which exhibits a dramatic drop-off (Uteshev & Pennefather, 1996). This drop-off is driven by a number of biophysical factors discussed in Section 3 of this thesis. Only ~50 of 100 uniformly spaced receptors are expected to open when placed 10 nm apart (about the width

of the receptor) on a rectangular grid following the release of 2,000 glutamate molecules over the center of the grid. Increasing the spacing between receptors by 4-fold leads to a further 50% reduction in channel open probability with only ~30% of PSD receptors opening (Wahl et al., 1996). Other models found that an AMPAR displaced by 100 nm from the presynaptic release site would generate a response 32% of a receptor directly across from the site of release, and the response of receptors as far away as 200 nm would almost be undetectable. This distance-dependent activation of postsynaptic receptors has been posited as a mechanism to strengthen AMPAR-mediated transmission following short-term and long-term plasticity (Xie et al., 1997; Savtchenko & Rusakov, 2013). Interestingly, the coefficient of variation, a measure of the volatility of synaptic responses (discussed in detail in Discussion Section 6.5) appeared to increase as receptors were displaced from the site of neurotransmitter release (Franks et al., 2003). This is surprising because it suggests postsynaptic receptor positioning may influence a parameter thought to be dominated by presynaptic properties. In Raghavachari & Lisman (2004), upon a spike of glutamate in a cleft, it was observed that 80% of all opened channels were within 240 nm of the release site, nearly consistent with the measurements of Franks et al. (2003). About 35 channels of 100 were bound to glutamate, only 50% of which underwent channel opening. Of these receptors that underwent channel opening, only 30% were bound to 3 glutamate molecules. The number of bound glutamate molecules increases single-channel conductance (as discussed in Section 3), thus, receptors closest to the site of release are more likely to drive the postsynaptic response amplitude, and their positioning closer to sites of release may enhance postsynaptic strength (Raghavachari & Lisman, 2004). Numerical models that involve the diffusion of glutamate and AMPAR kinetics, with

varied spatial distributions of receptors, quite clearly demonstrate that the distance of AMPARs to sites of release has a strong impact on both the likelihood of activation, as well as the kinetics of activated AMPARs. Both the likelihood of activation and kinetics of AMPAR channel opening will robustly impact the strength of the postsynaptic response.

Biological predictions regarding how nanostructure influences the properties of synaptic transmission should be carefully considered. For instance, the comparison of the average distance of receptors to release sites across two independent synaptic configurations of nano-alignment may not matter if one has triple the number of receptors of that of the other synapse. Base receptor density must be accounted for in the estimation of the cumulative receptor activation. While easy to control for in experimental models, these properties must be considered in biological experiments investigating the impact of nano-alignment of synaptic function. Several parameters may act to make nanostructural alignment less impactful. For example, a synapse with a greater average distance of receptors to neurotransmitter release sites may be just as strong in response to single vesicle release if the neurotransmitter-containing vesicles in the active zone contain significantly more glutamate. More theoretically, changes in the channel kinetics of synaptic AMPARs to have a higher affinity for glutamate may obviate any functional sensitivity to nanostructure, leaving only the number of receptors to determine postsynaptic strength. The balance of the biophysical parameters, previously discussed to impact AMPAR activation, enable the strength of transmission to be tuned by average receptor distance from sites of neurotransmitter release.

## 7.3 Hypothesis and experimental approach

Postsynaptic nanodomains of AMPARs are trans-synaptically aligned with RIM nanodomains. Evoked release preferentially takes place within RIM nanodomains. Therefore, AMPARs are aligned at the nanoscale to sites of evoked neurotransmitter release. The distance of AMPARs from sites of glutamate exocytosis is expected to influence AMPAR activation and postsynaptic strength. Thus, this trans-synaptic organization likely enhances the strength of the AMPAR-mediated component of basal synaptic transmission.

Mechanistic tests of AMPAR nano-alignment and the distance-dependence of AMPAR activation have as of yet only been performed using computer simulations. Our hypothesis is that AMPAR alignment to sites of evoked release at the nanoscale is important for AMPAR activation in basal glutamatergic transmission in neurons. In order to test this fundamental mechanism we must disrupt this organization in a way that rearranges AMPARs so that they are further from sites of neurotransmitter release, however the mechanisms that specifically position subsynaptic AMPARs across from sites of evoked release is not known. While more gross disruptions of AMPAR clustering or mobility may influence trans-synaptic nano-alignment, it does not always allow us to disambiguate the relative influences of AMPAR number from AMPAR positioning on synaptic strength. Thus, much consideration was given to which mechanisms are most likely involved in AMPAR nano-alignment to sites of evoked release.

## 7.4 Potential mechanisms of trans-synaptic nano-alignment

There are many potential mechanisms that could bring these molecular assemblies within close proximity across the synapse. As so few details are known about how this organization is achieved, the list of potential mechanisms remains quite broad. It is possible that diffusible signals traverse the cleft to induce clustering, receptors or other ion channels that reach into the cleft may help to bind other cleft-resident molecules from the pre- or postsynaptic membrane, and synaptic cell adhesion molecules may act in a similar manner through their protein-protein interactions (Figure 1; Taken from Biederer et al., 2017).

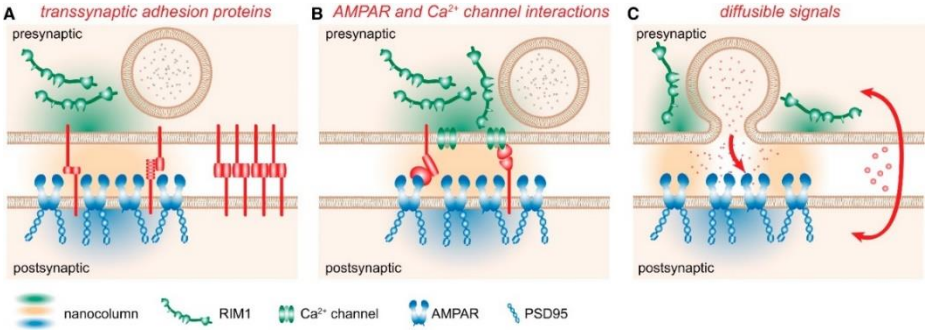


**Figure 1. Mechanisms of trans-synaptic nano-alignment from Biederer et al. (2017).** A) Schematic demonstrating the trans-synaptic interactions of synaptic cell adhesion molecules, B) AMPAR and Ca2+ channel interactions, and C) diffusible signals.

### 7.4.1 Diffusible signals

One way that the active zone could induce clustering in the postsynaptic density is through diffusible signals, where diffusible molecules are generated in the active zone and can traverse the cleft and postsynaptic membrane. This could happen because the signaling molecule is either cell-permeable or packaged in vesicles and released binding to cognate receptors that lead to local signaling. Many secreted, diffusible molecules can play a role in synapse formation or the stabilization of small dendritic protrusions. One issue that some

have raised is that these diffusible signals may act over longer distances than what would be required to maintain specific synaptic input, let alone directing nanostructure, but the range of action of these diffusible signals is not entirely understood (McAllister et al., 2007; Craig et al., 2006; Waites et al., 2005). Furthermore, it is possible that these diffusible signals are co-packaged with glutamate itself, which may help to control protein organization within close proximity to sites of neurotransmitter exocytosis (McAllister et al., 2007), where their local concentration would be at its peak before equilibrating in the extracellular space. One recent example in support of this idea is the secreted glycoprotein protein Noelin-1, which has been shown to bind AMPARs directly, limiting their synaptic mobility, and impacting short term plasticity (Pandya et al., 2018).

### 7.4.2 Contact between membrane proteins

A number of ion channels may also be involved in coordinating the trans-synaptic clustering and alignment of proteins. A prime example would be presynaptic calcium channels themselves, which are known in some cases to be tethered directly to neurotransmitter-containing vesicles through a number of scaffolding proteins. If calcium channels could bind to postsynaptic components, this would provide direct coordination of vesicles to postsynaptic receptors. One way this could be achieved is through the alpha subunit of calcium channels, α2δ (Dolphin et al., 2013), which is known, again, to be important for synaptogenesis and targeting axons to PSDs. This α2δ subunit may help to bridge calcium channels in complex with vesicles and potentially cluster postsynaptic proteins that may similarly influence how AMPARs are patterned within the PSD. Alternatively, α2δ has been shown to interact with many components of the extracellular

matrix, which may shape how the cleft is arranged and how AMPARs experience steric hindrance in the cleft (El-Awaad et al,, 2019).

AMPARs extend quite deep in the cleft, nearly 12 nm towards the active zone only 20 nm away (Sobolevsky et al., 2009), and bind to cleft proteins involved in calcium channel recruitment and release probability (O'Brien et al., 1998; Hoppa et al., 2012). AMPARs are known to bind to a number of different molecules (Bissen et al., 2019; Greger et al., 2017; Schwenk et al., 2012), and perhaps most notably PSD-95 through their association with TARPs (Rouach et al., 2005; Nicoll et al., 2006). Interactions with presynaptic transmembrane release machinery, or other release-associated molecules in the presynaptic membrane are limited to few known interactions. Of note, however, neuronal pentraxins are known to bind directly to AMPAR subunits, in addition to presynaptic C1q (Stevens et al., 2007). In addition to this, the neuronal pentraxins have been shown to form multimers, which would satisfy both a mechanism for trans-synaptic control and clustering of AMPARs (Kirkpatrick et al., 2000; O'Brien et al., 1999; Xu et al., 2003). However, AMPARs themselves are highly mobile, perhaps suggesting they depend on immobilized structures for their subsynaptic positioning, where subunit composition and auxiliary association likely contribute to which proteins they interact with.

Synaptic cell adhesion molecules are strong candidates to coordinate the positioning of AMPARs across from sites of neurotransmitter release. Despite their role in synaptogenesis, many synaptic adhesions are expressed and localized to synapses even much later in development, though their particular roles in established synapses are not well understood. There are several exciting candidates that may control the localization of glutamate receptors through their protein-protein interactions. For instance, EphB2 is

known to directly influence NMDAR mobility within synapses through specific residues (Washburn et al., 2020). Other cell adhesions like neuroligin-1 bind to a set of neurexins and their heparan sulfate attachments and is known to control AMPAR mobility through C-terminal interactions with PSD-95 (Mondin et al., 2011; Haas et al., 2018). Thus, through a set of indirect interactions with glutamate receptors themselves, synaptic cell adhesion molecules may be able to coordinate pre- and postsynaptic protein nano-organization.

Many potential molecules in all three synaptic compartments may act in unique ways as central coordinators that mediate receptor alignment to sites of neurotransmitter release. Calcium channel subunits in the active zone, secreted factors such as the neuronal pentraxins and noelin-1, and even diffusible signals co-packaged with glutamate may instruct protein nano-organization. Determining the relative contributions of all of these molecules in protein nano-organization will be important, and testing each potential mechanism will present specific challenges, and for this reason prioritizing the most likely candidates is a valuable endeavor.

## Section 8. Synaptic cell adhesion molecules as a transcellular structural linkage

### 8.1 Cell adhesion molecule general classes and functions

The trans-synaptic interactions of synaptic cell adhesion molecules may provide a transcellular structural linkage between pre- and postsynaptic nanodomains. CAM families are large, the roles they play are diverse, and the family members exhibit substantial redundancy upon knockout. Cell adhesion molecules are transmembrane proteins expressed on the cell surface and bind to other molecules on the surface of other cellular or non-cellular material, providing adhesion (Missler et al., 2012). Notably in neurons, cell adhesion molecules are important for establishing and maintaining cell-cell contact. Perhaps even more famously, *synaptic* cell adhesion molecules (Akins et al., 2006; Biederer et al., 2002) help to established axo-dendritic contact. This involves the accumulation of synaptic proteins at focal sites, which facilitates the formation of synapses, a process known as synaptogenesis (Irie et al., 1997). Many cell adhesion molecules are transcribed and translated as Type I membrane proteins. Commonly contained within these molecules are familiar motifs such as IgG domains, cadherin domains, fibronectin domains, and LNS domains (Missler et al., 2012). Synaptic CAMs have also been classified as mostly belonging to four unique groups, which include integrins, the immunoglobulin superfamily, cadherins, and neurexin/neuroligins (Benson et al., 2000). But recently, LRR-containing proteins gained attention as they make up several families of cell adhesion molecules commonly found at synapses, have roles in synapse formation, and bind to many molecules central to synapse function (Linhoff et al., 2009; Ko et al., 2012).

The trans-synaptic neurexin-neuroligin interaction has perhaps been studied in the most detail at mammalian synapses. However, an increasing number of trans-synaptic

partners are being identified as important for synapse formation, input specificity, basal synaptic transmission, and synaptic plasticity. For instance, FLRTs, SlitRKs, SALMs, EphB2, NGL, integrins and cadherins have been found to reside within synapses, and similarly bind to a partner located within the active zone (Sando et al., 2019; Ko et al., 2012; Um et al., 2014; Hruska et al., 2012; Mortillo et al., 2011). Interestingly, some CAMs associate with synaptic structures but are most commonly found at the edge, or perimeter, of synapses, such as, SynCAM1 at excitatory synapses or Cadherin-10 at inhibitory synapses (Biederer et al., 2002; Smith et al., 2017). For some time, it has been thought that synaptic CAMs are not only important for synapse formation, but that even in established synapses they play roles in regulating synaptic plasticity in support of learning and memory processes (Benson et al., 2000). Recent work has highlighted a novel neurexin ligand, Leucine Rich Repeat Transmembrane neuronal 2, or LRRTM2 (Linhoff et al., 2009), and has gained attention as it has been found to bind to a competing site where neuroligin-1 is also known to bind, and furthermore the binding of these two postsynaptic ligands is dependent upon the neurexin splice isoform at site 4 (Ichtchenko et al. 1995; Boucard et al., 2005; Siddiqui et al., 2010), perhaps suggesting some kind of differential trans-synaptic binding code. While the specific binding interactions at play may be complex, postsynaptic cell adhesion molecules that bind with neurexins may act as a structural mediators of trans-synaptic nano-alignment of receptors to sites of release.

## 8.2 Presynaptic neurexins and their role synapse function

Neurexins are single pass transmembrane proteins and notably consist of a series of LNS domains, though, this varies depending upon the splice isoform. α-Neurexins

consist of six LNS domains, and β-Neurexins are much smaller in size, and contain only a single LNS domain, which is identical to the sixth LNS domain contained within α-Neurexins. Neurexins are known to bind to a large number of postsynaptic ligands (Trotter et al., 2021, *bioRxiv*). In mammalian neurons, there are three genes that encode the neurexins: Nrxn1, Nrxn2, and Nrxn3, and these genes can be expressed by a number of different transcriptional promoters: α, β, γ (Gomez et al., 2021). Additionally, Neurexins have been shown to undergo extensive splicing (Ichtchenko et al., 1996; Chih et al., 2006; Rowen et al., 2002; Fuccillo et al., 2015). Neurexins are found at all synapses, but their location can be specific to their isoform, where it has been posited that specific neurexin isoforms instruct a code important for input specificity, but the details are not well-established (Siddiqui et al., 2010; Graf et al., 2004; Boucard et al., 2005).

Recently, it was discovered that neurexins can undergo a heparan sulfate modification, which classifies them as heparan sulfate proteoglycans (Condomitti & de Wit, 2018; Zhang et al., 2018). This is of interest, because other neurexin ligands were found to additionally bind to its heparan sulfate attachment at non-overlapping sites, increasing the valency of neurexin for these postsynaptic ligands (Yamagata et al., 2018). This opens up the opportunity for exploring other molecules already known to bind to heparan sulfates and examining whether these molecules interact with the heparan sulfate attachment of neurexins in a similar manner, determining their relative affinities.

Neurexins are synaptically enriched adhesion molecules (Chamma et al., 2016; Trotter et al., 2019). Interestingly, neurexins also demonstrate subsynaptic enrichment similar to scaffolds, receptors, and release machinery (Tang et al., 2016). However, it remains unknown whether neurexins are enriched within the trans-synaptic nanocolumn

structures observed in synapses. Neurexins have a C-terminal PDZ binding motif, which enables their binding to the presynaptic scaffolding molecule CASK (Hata et al., 1996), which forms a complex with calcium channels via Rab3a (Zhang et al., 2001), and even links neurexin to the neuronal cytoskeleton (Biederer & Sudhof, 2001). Furthermore, it has been shown that neurexins are also linked to Mints, which act as adaptors between neurexins and the priming factor Munc18 (Biederer & Sudhof. 2000; Tabuchi et al., 2002). Neurexins bind to a number of postsynaptic ligands, but perhaps the most well-studied are the neuroligin family and the LRRTM family proteins. Interestingly, binding with these two protein families is highly regulated by a single amino acid at splice site 4 (SS4) of neurexin, which can modify the affinity for neuroligin-1 and LRRTM2 (Siddiqui et al., 2010; Boucard et al., 2005). Not only do neurexins instruct the formation of synapses, but they also control presynaptic release probability by coupling $Ca^{2+}$ channels to synaptic vesicles (Missler et al., 2003). Neurexins enable synapse formation and proper synaptic function, but they may also relay important spatial information across the synaptic cleft which instructs the organization of key postsynaptic molecules.

## 8.3 The neurexin ligands Neuroligin-1 and LRRTM2 are key candidates in controlling AMPAR nano-alignment

Disruption of postsynaptic neuroligin-1 by expression of dominant negative mutants or prolonged incubation with interfering peptides does in fact alter receptor alignment with RIM, providing support for the idea. However, these extended treatments also prompt a complex set of other effects including altering synapse numbers, presynaptic vesicle release probability, and frequency of spontaneous transmission. The LRRTM

family are strong candidates to mediate transsynaptic alignment. A key abundant family member in hippocampus, LRRTM2, binds postsynaptic PSD-95 through a C-terminal motif and the presynaptic Neurexin-Heparan sulfate complex through 10 extracellular LRR repeats. LRRTM2 has been found to be important for evoked AMPAR-mediated, though not NMDAR-mediated, synaptic transmission independent of synaptogenesis. Furthermore, the extracellular domain of LRRTM2 alone is sufficient to rescue AMPAR-mediated synaptic transmission following LRRTM1,2 double knockout, a mechanism proposed to be achieved by altering AMPAR mobility in the PSD. LRRTM2 within synapses also forms nanoscale clusters of similar size to scaffold, receptor, and release machinery nanodomains.

## 8.4 LRRTM2 guides synapse formation by accumulating scaffolds and receptors

An unbiased screen of synaptogenic proteins revealed a novel neurexin ligand, LRRTM2, important for the recruitment of synaptic proteins through synaptogenesis, and which is highly expressed in mammalian hippocampus (Lauren et al., 2003; Linhoff et al., 2009). LRRTM2 was proposed to recruit these synaptic proteins through a C-terminal ECEV motif. Interestingly, beyond inducing VGluT1 accumulation, it was found to cluster functional postsynaptic sites of receptor activation in a co-culture assay, from which whole-cell recordings demonstrated the establishment of functional sites of neurotransmitter release.

In neurons, knockdown of LRRTM2 was shown to decrease the number of excitatory, but not inhibitory, synapses as shown by confocal imaging of immunostained

GluA1 and the scaffold PSD-95 (de Wit et al., 2009). Furthermore, coimmunoprecipitation of LRRTM mutants and AMPAR subunits and PSD-95 demonstrated that the extracellular domain of LRRTM2 was important for binding with both GluA1 and GluA2 subunits of AMPAR complexes. In addition to this, deletion of the predicted PDZ binding motif, prevent coimmunoprecipitation of LRRTM2 and PSD-95 in heterologous cells. Taken together, it seems that LRRTM2 not only induces presynaptic differentiation, but suggests it may be doing more to organize postsynaptic complexes. Beyond this, LRRTM2 was confirmed to be a neurexin ligand through mass spectrometry, soluble protein binding assays, and coimmunoprecipitation.

It was also demonstrated that LRRTM2 fails to bind to neurexins containing a single amino acid insert at splice site 4 of the $6^{th}$ LNS domain of neurexins, thus differentiating it from neuroligin-1 which binds to SS4+ and SS4- neurexins (Figure 2; Ko et al., 2009). This provided new evidence for the unique regulation of neuroligin-1 and LRRTM2, either with regard to synapse formation, or their organization of the postsynaptic density. In addition to this single point of regulation, detailed examination of the binding interactions between neurexins and neurexin ligands revealed that not only is SS4 critical for determining neurexins trans-synaptic binding interactions, but additionally that neuroligin-1 preferably interacts with only β-neurexins, whereas LRRTM2 binds to both α- and β-neurexins, as long as they were SS4- (Siddiqui et al., 2010). These findings refined a differential code by which neurexins and neurexin ligands will bind, depending on neurexin splice isoform. Furthermore, through these experiments, the binding surface between LRRTM2 and neurexins was established. Of note, it was also found that neuroligin-1 and LRRTM2 bind to the same surface on neurexins, thus establishing a

competitive interaction between these two ligands, perhaps suggesting that copy number or their postsynaptic distribution relative to neurexins may influence the degree to which they interact.

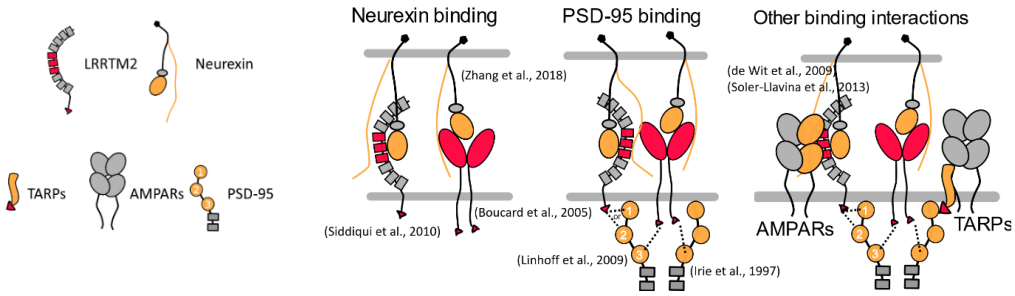


**Figure 2. The trans-synaptic interactions of LRRTM2 and Neuroligin-1.** Molecule list, left. Red indicates the postsynaptic cell adhesion molecule surface that has been implicated in protein binding, while orange indicates other protein surfaces that are important for these interactions.

## 8.5 Roles beyond synaptogenesis – LRRTM2 control of AMPARs in mature synapses

Given these unique rules for binding, and the potential for the segregation of various synaptic functions, Soler-Llavina et al. (2011) performed loss-of-function experiments targeting LRRTM1, LRRTM2, neuroligin-1, and neuroligin-3 at various developmental stages (before and after synapse formation) in order to determine whether they play similar roles *in vivo*. They found that elimination of the neuroligins at excitatory synapses had no effect on excitatory transmission during synaptogenesis but did impact transmission at later developmental stages. Interestingly, they found that LRRTM loss early on impacted AMPAR-mediated transmission but had no effect at later developmental stages (P21), perhaps suggesting an earlier role in synapse formation (Figure 3). Thus, in established synapses it seems that neuroligins and LRRTMs play divergent roles at the synapse.

However, further experiments indicated that LRRTM2 alone was necessary for the expression of LTP, even at later developmental stages (Figure 3; Soler-Llavina et al., 2013). It was suggested that this was not through LRRTM2's synaptogenic functions, but it was instead put forward that because AMPARs exocytosed after LTP are unable to be incorporated readily into synapses, perhaps suggesting LRRTM2 acts as an AMPAR anchor. Thus, the presence of LRRTM2 is better able to accommodate and stabilize an increased number of receptors.

Additional evidence demonstrated that Neurexin-3 was important for the surface stability of LRRTM2 and consequently AMPARs, but not neuroligin-1 (Aoto et al., 2013). This was observed following the constitutive inclusion of a single amino acid at SS4, which is known to significantly reduce Neurexin's affinity for the postsynaptic ligand LRRTM2, but not neuroligin-1. With the incorporation at SS4 of neurexin-3α, this led to reduced surface levels of LRRTM2, and the GluA1- and GluA2- containing AMPARs, both in their synapse number and content at synapses. Indirectly suggesting that LRRTM2 helps to link AMPARs with presynaptic neurexins, perhaps controlling their lateral mobility and synaptic incorporation, or even their nanoscale organization.

Further evidence for LRRTM2 in the control of AMPAR mobility comes from Bhouri et al. (2018), where LRRTM1 and LRRTM2 were conditionally knocked out following synapse formation. This manipulation recapitulated earlier findings where the AMPAR-mediated evoked currents were dramatically reduced in basal transmission, and the expression of LTP was nearly completely abolished (Soler-Llavina et al., 2013). However, they also performed an AMPAR mobility assay, which consisted of expressing a photo-activatable GFP tag on the N-terminus of AMPAR subunits. This permits transient

labeling of current spine-resident AMPARs, and quantification of their slow escape from synapses over time is then possible in order to draw conclusions about their stability in synapses or general mobility. In LRRTM-lacking synapses, a fraction of AMPARs escaped from spines much more quickly, again consistent with the idea that LRRTMs are responsible for the synaptic retention and surface mobility of AMPAR complexes.

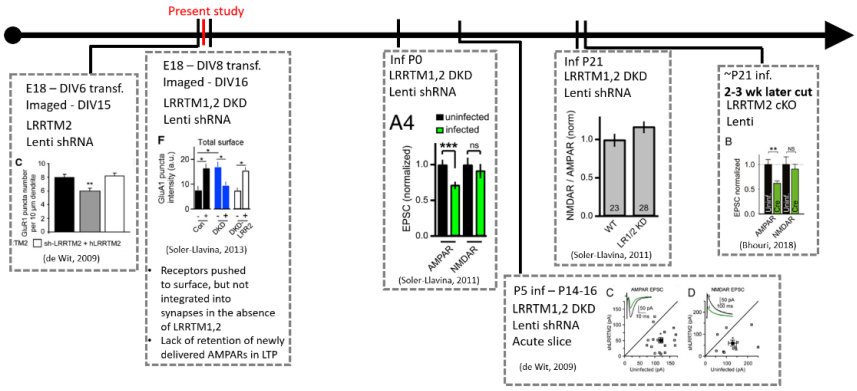


**Figure 3. Developmental time course of LRRTM2 perturbation and the effects of AMPAR-mediated transmission and synaptic organization.** X-axis represents age in development as indicated in the box by EXX, for embryonic cultures, or PXX, for intact ex-vivo slices or organotypic cultures. Red indicates the developmental stage at which the experiments in this thesis were conducted.

## 8.6 LRRTM2 is concentrated within subsynaptic nanodomains

This idea that LRRTM2 is perhaps controlling AMPAR mobility and perhaps even retention within synapses was an interesting observation, importantly because of its previously described nanoscale organization within synapses. Chamma et al. (2016a; 2016b) developed a novel method to label expressed LRRTM2 with a small tag, an effort to observe the nanoscale dynamics of the native protein more closely. They observed that LRRTM2 was much less mobile than neuroligin-1. Interestingly, though, they observed that LRRTM2 was highly synaptically enriched, and formed nanoscale clusters of a similar size to that of receptors, scaffolds, and release machinery (Tang et al., 2016). Thus, not

only might LRRTM2 influence AMPAR mobility, but it may do so in such a way that instructs its synaptic and subsynaptic position.

Not all synaptic cell adhesion molecules display this unique subsynaptic organization at synapses (Figure 4; Figure 5). SynCAM1, another synaptic cell adhesion molecule, has been shown to localize to peri-synaptic clouds, and it has been suggested that this may in some way contribute to its function (Perez de Arce et al., 2015; Cijsouw et al., 2018). Of course, there have been many other molecules that have been reported to localize towards the synapse periphery, such as NCAM180 and cadherin-10, but much of these reports are based on EM immunogold labeling, which does not produce a primary antibody labeling efficiency high enough to make strong conclusions, especially for low copy-number proteins.

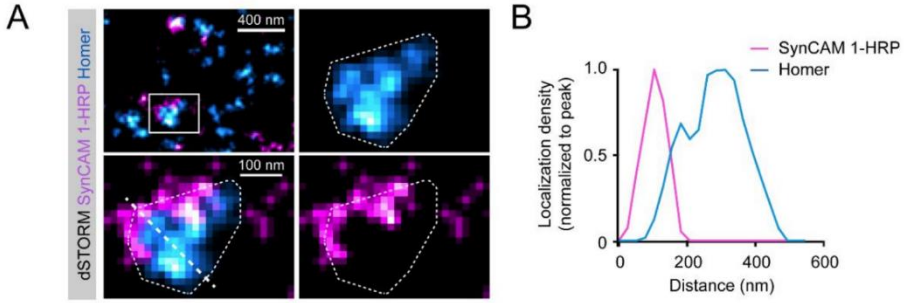


**Figure 4. Unique subsynaptic distributions of cell adhesion molecules.** Taken from Cijsouw et al. (2018). SynCAM1 (magenta) localizes to the edge of synapses as defined by Homer1 (cyan) via dSTORM. Right, line scan indicated in Panel A demonstrating the lateral organization of SynCAM1 relative to Homer1.

Consistent with this notion of trans-synaptic control of AMPAR mobility by the Neurexin-LRRTM2 complex was the finding that endogenous neurexins also display a tight subsynaptic distribution which can be co-enriched with postsynaptic receptors (Trotter et al., 2019). However, it still remains to be seen how the variety of neurexin splice

isoforms influence their number and position within synapses, and which subset are important in controlling synaptic AMPAR dynamics. New techniques are being applied for the endogenous labeling of many CAMs, allowing their visualization by single-molecule imaging techniques. For instance, Klatt et al. (2021) were able to knock-in a N-terminal GFP selectively in β-neurexins, permitting its endogenous detection. Interestingly, they found that β-neurexins were abundant at extrasynaptic sites, they were highly mobile on the cell surface, though, transiently confined at synaptic sites, and their mobility was modulated by activity. Imaging of endogenous molecules will be very important especially in consideration of synaptic CAMs, where overexpression artifacts are present in many other approaches, and protein copy number is expected to be important in the maintenance and formation of clusters.

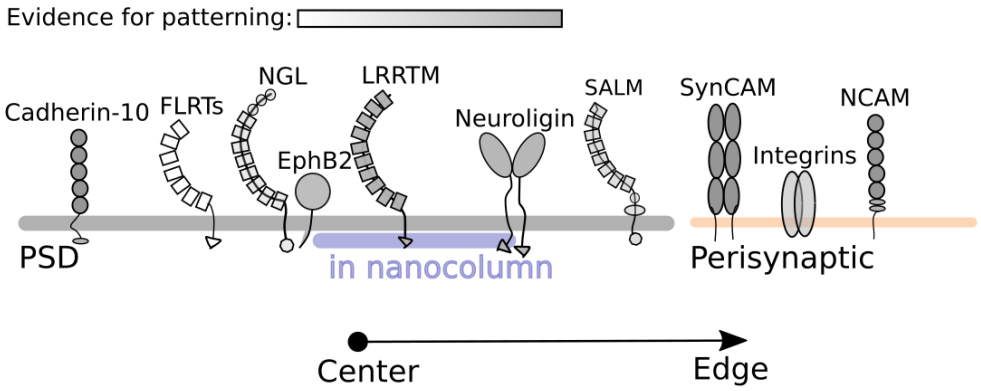


**Figure 5. The lateral postsynaptic distribution of synaptic cell adhesion molecules.** A summary of findings (both qualitative, light grey, and quantitative, dark grey) from electron microscopy immunogold labeling of various CAMs and other super-resolution imaging of CAMs.

Despite this collection of evidence that the LRRTM2-Neurexin complex mediates synaptic AMPAR dynamics and synaptic function, other trans-synaptic complexes are also thought to contribute to these complex processes. Disruption of the LGI1-ADAM22-

MAGUK complex was shown to decrease scaffold nano-alignment and contribute to the generation of epileptic seizures (Fukata et al., 2021). Additionally, the presynaptic CAM, PTPσ, has been shown to form a tripartite complex with Glypican-4, LRRTM4, and AMPARs, which is important for controlling their synaptic enrichment, perhaps acting as an AMPAR anchor (de Wit et al., 2013; Siddiqui et al., 2013; Farhy-Tselnicker et al., 2017; Ko et al., 2015; Roppongi et al., 2020).

My hypothesis is that the subsynaptic positioning of AMPARs across from sites of evoked neurotransmitter release is controlled by the cell adhesion molecule LRRTM2. Long-term manipulations can prompt substantial reorganization of synapses which makes deducing the native state difficult. To test the role of LRRTM2 while avoiding such effects, I used acute extracellular proteolysis of an engineered cleavage site to disrupt its extracellular interactions within seconds, thus uncoupling it from the postsynaptic membrane while avoiding complications of genetic compensation. With this approach, I found that LRRTM2 acutely controls the fine positioning of AMPARs relative to the site of release. The repositioning of AMPARs following loss of the LRRTM2 extracellular domain leads to reduction in the amplitude of evoked but not spontaneous responses. Further, the basal distribution of LRRTM2 is in nanoscale register with both RIM and AMPAR nanodomains. Together, these data suggest that postsynaptic LRRTM2 establishes a transcellular, structural linkage mediating nanocolumn alignment of AMPARs with preferential sites of evoked neurotransmitter release and provide strong evidence that AMPAR organization within the synapse is critical for the strength of basal synaptic transmission.

## CHAPTER 2: Methods

### Plasmids

All LRRTM2 plasmids were generated based on FCK-shLRRTM2 and pBOS-GFP-hLRRTM2-FL described previously (de Wit et al., 2009). For insertion of the thrombin cleavage site, the sequence coding the four Ser's (S386-S389) was replaced with a sequence coding the cleavage site (LVPRGS) with a flexible linker (GGGGS) on each side. For knockdown-rescue experiments in neurons, the H1 promoter and sh-LRRTM2 sequences from FCK-shLRRTM2 were subcloned into the pBOS-GFP-hLRRTM2-FL around the MluI site with IVA cloning (Biederer & Schieffele, 2007). For BRS-LRRTM2, GFP sequence was replaced with a sequence coding the α-bungarotoxin-binding sequence (WRYYESSLEPYPD; (Sekine-Aizawa et al., 2004)). GFP-Neuroligin1 and GFP-Neuroligin1-Thr were kind gifts from Michael Ehlers (Peixoto et al., 2012).

### Co-culture synaptogenesis assay

Co-culture assays were performed as described (Fukumoto et al., 2010). Briefly, neurons were dissociated from embryonic day 18 Sprague-Dawley rat hippocampi, plated at a density of 60,000 cells on 12 mm cover glasses pre-coated with 1 mg/ml poly-l-lysine (Sigma, P1274), and treated at 2 div for 24 with Ara-C (2 µM) to prevent glial growth. Neurons were cultured in Neurobasal medium (Invitrogen 21103-049) with 3% B27 (Invitrogen, 17504-001) and 1% Glutamax (Invitrogen, 35050-061) and incubated at 37°C in 5% CO2. When neurons reached 7 div, 70% confluent HEK293 cells were transfected using polyethylenimine in 6 well dishes at approximately 0.4 picomol plasmid per 9.5 cm2

well (Frost et al., 2010). Transfected HEK293 cells were suspended 24 h later and seeded onto 8 div neurons at a density of 5,000 HEK cells per 12 mm cover glass. Ara-C was added at 2 μM upon seeding to prevent HEK cell overgrowth. After 48 h, co-cultures were fixed on 10 div with 4% PFA, 4% sucrose in PBS, stained with primary antibodies diluted in 3% fetal bovine serum (FBS) and 0.01% Triton-X 100 in PBS, and incubated overnight at 4°C. Secondary antibodies were diluted in 3% FBS and applied for 4 hours at 4°C. Neuronal cultures were stained with mouse monoclonal antibodies against Bassoon (AssayDesigns Cat# VAM-PS003F, RRID: AB_2313991; 1:500) and BTX-Alexa-647. Secondary immunostaining was performed with Alexa dye-conjugated antibodies. Coverslips were mounted with Aqua/PolyMount (Fisher, NC9439247). Confocal microscopy was performed on a Leica TCS SP8. Images were acquired with an ACS APO 63x oil lens with 1.3 NA, using the same settings for each condition. During image acquisition and analysis, the researcher was blind to the condition. Images were analyzed using a custom written ImageJ script available upon request.

**Hippocampal Culture and Transfections**

All experimental protocols were approved by the University of Maryland School of Medicine Institutional Animal Care and Use Committee or the Institutional Animal Care and Use Committees at the University of Science and Technology of China (USTC) and the Chinese Academy of Sciences (CAS). Dissociated hippocampal neurons from E18 SD rats of both sexes were prepared as described previously (Frost et al., 2010). Neurons were transfected on DIV 7-10 with Lipofectamine 2000 and experiments were performed at least

7 days after the transfection (DIV 14–21). All experiments were repeated on 3 or more separate cultures unless otherwise specified.

**Immunocytochemistry**

Neurons were fixed in 4% paraformaldehyde, 4% sucrose in phosphate buffered saline (PBS) for 10 min at room temperature and processed for immunofluorescence with standard procedures as described previously (Tang et al., 2016). Primary antibodies were: rabbit anti-RIM1/2 (Synaptic System #140203, 1:500), mouse anti-PSD-95 (NeuroMab clone K28/43, 1:200), chicken anti-GFP (Chemicon ab13970, 1:200). Secondary antibodies were from Jackson ImmunoResearch (West Grove, PA), either already conjugated with Alexa 647 or unconjugated that we labelled with Cy3b (GE Healthcare). Labeling with the anti-GFP antibody was performed after fixation but prior to overt permeabilization.

Live cell α-bungarotoxin (BTX) recognition sequence (BRS) labeling with α-bungarotoxin conjugated to Alexa-647 was performed prior to fixation described above. Coverslips were inverted on 50 µl droplets of BTX-Alexa-647 (Thermofisher B35450, 1:100) in aCSF containing 2 mM Ca2+ and 2 mM Mg2+ and covered for 5 minutes at room temperature (21-24°C). Then, coverslips would be placed into a small weigh boat filled with aCSF, and gently agitated, removing and replacing the aCSF twice before mounting in the microscope imaging chamber.

For LRRTM2 and PSD-95 immunocytochemistry, neurons were fixed in 2% paraformaldehyde, 4% sucrose in cytoskeleton buffer (10 mM MES pH 6.8, 138 mM KCl,

3 mM MgCl2, 2 mM EGTA, 320 mM sucrose) for 8 minutes at room temperature. Coverslips were then washed 3 times for 5 minutes each with PBS/Gly. Cells were permeabilized with 0.3% TritonX-100 (TX-100) in PBS/Gly for 20 minutes at room temperature, then washed once in PBS/Gly with 0.1% TX-100 for 5 minutes. Blocking was performed with a solution containing 3% BSA, 5% goat serum, 5% donkey serum, and 0.1% TX-100 for 1 hour and 15 minutes. Coverslips were inverted and incubated with primary antibodies (αLRRTM2, IgG1A mouse, NeuroMab N209C/35.3, 1:10; αPSD-95, IgG2A, 1:80, stored in 50% glycerol) diluted in a 1:1 dilution of the blocking media and PBS/Gly overnight in a humidity chamber at 4°C. Coverslips were then washed 3x in PBS/Gly containing 0.1% TX-100 for 5 minutes. Secondaries (GαM IgG1A Alexa-647, Jackson, 115-605-205, Lot 143997, 1:200; DαM IgG2A, Jackson, Cat 20257, Lot 14C0225 1:200) were diluted in a 1:1 dilution of the blocking media and PBS/Gly and coverslips were inverted on secondary in a humidity chamber at room temperature for 1 hour. Then coverslips were washed 3x with PBS/Gly for 5 minutes. Cells were postfixed with 4% PFA, 4% sucrose in PBS for 15 minutes, then washed 3x with PBS/Gly for 5 minutes.

All imaging except for dSTORM and HEK co-culture assay was performed on an Andor Dragonfly spinning disk confocal on either an Olympus IX81 or a Nikon Ti2 microscope. In each case, a 60x/1.45 NA oil immersion objective and Zyla sCMOS camera were utilized, with image format of 103 nm/pixel. Except where indicated, experiments were conducted at room temperature (22-24°C). Otherwise, for imaging in culture medium, a stage-top incubator and objective heater (Tokai Hit) maintained the sample temperature at 37°C and CO2 at 5%.

**Proteolytic cleavage**

Thrombin from bovine plasma (Sigma, T4648-1KU, Lot # SLBV3604) was diluted in the imaging buffer (aCSF; 2 mM Ca2+, 2 mM Mg2+) at 100 Units per mL such that when added to the bath by pipette the final concentration became 10 Units per mL. Thrombin was added drop-wise away from the objective into the media containing cells in the imaging chamber at 24ºC. Thrombin was stored at -20ºC with a volume of at least 600 µl, and only underwent 1 freeze-thaw cycle. For imaging at 0.003 Hz, cells were maintained at 24ºC. Z-stacks were taken every 5 minutes, and a maximum intensity projection was used for analysis. For imaging at 20 Hz, cells were kept on the objective at 24ºC. Imaging was performed with 488 nm excitation during continuous acquisition at 20 Hz. Binning (2x2) permitted the identification of modestly expressing synaptic puncta at lowest possible laser power to prevent photobleaching. Exposure was 50 ms per frame. Data was smoothed with a sliding average window with a bin length of 3 frames (150 ms). For all experiments, chamber was thoroughly washed with deionized water and 70% ethanol accompanied by physical scrubbing in order to completely remove residual thrombin that can adhere to the plastics and rubber of the imaging chamber and O-ring. All synaptic ROI measurements were background subtracted and normalized to an average of each synapses own baseline.

**Quantification of protein retention at synapses**

Live (30 minute). Cells were co-transfected with GFP-Thr-LRRTM2* or BRS-Thr-LRRTM2* and PSD95-mCherry* or SEP-GluA1,2, respectively. For PSD-95 experiments, multiposition z-stacks were acquired every five min. For analysis, maximum intensity projections were calculated. ROIs of a fixed size (15 pixels) were drawn around synaptic

puncta containing both LRRTM2 and PSD95-mCherry* or SEP-GluA1/2 fluorescence. Integrated intensity was measured, background subtracted (an average of multiple ROIs across the field of view), then normalized to an average of the ROIs pre-thrombin baseline. Only spines that remained within the ROI for the duration of imaging were included.

Live (2 hour). Cells were co-transfected with SEP-GluA1,2 and BRS-LRRTM2* or BRS-Thr-LRRTM2*. Multiposition z-stacks were taken every 15 or 20 minutes. For analysis, maximum intensity projections were calculated. ROIs of a fixed size (25 pixels) were drawn around synaptic puncta containing both LRRTM2 and SEP-GluA1,2 fluorescence. Integrated intensity was measured, background subtracted (an average of multiple ROIs across the field of view), then normalized to an average of the ROIs pre-thrombin baseline. Only spines that remained within the ROI for the duration of imaging were included.

Fixed. Cells were co-transfected with GFP-Thr-LRRTM2* and mCerulean3. Cells were immunostained for PSD-95 and RIM1/2 as described above. All regions were acquired with the same imaging parameters on the Dragonfly confocal. For analysis, background subtracted (values taken from an average of multiple background regions across the field) integrated intensity within an ROI of a fixed size (15 pixels). Values were additionally normalized to the median intensity in the field which helped to normalize potential differences in any region to region variability in staining intensity. Normalization to median intensity did not appear to be skewed by artefactual puncta as these were avoided during acquisition or occupied a very small fraction of total pixels in the field.

24-hour post-thrombin. Cells were co-transfected with SEP-GluA1,2 and BRS-LRRTM2* or BRS-Thr-LRRTM2*. Both groups were treated with thrombin for 10 minutes and then returned to culture media. Then, 24 hours later cells were fixed and stained for GFP and

the BRS-tagged LRRTM2 ECD as described above. All regions were acquired with the same imaging parameters on the Dragonfly confocal spinning-disk (Andor). For analysis, maximum intensity projections were calculated. ROIs of a fixed size (15 pixels) were drawn around αGFP puncta. Integrated intensity was measured, routinely background subtracted (an average of multiple ROIs across the field of view).

**Quantification of PSD-95 puncta density**

Cells were transfected with cytosolic mCerulean3 alone or paired with either pBOS-shLRRTM2 (tgctattctactgcgactcde;(de Wit et al., 2009)), GFP-Thr-LRRTM2* (this paper), or pBOS-GFP-Thr-LRRTM2 (this paper). Cells were then fixed and immunostained for PSD-95 (described above). mCerulean fluorescence was used to demarcate the dendrites of transfected cells. Using mCerulean fluorescence alone, in order to remain blinded to the transfection condition, up to the first 6 transfected cells were selected for imaging and further analysis in order to reduce bias. Regions were chosen at least ~75 μm from the soma when dealing with a clear primary dendrite to avoid volume effects. Distance was calculated by drawing a line in ImageJ (total pixel number x pixel size). All images were thresholded the same. Each punctum had to consist of at least 4 suprathreshold pixels. Experimenter was blind to the condition during image analysis.

**Quantification of spine morphology**

Cells (DIV 4-6) were transfected with mCerulean3 alone or mCerulean3 paired with GFP-Thr-LRRTM2*. Cells were imaged at DIV 14-16. Maximum intensity projections of the

confocal stacks were analyzed in ImageJ by an observer blinded to conditions. Analysis between groups were always performed within the same culture. For spine length, a line was drawn from the edge of the spine head to the edge of the dendrite, parallel to the long axis of the spine (total pixel number x pixel size). For spine area, an ROI was drawn around the spine head. The images were thresholded based on intensity and area was measured in ImageJ. Experimenter was blind to the condition during image analysis.

**Colocalization analysis**

Cells were transfected with GFP-Thr-LRRTM2*. Synapses were picked based on colocalization with dendritic spines. Five consecutive spine-resident, GFP-positive puncta were selected randomly from at least 4 separate dendritic regions per cell when possible. When few branches were present, selection of dendritic regions of interest were as evenly distributed throughout the image as possible. The data represent the number of those randomly selected GFP-positive puncta which also contained at least 4 suprathreshold pixels of PSD-95 or RIM1/2 staining. Analysis was performed using ImageJ. Experimenter was blind during data analysis.

**3D-STORM imaging**

Imaging was performed essentially as described (Tang et al., 2016) on an Olympus IX81 ZDC2 inverted microscope with a 100×/1.49 TIRF oil-immersion objective. Excitation light was reflected to the sample via a 405/488/561/638 quad-band polychroic (Chroma) with an incident angle near but less than the critical angle. The typical incident power out

of objective was ~30 mW for 647 nm and ~60 mW for 561 nm. Emission was passed through an adaptive optics device (MicAO, Imagine Optic) which corrected the aberrations and introduced astigmatism for 3D imaging. A Photometrics DV2 was insert before an iXon+ 897 EM-CCD camera (Andor) for simultaneous collection of the red and far-red emissions. All hardware was controlled via iQ software (Andor), except the MicAO which was controlled via Micromanager. Z stability was maintained by the Olympus ZDC2 feedback positioning system. Imaging of NL1 experiments was carried out on a Nikon ECLIPSE Ti2 inverted microscope equipped with a perfect focusing system and an 100×/1.49 TIRF oil-immersion objective controlled with NIS-Elements AR 4.30.02 software; emission was collected with a CMOS camera (ORCA-Flash4.0, Hamamatsu); localization detection, calibration and drift correction were done using the NIS-Elements AR analysis 4.40.00 software. Lateral drift was corrected with a cross-correlation drift correction approach24. Samples were imaged in a STORM imaging buffer freshly made before experiments containing 50 mM Tris, 10 mM NaCl, 10% glucose, 0.5mg/ml glucose oxidase (Sigma), 40 μg/ml catalase (Sigma), and 0.1M cysteamine (Sigma). TetraSpeck beads (100 nm; Invitrogen) immobilized within a thin layer of 4% agarose on a coverslip were localized across a z-stack with 30-nm steps to get the 3D calibration and correct alignment between the two channels as described previously. The average deviation of the bead localizations after correction was <15 nm in x/y directions and 40–50 nm in z.

**Single-molecule localization and analysis of synaptic clusters**

All data analysis was performed offline using custom routines in MATLAB (Mathworks). The lateral (x, y) and axial (z) coordinates of single fluorophores were determined from the

centroid position and ellipticity of the fitted elliptical 2D Gaussian function to a 7×7 pixel array (pixel size 160 nm) surrounding the peak. Poorly localized peaks were removed with a set of rejection criteria including an x–y precision <10 nm, fitting R2 > 0.6, and comprising >200 photons, and the shape of peaks24. For peaks lasting for more than one frames, only the localizations in the first frame were included in further analysis.

Synapses were identified as a juxtaposed pair of localization clusters of synaptic proteins and only those with clear pre- and postsynaptic components were selected for further analysis. A DB-SCAN filter was applied to the selected synaptic localizations with MATLAB function 'DBSCAN.m' created by S. M. K. Heris to define the boundaries of synaptic clusters. Only those localizations with a minimum of 60 localizations (MinPts = 60) within a radius of 5 times mean nearest neighboring distance (epsilon = 5 x MNND ≈ 100-120 nm) were considered within the synaptic cluster. The cluster boundaries were defined by an alpha-shape with $\alpha = 150$ nm.

**Nanocluster detection and protein enrichment analysis**

Nanoclusters within synaptic clusters were automatically identified based on local densities defined as the number of localizations within a certain distance (d) from each localization. To account for the variation in localization density across different synaptic clusters, we defined d as $2.5_{x}$ MNND instead of a fixed value (78). The threshold of local density for nanocluster detection was defined as Mean(LD0) + 4 x Std(LD0), where LD0 is the local density of a randomized cluster with the same overall density as the synaptic cluster. The threshold we used represented the 99.95% confidence that the measured density differs from chance.

All localizations above the threshold were then ranked based on their local densities in a descending order and assigned each localization sequentially as the peak of a new nanocluster or a part of an existing nanocluster based on whether it was further enough from peaks of all existing nanoclusters. The localization with highest local density, if above the threshold, was defined as the peak of the first nanocluster. The second-highest-density localization would be considered as the peak of another potential nanocluster if the distance between the first peak to this potential second peak was larger than the defined cutoff distance; otherwise, the second localization was considered a part of the first nanocluster. The minimum peak-to-peak distance was set as 80 nm, which is about the average size of synaptic nanoclusters (MacGillavry et a., 2013; Tang et al., 2016; Chen et al., 2020). Then, each potential nanocluster was further divided into sub-clusters based on the point-to-point distance with a cutoff of 2 x MNND using MATLAB function 'clusterdata', and only the sub-cluster having the original peak localization of this potential nanocluster was selected. Finally, the sub-clusters had to include at least 4 localizations to be accepted as a nanocluster.

The enrichment analysis is based on the prediction that if the pre- and postsynaptic nanoclusters align across the cleft, the presence of a nanocluster on one side will predict a higher local protein density around its projected point on the other side. The synaptic cluster pair was first translated to overlap with each other based on their general shape without bias towards local densities (Tang et al., 2016, Chen et al., 2020). The enrichment was then quantified as the average local density of protein A over the distance from the projected peak of a protein B nanocluster. In case of a positive alignment, this curve would start from a local density significantly higher than the average at the small distance and

then decay to the average. More details and the defined MATLAB function for nanocluster detection and protein enrichment analysis could be found in (Chen et al., 2020). Experimenter was blind during image analysis.

**Automatic enface projection and averaging of synapses**

A plane parallel to the cleft was defined by fitting all localizations after the translation (least square of the normal distance to the plane). The two-dimensional enface projection was achieved with calculation of the projected coordinates of all localizations along the fitted plane. To avoid the potential dilution of local density after the collapse of one dimension, maximal projection of 3D local density was made to generate the density map of projected cluster. To visualize the enface distribution of both RIM1/2 and PSD-95 around PSD-95 nanoclusters, we averaged both normalized density maps centered around the projected peaks of PSD-95 nanoclusters. Meanwhile, to avoid any artifact created by the bordering effect, all values outside the synaptic cluster were replaced with 1 before averaging was performed (Chen et al., 2020).

**Numerical model to estimate peak open probability of AMPARs**

We used a constrained deterministic approach to test how different AMPAR organizations could impact the peak open probability of AMPARs at individual synapses based on key biological measurements. The calculation of ∑[peak open probability], also denoted as∑[peak p(o)], is adapted from previous stochastic modeling (Tang et al., 2016, Raghavachari & Lisman, 2004), where the probability of channel opening characteristically decays as a function of the distance to the position of glutamate

exocytosis. This relationship has been modeled here as Po(r) = 0.42e-r/88, as described previously (Tang et al., 2016).

AMPAR positions were randomly generated in MATLAB using cirrdnPJ.m which creates points within a circle of a specified size, essentially building a map of randomized AMPAR positions with 2D coordinates. We considered this the modeled PSD area, and this area was determined by values taken from prior EM work (Matsuzaki et al., 2001). The number of points to be generated within the PSD area was taken from prior work (Harris & Stevens, 1989). Using a separate loop of cirrdnPJ.m, another smaller radius could be specified within the larger PSD area, in which points were randomly generated. We considered this the modeled nanodomain, and it contained the average number of AMPARs suggested to form these nanodomains (Nair et al., 2013).

These modeled AMPAR organizations containing a single nanodomain were examined using our spatial analysis. The autocorrelation measurement, as described previously (Tang et al., 2016) for both biological and modeled localization data, was used to measure the size of these modeled subsynaptic clusters. The detected size of the modeled nanodomain was similar to the subsynaptic organizations observed in the biological data where the profile decays back to 1 at ~80 nm indicating the size of the modeled nanodomain. Of course, AMPAR nanodomains found in biological synapses can range in number impacting the amplitude of this measurement due to the increased frequency of the signal, and multiple nanodomains in one synapse will show a larger amplitude when measured by the autocorrelation. Since we only model a single nanodomain within the synapse, the autocorrelation correctly demonstrates a lower amplitude than the measured biological data.

These modeled AMPAR organizations were examined using our enrichment analysis (Tang et al., 2016, Chen et al., 2020). This analysis measures the density of points as a function of distance beginning at a specified position and moving out radially at determined step sizes (distance in nm). Using the previously described baseline parameters, and in agreement with the autocorrelation, the enrichment analysis successfully demonstrated that these modeled AMPAR positions show subsynaptic enrichment decaying to the average synaptic density by ~80 nm, and this measure was expectedly sensitive to the number of AMPARs included in the nanodomain. Then, the sensitivity of the threshold-based nanocluster detection algorithm, which can detect the number of points included in a subsynaptic cluster was adjusted until it successfully indicated that on average ~27 AMPARs were in-nanodomain.

In order to reflect the redistribution of AMPARs within synapses observed in the biological data by dSTORM, some number of AMPARs had to be removed from the nanodomain, but not lost from the PSD (Fig. 2, Fig. 6), which is referred to here as 'redistribution.' The specific mechanisms driving AMPAR position after this redistribution remain unclear, for instance, whether AMPARs are specifically excluded following LRRTM2 cleavage has not been determined. To reflect this in our model, AMPARs were simply placed back randomly into the modeled PSD, thus not specifically excluded from the nanodomain area after redistribution. Then using the enrichment profile and enrichment index as readouts of this reorganization, AMPARs were redistributed using this approach until the modeled enrichment index and modeled enrichment profile closely approximated the difference in the measured enrichment index and measured enrichment profile of AMPARs in biological synapses compared to their respective controls. Then, using the nanocluster detection

algorithm adjusted to detect the modeled 'ground truth' number of AMPARs previously, we redistributed AMPARs and quantified how many AMPARs were still considered to be 'in nanodomain' after redistribution. Interestingly, some nanodomains were no longer detectable given the magnitude of reorganization, which is consistent with our observations in Fig. 4l.

The open probability of AMPARs is thought to critically depend on the distance to the site of glutamate exocytosis. Release position has been thought to occur in spatially distinct subregions of the active zone given different modes of neurotransmitter release, thus influencing this key parameter. To understand how different constraints on release position in the active zone impact AMPAR open probability, we modeled two modes of release, again using cirrdnPJ.m to randomize AMPAR positions within a specified area. Release constrained to the nanodomain is referred to here as 'evoked release,' as it is thought to occur over a smaller fraction of the PSD and aligned with postsynaptic AMPAR nanodomains. We refer to release over the entire area of the PSD as 'spontaneous release', as it does not demonstrate a similar constraint in release position distribution determined by live-imaging of vesicle fusion events (Tang et al., 2016).

Then, using the baseline parameters as a starting point, and our modeled redistribution of AMPARs given the data from Fig. 4F,M (as described above), we calculated the open probability of each AMPAR in the modeled PSD. This was done by indexing the distance of each AMPAR to the modeled vesicle release position. Then by summing these probabilities across every AMPAR in the modeled PSD, we could estimate the number of AMPARs on average that would generally be expected to open in response to spontaneous or evoked release. This informed the interpretations of the electrophysiology from neurons

that underwent LRRTM2 cleavage and subsequent AMPAR redistribution. To test how these various spatial parameters ('PSD area', 'proportion of AMPARs in the nanodomain', and the 'decay constant of the decay profile') used in the model influenced AMPAR open probability, we kept the baseline parameters constant except for the parameter being tested and repeated the redistribution of AMPAR positions described above over a reasonable biological range.

**Electrophysiology**

Whole-cell recordings were made on neurons from DIV13-17 with 5-8 MΩ pipettes filled with an internal solution that contained (in mM): 130 CsMeSO3, 6 NaCl, 10 HEPES, 1 MgCl2, 2 BAPTA-K, 0.2 CaCl2, 3 Mg-ATP, 0.3 Tris-GTP, pH 7.3 with CsOH, 290-295 mOsm. Neurons were hold at -70 mV at which the GABAergic current were minimal. The bath solution consisted of (in mM): 130 NaCl, 2.5 KCl, 1 NaH2PO4, 10 HEPES, X CaCl2, 4-X MgSO4, and 10 Glucose. Lower [Ca2+]o (X = 0.5-1) was used for eEPSC recordings to reduce the recurrent activity, while for mEPSC recordings normal [Ca2+]o (X = 2) combined with TTX (1 μM) and picrotoxin (50 μM) was used. Evoked EPSCs were elicited with 1-ms extracellular field stimuli through a bipolar electrode made from θ-shape glass pipette with opening of 2 to 3 μm. The stimulation electrode was held a few μm above the cells and moved around to locate at a position where single-peak, monosynaptic currents were reliably evoked. The paired stimuli with a 50 ms interval were delivered every 10 s. For miniature EPSCs, glass pipettes were pulled to have a resistance of 3-6 MΩ. An internal solution containing 130 mM K-gluconate, 5mM KCl, 2 mM MgCl6-H2O, 10 mM HEPES, 4 mM Mg-ATP, 0.3 mM Na2-GTP, 10 mM Na2-phosphocreatine, and 1 mM EGTA was

used to record at room temperature (21-24°C). The series resistances were monitored and data with changes of >20% were discarded. The capacitance and input resistance were not significantly different between different groups of neurons. Data were collected with MultiClamp 700B amplifiers (Molecular Devices) and digitized at 5 kHz with Digidata 1440 and Clampex 10 software (Molecular Devices). mEPSCs were detected by fitting to a variable amplitude template using pClamp 10 analysis software. Experimenter was blinded to condition during data analysis.

**Statistical analysis**

We used two-tailed Student's T or Mann-Whitney rank sum tests for comparisons between 2 groups. We used a one-way ANOVA with posthoc Dunnett's Test for multiple comparisons of three groups. Data are presented as means ± SEM except otherwise noted. Significance levels displayed as follows: n.s., not significant, $p > 0.05$; * $p < 0.05$, ** $p < 0.01$, *** $p < 0.001$, **** $p < 0.0001$. These tests were performed in Prism 8.2.0 (GraphPad).

## CHAPTER 3: Results

### Section 1. Acute and specific cleavage of the LRRTM2 extracellular domain

To test the role of LRRTM2 extracellular interactions in synapse structure and function independent of synaptogenesis and genetic compensation, we adapted a previous approach (Peixoto et al., 2012) and inserted the short recognition sequence for the endoprotease thrombin (LVPRGS) at an extracellular, juxtamembrane position within human LRRTM2 (Fig. 1A). To visualize the molecule and enable live-cell measurement of its cleavage in neurons, we appended EGFP to the N-terminus, and used this to replace endogenous LRRTM2 following knockdown with published shRNA targeting sequences. We denote the molecule GFP-Thr-LRRTM2*, where * indicates the human sequence designed to be resistant to the shRNA (de Wit et al., 2009; Ko et al., 2009).

**Fig. 6. Acute and specific cleavage of the LRRTM2 extracellular domain. (A)** Schematic demonstrating the juxtamembrane insertion of the thrombin recognition sequence (Peixoto et al., 2012) and the N-terminal GFP* denotes co-packaging of an shRNA (de Wit et al., 2009) that targets endogenous LRRTM2 expressed in the same vector as GFP-Thr-LRRTM2. **(B)** Expression of GFP-Thr-LRRTM2* in cultured hippocampal neurons and immunostaining of endogenous PSD-95 and RIM1/2 visualized by confocal microscopy. Scale bar, left: 30 µm, right: 10 µm. **(C)** Quantification of the colocalization between expressed GFP-Thr-LRRTM2*, RIM1/2, and PSD-95. ($n$ = 120 synapses/6 neurons/2 independent cultures per condition). **(D)** Quantification of Bassoon recruitment by LRRTM2 in an HEK-neuron coculture synaptogenesis assay alongside positive (CFP-NL1) and negative (CFP alone) controls. CFP alone ($n$ = 30 cells/2 independent cultures), CFP-NL1 ($n$ = 34/2), BRS-Thr-LRRTM2* ($n$ = 24/2), GFP-Thr-LRRTM2* ($n$ = 25/2), GFP-LRRTM2* ($n$ = 32/2). **(E)** Quantification of PSD-95 puncta density in neurons expressing GFP-Thr-LRRTM2* (KDR, $n$ = 19 neurons/3 independent cultures), GFP-Thr-LRRTM2 (OE, $n$ = 16/3), or cytosolic mCerulean3 (Cer3, $n$ = 15 /3). **(F)** Quantification of spine density. ($n$ = 10 neurons/3 independent cultures per condition). **(G)** Quantification of spine length. ($n$ = 10/3). **(H)** Quantification of spine area. ($n$ = 10/3). **(I)** Representative images from a confocal time series of GFP-Thr-LRRTM2* cleavage following thrombin application (red arrow, 10 units $ml^{-1}$). Scale bar: 10 µm. **(J)** Quantification of GFP-Thr-LRRTM2* ($n$ = 100 synapses/5 neurons/3 independent cultures) and GFP-LRRTM2* ($n$ = 40/2/2) cleavage. **(K)** Quantification of GFP-LRRTM2* ($n$ = 100/5/2) or GFP-Thr-LRRTM2* ($n$ = 120/6/2) for up to 60 minutes post thrombin exposure. One-way ANOVA with posthoc Dunnett's Test was used in E-H. Data are presented as mean ± SEM, * $p \leq 0.05$, ** $p \leq 0.01$.

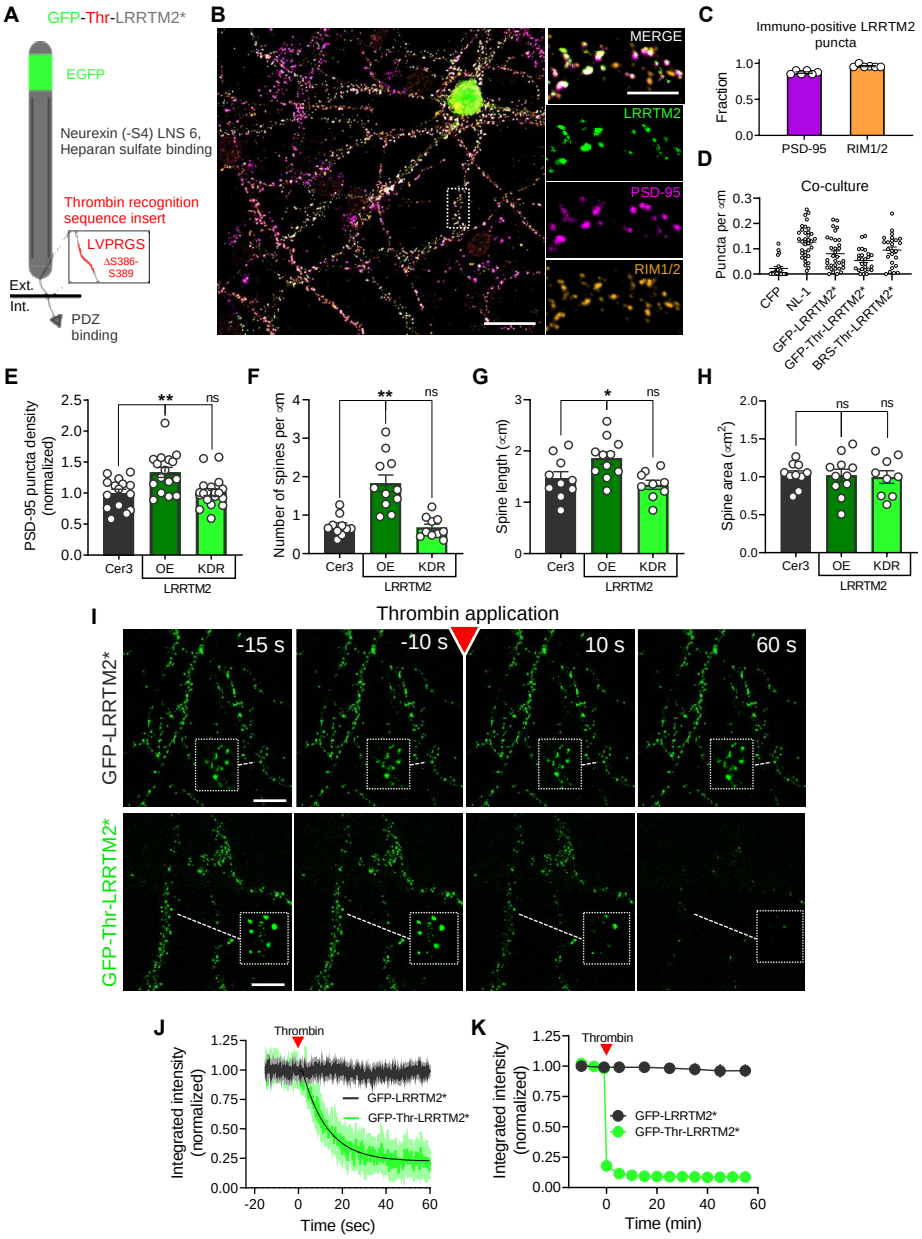
A
GFP-Thr-LRRTM2*
EGFP
Neurexin (-S4) LNS 6,
Heparan sulfate binding
Thrombin recognition
sequence insert
LVPRGS
ΔS386-
S389
Ext.
Int.
PDZ
binding
B
MERGE
LRRTM2
PSD-95
RIM1/2
C
Immuno-positive LRRTM2
puncta
Fraction
PSD-95
RIM1/2
D
Co-culture
Puncta per μm
CFP
NL-1
GFP-LRRTM2*
GFP-Thr-LRRTM2*
BRS-Thr-LRRTM2*
E
PSD-95 puncta density
(normalized)
F
Number of spines per μm
G
Spine length (μm)
H
Spine area (μm²)
Cer3
OE
KDR
LRRTM2
ns
I
Thrombin application
-15 s
-10 s
10 s
60 s
GFP-LRRTM2*
GFP-Thr-LRRTM2*
J
Thrombin
Integrated intensity
(normalized)
Time (sec)
K
Time (min)

These modifications of LRRTM2 did not appear to disrupt its function. When expressed in cultured rat hippocampal neurons, GFP-Thr-LRRTM2* clustered avidly in small puncta that colocalized nearly exclusively with synapses immunolabeled for PSD-95 and RIM1/2 (Fig. 1B-C), though some puncta appeared in the dendritic shaft apart from synapses. In addition, when expressed in HEK cells, GFP-Thr-LRRTM2* trafficked strongly to the plasma membrane and retained the synaptogenic ability of wild type LRRTM2 to cluster presynaptic markers in the axons of co-cultured wild type neurons (Fig 1D, Supplementary Fig. 1A).

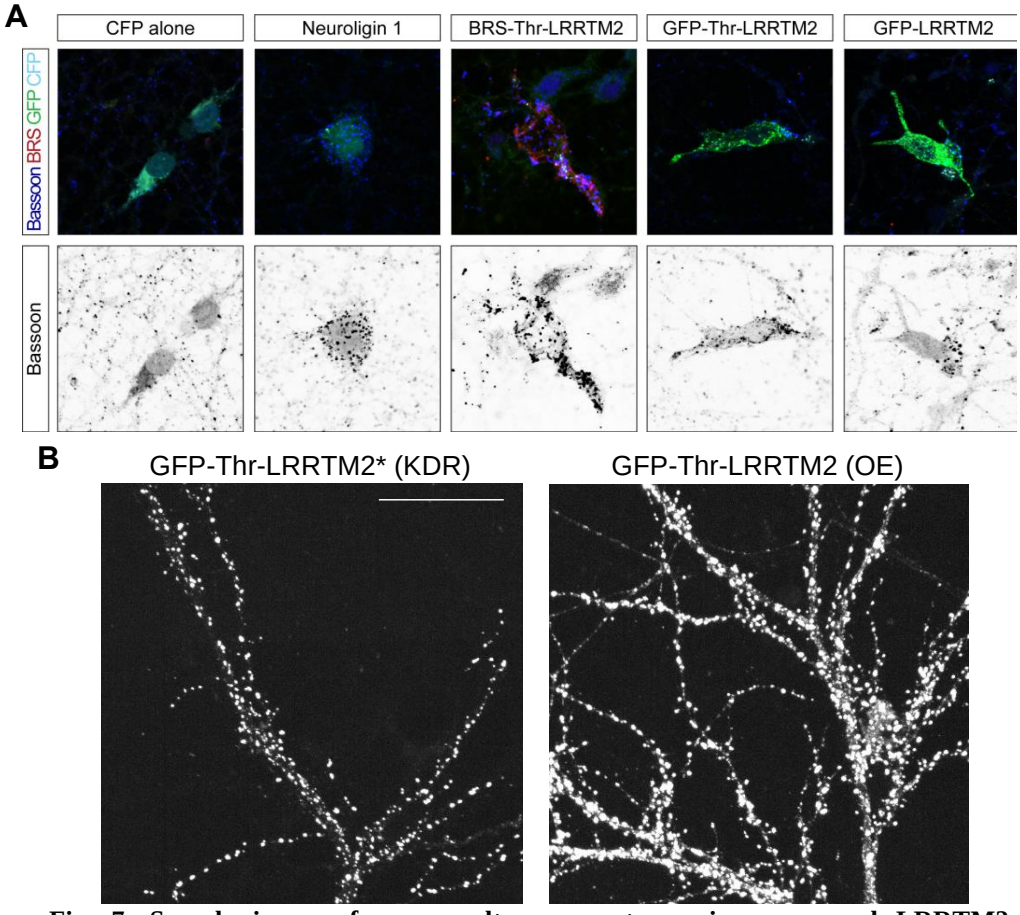


**Fig. 7. Sample images from co-culture synaptogenesis assays and LRRTM2 overexpression. (A)** Representative images from HEK-neuronal co-culture synaptogenesis assay. **(B)** Representative images from neurons expressing the knockdown-replacement vector GFP-Thr-LRRTM2* or overexpressing GFP-Thr-LRRTM2 demonstrating elevated synaptic enrichment of LRRTM2 in the knockdown-replacement. Scale bar: 20 µm.

Though knockdown of LRRTM2 was successful (Supplementary Fig. 2), typical rescue strategies can still result in overexpression. Since overexpression of LRRTM2 in cultured neurons increases excitatory synapse density (de Wit et al., 2009; Ko et al., 2009), we tested for functional effects of LRRTM2 overexpression by measuring synapse density via PSD-95 immunolabeling. As expected, expression of GFP-Thr-LRRTM2* without concurrent knockdown resulted in a ~1.3-fold increase in PSD-95 puncta compared to controls expressing cytosolic mCerulean3 alone (Fig. 1E). However, puncta density was unchanged following knockdown of endogenous LRRTM2 and replacement with GFP-Thr-LRRTM2*. Similarly, compared to mCerulean transfected neurons, spine numbers were increased by GFP-Thr-LRRTM2* overexpression, but were unchanged following knockdown and replacement (Fig. 1F). Overexpression also resulted in an increase in spine length though not spine area, but we found no changes in either measure with the knockdown-replacement approach (Fig. 1G-H). The replacement strategy also minimized non-synaptic localization of GFP-Thr-LRRTM2*, which was enriched much more specifically in synapses when endogenous LRRTM2 was knocked-down as judged by the levels of thrombin-sensitive extrasynaptic fluorescence (Supplementary Fig. 1B). These data suggest that GFP-Thr-LRRTM2* incorporates readily into excitatory synapses without disrupting synaptogenesis and with minimal effects of overexpression.

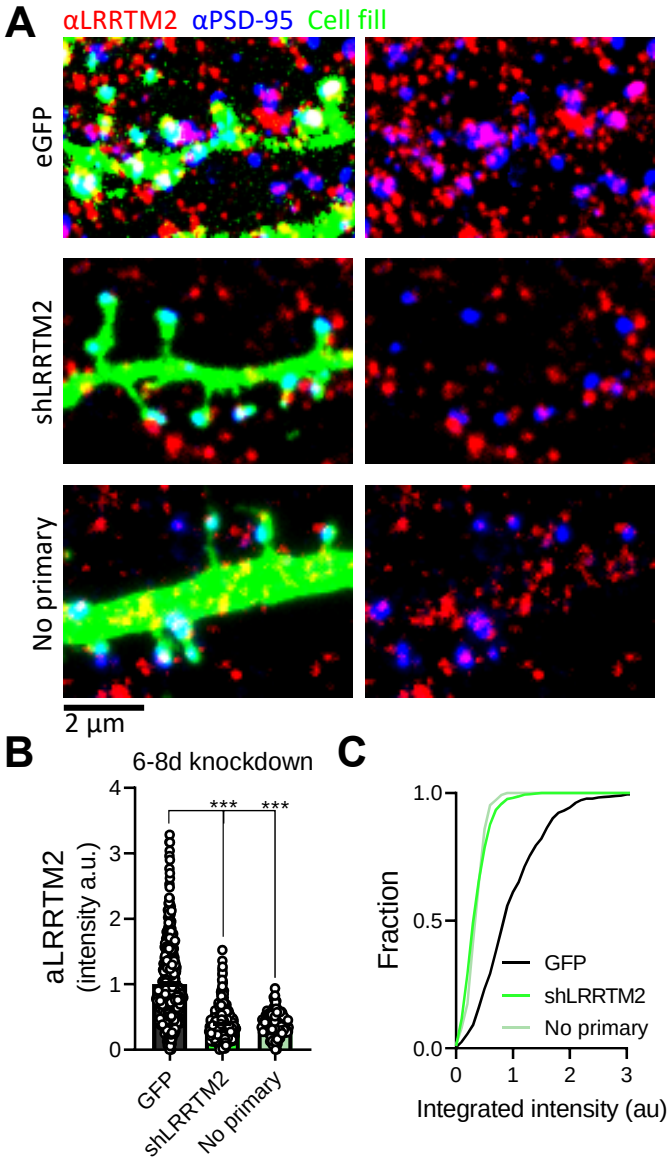


**Fig. 8. Knockdown of LRRTM2.** (A) Representative images from neurons transfected with cytosolic GFP (22 neurons/550 synapses/2 cultures), LRRTM2 shRNA (20/500/2), and staining lacking the primary antibody against LRRTM2 (175/7). (B) Quantification of LRRTM2 signal at PSD-95 positive spines normalized to control. (C) Cumulative distribution of LRRTM2 signal intensity Scale bar: 2 µm. Kruskal-Wallis with Dunn's multiple comparisons test, $p < 0.05$ = *, $p < 0.01$ = **, $p < 0.0001$ = ***.

Next, we tested whether thrombin successfully cleaved GFP-Thr-LRRTM2* in synapses, particularly at low working concentrations to avoid potential effects which could be mediated via PAR receptors (Mrozkova et al., 2016). Following baseline measurements of EGFP fluorescence, we bath-applied thrombin at 10 units/mL. This prompted the rapid and robust loss of GFP fluorescence from puncta in dendritic spines (Fig. 1I, below). Thrombin application to neurons expressing GFP-LRRTM2* (with no thrombin recognition sequence) resulted in no decrease in fluorescence, indicating the loss was due to cleavage of the extracellular domain (ECD) and not non-specific effects of thrombin (Fig. 1I, above). The LRRTM2 ECD was lost with a time constant of $\tau = 11.08$ seconds (95% C.I 10.74 to 11.43 sec; Fig. 1J), surprisingly rapid given its presumed interactions within the synaptic cleft. Incubations in thrombin for up to 1 hour showed sustained loss of GFP-Thr-LRRTM2* (Fig 1K; fractional fluorescence remaining; $0.09 \pm 0.02$ compared to baseline; mean ± SEM), but no loss of the LRRTM2 ECD in GFP-LRRTM2* transfected neurons (Fig 1K; fraction remaining; $0.96 \pm 0.05$, compared to baseline). The rate of cleavage is likely limited by the speeds of perfusion and proteolysis, but regardless suggests that LRRTM2 ECD interactions are insufficient to immobilize it for substantial periods within the synaptic cleft. In addition, the quick action and extensive loss of fluorescence confirms that GFP-Thr-LRRTM2* was trafficked to the cell surface as expected, and suggests that LRRTM2 is only minimally retained intracellularly at steady state in these neurons. Overall, these results demonstrate that expressed GFP-Thr-LRRTM2* localizes appropriately to excitatory synapses, retains its synaptogenic activity, induces no observable morphological changes in spines, and can be proteolytically cleaved acutely and specifically on demand.

## Section 2. No rapid loss of AMPARs following removal of the LRRTM2 extracellular domain

The role of LRRTM2 in synaptogenesis has been well studied, but its functions in established synapses have been explored in far less detail. The four C-terminal amino acids in its intracellular domain form a PDZ-binding motif which is thought to play a role in the recruitment of PSD-95 in developing synapses (de Wit et al., 2009), through interactions with the first and second PDZ domains of PSD-95 (Linhoff et al., 2009). We considered whether maintenance of PSD-95 at established synapses depends on stable LRRTM2 extracellular interactions. To test this, we co-transfected neurons with GFP-Thr-LRRTM2* and PSD95*-mCherry (MacGillavry et al., 2013) (here, * also denotes resistance to co-expressed shRNA) and measured their fluorescence intensity over the course of a 30 min thrombin application. Strikingly, despite a large and sustained reduction in the GFP-Thr-LRRTM2* fluorescence (fraction remaining: 0.15 ± 0.07, Fig. 2A-C), PSD95*-mCherry fluorescence at synapses remained unchanged (fraction remaining: 0.94 ± 0.05, Fig. 2A-C). Immunocytochemical analysis of synaptic PSD-95 content after thrombin cleavage (discussed below) confirmed this result. Thus, the interactions of LRRTM2 within the synaptic cleft are not necessary for the retention of PSD-95 in established synapses.

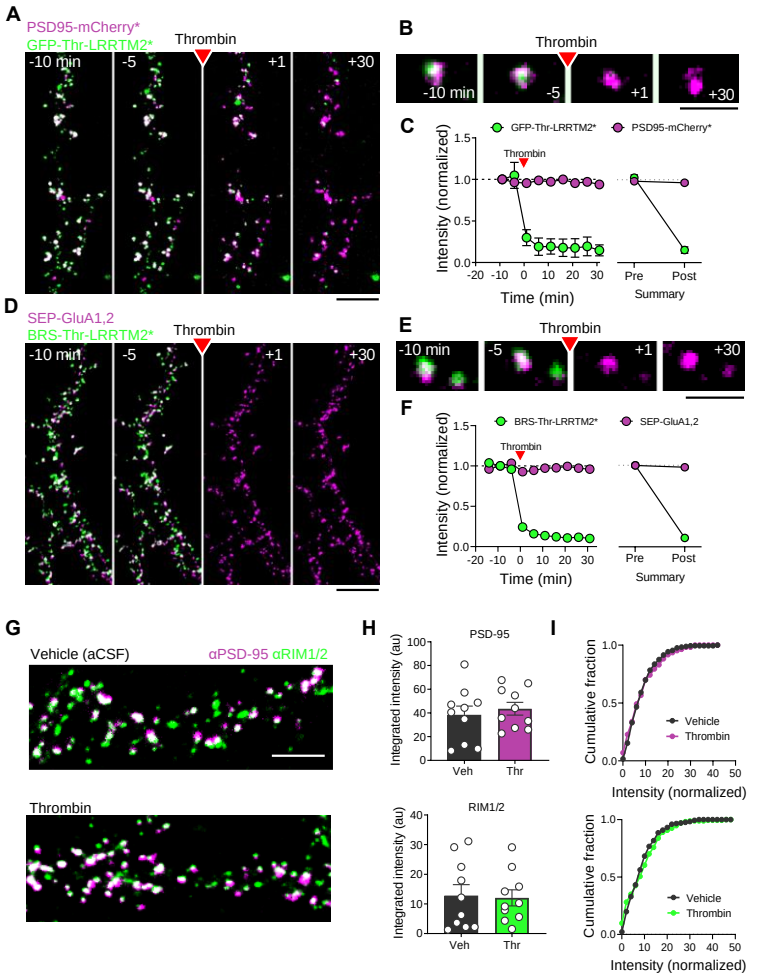


**Fig. 9. No rapid loss of AMPARs following removal of the LRRTM2 extracellular domain. (A)** Representative images of neuronal dendrites co-expressing GFP-Thr-LRRTM2* and PSD95-mCherry*. Red arrow indicates the bath application of thrombin (10 units $ml^{-1}$). Scale bar: 10 µm. **(B)** Enlarged view. Scale bar: 2 µm. **(C)** Left, quantification of fluorescence intensity of both GFP-Thr-LRRTM2* and PSD95-mCherry*. Right, summary of baseline measurements compared to 30' post thrombin application. (*n* = 14 neurons/3 independent cultures). **(D)** Representative images of neuronal dendrites co-expressing BRS-Thr-LRRTM2* and SEP-GluA1/2. Red arrow indicates the bath application of thrombin (10 units $ml^{-1}$). Scale bar: 10 µm. **(E)** Enlarged view. Scale bar: 2 µm. **(F)** Left, quantification of fluorescence intensity of both BRS-Thr-LRRTM2* labeled with α-bungarotoxin conjugated to Alexa-647 and SEP-GluA1/2 over time normalized to their respective baseline. Right, summary of baseline measurements compared to 30' post thrombin application. (*n* = 11 neurons/3 independent cultures). **(G)** Representative images of immunocytochemical staining of endogenous RIM1/2 and PSD-95 from cultured hippocampal neurons expressing GFP-Thr-LRRTM2* and mCerulean3 treated with either vehicle (aCSF, above; n = 173 synapses/9 neurons/3 independent cultures) or thrombin (below, 10 units $ml^{-1}$ for 10 minutes; n = 176/9/3). Scale bar: 5µm. **(H)** Quantification of synaptic staining intensity for PSD-95 (above) and RIM1/2 (below). **(I)** Cumulative distribution of synaptic staining intensities for cells treated with vehicle (aCSF, grey) or thrombin (magenta for PSD-95 and green for RIM1/2). Data are presented as mean ± SEM.

LRRTM2 is important for both establishing the number of GluA1-containing synapses as well as basal synaptic content of GluA1 and GluA2 (de Wit et al., 2009; Soler-Llavina et al., 2013; Aoto et al., 2013). In neurons at rest, many AMPARs continuously diffuse within the synapse and exchange between synaptic and extrasynaptic domains on a time scale of seconds to minutes (Choquet & Triller, 2003), but the mechanisms that counteract diffusion and enrich them in the PSD are incompletely understood. Extracellular interactions in the synaptic cleft may be important, and it is conceivable that the ECD interactions of LRRTM2 could assist in the stabilization of both LRRTM2 and additionally GluA1-containing AMPARs in established synapses. To visualize synaptic AMPAR content during live imaging before and after cleavage of LRRTM2, we utilized super-ecliptic pHluorin (SEP)-tagged GluA1 and GluA2, as previously described (Kerr et al., 2012). We expressed these receptors along with a version of LRRTM2* in which the GFP was replaced with the smaller α-bungarotoxin recognition sequence (Sekine-Aizawa et al., 2004) (BRS-Thr-LRRTM2*) which retained its synaptogenic activity (see Fig 1D, Supplementary Fig. 1) and allowed us to select the wavelength of the labeled α-bungarotoxin. Alexa-647 conjugated to α-bungarotoxin was applied to live cells, resulting in synapse-specific labeling and visualization of the LRRTM2 ECD in co-transfected neurons. We predicted that if the LRRTM2 ECD interacts directly or indirectly with the GluA1 extracellular domain, its acute loss would reduce SEP-GluA1,2 content in synapses. As with GFP-Thr-LRRTM2*, thrombin application produced a rapid and dramatic loss of α-bungarotoxin-Alexa-647 fluorescence (fraction remaining: 0.10 ± 0.02, Fig. 2D-F) indicating cleavage and dispersal of the LRRTM2 ECD. However, SEP-GluA1,2 fluorescence colocalized with LRRTM2 puncta did not decrease even after 10 or 30 min

(fraction remaining: 0.96 ± 0.03, Fig. 2D-F), suggesting no changes in the number of receptors present within the PSD. Furthermore, neurons expressing SEP-GluA1/2 along with the cleavable or non-cleavable versions of LRRTM2*, showed no difference in the SEP-GluA1,2 synaptic cluster localization density as measured by dSTORM after a 10-min thrombin treatment (Mann-Whitney Test, p = 0.85; data discussed below, Supplementary Fig. 3). These data suggest that the LRRTM2 ECD is not required for the synaptic retention of AMPARs within a time frame of 30 minutes, during which many receptors exchange in and out of the synapse (Choquet & Triller, 2013).

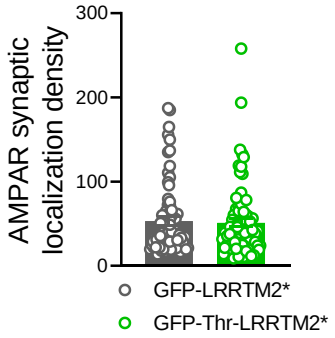


**Fig. 10. Synaptic localization density of AMPARs.** Accompanies Fig 2. Expression of GFP-LRRTM2* (grey) or GFP-Thr-LRRTM2* (green) in cultured hippocampal neurons and immunolabeling of SEP-GluA1/2 and RIM1/2 following 10-minute treatment with thrombin. Quantification of the synaptic localization density of AMPARs analyzed in Fig. 4c (non-cleavable, grey; 77/15/3; cleavable, green; n = 73/11/3).

This result was surprising because conditional knockout of LRRTM1 and 2 leads to a reduction in AMPAR content and EPSC amplitude at established synapses (Bhouri et al., 2018). One major difference between the conditional deletion and the acute cleavage is the vastly differing time scales of the two approaches. To test whether the prolonged loss of the LRRTM2 ECD affects AMPAR retention in spines, we performed live-cell imaging for up to 2 hours post-cleavage. In fact, synaptic AMPAR content remained almost

completely unchanged for at least 60 min after LRRTM2 cleavage. Only after this, a slow decline set in, and 2 hours after cleavage there was a 23.55% ± 0.08% reduction in AMPAR content compared to non-cleavable controls (Supplementary Fig. 4). To examine longer time points, we fixed transfected neurons 24 hours after thrombin treatment and stained for surface SEP-GluA1,2. Compared to controls expressing non-cleavable BRS-LRRTM2*, neurons that underwent LRRTM2 cleavage displayed much weaker surface SEP-GluA1,2 expression (Supp. Fig. 4). These data corroborate the previously reported idea that LRRTM2 is important for AMPAR stability in synapses (Bhouri et al., 2018), but show that this effect plays out only over extended periods without the LRRTM2 ECD.

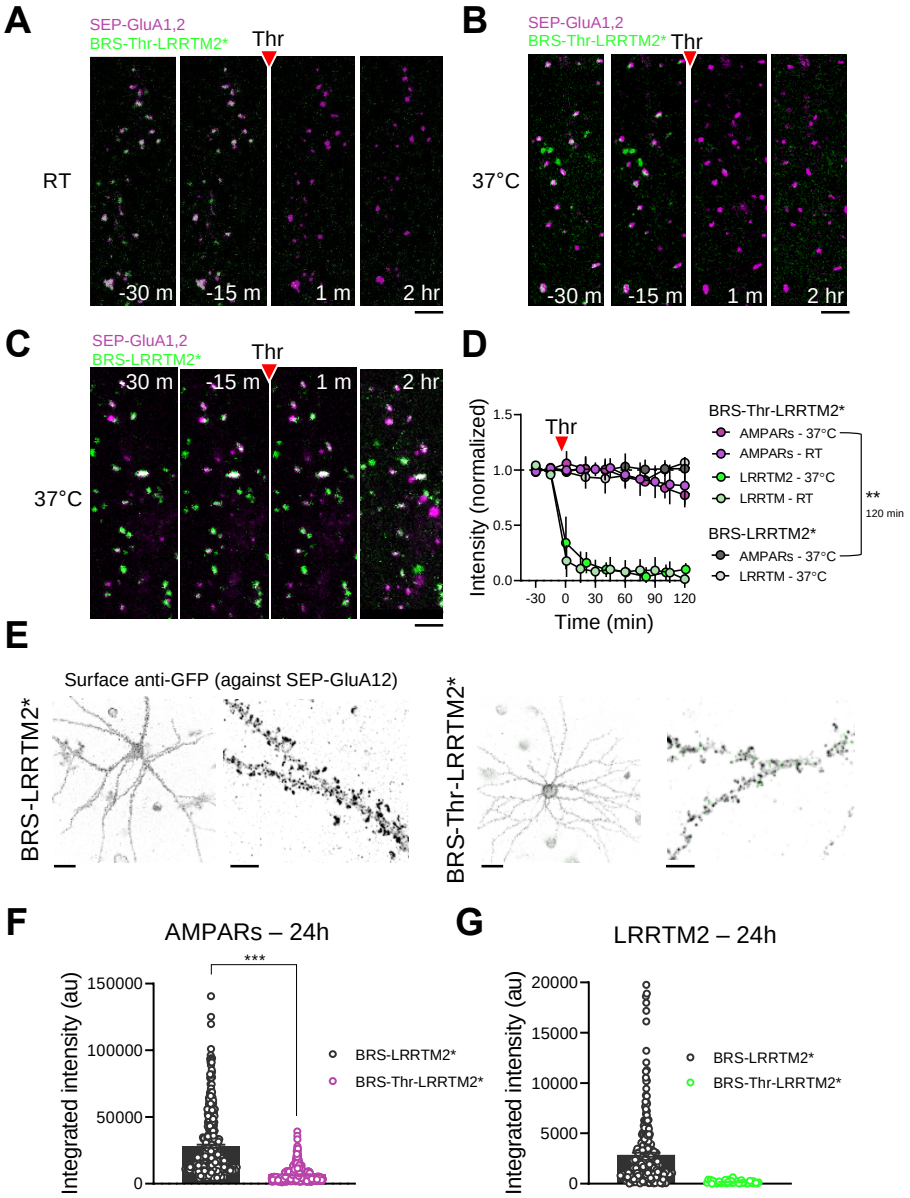


**Fig. 11. Prolonged disruption of LRRTM2 interactions.** (A) Representative images from time series from neurons expressing SEP-GluA1,2 and BRS-Thr-LRRTM2* at room temperature (RT) in aCSF (n = 8 neurons/160 synapses/3 cultures), (B) SEP-GluA1,2 and BRS-Thr-LRRTM2* at 37°C in culture media ($n$ = 6/120/2), or (C) SEP-GluA1,2 and BRS-LRRTM2* at 37°C in culture media ($n$ = 4/80/2). Scale bar: 2 µm. (D) Quantification from A-C. (E) Surface staining of SEP-GluA1,2 in cells expressing either BRS-LRRTM2* ($n$ = 8 neurons/400 synapses/2 cultures) or BRS-Thr-LRRTM2* (11/550/2) 24 hours after treatment with thrombin for 10 minutes. Scale bar: 25 µm, 5 µm. (F) Quantification of SEP-GluA1,2 staining intensity. (G) Quantification of LRRTM2 labeling intensity. (D) Student's t-test, (F) Mann Whitney rank-sum test, $p < 0.05$ = *, $p < 0.01$ = **, $p < 0.0001$ = ***.

Another possible role of LRRTM2 may be to instruct organization of presynaptic release machinery. To test this, we transfected cultured hippocampal neurons with GFP-Thr-LRRTM2* along with soluble Cerulean3 to identify transfected spines following elimination of the EGFP fluorescence post-cleavage. Then, following live-cell cleavage of LRRTM2 with 10 U/mL thrombin for 10 minutes, cells were fixed, permeabilized, and stained for endogenous PSD-95 and the critical presynaptic scaffolding molecule RIM1/2. Despite near complete elimination of EGFP fluorescence at transfected spines we observed no changes in endogenous RIM1/2 content (fraction remaining: 1.06 ± 0.06, compared to vehicle, Fig. 2G-I). These data suggest that LRRTM2 is not necessary for the retention of RIM in the active zone. Analysis of PSD-95 staining intensity further confirmed that cleavage of LRRTM2 in established synapses did not change PSD-95 content (fraction remaining; 1.02 ± 0.06, compared to vehicle, Fig. 2G-I) supporting our earlier observations during live imaging. Taking these data together, we conclude that although the LRRTM2 ECD is quickly lost after thrombin cleavage in established synapses, its acute removal does not rapidly lead to loss of other key molecules, including AMPARs.

**Section 3. LRRTM2 is enriched within the trans-synaptic nanocolumn**

Growing evidence indicates that different CAMs possess unique and distinct organizations within excitatory synapses (Chamma et al., 2016). For instance, both SynCAM1 and Neurexin-1 are enriched in a small number of subsynaptic ensembles, but the nanoclusters of SynCAM-1 are often found near or around the border of the synapse (Perez de Arce et al., 2015; Cijsouw et al., 2018) whereas Neurexin-1 nanoclusters tend to occur just slightly off-center within the PSD (Trotter et al., 2019). How these distributions subserve particular functions is not known. LRRTM2 forms tight clusters in the postsynaptic density (Chamma et al., 2016). Its enrichment within these nanoclusters in notably tighter than Neuroligin-1 (NL-1), which more homogeneously distributes through the synapse (Chamma et al., 2016), but neither the location nor function of LRRTM2 nanoclusters is known. We hypothesized that LRRTM2 may link pre- and postsynaptic nanodomains, and therefore predicted that it is enriched with other proteins found within the trans-synaptic nanocolumn (Tang et al., 2016).

To test whether LRRTM2 formed subsynaptic clusters within excitatory PSDs, we performed two-color 3D dSTORM in our LRRTM2 knockdown-replacement system using an anti-GFP antibody (Fig. 3A). Maps of the local density at each molecular location (Fig. 3B) showed that LRRTM2 is non-uniformly organized within the PSD, forming nanodomains of similar size and number to those previously reported for receptors and scaffolding molecules (Dani et al., 2010; MacGillavry et al., 2013; Chamma et al., 2016). To quantify the degree to which LRRTM2 was self-clustered, we calculated an autocorrelation measurement and found that LRRTM2 was robustly organized into clusters with a ~100 nm diameter within synapses (Fig. 3C).

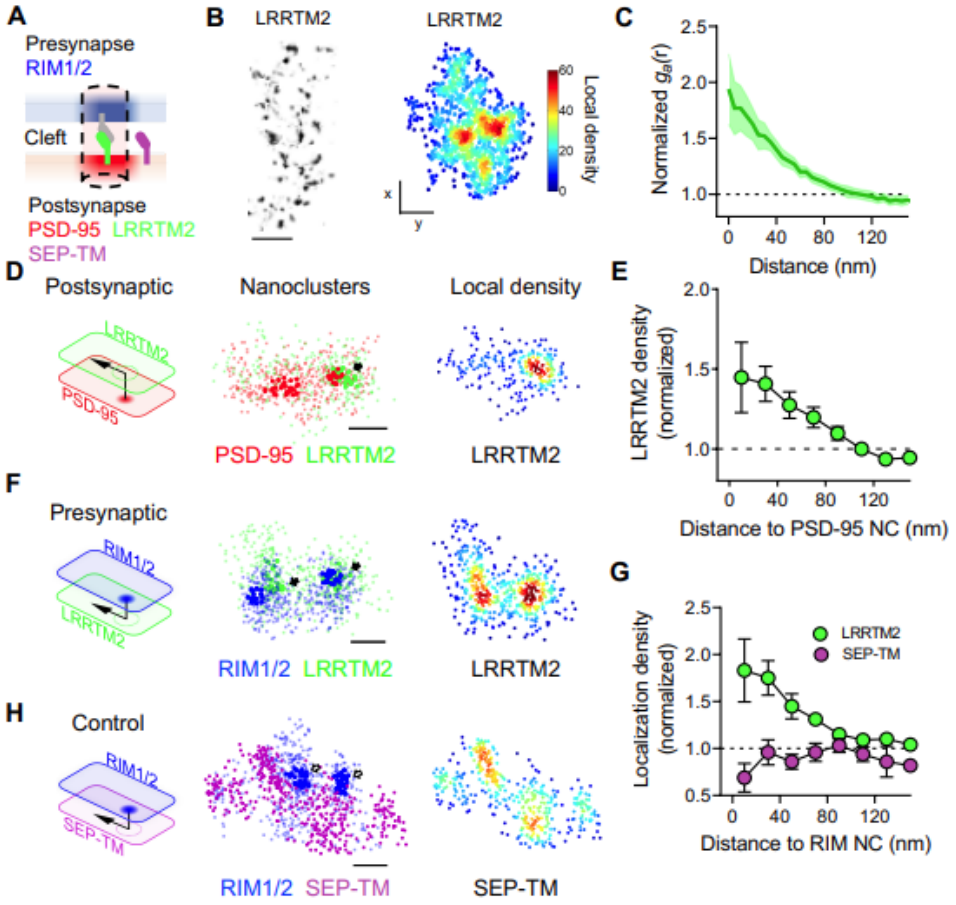


**Fig. 12. LRRTM2 is enriched within the trans-synaptic nanocolumn. (A)** Schematic demonstrating the trans-synaptic nanoscale organization of LRRTM2 relative to RIM and PSD-95. **(B)** Left, 3D dSTORM reconstruction of a dendrite from a neuron expressing GFP-LRRTM2*. Scale bar: 2 µm. Right, 3D dSTORM reconstructions of an individual synapse with localizations color-coded by local density (5x nearest neighbor distance (NND)). Scale bar: 100 nm. **(C)** Auto-correlation of LRRTM2 synaptic clusters. **(D)** Schematic demonstrating the measurement of 3D co-enrichment between protein pairs (LRRTM2 green, PSD-95 red). Middle, left, en face view of the localized positions of PSD-95 (red) and LRRTM2 (green) with detected nanoclusters indicated in bold. Middle, right, the same LRRTM2 localizations coded by their local density (5x NND). Scale bar: 100 nm. **(E)** Quantification of LRRTM2 density as a function of the distance to the PSD-95 nanocluster center. **(F)** LRRTM2 cross-enrichment with RIM1/2 as displayed in D-E. **(G)** Quantification LRRTM2 cross-enrichment with RIM1/2 nanoclusters. (*n* = 176 nanoclusters/16 neurons/5 independent cultures). **(H)** Cross-enrichment of a diffuse target, SEP-TM, across from presynaptic RIM1/2 nanoclusters displayed as in D-E. Scale bar: 100 nm. (*n* = 85/9/3). **(G)** Quantification of SEP-TM density as a function of the distance to the RIM1/2 nanocluster center. Data are presented as mean ± SEM.

To test how LRRTM2 was organized relative to nanocolumn-resident molecules, we measured the subsynaptic organization of GFP-Thr-LRRTM2* relative to endogenous PSD-95 (Fig. 3D-E) and RIM1/2 (Fig. 3F-G) using an enrichment assay reported previously (Tang et al., 2016). LRRTM2 was tightly enriched within PSD-95 nanodomains (enrichment index: 1.37 ± 0.13, Fig. 3E) and aligned with RIM1/2 nanodomains across the synaptic cleft (enrichment index: 1.56 ± 0.21%, Fig. 3G). To analyze the LRRTM2 distribution with respect to that of RIM1/2 or PSD-95 without requiring the identification of nanoclusters of either protein, we measured the cross-correlation between LRRTM2 and RIM1/2 or PSD-95 density distributions (Sup. Fig. 3). This demonstrated that the distribution of LRRTM2 and PSD-95 as well as LRRTM2 and RIM1/2 are highly similar to one another. To illustrate this similarity, we compared the distribution of LRRTM2 to a probe without nanocolumns enrichment. We used an engineered single pass transmembrane protein called SEP-TM containing an N-terminal extracellular super-ecliptic pHluorin (SEP) appended to the transmembrane domain from PDGFR (Li et al., 2016). SEP-TM traffics avidly to the plasma membrane (Supplementary Fig. 5), but we predicted that it would not be enriched within the nanocolumn because it lacks relevant binding via its N- or C-terminus. While LRRTM2 was tightly aligned across the cleft from RIM nanodomains, SEP-TM was not (enrichment index: 0.83 ± 0.12, Fig. 3G-H, Supplementary Fig. 6). This suggests that the subsynaptic positioning of LRRTM2 is actively determined by protein-protein interactions rather than arising as a general feature of transmembrane proteins in the dense synaptic environment. The distribution of LRRTM2 within the synapse, tightly clustered and colocalized with transsynaptically aligned protein nanodomains, suggests that it acts within the nanocolumn.

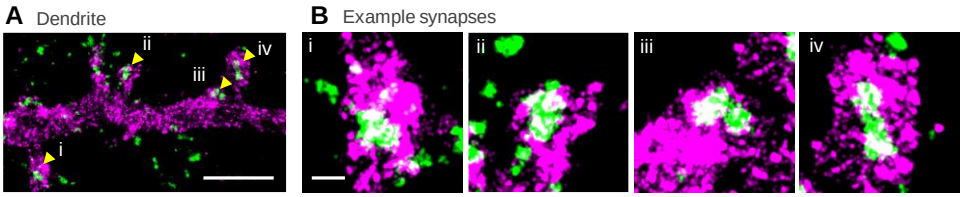


**Fig. 13. SEP-TM has a much broader cellular distribution than RIM.** Representative images of SEP-TM distribution in dendrites as measured by 3D dSTORM, demonstrating a much broader distribution than the synaptic marker RIM. Scale bar a, 2 µm, b, 250 nm.

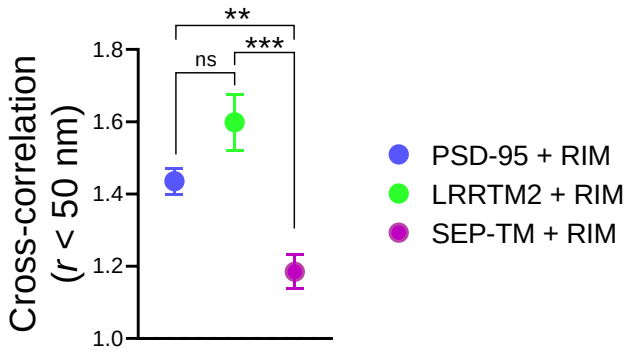


**Fig. 14. Cross-correlation of LRRTM2 with PSD-95 and RIM.** Cross-correlation for LRRTM2 (n = 99 synapses/5 independent cultures), PSD-95 (n = 60/2), and SEP-TM (n = 66/3), where the correlation is performed between each molecule's cluster distribution and the synaptic distribution of RIM1/2. Kruskal-Wallis with Dunn's multiple comparisons test, $p < 0.05$ = *, $p < 0.01$ = **, $p < 0.0001$ = ***.

**Section 4. LRRTM2 is critical for AMPAR enrichment with preferential sites of evoked neurotransmitter release**

Expression of LRRTM2 with mutations that disrupt its interaction with presynaptic neurexin decreases content of expressed mutant LRRTM2 at synapses and leads to lower synaptic AMPAR content and reduced AMPAR-mediated EPSCs (Bhouri et al., 2018; Aoto et al., 2013). However, it remains unclear whether LRRTM2 exerts ongoing control of synaptic transmission in established synapses. Given the location of LRRTM2 within the nanocolumn, we reasoned that its extracellular interactions may contribute to the nanoscale alignment of AMPARs to RIM nanodomains. To test this, we took advantage of the acute nature of the protease cleavage approach, which avoids the complications of compensation by other CAMs during the prolonged periods required for molecular expression.

Since we wanted to assure that we measured receptors only in cells where we manipulated LRRTM2 rather than nearby untransfected synapses, we first used two-color 3D dSTORM to measure the distribution of SEP-tagged AMPARs co-transfected with LRRTM2. Our previous work demonstrated that endogenous receptors are enriched in ~80 nm nanodomains aligned with surprising precision to presynaptic RIM nanodomains (Tang et al., 2016). As expected, SEP-GluA1/2 AMPARs in neurons co-transfected with BRS-Thr-LRRTM2* but treated only with vehicle formed nanodomains of ~80 nm, as judged by the autocorrelation of their distributions (Supplementary Fig. 7A,B). These were strongly enriched with RIM nanodomains across the cleft, decaying in enrichment over approximately 80 nm (Fig 4A, Supplementary Fig. 7C).

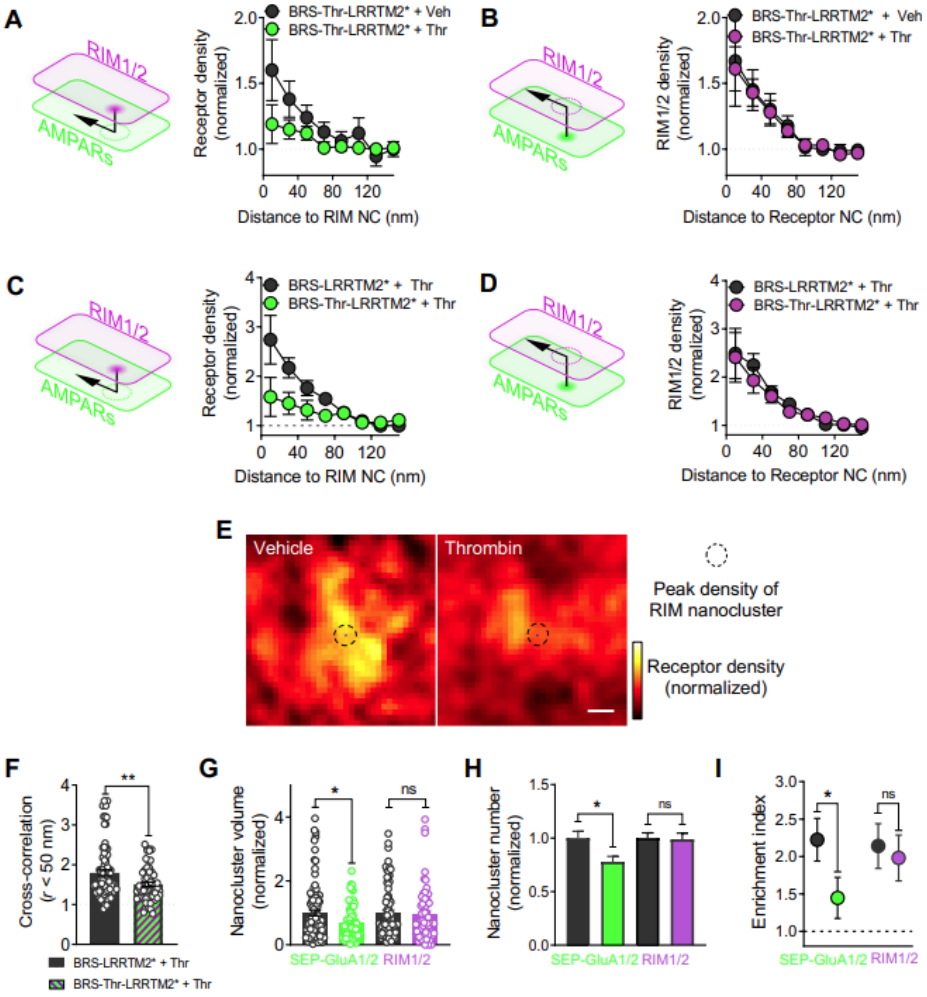


**Fig. 15. LRRTM2 is critical for AMPAR enrichment across from preferential sites of evoked neurotransmitter release. (A)** Schematic demonstrating the measurement of AMPAR localization density across from RIM1/2 nanoclusters (left). Quantification of AMPAR enrichment from neurons co-expressing BRS-Thr-LRRTM2* and SEP-GluA1/2 following treatment with thrombin (10 minutes, green) or vehicle (black). **(B)** RIM1/2 density across from AMPAR nanoclusters from neurons in A. **(C)** Quantification of AMPAR enrichment from neurons co-expressing either BRS-Thr-LRRTM2* (cleavable, green; n = 95 nanoclusters/11 neurons/3 independent cultures) or BRS-LRRTM2* (non-cleavable, black; 127/15/3) and SEP-GluA1/2 following treatment with thrombin (10 minutes). **(D)** RIM1/2 density across from AMPAR nanoclusters as displayed in B. Quantification (cleavable, magenta; n = 90/11/3) of BRS-LRRTM2* (non-cleavable, black; n = 103/15/3) and AMPARs following treatment with thrombin (10 minutes). **(E)** Representation of AMPAR density across from RIM1/2 peak density averaged across many synapses. Scale bar: 50 nm. **(F)** Paired cross correlation $g_c(r) < 50$ nm of synaptic protein pairs of SEP-GluA1/2 and RIM1/2 from thrombin treated neurons expressing BRS-LRRTM2* (black) or BRS-Thr-LRRTM2* (green). **(G)** Volume of AMPAR nanoclusters. **(H)** Number of detected AMPAR nanoclusters. **(I)** Enrichment indices ($g_r < 50$ nm) for AMPARs across from RIM1/2 nanoclusters (grey, green, left) and RIM1/2 across from AMPAR nanoclusters (grey, magenta, right). Data are presented as mean ± SEM, , * $p \leq 0.05$, ** $p \leq 0.01$, *** $p \leq 0.001$. Mann Whitney rank-sum test was performed for F-I.

In these neurons, we applied either vehicle (aCSF) or thrombin to test the acute regulation of AMPAR organization by LRRTM2's extracellular interactions. Remarkably, brief treatment with thrombin dramatically reduced the density of AMPARs directly across from RIM nanodomains (to 37.7 ± 9.1% of control enrichment index, Fig. 4A). Of note, RIM1/2 density across from detectable AMPAR nanodomains was unchanged (97.7 ± 12.2% of control, Fig. 4B), suggesting a strictly postsynaptic nanoscale re-organization of AMPAR patterning within the PSD, but also that the position of the detected AMPAR nanodomains relative to RIM1/2 nanoclusters were largely unchanged. Since we could not yet rule out that this was caused by specific or off-target effects of thrombin, we repeated the experiment except that neurons were transfected with either BRS-Thr-LRRTM2* or BRS-LRRTM2*, and both conditions received brief treatment with thrombin. Consistent with the prior result, thrombin treatment to neurons expressing the cleavable, but not the non-cleavable LRRTM2 resulted in a large reduction in AMPAR density across from RIM nanodomains (36.5 ± 27.3% of control enrichment index, Fig. 4C, Supplementary Fig. 7D), confirming that the effect is specific to the cleavage of the LRRTM2 ECD. Furthermore, RIM density across from these AMPAR nanodomains was again unaffected (92.5 ± 30.6% of control, Fig. 4D). To visualize this AMPAR de-enrichment another way, we calculated a 2D view of these data by aligning all receptor map data to the peak of their corresponding RIM1/2 nanocluster, producing a histogram of receptor density across from the RIM1/2 nanocluster peak averaged over all measured nanoclusters from many synapses (Fig. 4E). This output thus represents the average distribution of receptors arrayed in the synaptic membrane facing a vesicle that might fuse at the center of a RIM nanodomain. Following thrombin treatment, the peak of this receptor array is diminished, and receptors are

dispersed so that they are much less concentrated directly in line with the RIM nanodomain. Together, the rapid effect of thrombin in these experiments demonstrates that LRRTM2 via its extracellular domain is actively involved in the nanoscale organization of AMPARs within established synapses.

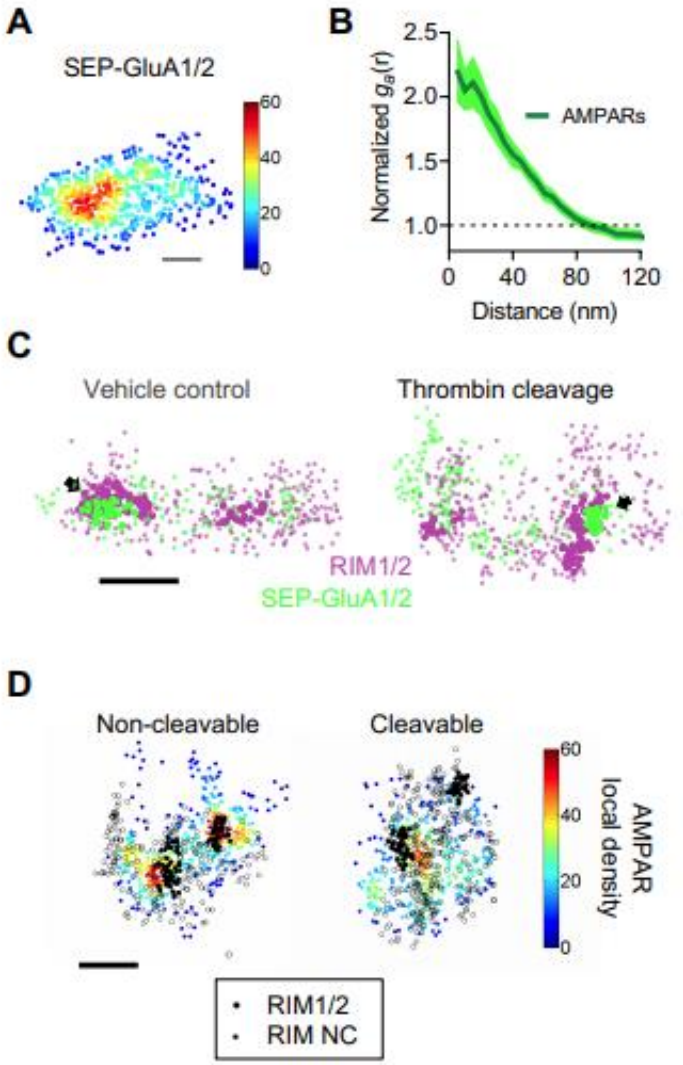


**Fig. 16. Representative images of RIM-AMPAR lateral distributions.** (A) En face view of SEP-GluA1/2 localizations coded by their local density (5xNN distance). Scale bar: 80 nm. (B) Auto-correlation of SEP-GluA1/2, decaying to 1 by ~80 nm. (n = 55 synapses, 5 neurons). (C) En face views of synapses treated with either aCSF (left, vehicle control) or thrombin (right) labeled for RIM1/2 (magenta) and SEP-GluA1/2 (green) imaged with 3D dSTORM. Arrows and bolded localizations indicate detected nanoclusters. Scale bar: 100 nm. (D) En face views of synapses treated with thrombin while expressing either BRS-LRRTM2* (non-cleavable) or BRS-Thr-LRRTM2* (cleavable) imaged with 3D dSTORM. RIM localizations are denoted by the open black circles and filled black circles represent nanocluster localizations. SEP-GluA1/2 localizations are denoted by the jet lookup table, coded by their local density (5X nearest neighbor distances) where warmer colors indicate a higher local density. Scale bar: 100 nm.

Changes in either the density or arrangement of these AMPAR nanodomains could have produced changes to the enrichment measurements. To further discriminate how AMPAR organization changed upon LRRTM2 cleavage, we assayed a number of properties that these AMPAR nanoclusters exhibited. To assess the effect on RIM-AMPAR alignment without explicitly identifying nanoclusters of either protein, we measured the cross-correlation between AMPAR and RIM1/2 density distributions from the same neurons transfected with BRS-Thr-LRRTM2* or BRS-LRRTM2*. This measure showed a reduction following LRRTM2 cleavage (63.8 ± 1.3% of control, Fig. 4F), indicating that their relative density distributions became less similar, consistent with the above. Receptor nanoclusters were 67.5 ± 0.7% the volume of control receptor nanoclusters (Fig. 4G), and 28.3 ± 0.8% less numerous (Fig. 4H), while RIM1/2 nanocluster number and volume were not altered (94 ± 10.9%, 98 ± 5.7%, respectively; Fig. 4G,H). Furthermore, the summary enrichment data (an average of the data within 50 nm of the opposite nanocluster) demonstrated a significant decrease following LRRTM2 cleavage for AMPARs, but not RIM1/2 (Fig. 4I). Taken together, these data are consistent with a model of a postsynaptic nanodomain-specific de-enrichment of AMPARs near RIM nanodomains. These data provide strong evidence that while not acutely required for controlling AMPAR number in the PSD (Fig. 2D-F), LRRTM2's ECD is critical for ongoing coordination of AMPAR density across from RIM nanodomains.

## Section 5. Numerical model to predict effects of LRRTM2 loss on synaptic transmission

These effects offer a unique opportunity to explore how changes in the nanoscale spatial organization of AMPARs in the PSD could alter receptor activation and synaptic transmission. To address this theoretically, we predicted the magnitude of the potential effect using a model based on prior work. Prior models of glutamate release and diffusion along with receptor opening kinetics have established that AMPAR open probability decreases characteristically as their distance to the site of release increases (Raghavachari & Lisman, 2004; Rusakov & Kullman, 1998). Beginning with this simplification enabled us to estimate the relative synaptic response after release given different receptor distributions within the PSD without explicitly simulating glutamate diffusion or receptor kinetics.

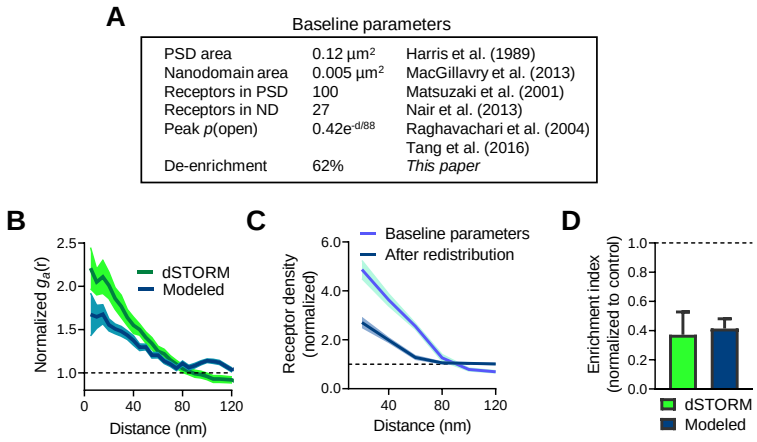


**Fig. 17. AMPAR activation model parameters.** (A) Baseline parameters incorporated into the model to estimate AMPAR peak open probability from modeled receptor organizations and release site positions. (B) Auto-correlation of measured SEP-GluA1,2 (from experiments in Fig. 4b, n = 55 synapses, 5 neurons) and modeled AMPAR organizations with a single modeled nanodomain (n = 100 randomizations). (C) Distribution of AMPAR density as a function of the distance to the modeled nanodomain normalized to the average synaptic density and the impact upon this self-enrichment following the redistribution of AMPARs from within the nanodomain to out of the nanodomain. (D) Normalized enrichment indices (gr(<50 nm)) for measured SEP-GluA1/2 (Fig. 4m) and modeled AMPARs following LRRTM2 cleavage and AMPAR redistribution, respectively.

We generated simulated receptor maps based on several key synapse features obtained from our measurements and the literature (Fig. 5A,B and Supplemental Fig 6A). When subjected to our spatial analysis, this basal arrangement of simulated receptor positions recapitulated the autocorrelation (Supplementary Fig. 8B) and well reflected both the relative change in the enrichment profile (Supplementary Fig. 8C) and the relative change in the enrichment index (Supplementary Fig. 8D) for receptors as measured in our cultured neurons. To deduce how many AMPARs would need to leave the nanodomain to result in de-enrichment to the same degree as observed after cleavage of LRRTM2 (Fig. 4F, 4M), we removed different numbers receptors from the modeled nanodomain, placed them randomly within the PSD, and then compared the enrichment profile of the redistributed synapse to that of the original modeled synapse. A loss of ~16 AMPARs from the modeled nanodomain resulted in a ~60% reduction in density within the nanodomain and well recapitulated the experimentally observed decrease in enrichment (Supplementary Fig. 6C,D).

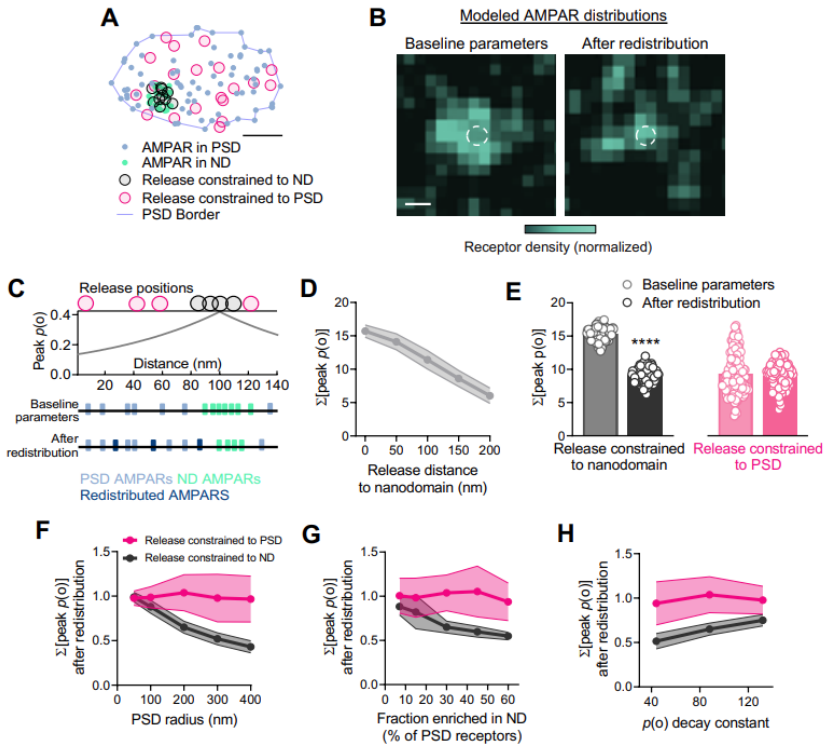


**Fig. 18. Numerical model to predict the effects of LRRTM2 loss on synapse function.** **(A)** Example of the distribution of randomized AMPAR positions within the PSD and nanodomain and the distribution of randomized vesicle release positions, where release is constrained to either the boundary of the nanodomain (black) or PSD (magenta). Scale bar: 100 nm. **(B)** Representative density histograms of individual modeled receptor distributions. **(C)** Schematic demonstrating the calculation of peak open probability of all AMPARs within the PSD given a randomized release position constrained as described in a. **(D)** Calculation of the summed peak open probability of AMPARs as the release position is offset from the nanodomain. **(E)** Calculation of the summed peak open probability of AMPARs for release positions constrained to the nanodomain (left) and release positions constrained to the PSD (right) using the modeled nanodomain parameters (grey, black) and redistribution of AMPARs (pink, magenta). **(F)** Calculation of the summed peak open probability of AMPARs as PSD diameter is adjusted. **(G)** Calculation of the summed peak open probability of AMPARs as the proportion of AMPARs included in the nanodomain is adjusted. **(H)** Calculation of the summed peak open probability of AMPARs from as the peak open probability as a function of distance decay constant is adjusted ± 50%. Data in F-H are normalized to the baseline parameters condition. Data are presented as mean ± SEM. For all modeled data $n$ = 100 randomizations/bin or 100 randomizations/condition. Mann Whitney rank-sum test was performed for E, **** $p \leq 0.0001$.

Increasing evidence suggests that evoked and spontaneous transmission involve separable presynaptic structures (Ramirez et al., 2011) and activate separated groups of receptors (Kavalali, 2015), but their potential differential dependence on receptor nano-organization is not known. To model the impact of receptor redistribution on these different

release modes, randomized release positions were constrained either to the nanodomain or the PSD as a whole to inform our predictions about evoked and spontaneous release, respectively (Fig. 5A, (Tang et al., 2016)). Then, by indexing the AMPAR peak open probability as function of distance from the vesicle fusion site (as in Tang et al., 2016, shown schematically in Fig. 5C, Tang et al., 2016), we calculated the mean summed peak open probability of all receptors in response to single glutamate release events before and after receptor redistribution. EPSC kinetics are not captured in such a model, but the mean summed peak open probability successfully indicated that release events closer to receptor nanodomains produce larger predicted responses (Fig. 5D) consistent with results observed from Haas et al. (2018).

To simulate the receptor reorganization observed after acute cleavage of LRRTM2, we removed the portion of the receptors from the nanodomain determined from the modeling above (16 of 27) and placed them randomly into the PSD outside the nanodomain. This manipulation substantially reduced the predicted response to release constrained to the receptor nanodomain (59.4 ± 0.1% of control; Fig. 5E, left). Thus, the model predicts that evoked transmission at "average" synapses would be reduced by roughly 60% after LRRTM2 cleavage. Strikingly, despite this strong effect, the response to release events occurring at randomized positions across the AZ was essentially unaltered (96.3% ± 0.1% of control; Fig. 5E, right). Interestingly, variability of response amplitude for spontaneous release was reduced upon redistribution (CV 33.03% for baseline parameters and 20.31% after redistribution), suggesting that heterogeneity of receptor density across the face of an individual PSD contributes to the response CV at that synapse.

This difference between the decrement of response to release at a nanodomain or across the synapse persisted over a range of parameters. For instance, we found that as PSD size increases, the proportional effect of receptor redistribution grows larger (Fig. 5F), suggesting that nano-alignment may be most critical for maximizing postsynaptic responsivity at large synapses. Similarly, positioning a greater fraction of receptors within the nanodomain resulted in a greater reduction in mean summed peak open probability upon redistribution (Fig. 5G) but again this only affected release constrained to the nanodomain, and no differences were observed in the mean of the responses with release constrained to the PSD.

A key parameter in the model is the decay profile in receptor open probability as a function of distance from the release site, here modeled by default as $Po(d) = 0.42e^{-d/88}$ adapted from previous work (Tang et al., 2016; Raghavachari & Lisman, 2004). To test whether the outcomes were robust to changes in this parameter, we varied this decay constant by 50% in either direction. This altered the magnitude of influence as expected but did not qualitatively affect the outcome. When the decay rate was decreased ($-d/44$) making receptors less sensitive to release position, the mean summed peak open probability after nanodomain release events was elevated (not shown) yet was still strongly reduced upon redistribution (Fig. 5H). Conversely, when the rate of decay was increased ($-d/132$), responses were lower but also strongly reduced after redistribution. Note that for all values of the decay constant, in response to the modeled spontaneous release events, the mean summed peak open probability was essentially unchanged by redistribution of receptors (Fig. 5H).

Together, these simulations most generally suggest that receptor distribution within a PSD strongly influences the amplitude of evoked but not average spontaneous neurotransmission at that synapse. Specifically, they predict that following LRRTM2 cleavage, the amplitude of evoked EPSCs but not spontaneous mEPSCs should decrease substantially.

**Section 6. LRRTM2 is critical for basal strength of evoked, but not spontaneous transmission**

To assess these predictions of functional effects of AMPARs nanostructural remodeling within the PSD following LRRTM2 cleavage, we performed patch-clamp recordings from cultured hippocampal neurons while stimulating nearby cells to evoke synaptic responses (Fig. 6A, Supplementary Fig. 9A). In untransfected neurons, thrombin application had no effect on EPSC amplitude (98.8 ± 7.7% after 10 min, n = 9, Fig. 6B), confirming a lack of non-specific or endogenous effects of the protease. Similarly, in cells transfected with LRRTM2 knockdown and rescued with the non-cleavable GFP-LRRTM2*, EPSCs were unaffected (95.5 ± 5.8%, n = 9, Fig 6B). However, in cells transfected with GFP-Thr-LRRTM2*, acute cleavage of the LRRTM2 ECD resulted in a 45.3% ± 7.6% reduction in EPSC amplitude (n = 12, Fig. 6B), consistent with our modeling results.

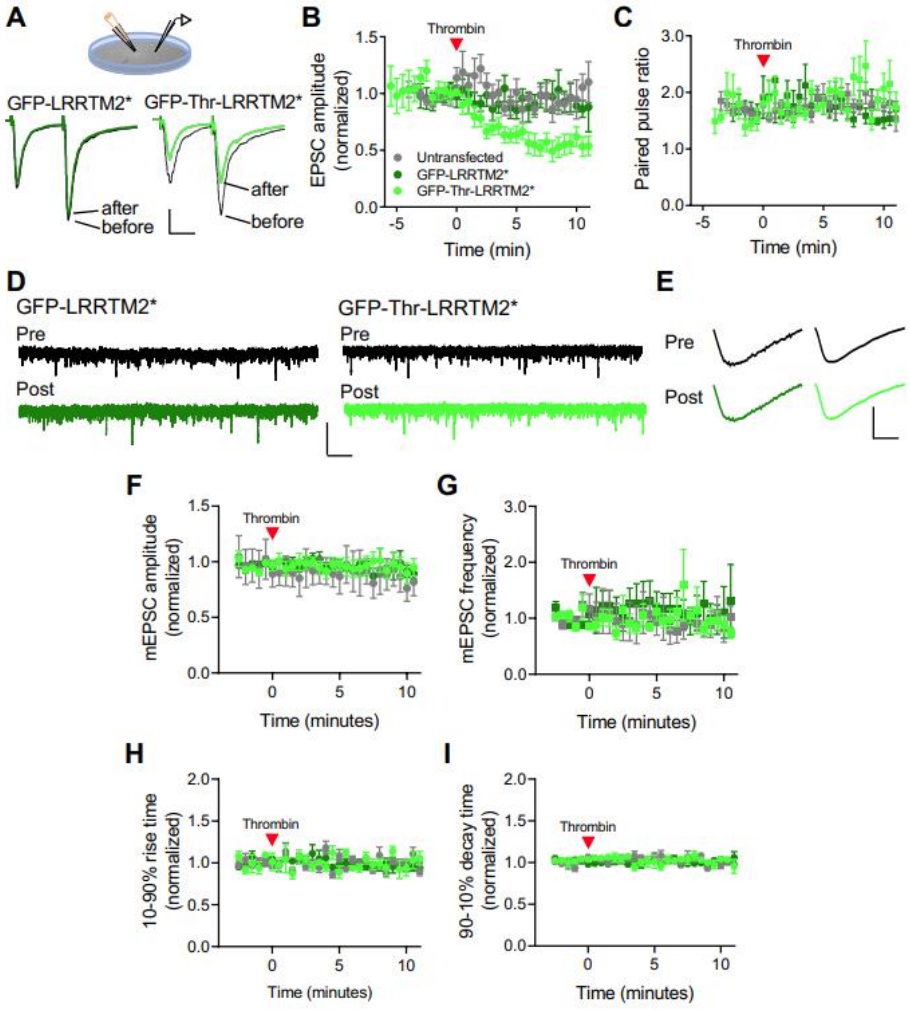


**Fig. 19. LRRTM2 is critical for basal strength of evoked but not spontaneous transmission. (A)** Schematic of whole-cell patch clamp recordings from cultured hippocampal neurons with bipolar electrode stimulation to evoke synaptic currents. Below, averaged traces of evoked synaptic events. Neurons transfected with GFP-Thr-LRRTM2* (light green, cleavable, post-thrombin), GFP-LRRTM2* (dark green, non-cleavable, post-thrombin), where black indicates their respective baselines. Scale bar: 100 pA, 20 ms. **(B)** Quantification of evoked synaptic current amplitudes normalized to their baseline measurements over time from neurons expressing GFP-LRRTM2* (dark green; n = 9 neurons/3 independent cultures), GFP-Thr-LRRTM2* (light green; n = 12/3), or untransfected neurons (grey; n = 9/3). **(C)** Quantification of the paired-pulse ratio. **(D)** Representative traces of miniature EPSC (mEPSC) recordings from cultured hippocampal neurons transfected with GFP-LRRTM2* (dark green) or GFP-Thr-LRRTM2*(light green) before and after the application of thrombin. Scale bar: 35 pA, 2 s. **(E)** Averaged traces of miniature synaptic currents. GFP-Thr-LRRTM2* (light green) and GFP-LRRTM2* (dark green). Scale bar: 5 pA, 2 ms. **(F)** Quantification of miniature synaptic current amplitudes from GFP-LRRTM2* (n = 8/3), GFP-Thr-LRRTM2* (n = 8/3), or untransfected neurons (n = 5/3) before and after the application of thrombin. **(G)** Quantification of miniature frequency before and after the application of thrombin. **(H)** Quantification of the 10-90% rise times of mEPSC events over time, before and after the application of thrombin. **(I)** Quantification of the 90-10% decay time of mEPSC events over time, before and after the application of thrombin. Data are presented as mean ± SEM.

Deficits in presynaptic release probability could have contributed to the decreased EPSC amplitude. To test this, we calculated the paired-pulse ratio of responses to stimuli 50 ms apart. Thrombin treatment had no effect on the paired-pulse ratio across GFP-Thr-LRRTM2*, GFP-LRRTM2*, and untransfected neurons (Fig. 6C), as well as compared to their own baselines. These data suggest changes in release probability did not drive the changes in the evoked response amplitude after LRRTM2 cleavage.

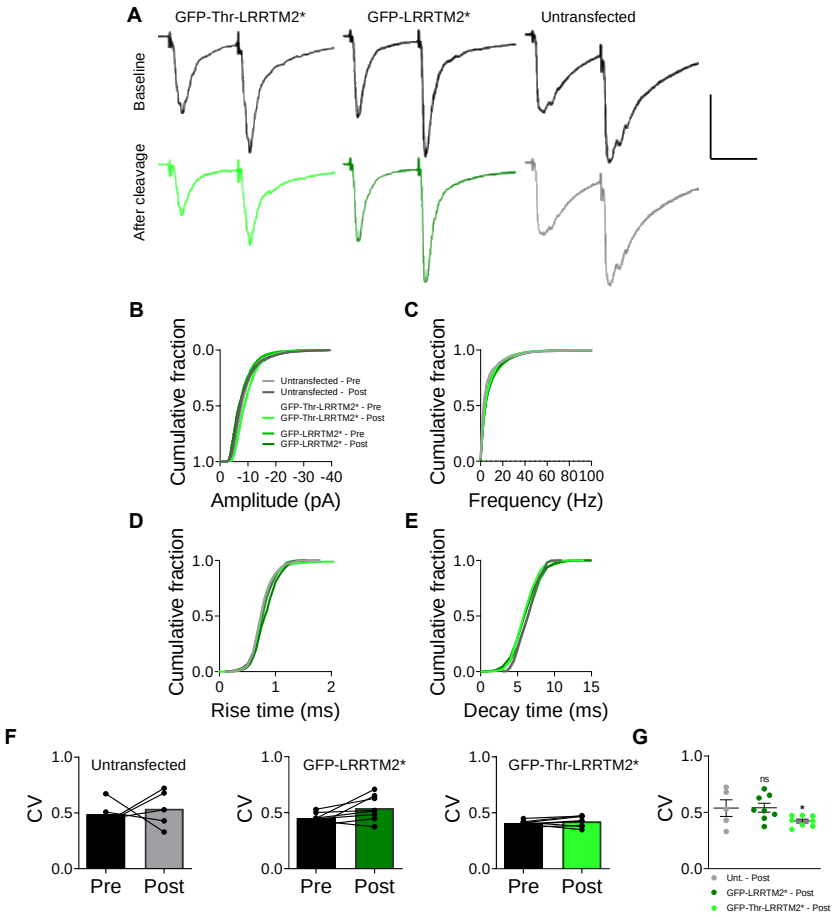


**Fig. 20. Synaptic responses before and after the application of thrombin.** (A) Traces from Fig 6a, replotted offset from one another for clarity. Scale bar, 100 pA, 20 ms. (B-G) Quantification of spontaneous mEPSCs from neurons transfected with GFP-LRRTM2* (n = 8 neurons/3 independent cultures), GFP-Thr-LRRTM2* (n = 8/3), or untransfected neurons (n = 5/3) before and after the application of thrombin. (B) Amplitude, (C) frequency, (D) 10-90% rise time, (E) 90-10% decay time, (F) and coefficient of variation (CV) for each neuron for pre- and post-thrombin bins. (G) Summary of post-thrombin CV among these groups. One-way ANOVA with Dunnett's multiple comparison, $p < 0.05$ = *.

To test the effect of LRRTM2 cleavage on the postsynaptic response to spontaneous release of glutamate, we measured miniature EPSCs (mEPSCs; Fig 6D-I) from neurons expressing GFP-LRRTM2* or GFP-Thr-LRRTM2*. Thrombin application did not change mEPSC amplitude in cells transfected with non-cleavable GFP-LRRTM2*. Neurons transfected with cleavable GFP-Thr-LRRTM2* also showed no changes to mEPSC amplitude following thrombin application (98.5 ± 3.7% of control, Fig. 6F, Supplementary Fig. 9B), consistent with the model's prediction. Nevertheless, the coefficient of variation of mEPSC amplitude was smaller after thrombin exposure in neurons expressing GFP-Thr-LRRTM2* vs GFP-LRRTM2* (Supplementary Fig 9G), as expected based on modeling (Fig 5E). Together, these results suggest that the number of synaptic AMPARs was not changed upon the acute loss of the LRRTM2 ECD, consistent with results in Fig. 2 that synaptic content of both surface AMPARs and PSD-95 was unchanged within 30 minutes following LRRTM2 cleavage.

To further test if loss of the LRRTM2 ECD alters presynaptic mechanisms, we quantified mEPSC frequency. Neurons transfected with the non-cleavable LRRTM2 showed no changes in frequency after 10 minutes of thrombin exposure (91.7 ± 19.4% of control, Fig. 6G, Supplementary Fig. 9C), consistent with the lack of nonspecific or endogenous protease effects. Interestingly, neurons transfected with GFP-Thr-LRRTM2* also showed no changes following 10 minutes of thrombin treatment (Fig. 6G), further strengthening the idea that the LRRTM2 extracellular domain does not acutely regulate presynaptic release probability. It was previously shown that extracellular cleavage of NL-1 reduced evoked EPSC amplitude without changing in mEPSC amplitude, and this was attributed to a reduction of presynaptic release probability (Peixoto et al., 2012). As NL-1

and LRRTM2 share presynaptic Nrx as a ligand, we examined whether NL-1 cleavage also resulted in reorganization of transsynaptic alignment. Interestingly, the acute cleavage of NL-1 did not change the relative nano-alignment of RIM and AMPARs (Supplementary Fig. 10). This further distinguishes the unique role of LRRTM2 in maintaining synapse nanoarchitecture.

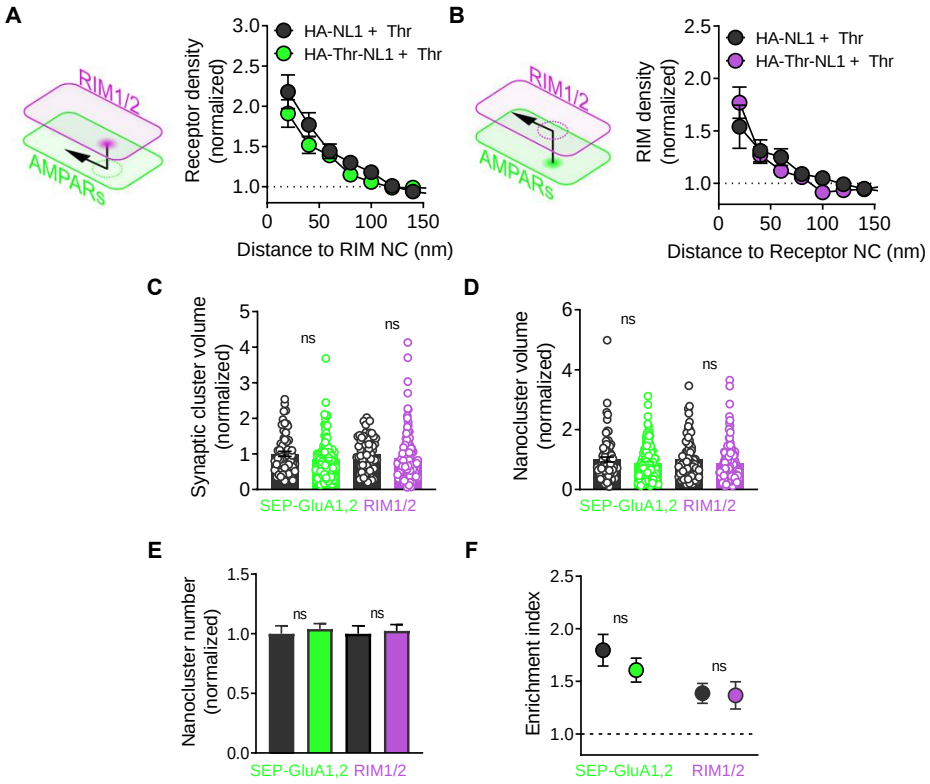


**Fig. 21. Acute cleavage of the neuroligin-1 extracellular domain does not change RIM-AMPAR nanostructure.** (A) Left, schematic demonstrating the measurement of AMPAR density across from RIM nanodomains in neurons transfected with SEP-GluA1,2 and HA-NL1-Thr or HA-NL both treated with thrombin. Right, quantification of receptor density as a function of distance to the RIM nanocluster. (B) Left, schematic demonstrating the measurement of RIM density across from AMPAR nanodomains in neurons transfected with SEP-GluA1,2 and HA-NL1-Thr or HA-NL both treated with thrombin. (C) Quantification of normalized synaptic cluster volume, (D) normalized nanocluster volume, (E) nanocluster number, and (F) enrichment indices. Data are presented as mean ± SEM, * $p \leq 0.05$, ** $p \leq 0.01$, *** $p \leq 0.001$. Mann Whitney rank-sum test was performed for C-F.

Numerical models of glutamate diffusion and AMPAR kinetics have demonstrated that glutamate release away from AMPARs delays the opening of these channels by decreasing the number of immediately doubly-bound receptors, leaving many in a singly-bound state and slowing the rise of the EPSC as the concentration of glutamate in the cleft quickly equilibrates (Franks et al., 2003). Unfortunately, the measured variability in EPSC kinetics in our approach (which did not stimulate single presynaptic neurons for analysis) appeared to be dominated by variation in axonal conduction and other presynaptic factors, precluding interpretation of EPSC kinetics. However, we tested whether mEPSC kinetics were disrupted after LRRTM2 cleavage. We quantified both normalized and raw 10-90% rise time (Fig. 6H, Supplementary Fig. 9C) and 90-10% decay times (Fig. 6I, Supplementary Fig. 9D) of mEPSCs from neurons transfected with either GFP-LRRTM2* and GFP-Thr-LRRTM2* before and after the application of thrombin. Representative averaged traces (Fig. 6E) and group quantification, however, demonstrated no change in either the rise time (101.8 ± 8.9% of control, Fig. 6H) or the decay time (100 ± 4.2% of control, Fig. 6I). These results in combination with the raw and normalized miniature amplitudes (Supplementary Fig. 6F, Supplementary Fig. 7B), which are also sensitive to changes in single channel kinetics, suggest no population changes in AMPAR single-channel kinetics following the cleavage of the LRRTM2 ECD. These results are consistent with our numerical model of AMPAR position within the PSD (Fig. 5), where the average distance of AMPARs to the modeled spontaneous release positions across the AZ was unchanged upon AMPAR redistribution.

Taking these data together, we conclude that the LRRTM2 extracellular domain is required for close positioning of AMPARs to sites of evoked vesicle fusion, and that this distribution of receptors preferentially enhances evoked, but not spontaneous postsynaptic response amplitude.

# CHAPTER 4: Discussion

## Section 1. Summary of major findings

I used acute proteolysis of the LRRTM2 extracellular domain to test the idea that transsynaptic interactions in the synaptic cleft control molecular organization and function of established synapses, independent of synapse formation and on rapid time scales. These results demonstrate that acute cleavage of LRRTM2 quickly led to dispersal of its extracellular domain from synapses and prompted a strong reduction in the strength of evoked but not spontaneous synaptic transmission. Based on several lines of evidence, I conclude that this reduction in transmission arose from nanoscale redistribution of AMPARs within the synapse away from sites of glutamate release. First, LRRTM2 is concentrated in the synaptic nanocolumn, heavily enriched in nanoscale subdomains containing PSD-95 and AMPARs and aligned trans-synaptically with RIM nanodomains in the active zone. Second, after cleavage of LRRTM2, AMPARs became less densely enriched across from RIM nanodomains, even though total AMPAR content in synapses as measured by immunostaining or live imaging was unchanged for at least 30 minutes. Third, despite marked alteration of AMPAR distribution, the acute disruption of LRRTM2 did not grossly alter synapse number, structure, or molecular content, and notably the total synaptic content of PSD-95 also did not change within this period of interest. Fourth, presynaptic function was unaltered, as judged by fully intact spontaneous release and evoked paired-pulse response ratio. Finally, numerical modeling of AMPAR activation based on our nanostructural measurements of AMPAR position well predicted the degree of reduction in evoked transmission, while also providing a mechanism for the lack of effect on the amplitude of spontaneous EPSCs. Together, these findings provide support

for a model in which the nanoscale patterning of AMPARs is dynamically controlled by interactions of LRRTM2 with cleft proteins enriched within the nanocolumn, and that this organization can dramatically enhance AMPAR activation during evoked synaptic transmission. The differential control of evoked and spontaneous transmission at single PSDs may mediate discrete forms of activity-dependent regulation even at individual synapses. CAM-mediated nano-organization of AMPARs also has both functional and structural implications for synaptic plasticity both upstream and downstream of induction.

## Section 2. Receptor distribution within synapses affects synaptic strength

2.1 Altered distance from release site, without loss of receptors, decreases activation

The close correspondence between our measurements and the predictions from numerical modeling provide experimental support for the longstanding notion that receptor distribution within synapses affects synaptic strength (Biederer et al., 2017; Tang et al., 2016; Heine & Holcman, 2020). Modeling indicates that the combination of the sharp decay of glutamate concentration away from the site of fusion with the rapid kinetics of AMPAR activation and desensitization necessitate that AMPARs positioned closest to the site of glutamate exocytosis contribute proportionally most to EPSCs (Freche et al., 2011; Raghavachari & Lisman, 2004). The quick relaxation of EPSC amplitude towards a reduced steady state that I observed following LRRTM2 cleavage indicates that this mechanism likely plays a role in maintaining basal synaptic strength. In further support of this mechanism, sustained disruption of NL-1 also reduces alignment of AMPARs with RIM (Haas et al., 2018), suggesting that neurexin binding partners may be central to maintaining functional synaptic nanoarchitecture over multiple time scales. Mechanisms that maintain synaptic strength absent the active induction of plasticity are not clear, but have been postulated to involve adhesion systems (Benson et al., 2000). Taken most broadly, our findings suggest that mechanisms of synaptic maintenance may be divided into those which establish the molecular constituent list including AMPAR number, and those which facilitate appropriate nanostructural organization. It is interesting to consider whether synapses of limited molecular complexity may adopt a somewhat disorganized configuration "by default," whereas the presence of LRRTM2 enables organization into a configuration of higher synaptic potency.

## 2.2 Postsynaptic neurexin ligands control AMPAR nano-alignment

Trans-synaptic protein interactions are expected to influence synaptic nano-organization. Neurexins interact with a large number of postsynaptic proteins, including those which mediate interactions with receptors (Südhof, 2018). Two neurexin ligands are key candidates in controlling the alignment of AMPARs to sites of glutamate release: LRRTM2 and NL-1. Both LRRTM2 and NL-1 have been proposed to mediate AMPAR number and mobility within synapses (Aoto et al., 2013; Bhouri et al., 2018; Mondin et al., 2011). However, the mechanisms through which LRRTM2 and NL-1 control AMPAR mobility in synapses are markedly different. Experiments from this thesis further test how these two CAMs influence synaptic nanostructure and transmission. Depending on the type of manipulation of these proteins, a number of differences in synaptic organization and function have been observed. Different outcomes of manipulating LRRTM2 and NL-1 may be attributed to these proteins' subcellular distributions, subsynaptic distributions, mobility, ability to dimerize, and protein interactions. Discussion of these findings in detail will hopefully make clearer how these molecules may be involved in nanocolumn organization. These neurexin ligands may control distinct aspects of the coordination between glutamate release and AMPAR positioning.

The neurexin ligand NL-1, which is important for the diffusional trapping of AMPARs through intracellular interactions with PSD-95 (Mondin et al., 2011), is hypothesized to align AMPARs across from RIM at submicron scales (Haas et al., 2018). To test this, Haas et al. used single-molecule imaging, electrophysiology, and numerical estimations of receptor activation to link the functional roles of NL-1 to synaptic nanostructure. Rather than a traditional loss of function approach like a knockout or

knockdown, NL-1's intracellular protein interactions were disrupted by expressing C-terminal deletion mutants or incubation with biomimetic peptides of NL-1's C-terminus. These intracellular manipulations aimed to provide key molecular information about which domains of NL-1 are important for the observed structural and functional outcomes. Importantly, the C-terminal mutant expression experiments were performed in the context of overexpression, with both manipulations taking effect over the course of days. It should be noted that Haas et al. state that the overexpression of NL-1 ΔC-terminal mutants produce a greater number of synapses, AMPAR content, presynaptic function, and changes to the CV (discussed later). This greatly reduces confidence in NL-1 specific control of nanostructure and any implication that nanostructure directly influences synaptic strength. The time course of these manipulations may permit homeostatic changes in synapse function (i.e., within 48 hours; Hou et al., 2017; Turrigiano et al., 1998), which makes forming conclusions about the ongoing role of NL-1 difficult. Furthermore, the peptide used was a biomimetic peptide that constituted that last 15 amino acids of NL-1, which is known to bind to PSD-95 (Irie et al., 1997). Thus, any number of PSD-95 interacting molecules may be non-specifically disrupted over the days-long incubation, including LRRTM2 (Haas et al., 2018). Taken together, the time course of the manipulations, the context of overexpression, and the non-specificity of the peptide incubation make conclusions difficult.

Using a fairly standard colocalization analysis (Manders et al., 1993), they found that there was decreased colocalization between RIM and endogenous AMPARs following expression of ΔC-terminal mutants or incubation with biomimetic peptides of the C-terminus of NL-1. They found that RIM and GluA2 clusters were of a typical area and

density compared to controls, but following both manipulations there is a greater distance between clusters. They propose a model where there was a nanoscale (range: 0-800 nm) shuffling of intact AMPAR nanodomains away from RIM clusters. Unfortunately, they do not make the effort to distinguish what constitutes synaptic AMPARs from those concentrated in subsynaptic domains and perform analysis on all clusters larger than the size of a single emitter (~0.005 $\mu m^2$). Interestingly, our manipulation of LRRTM2 led to much different results, despite both being neurexin ligands. Acute proteolytic cleavage of the LRRTM2 ECD led to the dispersal of AMPAR nanodomains and redistribution of AMPARs throughout the entire area of the PSD. One technical note is that our analysis involves intact tightly juxtaposed 3D synaptic clusters of pre- and postsynaptic molecules. AMPARs redistributed within the PSD, and these synaptic cluster positions relative to one another were not affected. However, the distance between objects is what Haas et al. predominantly captured with their 2D analysis, perhaps suggesting that AMPARs were no longer synaptic. In our manipulation of the ECD of LRRTM2, the cross-correlation, cross-enrichment analysis, nanocluster volume, and nanocluster number were consistent with a strictly postsynaptic nanodomain-autonomous dispersal of AMPARs away from RIM nanodomains, but not prompting their exit from the synaptic cluster, as confirmed by live-cell confocal imaging. The intracellular disruption of NL-1 interactions implicate NL-1 in the positioning of AMPARs relative to RIM. Meanwhile, the extracellular interactions of LRRTM2 are important in controlling the subsynaptic distribution of AMPARs. The results of both studies are interpreted to uncouple the trans-synaptic coordination of receptor positioning and sites of neurotransmitter release, with the phenotype observed

with NL-1 perturbation seeming more severe, perhaps due to the loss of synaptic AMPARs, which could not be established by their analysis (Haas et al., 2018; Ramsey et al., 2021).

The acute elimination (on the scale of minutes) of the LRRTM2 ECD led promptly to a decrease in the evoked EPSC amplitude, but not spontaneous response amplitude, with no effect on presynaptic function (Ramsey et al., 2021). Disruptions to NL-1 intracellular interactions led to decreases in evoked, spontaneous, and asynchronous response amplitudes, and some difficult to interpret impacts on presynaptic function in the cases of NL-1 overexpression (Haas et al., 2018). However, extracellular cleavage of the NL-1 ECD by other groups led quickly to a reduction in neurexin content and release probability (Peixoto et al., 2012). It should be noted that in Haas et al. (2018) the target of the manipulation in both cases was against the C-terminus in an effort to disrupt its scaffold interactions, and the different termini of the protein could play very different roles in synapse organization and function. However, it remains unclear how spontaneous release was impacted by the proposed internal rearrangement of the *same number* of receptors. Our model demonstrated that spontaneous release would only be affected if AMPARs were lost. This leaves open many questions regarding the differential regulation of spontaneous and evoked receptor activation. It is possible that the distance between RIM and GluA2 clusters and the internal rearrangement of postsynaptic AMPARs depend upon different mechanisms, something beyond just AMPAR distance to sites of vesicle fusion. Regardless, it could be interpreted that intracellular manipulations of NL-1 and extracellular manipulations of LRRTM2 lead to distinct nanostructural effects that effectively increased the average distance of AMPARs from sites of release. This increased distance between AMPARs and the site of glutamate exocytosis is expected to decrease

receptor activation. However, changes to AMPAR distance to sites of release was accompanied by a range of effects in Haas et al. (2018), perhaps requiring further dissection of the mechanisms at play.

The general model arrived at in Haas et al. (2018) is one where intact nanoclusters of AMPARs are aligned across from various different kinds of neurotransmitter release sites (evoked, spontaneous, and asynchronous), which is quite a striking concept. There is evidence that these release sites occur at different subsynaptic compartments of the active zone (Tang et al., 2016; Li et al., 2021).The results from Haas et al. suggest that NL-1 mediates AMPAR alignment at many different subsynaptic sites. The Haas et al. functional outcomes suggest that NL-1 is important for alignment of AMPARs to all major sites of neurotransmitter release. This is perhaps consistent with the finding that NL-1 is more broadly distributed within synapses than LRRTM2 (Chamma et al., 2016). It still remains possible that the number of AMPARs at the synapse were reduced after the intracellular disruption of NL-1, but that changes in synaptic AMPAR number were not able to be captured by the imaging approach or analysis. In fact, the loss of AMPARs from synapses may be expected. The PDZ interactions of PSD-95 are known to anchor AMPARs at synapses but were likely saturated or greatly disrupted by their biomimetic peptide experiments (Bats et al., 2007; Sainlos et al., 2011). Even acute disruption of PSD-95-mediated protein interactions can lead to as much as an ~80% reduction in GluA2 surface staining (Yudowski et al., 2013). Furthermore, expression of the NL-1 C-terminal mutant fails to immobilize and accumulate AMPARs to PSDs relative to WT NL-1 and leads to a reduction in synaptic AMPAR number and excitatory transmission (Chih et al., 2005; Nam & Chen, 2005; Mondin et al., 2011). There is no discrimination between synaptic and non-

synaptic AMPAR content following the manipulations, making it difficult to attribute any of the observed functional effects to the nanoscale organization of AMPARs rather than simply their number in the PSD. Additionally, I found that the acute cleavage of the neuroligin-1 ECD produced no observable changes in AMPAR nanostructure, but this result could indicate that it is NL-1's intracellular interactions with PSD-95 as the mechanism by which AMPARs are organized within synapses. The combination of the molecular details of the manipulation, limited spatial analysis, and the broad functional effects complicate the conclusions of Haas et al., where it is put forward that the coupling of AMPARs to active zone proteins that instructs their alignment, while the results seem more consistent with a loss of synaptic AMPARs.

## 2.3 The functional impact of trans-synaptic nanostructure

There are many different ways that synaptic transmission could be influenced given the nanoscale organization of AMPARs and neurotransmitter release sites. If pre- and postsynaptic nanoclusters display standard properties, but are not located nearby one another in the synapse, then the strength of transmission would be reduced. AMPAR nanodomains weight the average density of receptors directly across from sites of release under basal conditions. AMPAR nanodomains are thought to consist of a large fraction of PSD AMPARs (Nair et al., 2013). If an AMPAR nanodomain is not aligned with release, then the average closest distance of receptors nearby release sites will be reduced (Haas et al., 2018). Similarly, if presynaptic nanostructure is observed to be typical, and AMPARs are simply redistributed from within nanodomain to random areas of the PSD, then receptor distance from release sites will increase, and affect receptor activation (Ramsey et al.,

2021). The difference between these scenarios is that if typical nanodomains of AMPARs are misaligned with release sites, they sequester a large fraction of AMPARs in the PSD away from potential sites of release. Exactly how far that AMPAR nanodomain translocates away from release sites is then important, since a short distance away will still keep a large number of receptors a short distance away, but a large distance away keeps a large fraction of receptors a large distance away (Haas et al., 2018). Alternatively, if postsynaptic AMPARs simply disperse from nanodomains randomly, the degree of impact is based on how many fractional PSD receptors leave the nanodomain and the area of the PSD (Ramsey et al., 2021). Additionally, the mechanisms which constitute clustering of receptors at the nanoscale will always impact nano-alignment, but the mechanisms that constitute nano-alignment do not necessarily impact the properties of AMPAR nanodomains. Studies of disruptions to the trans-synaptic interactions of adhesion molecules have now produced well-defined biological examples of at least these two mechanisms by which synaptic nanostructure can impact function (Haas et al., 2018; Ramsey et al., 2021). Alternatively, evoked release sites could be selectively impaired, disassembling their molecular constituents, which could lead evoked fusion to exhibit a less concentrated spatial distribution of release positions more similar to that of spontaneous transmission (Tang et al., 2016). This scenario would likely additionally lead to an overall lower release probability. If functional release positions became more random across a larger area of the PSD, it decreases the likelihood of the greatest number of receptors nearby, thus impacting postsynaptic receptor activation *q*, in chorus with release probability *p*. Interestingly, this has yet to be observed in biology, but some similar mechanisms may exist in homeostatic potentiation of active zones (Mrestani et al., 2021).

No matter the hypothetical scenario, it is now clear that it is paramount to understand the nanoscale relationship between release and receptor positions when deficits to synaptic transmission are observed in order to truly understand the factors underlying the phenomenon. It no longer seems useful or sufficient to consider deficits in synaptic transmission as presynaptic or postsynaptic based on a few experimental readouts, and that prior terminology, *n*, as the number of functional release sites and *q* as the number of activated receptors in response to a single vesicle, in fact more appropriately help to explain these deficits in synaptic transmission. And additionally, the synaptic parameters of *n*, *p*, and *q* need to be understood as readouts that can be impacted by the spatial organization of proteins within synapses.

Although our rather simple numerical model was sufficient to explain the observed phenomena, there are certainly features that can be improved. Most notably, our numerical model that takes into account the AMPAR distribution of single synapses and the active zone distribution of various release modes, where the model hard codes these receptors and release positions as a set position, rather than a probability. The current model considers only a single slice of time wherein these receptors and release sites occupy these set positions. Though, these set positions are representative of their average positions, it would strengthen future predictions to integrate release likelihood and receptor position likelihood, in addition to the open likelihood of receptors and their relevant kinetic schemes. Unfortunately, this vesicle fusion likelihood for varying release modes is not well understood, but good progress has been made toward better understanding it in the spatial coordinates of active zones (Tang et al., 2016; Li et al., 2021; Martinez-Sanchez et al., 2021), despite these exemplary cases, spatial and temporal resolution of single vesicle

release positions in the active zones of live cells remains a challenge. Stochastic models that also incorporate the probability of specific modes of vesicle release site distributions, stochastic protein binding interactions, and receptor kinetics will be a next large step *in silico*.

As laid out in the introduction, there are many biophysical constraints that come together to explain the distance-dependent nature of transmission at excitatory hippocampal synapses. The sensitivity of any given synapse in the hippocampus or otherwise to the subsynaptic relationship between receptors and sites of release may be quite variable. This organization is likely not to be guaranteed for all synapse types or sizes. It is expected that at the otherwise "average" hippocampal synapses with a smaller area will be less sensitive to the arrangement of receptors relative to sites of release. However, as laid out in the introduction, Schaeffer collateral synapses possess an apt set of biophysical properties spanning the synapse that confer a large degree of the postsynaptic response amplitude through the subsynaptic organization of AMPARs. Importantly, the sensitivity of a synapse to this distance-dependent mechanism of receptor activation includes a number of factors, but perhaps the most prominent are synapse geometry, the molecular profile of these synapses (and their propensity for forming aligned pre- and postsynaptic nanoclusters), the lateral distribution of receptors, their propensity for evoked single vesicle versus multivesicular release (generally low *p* synapses), and how glutamate is packaged into vesicles at those synapses.

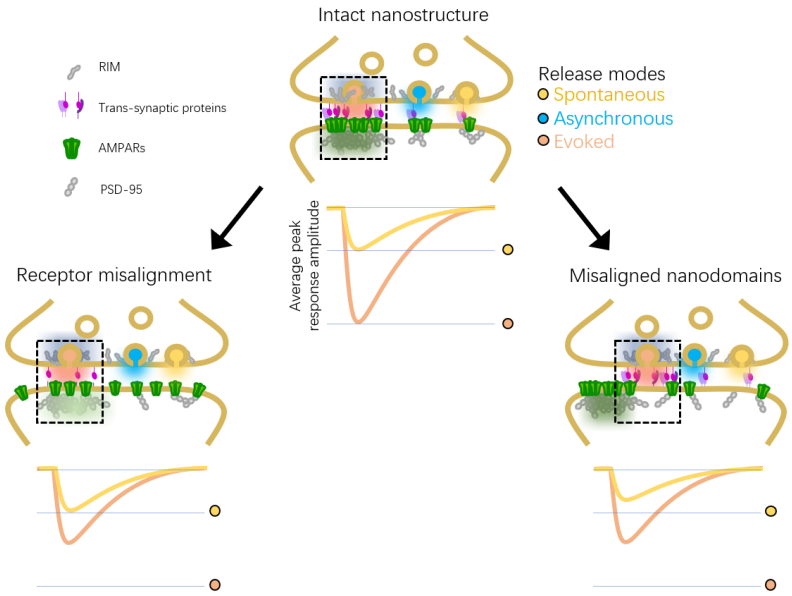


**Figure 22. Cell adhesions control unique modes of transmission through spatial organization.** Schematic depicting the nanostructural mechanisms underlying functional changes at individual synapses. Displayed molecules, top left. A synapse with typical protein distributions and postsynaptic responses, top middle. Bottom left, AMPAR redistribution away from evoked neurotransmitter release sites led to decreases in evoked (orange), but not spontaneous (yellow) release (Ramsey et al., 2021). In these experiments asynchronous release (blue) was untested. Right, intact AMPAR nanodomains are misaligned from evoked, spontaneous, and asynchronous release sites, causing a reduction in postsynaptic responsivity in both evoked and spontaneous synaptic transmission (Haas et al., 2018).

## 2.4 Stability of subsynaptic compartments over time

Many molecular constituents of these nanocolumn structures are dynamic under basal conditions (Kerr et al., 2012; MacGillavry et al., 2013) and in response to activity (Tang et al., 2016; Hruska et al., 2018). It remains a challenge to capture their dynamic nature in live cells with a high enough spatial and temporal resolution. In the past, people have performed live-cell PALM to understand how the distribution of the molecule within a PSD changes over the course of minutes, but PALM is a localization-based approach to single-molecule imaging. Therefore, a requisite number of frames must be collected to build an accurate map of the molecule's density within the synapse, which leads to poor temporal resolution. Additionally, it lacks a second channel needed to designate these

postsynaptic clusters as a part of this nanocolumn structure. However, even on the scale of minutes it was clear that these subsynaptic structures changed in size and shape, while remaining stable in some cases, and forming and disappearing in others (MacGillavry et al., 2013). One approach to capture how the spatial arrangement of multiple molecules changes over time has been to use 3D STORM of pre- and postsynaptic proteins at different timepoints following LTP- or LTD-inducing stimuli (Tang et al., 2016). Another approach, known as zap-and-freeze, involves the powerful combination of optogenetics to induce vesicle fusion and high-pressure cryofixation within ms after, allowing direct spatial measurements of fused vesicles with respect to immunogold labeled receptors (Li et al., 2021). Interestingly, an approach has been developed using structured illumination microscopy (SIM) to collect live-cell, 3-color images of synaptic proteins (Crosby et al., 2019). Although lacking in spatial resolution compared to STORM, this permits finer scale temporal resolution to observe dynamic changes to the trans-synaptic relationship of these proteins, helping us to estimate their stability. Unfortunately, likely only larger scale, or more dramatic, changes will be observable given the spatial resolution of SIM, but this is an important step forward in understanding the dynamics and stability of these trans-synaptic molecular relationships. This is a common trade-off in the super-resolution field, and our understanding will only be facilitated by new approaches that decrease sacrifices to spatial or temporal resolution and are compatible with living neurons. One such approach is that of Hruska et al. (2018) who were able to optimize live-cell Stimulated Emission Depletion (STED) microscopy to visualize the incorporation of synaptic nanomodules in response to plasticity-inducing stimuli. What remains unanswered given our spatiotemporal resolution constraints is how quickly these nanodomains can assemble

and disassemble, and how long a single domain remains stable. Understanding the temporal nature of these trans-synaptic nanostructures will help to form predictions about how they may support sustained basal transmission, short term plasticity, and even various incremental phases of long-term plasticity. Of course, these nanodomains could be critical for protein retention within synapses beyond simply positioning and may even be important for the stable incorporation of new molecules into synapses. Ultimately, the stability and spatial arrangement of these nanoscale domains may be involved in the flexibility of transmission, how it is maintained, and how the nano-organization of proteins responds to patterned activity.

## Section 3. A specific role for the LRRTM2 extracellular domain

### 3.1 Cleft, but not intracellular, interactions are critical for upholding function

The extracellular domain of LRRTM2 contains 10 leucine rich repeats (Linhoff et al., 2009), which in crystal structures suggest they form a shotel-like shape (Stone, 1999, 0-486-40726-8, p. 562). Neurexin (SS4-) binding has been suggested to take place in two separate positions on the extracellular domain: either nearby the C-cap which is located at a juxtamembrane position (Paatero et al., 2015; Yamagata et al., 2018), or at LRR repeats 5-7 (Zhang et al., 2018; Siddiqui et al., 2010). Most work seeking to understand the extracellular binding interactions of LRRTM2 at the level of individual residues has focused on neurexin binding (Siddiqui et al., 2010; Ko et al., 2009). However, it has been suggested that for LRRTM2 it may interact directly with the GluA1 and GluA2 subunit of AMPARs (de Wit et al., 2009; Soler-Llavina et al., 2013), though it remains unclear which residues are responsible, and could be mediated by other factors. LRRTM4, which shares 43% amino acid identity with LRRTM2 (Lauren et al., 2003), is considered to be a direct interactor with AMPAR subunits (Schwenk et al., 2012). Interestingly, it was also recently found that LRRTM2 binds directly to the heparan sulfate modification of neurexin, suggesting that it may bind to other HSPGs through heparan sulfate as well (Zhang et al., 2018; Roppongi et al., 2020), which would greatly diversify its extracellular binding interactions. These interactions may play a role in the clustering of AMPARs at the nanoscale, but specific identification of the role of these reactions is yet to be determined. And importantly, the combination of these interactions may help to induce AMPAR clustering at the nanoscale in the postsynaptic density.

The role of the transmembrane and intracellular domain of LRRTM2 is poorly understood. In fact, deletion mutants lacking the intracellular domain of LRRTM2 still traffick properly to synapses, and can induce presynaptic differentiation (de Wit et al., 2009), and even rescue LTP in LRRTM1,2 double knockout animals (Soler-Llavina et al., 2013; Bhouri et al., 2018). It was originally posited that the -ECEV C-terminal motif of LRRTM2, a sequence expected to bind to PSD-95, was necessary for the recruitment of synaptic proteins (Linhoff et al., 2009). However, it is unclear what the role of this intracellular domain is in established synapses. The role of the transmembrane and intracellular domains remains completely untested in this dissertation, but it will be important to test the role of these domains in the stabilization of PSD-95 or other MAGUKs on short or long time scales in established synapses. This could perhaps be tested using acute incubation with interfering peptides. Of course, the intracellular domain of LRRTM2 is small and unstructured (Chamma et al., 2020). Recently, it was found that an intracellular motif of LRRTM2 controls AMPAR mobility and synaptic immobilization (Liouta et al., 2021). Both the predicted -ECEV motif and another YxxC motif were found to have an effect on LRRTM2 mobility and confinement within synapses as synapses matured (Liouta et al., 2021). These sequences not only changed the synaptic enrichment of LRRTM2, but also influenced the number of subsynaptic clusters at synapses, which may have implications for how LRRTM2 acts to induce the cluster of AMPARs across from sites of neurotransmitter release. Serving as an example, neuroligin-1 has even been discovered to have intracellular non-PDZ functions (Shipman et al., 2011). Thus, even though the PDZ domain binding of LRRTM2 may be expected to exert control over PSD-95 organization, it may have other functions that are undescribed. For the time being, it remains mysterious

whether LRRTM2's intracellular domain will act to retain scaffolding molecules with PDZ type I and II domains and how these actions even relate to AMPAR nano-alignment in established synapses. Precise functional characterization of LRRTM2 PDZ-binding mutants may shed light on how they might be expected to contribute to nanostructure.

It remains generally difficult to relate our work to the findings of others that took place under a distinct experimental context, especially weeks-long knockout experiments (Soler-Llavina et al., 2013; Bhouri et al., 2018). However, these experiments are performed in mature synapses, independent of synaptogenesis, and therefore are worth comparison. Evidence for a specific role of the extracellular domain come from tests in mature synapses, where conditional deletion of LRRTM1,2 leads to deficits in postsynaptic AMPAR transmission and LTP. The importance of the LRRTM2 ECD is clear since these deficits are rescued with a GPI-anchored version of just the ECD of LRRTM2, whereas even full length LRRTM4 is not sufficient to rescue the cdKO phenotype. Despite clear experimental differences relative to our work (age, preparation, and approach to perturbation), quite robustly, postsynaptic control of AMPAR-mediated transmission seems to be a specific role of the LRRTM2 ECD (Bhouri et al., 2018). It will be interesting to see exactly which residues on LRRTM2 are critical for regulating AMPAR-mediated transmission. Replacement with a version of LRRTM2 that cannot bind neurexin also fails to rescue LTP, implicating presynaptic protein control, but exactly how LRRTM2 controls AMPAR organization is yet to be determined (Bhouri et al., 2018; Aoto et al., 2013). Indeed, it may require selective disruptions to the intracellular domain on short and longer time scales to deduce exactly what role it has in controlling synaptic scaffold organization and content. While the extracellular domain of LRRTM2 seems to clearly contribute to many synaptic

functions, the intracellular domain has been explored far less. Additionally, it remains unexplored how the transmembrane domain influences how LRRTM2 traverses the surface plasma membrane, how it influences its protein interactions, or how it aids in the translation of extracellular-to-intracellular signaling by conformational changes, should any of these properties even exist. Even these three hypotheticals, given LRRTM2's major role in the determination of AMPAR-mediated transmission, may greatly influence synaptic transmission, or may even possibly serve other functions.

### 3.2 LRRTM2 has a specific within-family role

Despite within-family similarities in protein structure, LRRTM2 seems to play a specific role at synapses. Single-cell knockout of LRRTM1 and 2 in young adult mice reduced AMPAR-mediated evoked transmission and destabilized AMPARs as measured by photo-activatable GFP-tagged AMPARs and their escape rates from synapses, without affecting synapse number, release probability, or NMDAR-mediated transmission (Bhouri et al., 2018; Soler-Llavina et al., 2013), suggesting that in established synapses, LRRTMs may serve as anchors for AMPARs in the PSD. However, the role of LRRTM1 in this process appears limited, since LRRTM1 knockdown alone has no effects on evoked or spontaneous EPSC amplitudes. However, LRRTM1 knockdown has substantial impact on mEPSC frequency, spine density, and synaptic vesicle distribution (Schroeder et al., 2018) its function may principally be limited to presynaptic roles following synaptogenesis. These findings strongly suggest that LRRTM2 plays a unique role for AMPAR retention. However, disruption of LRRTM2 did not lead to loss of AMPARs from the synapses within 30 to 60 minutes, even though it eventually produced large changes in AMPAR stability in

spines. Thus, LRRTM2 alone may not be sufficient to fulfill the functional role of "slots" hypothesized to anchor AMPARs (Opazo et al., 2012; Ashby et al., 2006). Further, I cannot rule out that the transmembrane and intracellular domains of LRRTM2 that remain after thrombin cleavage may contribute to the synaptic retention of AMPARs. This would be intriguing intramolecular segregation of function within LRRTM2 for overall retention vs positioning of AMPARs. However, GPI-anchored LRRTM2 ECD fully rescues the deficit in LTP during conditional deletion of LRRTM1 and 2, suggesting a specific role for the LRRTM2 extracellular domain.

The extracellular interactions of LRRTM2 mediate postsynaptic organization and function. Effects on synapse organization and function, including LTP, are rescued by the extracellular domain of LRRTM2, even with knockout of additional family member, LRRTM1 (Bhouri et al., 2018; Soler-Llavina et al., 2013). Neurexin binding appears important for the postsynaptic accumulation of AMPARs and synaptic function, further implicating the extracellular domain (Aoto et al., 2013; Bhouri et al., 2018). There does not appear to be reported directed within-family competition or redundancy for the LRRTM family of proteins, and this cautionary warning may not apply to this family of proteins. While LRRTM1,2 are expressed in CA1 hippocampal neurons, LRRTM3,4 are preferentially expressed in the dentate gyrus (DG). Even though LRRTM1 and LRRTM2 may be highly expressed at Schaeffer collaterals, they control strictly presynaptic and postsynaptic properties, respectively. Thus, LRRTM family members seem to exhibit quite little redundancy, and contribute to extremely different functions at synapses.

## Section 4. Precise mechanisms for controlling the number and subsynaptic distribution of AMPARs

At the subsynaptic scale, the patterned distribution of AMPARs is generally thought to be stabilized by a combination of factors in spite of continuous receptor diffusion in the plasma membrane (MacGillavry et al., 2013; Ashby et al., 2006; Groc & Choquet, 2020): a heterogenous affinity landscape in the synapse created by the distribution of direct AMPAR binding partners (Garcia-Nafria et al., 2016), and an array of steric obstacles which creates macromolecular crowding and hinders their motion within the dense synaptic environment (Li et al., 2016; Renner et al., 2010). I suspect both these mechanisms may be involved in how LRRTM2 controls the AMPAR pattern. There is some evidence that the LRRTM2 ECD can interact directly with AMPARs (de Wit et al., 2009; Soler-Llavina et al., 2013; but see Schwenk et al., 2012), and LRRTM2 through its interaction with PSD-95 might dynamically organize intracellular scaffolds (Linhoff et al., 2009; de Wit et al., 2009). At the same time, its loss may trigger reorganization or even loss of synapse-resident proteins which could alter the steric hindrance experienced by receptors in the cleft by their large extracellular domains or in the substantially denser PSD by their smaller intracellular domains. In addition, partitioning of the PSD via liquid-liquid phase separation is being actively investigated as a potential organizing mechanism of synaptic nanostructures (Wu et al., 2020). Due to multivalent interactions facilitated by LRRTM2 in the synaptic cleft, its presence could serve to establish a nanoscale, phase-separated synaptic subdomain into which AMPARs partition, and which would be disturbed by the cleavage of the LRRTM2 ECD (though I do not know of evidence that LRRTM2 is cleaved endogenously). Overall,

regardless of the mechanism, my data indicate that the nanoscale organization of AMPARs is both modulated by the LRRTM2 ECD and capable of rapid reorganization.

## 4.1 The definition of an AMPAR anchor

Anchor is a phrase that we commonly use to indicate that the presence of one protein in a synapse, or other given compartment, helps to bind and restrict the mobility of another protein within that same compartment, often by a robust direct interaction. Anchors are thought to determine AMPAR number and mobility within synapses, concepts directly relevant to this thesis. Although the specific benchmark for what constitutes one protein as an anchor is not explicit, there do seem to be a few general rules for earning the title of anchor. For instance, clear evidence of a direct interaction or an interaction with an already well-established anchor (Matt et al., 2018), often even supported by more than one point mutation in each protein, that alone prevent the proteins from interacting. While there are no specific affinity requirements between the anchor and the anchored, the absence of the anchor or disruption of their relevant interactions should lead to lower levels of the anchored protein at the site to which the anchor is typically enriched (e.g. synapses). Interestingly, though, even molecules involved in the synaptic removal of AMPARs, such as GRIP1, have been considered an anchor because it displays a direct interaction with AMPAR subunits and directs their subcellular localization, e.g. into the endocytic pathway (Liu et al., 2005).

So, perhaps more simply, a protein anchor can directly position another protein to a specific compartment, either through direct interactions established by point mutations of each protein, or indirectly, by anchoring another anchor of said protein. An anchor may act alone, using the analogy of a ship's anchor in the sea, through its weight alone, or

perhaps, should the seas be turbulent, the anchor itself requires being wedged against a rock, helping to keep the ship in a specified location. Thus, a "synaptic anchor" would be a protein that influences the abundance of another protein known to tightly bind AMPARs. And even further, an "AMPAR anchor" would be a protein that influences the localization of the TARP-AMPAR complex in a native location or pathway, such as PSD-95 at synapses or GRIP1 and how it bridges synapses and the endocytic pathway, which clearly influence the location of AMPARs. However, others have put forward even more general models of synaptic anchors, where the simple qualification is counteracting free diffusion at sites nearby neurotransmitter release (Hayer et al., 2005).

Using these simple definitions, it is interesting to consider whether LRRTM2 falls into the category of anchor, synaptic anchor, or AMPAR anchor. On short time scales under that of an hour, LRRTM2 does not influence the synaptic enrichment of AMPARs, but is important for their subsynaptic localization, a characteristic not previously considered in the criteria for what constitutes and AMPAR anchor. On short time scales, thus, LRRTM2 does not appear to be a synaptic anchor for AMPARs. And yet, on these short time scales the subsynaptic positioning of AMPARs is controlled by LRRTM2. This is in turn detrimental to action-potential evoked transmission, perhaps earning it the title of AMPAR anchor, but not synaptic anchor, as it localizes AMPARs to a site where LRRTM2, the anchor, is typically enriched, i.e. the nanocolumn on these short time scales. By contrast, after prolonged loss of LRRTM2, AMPARs do eventually depart from synapses, satisfying one of the other common criteria for a synaptic anchor. Even in a physiological context the turnover of a large number of LRRTM2 molecules from synapses, perhaps even by endocytosis or endogenous cleavage, could lead to slow changes in AMPAR synaptic

enrichment. This may suggest that LRRTM2 is a synaptic AMPAR anchor (Aoto et al., 2013). However, no conclusions can be made about LRRTM2's designation as an anchor until multiple point mutations can be verified to independently disrupt a direct AMPAR-LRRTM2 interaction, or the interaction of LRRTM2 with a protein that similarly meets those qualifications. If indirect, to be considered a synaptic anchor or synaptic AMPAR anchor, point mutations to disrupt binding of LRRTM2 to the true anchor, or the loss of LRRTM2, must lead to the loss of the true anchor from the compartment in which LRRTM2 typically occupies, at which point LRRTM2 could be considered also to anchor AMPARs within synapses, such as how actin is considered an AMPAR anchor (Matt et al., 2018). While the definition of an AMPAR anchor is not set in stone, those proteins which share the moniker have certain properties in common, and investigations into LRRTM2 have yet to meet certain criteria. Further investigations that establish single residue interactions between LRRTM2 and AMPARs or AMPAR anchors are required to establish LRRTM2 as a true AMPAR anchor.

## 4.2 Reconciling the notions of a binding slots, nanodomains, and the dynamic lateral mobility of AMPARs

AMPARs freely diffuse in and out of synaptic compartments on the dendritic surface. Synapses with a number of anchoring molecules provide a mechanism to counteract diffusion, and these anchoring molecules bind together and form a number of open slots for receptors to bind, and binding sites occupied by non-receptor proteins can limit the number of available slots (Ward-Walkup et al., 2016). Nanodomains, which are simply a collection of many receptor anchors at a relatively elevated density compared to

the average synaptic cluster density, are additional compartments in which an even higher number of anchors are capable of counteracting AMPAR diffusion. These nanodomains can be contained within trans-synaptic structures known as nanocolumns (Tang et al., 2016). Here I will define how I consider the terms slot and nanodomain in relation to trans-synaptic nanocolumns.

Any available subsynaptic compartment, whether in or out of the nanocolumn, may be capable of counteracting the free diffusion of the TARP-AMPAR complex and could be considered a slot (Opazo et al., 2012). It still remains uncertain how exactly the enrichment of so many multivalent proteins influences additional protein interactions, i.e., whether this aids in cooperative binding, and the general mechanisms for this nanoscale clustering are just beginning to be understood. Operationally, an individual slot, or an unoccupied anchor, is a smaller unit than what we would consider a nanodomain, and it requires many slots to establish a nanodomain, because each slot theoretically holds one receptor complex and nanodomains contain many AMPARs. However, slots also occupy the full area of a PSD within non-nanodomain areas, whereas nanodomains are restricted to ~1-6 subcompartments of the PSD (Tang et al., 2016), and may not include all available slots. Slots may be considered as any mechanism which counteracts the diffusion of AMPARs and helps to stabilize them within the PSD, which will occur within and outside of nanodomains. How the behavior of slots differentially counteract the diffusion of AMPARs in the nanodomain versus out of the nanodomain is not yet understood.

Interestingly, it is possible that slots in a nanodomain may be more fully occupied and therefore have a smaller influence on freely diffusing molecules, but rather establish a stable central organization with a slower turn-over rate. Nanocolumns may have slower

protein turnover than nanodomains or non-nanodomain regions of the PSD, for instance potentially because a higher density of interacting partners stabilizes their constituents. Nanocolumns may have slower protein turnover than nanodomains or non-nanodomain regions of the PSD, potentially because there are more binding partners or more steric hindrance to slow diffusion. On the other hand, unoccupied slots in non-nanodomain areas may more readily stabilize diffusing receptors, aiding in synaptic retention of certain proteins, whereas the dense nanocolumn regions may more readily block the path of AMPARs, redirecting them to non-nanocolumn slots (Li et al., 2016). What regulates the occupation of these slots, either in or out of the nanodomain, is mostly undescribed, and will require, in part, highly complicated models of protein affinities and their diffusion in simulated PSDs. Of great interest are the mechanisms that dynamically change the number of available slots. For instance, activity-triggered unbinding of the high-copy-number SynGAP1, which can bind to PDZ domains of MAGUKs, is thought to increase the number of open slots (Ward-Walkup IV et al., 2016; Opazo et al., 2012), though it is not known where within an individual synapse that this occurs. Another example is the phosphorylation of TARP-γ8, which allows it to reach deeper into the PSD, enabling it to bind to PDZ domains located further away from the membrane, thus effectively increasing the number of potential slots. The dynamic mechanisms that change the slot landscape of the PSD and how this happens in nanoscale space relative to PSD nanodomains will evidently influence basal transmission and synaptic plasticity. Understanding them will thus be critical, though the technical nature of experiments to determine them will likely be daunting.

## 4.3 Distinct time courses expose a deeper understanding of the role of LRRTM2 within synapses

What is now interesting about the potential role of LRRTM2 as an anchor for synaptic AMPARs is that we know that LRRTM2 occupies nanodomain and non-nanodomain regions of synapses. Additionally, it remains unclear whether LRRTM2 is a direct anchor, an anchor for another AMPAR anchor, or simply provides steric hindrance nearby scaffold nanodomains. There are many scaffolds within synapses that potentially mediate AMPAR positioning. Upon the cleavage of LRRTM2, the number of total synaptic slots is unlikely be dramatically reduced, though the composition of available slots inevitably shifts seeing as AMPARs leave 24 hours later. The loss of these potential slots (in terms of where LRRTM2 is positioned) may mean fewer molecules to counteract AMPAR diffusion preferentially within the nanocolumn. While the total number of slots is not changing, the ones that are affected were typically enriched within the nanocolumn. In the absence of the implementation of a hypothetically instantaneous point mutant to disrupt LRRTM2-AMPAR binding, I used acute proteolysis of the entire extracellular domain, which could concomitantly decrease steric hindrance of AMPARs traversing the PSD and individual nanodomains. Thus, upon acute cleavage of LRRTM2, AMPARs reposition from being within nanocolumn to other positions in the PSD, potentially where slots are more readily available to counteract their diffusion. This manipulation could also reduce steric hindrance within the nanocolumn, where LRRTM2 is highly enriched, perhaps affecting the incidence of counteracting receptor diffusion. Slots outside of nanodomains may be important for the synaptic retention of proteins, though may have generally lower incidences of interactions with synaptic proteins under basal conditions.

Disruptions to postsynaptic nanodomain valency may result in the shift in protein distribution to these more distributed slot proteins and various scaffolds.

There are many mechanisms which may control AMPAR number within synapses independently of their subsynaptic organization. The LRRTM2 ECD indeed seems to impact these two parameters independently when lost over short time scales. However, on longer time scales AMPARs are lost from synapses, which may suggest distinct mechanisms which regulate pattern versus number in the PSD. In this section I considered the classification of traditional mechanisms that immobilize AMPARs within nanodomains and within the PSD. Receptor occupancy in nanodomains may differ greatly from that of non-nanodomain areas of the PSD, and this may differentially influence receptor diffusion and exchange at these compartments. Thus, it will be important to understand the mechanisms that distinguish AMPAR number from their pattern within the PSD, and especially as it relates to sites of neurotransmitter release.

## Section 5. Cell adhesion molecule control of AMPAR positioning in basal synapse function and plasticity

A reduction in AMPAR nano-organization and AMPAR activation following the loss of the LRRTM2 ECD are particularly interesting given that strong evidence also implicates LRRTM2 in LTP (Soler-Llavina et al., 2013). Conditional deletion of LRRTM1 and 2 in mature mice reduces LTP in vivo, and expression of the LRRTM2 ECD alone, but not LRRTM4, is sufficient to rescue these deficits (Bhouri et al., 2018), clearly consistent with our observation that acute loss of the ECD regulates synaptic strength. Similarly, point mutations to the LRRTM2 ECD which disrupt presynaptic neurexin binding fail to completely rescue LTP (Bhouri et al., 2018), suggesting that neurexin binding may help explain how LRRTM2 specifically organizes AMPARs with respect to active zone nanodomains. LRRTM2 has been proposed as an anchor that stabilizes AMPARs during LTP induction (Bhouri et al., 2018; Soler-Llavina et al., 2013). Our work extends this by implying synaptic nanostructure shaped by LRRTM2 may play several roles in functional plasticity. Most simply, LRRTM2-augmented AMPAR activation may lower the threshold of activity needed to trigger plasticity. Existing LRRTM2 nanodomains could also facilitate the stabilization of recently exocytosed or otherwise labile receptors (Huganir & Nicoll, 2013). Similarly, it is conceivable that LRRTM2 could nucleate new nanoclusters added during LTP (Hruska et al., 2018; Lisman, 2017), though activity-dependent trafficking of LRRTM2 remains uninvestigated. In addition, our prior observation that chemical LTP induction “sharpens” the AMPAR distribution under RIM nanodomains (Tang et al., 2016) may suggest further that graded levels of AMPAR organizational tuning could be facilitated by LRRTM2. Most broadly, it is a natural extension of our findings

here to suggest that behavioral or disease-relevant plasticity mechanisms, even regardless of the potential involvement of LRRTM2, may regulate synaptic strength not only by regulating AMPAR number but through controlling synapse nanostructure.

## 5.1 LRRTM2 may act as a trans-synaptic structural component of LTP

Long-term potentiation leads to changes in both synapse function and organization. The structural changes are so dramatic that spine size can increase, and entirely new spines can form (Harris et al., 2020; Watson et al., 2016; Matsuzaki et al., 2004). These changes to spines are also accompanied by changes to the synapses themselves. Perhaps most notably, synapses that have undergone potentiation display an increased capacity to sequester AMPARs (Makino et al., 2009). However, there are other processes that act to accommodate this increased capacity to anchor AMPARs. Of course, much of this is related to the number of available binding sites for the TARP-AMPAR complex. Examples include the above discussed SynGAP1 unbinding and TARP-γ8 phosphorylation and extension (Araki et al., 2015; Constals et al., 2015). These processes act to accommodate additional AMPARs within the PSD following LTP, but where these newly incorporated AMPARs are positioned subsynaptically is not understood. If additional AMPARs are incorporated across from sites of release they will be more likely to contribute to the increased EPSC observed following LTP induction. How LRRTM2 may be acting in a structural manner to accommodate additional AMPARs or adjust their positioning relative to sites of neurotransmitter release is not known, but its conditional deletion prevents the stable expression of LTP and immobilization of AMPARs. Thus, LRRTM2 may have an additional role in positioning newly added AMPARs across from sites of neurotransmitter

release. LRRTM2 may also be responsible for accommodating the general number of synapses in the PSD, but this would depend on whether LRRTM2 is a synaptic AMPAR anchor, which is so far unknown (discussed above). What happens to the normal complement of LRRTM2 in the PSD upon LTP induction is unknown. LRRTM2 may undergo re-organization which may help to position a greater fraction of AMPARs closer to sites of evoked release. An increase in the number of LRRTM2 molecules at synapses may also help to alter the size and density of AMPAR nanodomains. Alterations in the copy number of LRRTM2 following LTP could even act to form new nanoclusters and even instruct their alignment to new sites of evoked release. It is possible that LRRTM2 and its enrichment within the nanocolumn may help to accommodate additional AMPARs directly across from sites of release.

## 5.2 LRRTM2-mediated nano-alignment may facilitate LTP induction

During basal synaptic transmission, LRRTM2 brings AMPARs within close proximity to sites of evoked release to enhance the strength of transmission. Long-term potentiation in part requires postsynaptic depolarization sufficient to relieve the magnesium block of NMDARs, which is AMPAR-dependent. The amount of AMPAR current passed depends on the number of activated channels and their individual conductance. Both of these parameters are thought to be controlled by AMPAR distance to the site of glutamate exocytosis. Modulation of LRRTM2-mediated alignment of AMPARs to sites of release may increase the ease with which an individual synapse is able to be depolarized and alleviate the magnesium block of NMDARs. This would then suggest that LRRTM2 could mediate the likelihood that an individual synapse achieves sufficient

postsynaptic depolarization to induce LTP. Determination of LRRTM2's role as a synaptic AMPAR anchor is important, before extending conclusions about its role in plasticity.

LRRTM2-mediated nano-alignment, even during basal conditions, enhances AMPAR activation. Therefore, a natural extension of this is whether this configuration is tuned during LTP. A number of mechanisms which regulate LRRTM2 upstream may also influence synaptic strength. LRRTM2 may therefore mediate a number of potential mechanisms of the induction or expression of synaptic plasticity. For instance, whether LRRTM2 adopts an increased density and area across from neurotransmitter release sites to further enhance LTP and guide the insertion of new AMPARs. Or perhaps to avoid excitotoxicity, does LRRTM2 flatten its distribution to accommodate an increased number of synaptic AMPARs in the PSD following LTP? LTP is a complex phenomenon, that involves a number of different proteins, signaling cascades, and changes to gene expression and protein trafficking. LRRTM2 itself or other influences on its behavior are likely impacted by LTP, but the cellular trafficking of LRRTM2 nor its nanoscale distribution following LTP is not known. The components that are influenced by LTP that are most likely to involve or influence LRRTM2 itself are changes in LRRTM2 expression or trafficking (i.e. changes to LRRTM2 copy number), post-translational modifications of LRRTM2 which could inform its binding interactions or conformation, or potential cleavage of competing neuroligin-1 interactions (i.e. biasing towards increased binding towards LRRTM2-Neurexin or LRRTM2-AMPARs). Understanding how LRRTM2 is regulated following LTP will be important to evaluate these hypotheticals. If the presence of LRRTM2 increases the sensitivity of the postsynapse to undergo LTP, then LTP may be differentially impacted at synapses with LRRTM2. If a synapse entirely lacks LRRTM2,

these synapses may require additional firing, or other presynaptic mechanisms that increase the ability of AMPARs or NMDARs to be activated. These synapses may exhibit a high *p* or elevated VGLuT1 expression. These factors would decrease the necessity of LRRTM2 for the induction of plasticity. Though, LRRTM2 may play a structural role in accommodating or stabilizing the synaptic influx of new receptors, which LRRTM-lacking synapses may have to compensate for in other ways.

## 5.3 A nanoscale hub for labile AMPARs

Given their relative lateral mobilities (Chamma et al., 2016), LRRTM2 appears more likely to instruct the immobilization of AMPARs than the inverse case of AMPARs immobilizing LRRTM2. The mechanisms restraining LRRTM2 mobility are not clear, but it has been presumed to stem from PDZ binding or neurexin binding. These high affinity protein interactions may restrict LRRTM2's lateral mobility, but from our acute cleavage assay, this is not entirely clear. It is possible that there is a very high avidity for LRRTM2 within synapses, and likely the majority of this avidity is exerted by its extracellular domain, since LRRTM2 trafficks and concentrates in synaptic puncta in the absence of its C-terminal domain, which harbors a PDZ binding motif (Linhoff et al., 2009; Siddiqui et al., 2010). Unfortunately, it remains unclear whether a direct interaction between LRRTM2 and AMPARs even exists, or if so, whether LRRTM2 engages the receptor N-terminal or ligand binding domain. Interaction with these different domains may affect how LRRTM2 could exert control over the receptor. The AMPAR NTD is involved in synaptic trafficking of AMPARs during basal transmission and LTP (Diaz-Alonso et al., 2017; Watson et al., 2017). Additionally, binding to the NTD or LBD may have implications in controlling AMPAR gating and synapse function, much like the actions of TARP-γ8 (Cais et al., 2014).

Because AMPAR gating is related to its lateral mobility via conformational changes (Constals et al., 2015), the two concepts may be intertwined when it comes to a potentially direct interaction with LRRTM2. Thus, LRRTM2 interactions with the extracellular region of AMPARs may differentially impact AMPAR incorporation or subsynaptic positioning through the NTD, or could influence channel kinetics through interactions with the LBD. Understanding the suspected binding interface between LRRTM2 and AMPAR subunits will give many clues regarding the role of this interaction, should it exist.

Should LRRTM2 directly bind to AMPARs, the location of the binding may inform how LRRTM2 acts to instruct AMPAR organization or channel properties following LTP. LRRTM2 may act to seed new nanoclusters that are important for immobilizing AMPARs. The construction of new LRRTM2-mediated nanodomains for AMPAR clustering may help to stabilize additional receptors and may instruct release sites in the active zone directly across from them. This could be achieved through LRRTM2 accumulation of PSD-95, direct binding of AMPARs, or other indirect protein interactions such as those involving heparan sulfate. LRRTM2 may control nano-organization in a functional manner where existing AMPARs are configured closer to sites of neurotransmitter release, or LRRTM2 could instruct new hubs for the immobilization of AMPARs following the induction of plasticity. If LRRTM2 indeed interacts with the NTD of AMPARs, it may be important for stabilizing newly fluxing AMPARs within the nanocolumn following LTP. If LRRTM2 interacts with the LBD, it may act to stabilize AMPARs with certain channel kinetics within the nanocolumn. However, in addition to their subsynaptic position, it is possible that LRRTM2 also influences the total number of AMPARs within synapses following LTP. Regardless, mechanisms regarding LRRTM2 trafficking or those which

implicate it as an AMPAR slot will be necessary to determine. Elucidation of these mechanisms will inform us about how LRRTM2 responds to plasticity to instruct AMPAR incorporation central to synaptic function.

## Section 6. The role of LRRTM2 in the nanostructural segregation of release mode regulation

Surprisingly, I found the average postsynaptic response to spontaneous release was rather insensitive to AMPAR nano-organization, though it remains to be seen if this holds for all synapse geometries (e.g. small synapses). Our model and others predict that different forms of release may produce different postsynaptic responses depending on the subsynaptic distribution of release sites. There is indeed evidence that mEPSCs as well as univesicular EPSCs evoked in the presence of $Sr^{2+}$ differ in CV and amplitude from AP-evoked EPSCs in the same neurons (Bekkers & Clements, 1999; Bolshakov & Siegelbaum, 1995), and our findings provide novel experimental support for the idea. However, one shortcoming in previous work as well as our own is that due to the large variation in synaptic potency even on single neurons, precise measures of both mEPSCs and evoked quantal size from the same synapses not merely the same cells will be needed for thorough experimental validation of these predictions. Differences in the regulation of evoked and spontaneous transmission may allow differential control of synaptic stabilization during spontaneous transmission and the propensity for a synapse to undergo plasticity during evoked transmission. While the roles of spontaneous synaptic transmission remain unclear, it has been suggested to stabilize the basal structure and function of the postsynapse (Sutton et al., 2006; McKinney et al., 1999; Raghavachari & Lisman, 2004). Local activity driven by spontaneous neurotransmitter release is also important for restricting the lateral mobility of AMPARs, helping to trap them in the PSD (Ehlers et al., 2007). Implicating transcellular mechanisms in the distinct regulation of evoked and spontaneous transmission further distinguishes these two forms of transmission already known to operate with heterogeneity

at different active zones (Peled & Isacoff, 2011). In this section, I will discuss how the nano-structural organization effectively impacted evoked and spontaneous release.

## 6.1 Subsynaptic AMPAR positioning following LRRTM2 cleavage differentially impacts evoked and spontaneous release

Acute disruption of the trans-synaptic interactions of LRRTM2 caused AMPARs within individual synapses to undergo rapid reorganization. Specifically, using 3D single-molecule imaging, I observed that the distribution of synaptic AMPARs become more homogenous within the PSD. Peaks of AMPAR local density directly across from RIM nanoclusters become severely blunted following LRRTM2 cleavage but are not lost from synapses (Fig. 2D-F). Importantly, the proximity of these receptors relative to sites of specific modes of neurotransmitter release are dynamically shifted. Nanoclusters of active zone proteins with different molecular compositions may comprise different types of neurotransmitter release sites. It remains unclear how the subsynaptic organization of AMPARs impacts unique modes of neurotransmitter release which may be established in different sub-active-zone regions (Tang et al., 2016; Haas et al., 2018; but see Li et al., 2021). There are very few postsynaptic mechanisms within single synapses that uphold any kind of differential regulation between release modes (Atasoy et al., 2008; Sara et al., 2011). By contrast, the loss of AMPARs from a synapse would be expected to impact all forms of transmission. However, with our acute and specific manipulation, I was able to delineate this role for the LRRTM2 extracellular domain. In fact, our manipulation led to fewer AMPARs directly across from preferential sites of evoked release, without their loss from synapses. This reduced the average density of AMPARs across from evoked sites.

Spontaneous sites of release are thought to be more broadly distributed, thus our manipulation did not change the average density of AMPARs across from spontaneous release sites.

The subsynaptic positioning of AMPARs across from different types of neurotransmitter release (e.g. evoked and spontaneous) is not well understood. Our results suggest that there are mechanisms which can control AMPAR distributions independently of their number within the PSD. The loss of AMPARs from synapses would be expected to impact all types of neurotransmitter release as it directly affects the density of AMPARs in the PSD. Exactly how synaptic content, versus the subsynaptic positioning of AMPARs is regulated is not well understood. It has been posited that it involves C-terminal and N-terminal regions of AMPAR subunits, respectively (Watson et al., 2021). In the context of our experiments, it remains unclear which molecular interactions allow for changes in the subsynaptic positioning of AMPARs, but not their loss from synapses (Bissen et al., 2019; Garcia-Nafria et al., 2016). It is possible that LRRTM2 mediates protein interactions which give rise to the differential N- and C-terminal control of AMPAR positioning and number in the PSD (Watson et al., 2021). AMPAR intracellular interactions are important for synaptic AMPAR number, while the NTD more specifically impacts the subsynaptic distribution of AMPARs (Watson et al., 2021). LRRTM2 has been suggested to control AMPARs through both intracellular and extracellular domains (Linhoff et al., 2009; Soler-Llavina et al., 2013; Aoto et al., 2013; Bhouri et al., 2018). Thus, the complete loss of LRRTM2 may impact the subsynaptic positioning and the number of synaptic AMPARs. In fact, LRRTM2 knockout leads to the loss of synaptic AMPARs, and reduces their mobility within synapses (Bhouri et al., 2018). Though the lateral mobility of AMPARs is

thought to influence AMPAR subsynaptic organization, this was not directly tested in Bhouri et al., but is consistent with the idea that LRRTM2 may mediate both intracellular and extracellular interactions that control AMPARs. However, this is not the case with the acute cleavage of the LRRTM2 extracellular domain alone, where only the subsynaptic distribution of AMPARs is impacted. Again, consistent with the model of Watson et al. (2021). It is possible that the remaining ICD interactions of LRRTM2 may be undisrupted in our manipulation, which leaves AMPAR number in synapses unaffected.

Though it is difficult to understand how AMPAR positioning can be affected without impacting the number of AMPARs retained within a synapse. One explanation is that the intracellular domain of LRRTM2 may be acting in a dominant-negative manner when the molecule is fully intact, perhaps through competitive intracellular interactions. Essentially, LRRTM2's intracellular interactions may negatively impact the synaptic stabilization and total number of AMPARs, perhaps because other intracellular interactions retain AMPARs more effectively, and binding is competed for by the LRRTM2 intracellular domain. It is possible that upon the uncoupling of the LRRTM2 extracellular domain from the intracellular domain, proteins that are more effective at retaining AMPARs may take over. Upon cleavage, and elimination of LRRTM2's extracellular interactions, it is possible that this dominant-negative effect of the intracellular domain on AMPAR synaptic retention is lifted, and other molecules act to compensate and retain AMPARs more efficiently through their C-terminal domains. Additionally, the extracellular domain of LRRTM2 may be important to varying degrees for both synaptic retention and the instruction of the subsynaptic distribution of AMPARs. Thus, upon its removal, and relief of the dominant-negative effect through its C-terminal domain,

AMPARs reorganize in a random fashion within the PSD without being lost from the synapse, resulting in differential effects on unique modes of transmission understood to be uniquely distributed within the active zone.

## 6.2 The homogenization of the postsynaptic AMPAR distribution decreases *q* and detriments in evoked responses

The data presented in this thesis suggests that the homogenization of AMPARs in the PSD increases the average distance of receptors from sites of evoked glutamate exocytosis, and in turn this results in weaker activation of AMPARs due to the biophysical constraints of AMPAR-mediated transmission. Under conditions that facilitate enhanced neurotransmitter release, such as higher concentrations of extracellular calcium, it would be expected that nano-alignment would have a significantly reduced influence on receptor activation. However, there may be several ways that high probability of release conditions (such as high calcium) can influence evoked transmission. Sites of evoked release are thought to be concentrated at nanodomains of RIM, which are expected to be in a complex with VGCCs and SVs. This brings SVs within close proximity to sources of calcium influx, and since calcium is well-buffered in the intracellular active zone compartment, low extracellular concentrations of calcium mean that calcium likely does not diffuse at high concentrations over long distances upon entry into the cell, leaving only SVs nearest to the RIM nanodomains to undergo fusion. But, in conditions where the extracellular concentration of calcium is increased dramatically, more calcium is able to flux into the cell. This would quench various intracellular calcium buffers, traveling further radially, and triggering release at primed SVs more physically distant from these RIM nanodomains.

This means that the radius of evoked release positions would be wider radially from these RIM nanodomains. This would introduce variability in vesicle fusion directly across from AMPAR nanodomains, in turn making the amount of glutamate these AMPAR nanodomains are exposed to more variable. In this way, neurotransmitter release would be expected to be less effective at activating postsynaptic receptors, and its disruption would not have as large of an impact in comparison to low probability of release conditions, where SVs closest to the RIM nanodomains in alignment with receptors preferentially undergo fusion.

Alternatively, in higher probability of release conditions, multivesicular release (MVR) is more frequent when extracellular concentrations of calcium are elevated, and MVR is known to happen more frequently at different synapse types (Christie & Jahr, 2006; Molnar et al., 2016). The consequence of this would be an increase in the amount of cleft glutamate given a presynaptic action potential, somewhat similar to the issue discussed above, with the exception that in this case dramatically increasing the amount of glutamate in the cleft, which would lead to more AMPARs experiencing a higher concentration of glutamate, increasing their likelihood of activation. Of course, something similar could be achieved with single vesicle release if glutamate transporters were able to package more glutamate, but higher probability release synapses may achieve this through simply releasing more than a single quantum of glutamate, making reuptake slower and reducing desensitization as more receptors, even those more distant from the site of vesicle fusion, bind more than one molecule of glutamate (Franks et al., 2002). Both the potential spatial component of vesicle fusion and consequent site of fusion and regulation of the amount of cleft glutamate through MVR would suggest that nano-alignment is expected to

be most impactful at low probability release synapses, which perhaps suggests quite the dynamic role for nano-alignment in the hippocampus where release probability varies greatly (Stevens & Wang, 1995; Hjelmstad et al., 1997; Christie & Jahr 2006).

## 6.3 Spontaneous release is insensitive to the state of nano-alignment

The observation in deficits to evoked, but not spontaneous transmission was striking. This could be explained by the average density of AMPARs across from sites of these two release modes. The role of spontaneous transmission signaling is not understood but has been suggested to have separable roles from action-potential evoked transmission (McKinney et al., 1999; Sara et al., 2005; Zucker et al., 2005; Chung & Kavalali, 2006; Chung et al., 2010; Sutton et al., 2006; Choi et al., 2014). Changes to AMPAR nano-organization similar to our findings maintain the amplitude of spontaneous transmission but reduce the amplitude of evoked transmission at individual synapses. The nano-organization of AMPARs can therefore seemingly differentially regulate processes dependent on evoked and spontaneous transmission. Action-potential evoked transmission is thought to transmit the majority of synaptic information (Zucker et al., 2005), whereas spontaneous transmission has been found to be important for both maintaining spine morphology and number (McKinney et al., 1999), propensity for homeostatic scaling and AMPAR composition (Sutton et al., 2006; Chung & Kavalali, 2006), and the diffusional trapping of AMPARs in the PSD (Ehlers et al., 2007). If AMPAR nano-organization can be regulated on short time scales, then the homogenization of the AMPAR nano-distribution within synapses may act as a mechanism which can temporarily and reversibly blunt information being transmitted from action-potential evoked release, while

maintaining the structural and functional integrity of those synapses through spontaneous transmission, without involving AMPAR trafficking pathways.

Spontaneous and evoked transmission can be achieved through unique molecular pathways, suggesting unique regulation and perhaps even separable synaptic functions. Some vSNAREs such as synaptotagmin-12, regulate spontaneous neurotransmitter release, but not evoked neurotransmitter release (Maximov et al., 2007), while synaptotagmin-1 has been found to be important for evoked, but not asynchronous or spontaneous release (Geppert et al., 1994). This independent regulation of these exocytic pathways may indicate that neurons at times regulate these functions independent of one another, and the postsynaptic nano-distribution of AMPARs may be one such mechanism to achieve this on unprecedented time scales. This segregation over the control of synaptic function isn't unique to mammalian synapses. Distinct mechanisms in *Drosophila*, spontaneous transmission is necessary for Trio guanine nucleotide exchange factor (GEF) and Rac1 GTPase signaling in development but has no impact on evoked release (Choi et al., 2014). And interestingly, again in *Drosophila*, visualizing evoked and spontaneous events using GCaMP3 showed little overlap between synapses that participate in these two pharmacologically isolated processes (Peled et al., 2014). These results showed that evoked and spontaneous release occur with different probabilities at separate synapses. Our experiments show that this separation of regulation between evoked and spontaneous transmission can be driven by postsynaptic mechanisms and can be differentially regulated within single synapses.

## 6.4 Asynchronous release is likely to sit somewhere in-between

Another form of neurotransmission, not addressed in the present study, and is often used to estimate the postsynaptic response to single vesicle events, without blocking action potential dependent transmission, is asynchronous release. Typically, this mode of release occurs in a delayed manner following action potential evoked release and notably lasts for tens to hundreds of milliseconds, where single vesicles are capable of fusing in an intermittent fashion (Rozov et al., 2019). While recent evidence was able to demonstrate the spatial distribution of evoked and spontaneous release events within the active zone (Tang et al., 2016), the subsynaptic distribution of asynchronous release events was recently reported to engage NMDARs most effectively (Li et al., 2021). Historically, asynchronous events and miniature events alike have been used to estimate the postsynaptic response to single vesicle release. This was a well-accepted practice, because asynchronous and miniature events both elicit very similar events, especially in contrast to evoked transmission. However, upon closer examination raw histograms of asynchronous and miniature events collected side by side suggest that asynchronous events are slightly larger on average than miniature events (Bekkers & Clements, 1999).

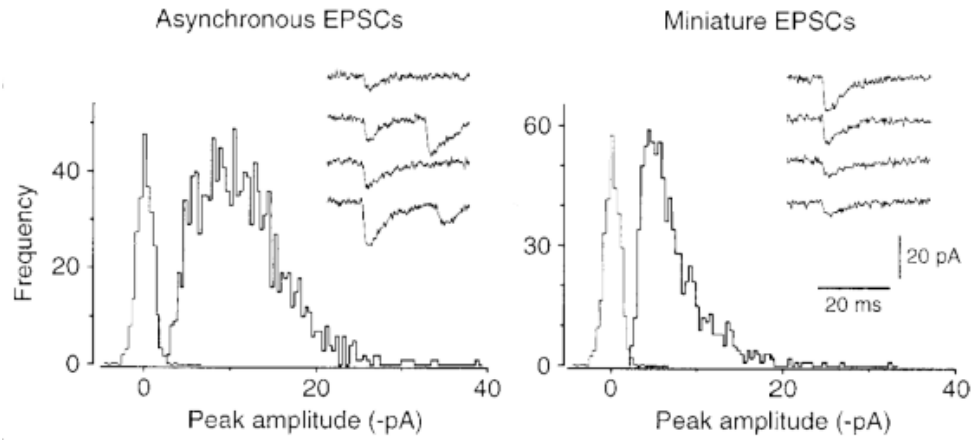


**Fig 23. Histograms displaying peak amplitudes of asynchronous (left) and miniature (right) EPSCs.** Taken from Bekkers & Clements (1999). Histogram of asynchronous EPSCs is slightly right shifted towards a larger magnitude than those of miniature EPSCs, perhaps explained by where asynchronous release happens within the synapse.

It is important to note that in these experiments, $Sr^{2+}$ is used to desynchronize AP-evoked release, as it possesses a weaker affinity for $Ca^{2+}$-dependent sensors of vesicle fusion. This weaker affinity leads to a long distance of action, thus permitting release further from the nanocolumn, where the majority of evoked release is expected to occur. Thus, it is possible that asynchronous release occurs well outside the nanocolumn, and likely has a radius of effective release somewhere between that of evoked and spontaneous release and may explain why asynchronous events from the same synapses exhibit slightly larger amplitudes given the relatively shorter distance to a greater number of AMPARs.

## 6.5 The coefficient of variation may be an indicator of a more structured subsynaptic environment

The coefficient of variation has historically been a very useful measure for synaptic electrophysiologists. Typically, it was used to compare changes before and after a

treatment (e.g. LTP induction), or at different synapses (e.g. DG-CA3 versus CA3-CA1), and it helps us to relate the standard deviation to the mean amplitude of the responses. In my results, I found that LRRTM2 cleavage and the redistribution of synaptic AMPAR distributions led to a reduction in the CV as determined from our numerical model of AMPAR positions in receptor activation and miniature recordings. This suggests that synapses which possess a more homogenous AMPAR distribution display a lower CV than those with a more heterogenous, or clustered, distribution.

CV is a biologically complex measure and can generally be thought of as a readout of the volatility of postsynaptic responsivity, which is classically considered to be influenced by presynaptic properties (Berninger et al., 1999). Practically, it is often used in two ways to determine the nature and locus of biological changes at a synapse or set of synapses upon treatment with particular stimuli. The first way is by looking at a standard CV analysis plot, which lists $1/CV^2$ on the Y-axis and the mean, μ, on the X-axis, and assessing whether in the responses from the treated group show a change in the mean, which would indicate whether LTP or LTD occurred at those synapses. The second way is by looking for whether $1/CV^2$ was altered in a specific manner, which is usually indicative of presynaptic changes in function (Bekkers & Stevens, 1990; Malinow & Tsien, 1990; Faber & Korn, 1991; Brock et al., 2020), however, these interpretations are made under strict biological qualifications and assumptions (Faber & Korn, 1991).

Interestingly, the initial CV was found to be significantly correlated with the end result of BDNF-induced synaptic potentiation and the degree to which paired-pulse facilitation could be induced (Berninger et al., 1991). Ultimately, there a complex set of parameters that establish CV at various synapse types, and depending on what that

arrangement is, the CV may be predictive of how those synapses respond to certain stimuli intended to induce changes in synaptic signaling and function. Not only is the CV susceptible to many synaptic parameters, but the subsynaptic distribution of AMPARs relative to evoked and spontaneous release sites may also contribute to the volatility that influences the CV. Thus, existing synaptic nanostructure may be indicative of the types of plasticity that a synapse can undergo.

## Section 7. Competitive, cooperative, or redundant? The nuanced roles of the neurexin ligands

The effects of disrupting LRRTM2 and NL-1 differ in several ways both electrophysiologically and molecularly. Perhaps most dramatically, our experiments showed that acute manipulation of LRRTM2 but not NL-1 quickly prompted disorganization of AMPARs, whereas in similar experiments, proteolytic cleavage of NL-1 rapidly altered synaptic neurexin content and reduced presynaptic release probability (Peixoto et al., 2012). Thus, even adhesion molecules that share binding partners may play unexpectedly divergent roles in maintaining organization of synaptic molecular complexes. More broadly, these results suggest that many specific aspects of synapse structure and function are maintained by unique subsets of the diverse cell adhesion systems present within single synaptic clefts. Indeed, growing evidence demonstrates that synaptic CAMs themselves are found in distinct subsynaptic patterns (Biederer et al., 2017; Chamma et al., 2016; Perez de Arce et al., 2015; Cijsouw et al., 2018; Trotter et al., 2019). Clearer understanding of CAM organization within synapses will provide insight into their contribution to synapse nanoarchitecture and to their cooperative or even redundant functional roles.

### 7.1 Neuroligin-1 and LRRTM2 seemingly play unique roles on short time scales, despite similarities in protein interactions

At the cellular level, as discussed in the introduction, the roles of NL-1 and LRRTM2 are quite similar, as synaptic cell adhesion molecules (Biederer et al., 2001;

Linhoff et al., 2009). They are both thought to recruit postsynaptic molecules, namely PSD-95, through C-terminal interactions with various neurexins (Linhoff et al., 2009; Song et al., 1999). Interestingly though, examination of their roles beyond synaptogenesis has led to several observations that they play quite unique roles in established synapses (Soler-Llavina et al., 2011). This is surprising only given a handful of common features, such as binding partners, and much remains to be explored in how they differentially interact with synaptic environments and how they are organized at the subsynaptic scale. Of particular interest, is how these molecules are differentially trafficked and incorporated into synapses, and whether this plays into their synaptic functions. Interestingly, it seems that dimerization of neuroligin-1 is required for proper trafficking and effecting changes in spine morphology, synapse number, and an increased miniature frequency (Shipman et al., 2012). How the requirement for dimerization influences their nanoscale distribution and more subtle synaptic functions is not known.

Using acute cleavage, I now have a comparison of how both of these neurexin ligands act on short time scales (Peixoto et al., 2012; Ramsey et al., 2021). However, a few caveats should be considered in order to assess their relative functions within synapses. In Peixoto et al. (2012), their cleavable NL-1 was overexpressed. NL-1 overexpression has been known to induce a number of morphological phenotypes (Schnell et al., 2012), leaving the possibility to influence synaptic organization and function. However, one similarity in the acute elimination of both LRRTM2 and NL-1 was synaptic stability of PSD-95 content within synapses for up to one hour after the loss of their extracellular domains. In addition to this, it seems as though the observed loss of neurexin was specific to the NL-1 extracellular domain, as cleavage did not lead to the loss of other presynaptic

proteins such as synaptophysin or RIM (Peixoto et al., 2012; Ramsey et al., 2021). In addition to this, acute cleavage of LRRTM2 did not lead to the loss of RIM, suggesting that general active zone organization does not require the extracellular domains of these neurexin ligands.

Interestingly, on short time scales, NL-1 and LRRTM2 seem to play drastically different roles. While acute cleavage of NL-1 leads to the loss of neurexin-1 and a concomitant reduction in release probability, the acute cleavage of LRRTM2 leads to disruption of postsynaptic AMPAR nano-alignment and selectively in evoked transmission (Ramsey et al., 2021). At the subsynaptic level NL-1 is thought to have a much broader subcellular distribution and is thought to be much more mobile than LRRTM2 (Chamma et al., 2016a; Chamma et al., 2016b). Interestingly, it seems that there is a developmental component that regulates LRRTM2 mobility and subsynaptic organization, which appears to be mediated by its intracellular domains, specifically a YxxC motif and a PDZ binding motif (Liouta et al., 2021). How these various properties influence the molecules constitutive roles in synapse organization and function is not well understood. However, given a number of similar binding interactions and partially overlapping functions, it seems likely that they will at times perhaps act redundantly, such as in PSD-95 stability at synapses, and perhaps divergently for other roles, such as the maintenance of release probability.

7.2 A series of complicated principles and assumptions required for testing this question

Our acute manipulation is well-suited to address the potentially coordinated roles of these molecules within synapses. Other attempts to tease apart their roles have used traditional loss of function approaches, like knockouts, which of course can suffer in their interpretations from genetic compensation or molecular compensation on even shorter times scales, from other family members or other molecular families. The acute nature of the exogenous cleavage approach and the high specificity of proteases would permit each molecules interactions to be disrupted within seconds. However, this leaves a complicated set of principles to be addressed by the experimenter.

The list of expression constructs could quickly become unwieldy, especially if other constructs are to be expressed concurrently (e.g., GCaMP or other SEP-tagged proteins of interest). It would be important to express the molecule of interest with the cleavable modifications as well as the tag for visualization, and all necessary controls to ensure these modifications do not modify protein function. And additionally limiting the effects of overexpression to couple this with a method to limit the amount of the endogenous protein, such as on a knockout background or concurrent knockdown. In consideration of the knockdown of endogenous protein and replacement with exogenous protein with modifications, one should consider what conclusions they hope to draw once the experiments have been completed. For instance, to knockdown only NL-1 and replace with a cleavable, tagged NL-1, it is possible that some components of NL-1 function are actively compensated for by NL-3 also known to be at excitatory synapses and even form heterodimers with NL-1. Thus, experiments may need to be conducted in such a way where other neuroligin family members are present in one condition and absent in the other

condition, in order to draw conclusions about which aspects of NL-1 function are readily compensated for by other neuroligin family members. And indeed, a similar set of control experiments would need to be performed for LRRTMs as well. One thing to consider may be to create a knockin of the cleavable sequence and N-terminal tags, though it still remains challenging to observe a high yield of knock-in. Additionally, estimation of whether a knock-in is biallelic on a cell-by-cell basis also remains a challenge for the field.

In addition to this, each of the knockdown constructs being used must be validated. Unfortunately, a benchmark for which phenotypes must be tested is likely far from being established and agreed upon, thus one must be robust in their quantification of the state of a neuron expressing the potentially various knockdown constructs. For instance, gross neuronal morphology, synaptic content, synapse density, etc. are just a few parameters which could be quantified in order to validate the lack of off-target effects of the miRNA targeting the endogenous protein. However, this becomes complicated, because some of these knockdowns of other family members (in an effort to avoid compensation), without replacement may be expected to show certain phenotypes and therefore must be taken into consideration for the experimenter's conclusions. The number of knockdown constructs that may potentially need to be expressed in the same vector, seeing as the size of the LRRTM or NL family is high, may range between 2 to 4 knockdown sequences. Chained miRNA expression is one approach which may be amenable to this, but the processing of 2 to 4 chained sequences is not commonly performed in neuronal preparations.

Regardless of how one decides to implement a system where your CAM of interest can be quickly eliminated in the absence of compensation, the original intent is to test the coordinated role of these molecules in a within-assay manner. One way that this can be

done is by co-packing the replacement construct within the same vector as the knockdown sequences. Once the set of constructs can be co-transfected or co-infected, it would then be possible to cleave Target A (LRRTM2) and cleave Target B (NL-1) in a controlled manner, with the inclusion of unique protease recognition sequences (e.g., TEV in NL-1 and Thrombin in LRRTM2). This then permits the cleavage of each molecule individually, combined, or in series (e.g., cleave Target A, then Target B). In doing so, it can be assessed within-assay whether these proteins were contributing to the same synaptic or cellular processes.

7.3 It is about time we invest in studying endogenous protein organization and function

Thankfully, many have been developing clever approaches to the endogenous labeling of synaptic proteins and cell adhesion molecules (Klatt et al., 2021; Fang et al., 2021; Getz et al., 2021; Willems et al., 2020). Although these approaches are difficult to implement often because of the knock-in efficiency, the few datasets able to be collected provide great value in the information they provide on endogenous protein distribution within cells and at the subsynaptic level. Because we think these distributions and protein copy number are important in the determination of synaptic nano-organization and function, it will be imperative to begin quantifying the endogenous distribution and amount of various synaptic cell adhesion molecules. Much previous work in the estimation of the cellular and synaptic distribution of CAMs has either relied on immunogold labeling in electron microscopy preparations. Unfortunately, this approach suffers greatly in its labeling efficiency, as discussed previously. For convenience, many often rely on the overexpression of tagged molecules, which may change how these molecules behave. It will be important to observe the endogenous protein to come to a more physiological

understanding of even the most basic information. As we begin to optimize these approaches for the manipulation and visualization of endogenous synaptic cell adhesion molecules we may eventually be able to move into *in vivo* or even awake and behaving animal models. This feat would provide an unprecedented look into how these molecules operate at synapses to influence behavior through their regulation of synapse and circuit efficacy, and with animal behavior as a robust benchmark in successful operation of neuronal processes, we may begin to understand exactly how these molecules contribute to how we process and act in the world.

The experiments in this thesis demonstrate that the trans-synaptic nanoscale alignment of AMPARs to sites of neurotransmitter release enhance basal AMPAR-mediated synaptic transmission. The distance of AMPARs at the nanoscale to sites of evoked neurotransmitter release is important in determining the strength of the postsynaptic response. The alignment of AMPARs to RIM nanodomains is served by LRRTM2 acting as a trans-synaptic structural linkage. The nanoscale organization of AMPARs to sites of release is constitutively maintained on the scale of minutes. Determining how endogenous proteins control nano-alignment will be important for assessing the role in native circuits, and many proteins may be expected to contribute to this nanoscale organization. Nano-alignment may enable efficacious circuit function and promote behavioral performance or the generation of internal states. Tests of nano-alignment in intact circuits and using behavior as a benchmark for circuit performance will establish the role of nano-alignment as a fundamental neurobiological mechanism.

## REFERENCES


Akins, M. R., & Biederer, T. (2006). Cell–cell interactions in synaptogenesis. Current Opinion in Neurobiology (Vol. 16, Issue 1, pp. 83–89). https://doi.org/10.1016/j.conb.2006.01.009

Aoto, J., Martinelli, D. C., Malenka, R. C., Tabuchi, K., & Südhof, T. C. (2013). Presynaptic Neurexin-3 Alternative Splicing trans-Synaptically Controls Postsynaptic AMPA Receptor Trafficking. Cell (Vol. 154, Issue 1, pp. 75–88). https://doi.org/10.1016/j.cell.2013.05.060

Araki, Y., Hong, I., Gamache, T. R., Ju, S., Collado-Torres, L., Shin, J. H., & Huganir, R. L. (2020). SynGAP isoforms differentially regulate synaptic plasticity and dendritic development. eLife (Vol. 9). https://doi.org/10.7554/elife.56273

Arendt, K. L., Royo, M., Fernández-Monreal, M., Knafo, S., Petrok, C. N., Martens, J. R., & Esteban, J. A. (2009). PIP3 controls synaptic function by maintaining AMPA receptor clustering at the postsynaptic membrane. Nature Neuroscience (Vol. 13, Issue 1, pp. 36–44). https://doi.org/10.1038/nn.2462

Armstrong, N., & Gouaux, E. (2000). Mechanisms for Activation and Antagonism of an AMPA-Sensitive Glutamate Receptor. Neuron (Vol. 28, Issue 1, pp. 165–181). https://doi.org/10.1016/s0896-6273(00)00094-5

Ashby, M. C., Maier, S. R., Nishimune, A., & Henley, J. M. (2006). Lateral Diffusion Drives Constitutive Exchange of AMPA Receptors at Dendritic Spines and Is Regulated by Spine Morphology. Journal of Neuroscience (Vol. 26, Issue 26, pp. 7046–7055). https://doi.org/10.1523/jneurosci.1235-06.2006

Atasoy, D., Ertunc, M., Moulder, K. L., Blackwell, J., Chung, C., Su, J., & Kavalali, E. T. (2008). Spontaneous and Evoked Glutamate Release Activates Two Populations of NMDA Receptors with Limited Overlap. Journal of Neuroscience (Vol. 28, Issue 40, pp. 10151–10166). https://doi.org/10.1523/jneurosci.2432-08.2008

Atasoy, D., Schoch, S., Ho, A., Nadasy, K. A., Liu, X., Zhang, W., Mukherjee, K., Nosyreva, E. D., Fernandez-Chacon, R., Missler, M., Kavalali, E. T., & Sudhof, T. C. (2007). Deletion of CASK in mice is lethal and impairs synaptic function. Proceedings of the National Academy of Sciences (Vol. 104, Issue 7, pp. 2525–2530). https://doi.org/10.1073/pnas.0611003104

Augustin, I., Rosenmund, C., Südhof, T. C., & Brose, N. (1999). Munc13-1 is essential for fusion competence of glutamatergic synaptic vesicles. Nature (Vol. 400, Issue 6743, pp. 457–461). https://doi.org/10.1038/22768

Augustine, G. J., Burns, M. E., DeBello, W. M., Hilfiker, S., Morgan, J. R., Schweizer, F. E., Tokumaru, H., & Umayahara, K. (1999). Proteins involved in

synaptic vesicle trafficking. The Journal of Physiology (Vol. 520, Issue 1, pp. 33–41). https://doi.org/10.1111/j.1469-7793.1999.00033.x

Barbour, B. & Hauser, M. (1997). Intersynaptic diffusion of neurotransmitter. Trends in Neurosciences (Vol. 20, Issue 9, pp. 377–384). https://doi.org/10.1016/s0166-2236(96)20050-5

Barbour, B. (2001). An Evaluation of Synapse Independence. The Journal of Neuroscience (Vol. 21, Issue 20, pp. 7969–7984). https://doi.org/10.1523/jneurosci.21-20-07969.2001

Barrera-Ocampo, A., & Chater, T. E. (2013). Contribution of Postsynaptic Molecules to AMPA Receptor Nanodomain Organization. Journal of Neuroscience (Vol. 33, Issue 49, pp. 19048–19050). https://doi.org/10.1523/jneurosci.4273-13.2013

Bats, C., Groc, L., & Choquet, D. (2007). The Interaction between Stargazin and PSD-95 Regulates AMPA Receptor Surface Trafficking. Neuron (Vol. 53, Issue 5, pp. 719–734). https://doi.org/10.1016/j.neuron.2007.01.030

Bekkers, J. M., & Clements, J. D. (1999). Quantal amplitude and quantal variance of strontium-induced asynchronous EPSCs in rat dentate granule neurons. The Journal of Physiology (Vol. 516, Issue 1, pp. 227–248). https://doi.org/10.1111/j.1469-7793.1999.227aa.x

Bekkers, J. M., & Stevens, C. F. (1990). Presynaptic mechanism for long-term potentiation in the hippocampus. Nature (Vol. 346, Issue 6286, pp. 724–729). https://doi.org/10.1038/346724a0

Bellingham, M. C., Lim, R., & Walmsley, B. (1998). Developmental changes in EPSC quantal size and quantal content at a central glutamatergic synapse in rat. The Journal of Physiology (Vol. 511, Issue 3, pp. 861–869). https://doi.org/10.1111/j.1469-7793.1998.861bg.x

Benke, T. A., Lüthi, A., Isaac, J. T. R., & Collingridge, G. L. (1998). Modulation of AMPA receptor unitary conductance by synaptic activity. Nature (Vol. 393, Issue 6687, pp. 793–797). https://doi.org/10.1038/31709

Benson, D. (2000). Making memories stick: cell-adhesion molecules in synaptic plasticity. Trends in Cell Biology (Vol. 10, Issue 11, pp. 473–482). https://doi.org/10.1016/s0962-8924(00)01838-9

Betzig, E., Patterson, G. H., Sougrat, R., Lindwasser, O. W., Olenych, S., Bonifacino, J. S., Davidson, M. W., Lippincott-Schwartz, J., & Hess, H. F. (2006). Imaging Intracellular Fluorescent Proteins at Nanometer Resolution. Science (Vol. 313, Issue 5793, pp. 1642–1645). https://doi.org/10.1126/science.1127344

Bhouri, M., Morishita, W., Temkin, P., Goswami, D., Kawabe, H., Brose, N., Südhof, T. C., Craig, A. M., Siddiqui, T. J., & Malenka, R. (2018). Deletion of LRRTM1 and LRRTM2 in adult mice impairs basal AMPA receptor transmission and LTP in hippocampal CA1 pyramidal neurons. Proceedings of the National Academy of Sciences (Vol. 115, Issue 23, pp. E5382–E5389). https://doi.org/10.1073/pnas.1803280115

Biederer, T. (2002). SynCAM, a Synaptic Adhesion Molecule That Drives Synapse Assembly. Science (Vol. 297, Issue 5586, pp. 1525–1531). https://doi.org/10.1126/science.1072356

Biederer, T., & Scheiffele, P. (2007). Mixed-culture assays for analyzing neuronal synapse formation. Nature Protocols (Vol. 2, Issue 3, pp. 670–676). https://doi.org/10.1038/nprot.2007.92

Biederer, T., & Südhof, T. C. (2000). Mints as Adaptors. Journal of Biological Chemistry (Vol. 275, Issue 51, pp. 39803–39806). https://doi.org/10.1074/jbc.c000656200

Biederer, T., & Südhof, T. C. (2001). CASK and Protein 4.1 Support F-actin Nucleation on Neurexins. Journal of Biological Chemistry (Vol. 276, Issue 51, pp. 47869–47876). https://doi.org/10.1074/jbc.m105287200

Bissen, D., Foss, F., & Acker-Palmer, A. (2019). AMPA receptors and their minions: auxiliary proteins in AMPA receptor trafficking. Cellular and Molecular Life Sciences (Vol. 76, Issue 11, pp. 2133–2169). https://doi.org/10.1007/s00018-019-03068-7

Böhme, M. A., McCarthy, A. W., Grasskamp, A. T., Beuschel, C. B., Goel, P., Jusyte, M., Laber, D., Huang, S., Rey, U., Petzoldt, A. G., Lehmann, M., Göttfert, F., Haghighi, P., Hell, S. W., Owald, D., Dickman, D., Sigrist, S. J., & Walter, A. M. (2019). Rapid active zone remodeling consolidates presynaptic potentiation. Nature Communications (Vol. 10, Issue 1). https://doi.org/10.1038/s41467-019-08977-6

Bolshakov, V. Y., & Siegelbaum, S. A. (1995). Regulation of Hippocampal Transmitter Release During Development and Long-Term Potentiation. Science (Vol. 269, Issue 5231, pp. 1730–1734). https://doi.org/10.1126/science.7569903

Borgdorff, A. J., & Choquet, D. (2002). Regulation of AMPA receptor lateral movements. Nature (Vol. 417, Issue 6889, pp. 649–653). https://doi.org/10.1038/nature00780

Borges-Merjane, C., Kim, O., & Jonas, P. (2020). Functional Electron Microscopy, "Flash and Freeze," of Identified Cortical Synapses in Acute Brain Slices. Neuron (Vol. 105, Issue 6, pp. 992-1006.e6). https://doi.org/10.1016/j.neuron.2019.12.022

Boucard, A. A., Chubykin, A. A., Comoletti, D., Taylor, P., & Südhof, T. C. (2005). A Splice Code for trans-Synaptic Cell Adhesion Mediated by Binding of Neuroligin 1 to α- and β-Neurexins. Neuron (Vol. 48, Issue 2, pp. 229–236). https://doi.org/10.1016/j.neuron.2005.08.026

Boulter, J., Hollmann, M., O'Shea-Greenfield, A., Hartley, M., Deneris, E., Maron, C., & Heinemann, S. (1990). Molecular Cloning and Functional Expression of Glutamate Receptor Subunit Genes. Science (Vol. 249, Issue 4972, pp. 1033–1037). https://doi.org/10.1126/science.2168579

Bowie, D., & Mayer, M. L. (1995). Inward rectification of both AMPA and kainate subtype glutamate receptors generated by polyamine-mediated ion channel block. Neuron (Vol. 15, Issue 2, pp. 453–462). https://doi.org/10.1016/0896-6273(95)90049-7

Brock, J. A., Thomazeau, A., Watanabe, A., Li, S. S. Y., & Sjöström, P. J. (2020). A Practical Guide to Using CV Analysis for Determining the Locus of Synaptic Plasticity. Frontiers in Synaptic Neuroscience (Vol. 12). https://doi.org/10.3389/fnsyn.2020.00011

Brunger, A. T., Weninger, K., Bowen, M., & Chu, S. (2009). Single-Molecule Studies of the Neuronal SNARE Fusion Machinery. Annual Review of Biochemistry (Vol. 78, Issue 1, pp. 903–928). https://doi.org/10.1146/annurev.biochem.77.070306.103621

Burger, P. M., Mehl, E., Cameron, P. L., Maycox, P. R., Baumert, M., Lottspeich, F., De Camilli, P., & Jahn, R. (1989). Synaptic vesicles immunoisolated from rat cerebral cortex contain high levels of glutamate. Neuron (Vol. 3, Issue 6, pp. 715–720). https://doi.org/10.1016/0896-6273(89)90240-7

Cais, O., Herguedas, B., Krol, K., Cull-Candy, S. G., Farrant, M., & Greger, I. H. (2014). Mapping the Interaction Sites between AMPA Receptors and TARPs Reveals a Role for the Receptor N-Terminal Domain in Channel Gating. Cell Reports (Vol. 9, Issue 2, pp. 728–740). https://doi.org/10.1016/j.celrep.2014.09.029

Calloway, N., Gouzer, G., Xue, M., & Ryan, T. A. (2015). The active-zone protein Munc13 controls the use-dependence of presynaptic voltage-gated calcium channels. eLife (Vol. 4). https://doi.org/10.7554/elife.07728

Catterall, W. A. (2011). Voltage-Gated Calcium Channels. Cold Spring Harbor Perspectives in Biology (Vol. 3, Issue 8, pp. a003947–a003947). https://doi.org/10.1101/cshperspect.a003947

Chamma, I., Letellier, M., Butler, C., Tessier, B., Lim, K.-H., Gauthereau, I., Choquet, D., Sibarita, J.-B., Park, S., Sainlos, M., & Thoumine, O. (2016). Mapping the dynamics and nanoscale organization of synaptic adhesion proteins using

monomeric streptavidin. Nature Communications (Vol. 7, Issue 1). https://doi.org/10.1038/ncomms10773

Chamma, I., Levet, F., Sibarita, J.-B., Sainlos, M., & Thoumine, O. (2016). Nanoscale organization of synaptic adhesion proteins revealed by single-molecule localization microscopy. Neurophotonics (Vol. 3, Issue 4, p. 041810). https://doi.org/10.1117/1.nph.3.4.041810

Chamma, I., Sainlos, M., & Thoumine, O. (2020). Biophysical mechanisms underlying the membrane trafficking of synaptic adhesion molecules. Neuropharmacology (Vol. 169, p. 107555). https://doi.org/10.1016/j.neuropharm.2019.02.037

Chang, C.-W., Hui, E., Bai, J., Bruns, D., Chapman, E. R., & Jackson, M. B. (2015). A Structural Role for the Synaptobrevin 2 Transmembrane Domain in Dense-Core Vesicle Fusion Pores. Journal of Neuroscience (Vol. 35, Issue 14, pp. 5772–5780). https://doi.org/10.1523/jneurosci.3983-14.2015

Chen, H., Roth, R. H., Lopez-Ortega, E., Tan, H. L., & Huganir, R. L. (2021). AMPA Receptors Exist in Tunable Mobile and Immobile Synaptic Fractions In Vivo. eNeuro (Vol. 8, Issue 3, p. ENEURO.0015-21.2021). https://doi.org/10.1523/eneuro.0015-21.2021

Chen, J.-H., Blanpied, T. A., & Tang, A.-H. (2020). Quantification of trans-synaptic protein alignment: A data analysis case for single-molecule localization microscopy. Methods (Vol. 174, pp. 72–80). https://doi.org/10.1016/j.ymeth.2019.07.016

Chen, L., Chetkovich, D. M., Petralia, R. S., Sweeney, N. T., Kawasaki, Y., Wenthold, R. J., Bredt, D. S., & Nicoll, R. A. (2000). Stargazin regulates synaptic targeting of AMPA receptors by two distinct mechanisms. Nature (Vol. 408, Issue 6815, pp. 936–943). https://doi.org/10.1038/35050030

Chen, X., Levy, J. M., Hou, A., Winters, C., Azzam, R., Sousa, A. A., Leapman, R. D., Nicoll, R. A., & Reese, T. S. (2015). PSD-95 family MAGUKs are essential for anchoring AMPA and NMDA receptor complexes at the postsynaptic density. Proceedings of the National Academy of Sciences (Vol. 112, Issue 50, pp. E6983–E6992). https://doi.org/10.1073/pnas.1517045112

Chen, X., Winters, C., Azzam, R., Li, X., Galbraith, J. A., Leapman, R. D., & Reese, T. S. (2008). Organization of the core structure of the postsynaptic density. Proceedings of the National Academy of Sciences (Vol. 105, Issue 11, pp. 4453–4458). https://doi.org/10.1073/pnas.0800897105

Chih, B., Gollan, L., & Scheiffele, P. (2006). Alternative Splicing Controls Selective Trans-Synaptic Interactions of the Neuroligin-Neurexin Complex. Neuron (Vol. 51, Issue 2, pp. 171–178). https://doi.org/10.1016/j.neuron.2006.06.005

Chih, B., Gollan, L., & Scheiffele, P. (2006). Alternative Splicing Controls Selective Trans-Synaptic Interactions of the Neuroligin-Neurexin Complex. Neuron (Vol. 51, Issue 2, pp. 171–178). https://doi.org/10.1016/j.neuron.2006.06.005

Choi, B. J., Imlach, W. L., Jiao, W., Wolfram, V., Wu, Y., Grbic, M., Cela, C., Baines, R. A., Nitabach, M. N., & McCabe, B. D. (2014). Miniature Neurotransmission Regulates Drosophila Synaptic Structural Maturation. Neuron (Vol. 82, Issue 3, pp. 618–634). https://doi.org/10.1016/j.neuron.2014.03.012

Choquet, D., & Hosy, E. (2020). AMPA receptor nanoscale dynamic organization and synaptic plasticities. Current Opinion in Neurobiology (Vol. 63, pp. 137–145). https://doi.org/10.1016/j.conb.2020.04.003

Christie, J. M. (2006). Multivesicular Release at Schaffer Collateral-CA1 Hippocampal Synapses. Journal of Neuroscience (Vol. 26, Issue 1, pp. 210–216). https://doi.org/10.1523/jneurosci.4307-05.2006

Chung, C., & Kavalali, E. T. (2006). Seeking a function for spontaneous neurotransmission. Nature Neuroscience (Vol. 9, Issue 8, pp. 989–990). https://doi.org/10.1038/nn0806-989

Chung, C., Barylko, B., Leitz, J., Liu, X., & Kavalali, E. T. (2010). Acute Dynamin Inhibition Dissects Synaptic Vesicle Recycling Pathways That Drive Spontaneous and Evoked Neurotransmission. Journal of Neuroscience (Vol. 30, Issue 4, pp. 1363–1376). https://doi.org/10.1523/jneurosci.3427-09.2010

Cijsouw, T., Ramsey, A., Lam, T., Carbone, B., Blanpied, T., & Biederer, T. (2018). Mapping the Proteome of the Synaptic Cleft through Proximity Labeling Reveals New Cleft Proteins. Proteomes (Vol. 6, Issue 4, p. 48). https://doi.org/10.3390/proteomes6040048

Citri, A., & Malenka, R. C. (2007). Synaptic Plasticity: Multiple Forms, Functions, and Mechanisms. Neuropsychopharmacology (Vol. 33, Issue 1, pp. 18–41). https://doi.org/10.1038/sj.npp.1301559

Clements, J. D. (1996). Transmitter timecourse in the synaptic cleft: its role in central synaptic function. Trends in Neurosciences (Vol. 19, Issue 5, pp. 163–171). https://doi.org/10.1016/s0166-2236(96)10024-2

Condomitti, G., & de Wit, J. (2018). Heparan Sulfate Proteoglycans as Emerging Players in Synaptic Specificity. Frontiers in Molecular Neuroscience (Vol. 11). https://doi.org/10.3389/fnmol.2018.00014

Constals, A., Penn, A. C., Compans, B., Toulmé, E., Phillipat, A., Marais, S., Retailleau, N., Hafner, A.-S., Coussen, F., Hosy, E., & Choquet, D. (2015).

Glutamate-Induced AMPA Receptor Desensitization Increases Their Mobility and Modulates Short-Term Plasticity through Unbinding from Stargazin. Neuron (Vol. 85, Issue 4, pp. 787–803). https://doi.org/10.1016/j.neuron.2015.01.012

Cooper, B., Hemmerlein, M., Ammermuller, J., Imig, C., Reim, K., Lipstein, N., Kalla, S., Kawabe, H., Brose, N., Brandstatter, J. H., & Varoqueaux, F. (2012). Munc13-Independent Vesicle Priming at Mouse Photoreceptor Ribbon Synapses. Journal of Neuroscience (Vol. 32, Issue 23, pp. 8040–8052). https://doi.org/10.1523/jneurosci.4240-11.2012

Coppola, T., Magnin-Lüthi, S., Perret-Menoud, V., Gattesco, S., Schiavo, G., & Regazzi, R. (2001). Direct Interaction of the Rab3 Effector RIM with Ca2+Channels, SNAP-25, and Synaptotagmin. Journal of Biological Chemistry (Vol. 276, Issue 35, pp. 32756–32762). https://doi.org/10.1074/jbc.m100929200

Craig, A. M., Graf, E. R., & Linhoff, M. W. (2006). How to build a central synapse: clues from cell culture. Trends in Neurosciences (Vol. 29, Issue 1, pp. 8–20). https://doi.org/10.1016/j.tins.2005.11.002

Craven, S. E., El-Husseini, A. E., & Bredt, D. S. (1999). Synaptic Targeting of the Postsynaptic Density Protein PSD-95 Mediated by Lipid and Protein Motifs. Neuron (Vol. 22, Issue 3, pp. 497–509). https://doi.org/10.1016/s0896-6273(00)80705-9

Crosby, K. C., Gookin, S. E., Garcia, J. D., Hahm, K. M., Dell'Acqua, M. L., & Smith, K. R. (2019). Nanoscale Subsynaptic Domains Underlie the Organization of the Inhibitory Synapse. Cell Reports (Vol. 26, Issue 12, pp. 3284-3297.e3). https://doi.org/10.1016/j.celrep.2019.02.070

Crosby, K. C., Gookin, S. E., Garcia, J. D., Hahm, K. M., Dell'Acqua, M. L., & Smith, K. R. (2019). Nanoscale Subsynaptic Domains Underlie the Organization of the Inhibitory Synapse. Cell Reports (Vol. 26, Issue 12, pp. 3284-3297.e3). https://doi.org/10.1016/j.celrep.2019.02.070

Czondor, K., Mondin, M., Garcia, M., Heine, M., Frischknecht, R., Choquet, D., Sibarita, J.-B., & Thoumine, O. R. (2012). Unified quantitative model of AMPA receptor trafficking at synapses. Proceedings of the National Academy of Sciences (Vol. 109, Issue 9, pp. 3522–3527).
Dani, A., Huang, B., Bergan, J., Dulac, C., & Zhuang, X. (2010). Superresolution Imaging of Chemical Synapses in the Brain. Neuron (Vol. 68, Issue 5, pp. 843–856). https://doi.org/10.1016/j.neuron.2010.11.021

Daniels, R. W. (2004). Increased Expression of the Drosophila Vesicular Glutamate Transporter Leads to Excess Glutamate Release and a Compensatory Decrease in Quantal Content. Journal of Neuroscience (Vol. 24, Issue 46, pp. 10466–10474). https://doi.org/10.1523/jneurosci.3001-04.2004

de Wit, J., O'Sullivan, M. L., Savas, J. N., Condomitti, G., Caccese, M. C., Vennekens, K. M., Yates, J. R., III, & Ghosh, A. (2013). Unbiased Discovery of Glypican as a Receptor for LRRTM4 in Regulating Excitatory Synapse Development. Neuron (Vol. 79, Issue 4, pp. 696–711). https://doi.org/10.1016/j.neuron.2013.06.049

Deng, F., Price, M. G., Davis, C. F., Mori, M., & Burgess, D. L. (2006). Stargazin and Other Transmembrane AMPA Receptor Regulating Proteins Interact with Synaptic Scaffolding Protein MAGI-2 in Brain. Journal of Neuroscience (Vol. 26, Issue 30, pp. 7875–7884). https://doi.org/10.1523/jneurosci.1851-06.2006

Denker, A., Krohnert, K., Buckers, J., Neher, E., & Rizzoli, S. O. (2011). The reserve pool of synaptic vesicles acts as a buffer for proteins involved in synaptic vesicle recycling. Proceedings of the National Academy of Sciences (Vol. 108, Issue 41, pp. 17183–17188). https://doi.org/10.1073/pnas.1112690108

Dexter, P.M., Caldwell, K.A. & Caldwell, G.A. A Predictable Worm: Application of Caenorhabditis elegans for Mechanistic Investigation of Movement Disorders. Neurotherapeutics 9, 393–404 (2012). https://doi.org/10.1007/s13311-012-0109-x

Diamond, J. S., & Jahr, C. E. (1997). Transporters Buffer Synaptically Released Glutamate on a Submillisecond Time Scale. The Journal of Neuroscience (Vol. 17, Issue 12, pp. 4672–4687). https://doi.org/10.1523/jneurosci.17-12-04672.1997

DiAntonio, A., Petersen, S. A., Heckmann, M., & Goodman, C. S. (1999). Glutamate Receptor Expression Regulates Quantal Size and Quantal Content at theDrosophilaNeuromuscular Junction. In The Journal of Neuroscience (Vol. 19, Issue 8, pp. 3023–3032). Society for Neuroscience. https://doi.org/10.1523/jneurosci.19-08-03023.1999

Díaz-Alonso, J., Sun, Y. J., Granger, A. J., Levy, J. M., Blankenship, S. M., & Nicoll, R. A. (2017). Subunit-specific role for the amino-terminal domain of AMPA receptors in synaptic targeting. Proceedings of the National Academy of Sciences (Vol. 114, Issue 27, pp. 7136–7141). https://doi.org/10.1073/pnas.1707472114

Dieck, S., Sanmartí-Vila, L., Langnaese, K., Richter, K., Kindler, S., Soyke, A., Wex, H., Smalla, K.-H., Kämpf, U., Fränzer, J.-T., Stumm, M., Garner, C. C., & Gundelfinger, E. D. (1998). Bassoon, a Novel Zinc-finger CAG/Glutamine-repeat Protein Selectively Localized at the Active Zone of Presynaptic Nerve Terminals. Journal of Cell Biology (Vol. 142, Issue 2, pp. 499–509). https://doi.org/10.1083/jcb.142.2.499

Dolphin, A. C. (2013). The α2δ subunits of voltage-gated calcium channels. Biochimica et Biophysica Acta (BBA) - Biomembranes (Vol. 1828, Issue 7, pp. 1541–1549). https://doi.org/10.1016/j.bbamem.2012.11.019

Dolphin, A. C., & Lee, A. (2020). Presynaptic calcium channels: specialized control of synaptic neurotransmitter release. Nature Reviews Neuroscience (Vol. 21, Issue 4, pp. 213–229). https://doi.org/10.1038/s41583-020-0278-2

Durand, G. M., Kovalchuk, Y., & Konnerth, A. (1996). Long-term potentiation and functional synapse induction in developing hippocampus. Nature (Vol. 381, Issue 6577, pp. 71–75). https://doi.org/10.1038/381071a0

Ehlers, M. D. (2000). Reinsertion or Degradation of AMPA Receptors Determined by Activity-Dependent Endocytic Sorting. Neuron (Vol. 28, Issue 2, pp. 511–525). https://doi.org/10.1016/s0896-6273(00)00129-x

Ehlers, M. D., Heine, M., Groc, L., Lee, M.-C., & Choquet, D. (2007). Diffusional Trapping of GluR1 AMPA Receptors by Input-Specific Synaptic Activity. Neuron (Vol. 54, Issue 3, pp. 447–460). https://doi.org/10.1016/j.neuron.2007.04.010

Ehlers, M. D., Heine, M., Groc, L., Lee, M.-C., & Choquet, D. (2007). Diffusional Trapping of GluR1 AMPA Receptors by Input-Specific Synaptic Activity. Neuron (Vol. 54, Issue 3, pp. 447–460). https://doi.org/10.1016/j.neuron.2007.04.010

Ehrlich, I. (2004). Postsynaptic Density 95 controls AMPA Receptor Incorporation during Long-Term Potentiation and Experience-Driven Synaptic Plasticity. Journal of Neuroscience (Vol. 24, Issue 4, pp. 916–927). https://doi.org/10.1523/jneurosci.4733-03.2004

Ehrlich, I. (2004). Postsynaptic Density 95 controls AMPA Receptor Incorporation during Long-Term Potentiation and Experience-Driven Synaptic Plasticity. Journal of Neuroscience (Vol. 24, Issue 4, pp. 916–927). https://doi.org/10.1523/jneurosci.4733-03.2004

El-Awaad, E., Pryymachuk, G., Fried, C., Matthes, J., Isensee, J., Hucho, T., Neiss, W. F., Paulsson, M., Herzig, S., Zaucke, F., & Pietsch, M. (2019). Direct, gabapentin-insensitive interaction of a soluble form of the calcium channel subunit α2δ-1 with thrombospondin-4. Scientific Reports (Vol. 9, Issue 1). https://doi.org/10.1038/s41598-019-52655-y

Elias, G. M., & Nicoll, R. A. (2007). Synaptic trafficking of glutamate receptors by MAGUK scaffolding proteins. Trends in Cell Biology (Vol. 17, Issue 7, pp. 343–352). https://doi.org/10.1016/j.tcb.2007.07.005

Eriksen, J., Li, F., & Edwards, R. H. (2020). The mechanism and regulation of vesicular glutamate transport: Coordination with the synaptic vesicle cycle. Biochimica et Biophysica Acta (BBA) - Biomembranes (Vol. 1862, Issue 12, p. 183259). https://doi.org/10.1016/j.bbamem.2020.183259

Faber, D. S., & Korn, H. (1991). Applicability of the coefficient of variation method for analyzing synaptic plasticity. Biophysical Journal (Vol. 60, Issue 5, pp. 1288–1294). https://doi.org/10.1016/s0006-3495(91)82162-2

Fang, H., Bygrave, A. M., Roth, R. H., Johnson, R. C., & Huganir, R. L. (2021). An optimized CRISPR/Cas9 approach for precise genome editing in neurons. eLife (Vol. 10). https://doi.org/10.7554/elife.65202

Farhy-Tselnicker, I., van Casteren, A. C. M., Lee, A., Chang, V. T., Aricescu, A. R., & Allen, N. J. (2017). Astrocyte-Secreted Glypican 4 Regulates Release of Neuronal Pentraxin 1 from Axons to Induce Functional Synapse Formation. Neuron (Vol. 96, Issue 2, pp. 428-445.e13). https://doi.org/10.1016/j.neuron.2017.09.053

Fenster, S. D., Chung, W. J., Zhai, R., Cases-Langhoff, C., Voss, B., Garner, A. M., Kaempf, U., Kindler, S., Gundelfinger, E. D., & Garner, C. C. (2000). Piccolo, a Presynaptic Zinc Finger Protein Structurally Related to Bassoon. Neuron (Vol. 25, Issue 1, pp. 203–214). https://doi.org/10.1016/s0896-6273(00)80883-1

Foster, T. C., & McNaughton, B. L. (1991). Long-term enhancement of CA1 synaptic transmission is due to increased quantal size, not quantal content. Hippocampus (Vol. 1, Issue 1, pp. 79–91). https://doi.org/10.1002/hipo.450010108

Franks, K. M., Bartol, T. M., & Sejnowski, T. J. (2002). A Monte Carlo Model Reveals Independent Signaling at Central Glutamatergic Synapses. Biophysical Journal (Vol. 83, Issue 5, pp. 2333–2348). https://doi.org/10.1016/s0006-3495(02)75248-x

Franks, K. M., Stevens, C. F., & Sejnowski, T. J. (2003). Independent Sources of Quantal Variability at Single Glutamatergic Synapses. The Journal of Neuroscience (Vol. 23, Issue 8, pp. 3186–3195). https://doi.org/10.1523/jneurosci.23-08-03186.2003

Freche, D., Pannasch, U., Rouach, N., & Holcman, D. (2011). Synapse Geometry and Receptor Dynamics Modulate Synaptic Strength. PLoS ONE (Vol. 6, Issue 10, p. e25122). https://doi.org/10.1371/journal.pone.0025122

Fremeau, R. T., Jr., Troyer, M. D., Pahner, I., Nygaard, G. O., Tran, C. H., Reimer, R. J., Bellocchio, E. E., Fortin, D., Storm-Mathisen, J., & Edwards, R. H. (2001). The Expression of Vesicular Glutamate Transporters Defines Two Classes of Excitatory Synapse. In Neuron (Vol. 31, Issue 2, pp. 247–260). Elsevier BV. https://doi.org/10.1016/s0896-6273(01)00344-0

Friedrich, R. W., Jacobson, G. A., & Zhu, P. (2010). Circuit Neuroscience in Zebrafish. Current Biology (Vol. 20, Issue 8, pp. R371–R381). Elsevier BV. https://doi.org/10.1016/j.cub.2010.02.039

Frischknecht, R., Heine, M., Perrais, D., Seidenbecher, C. I., Choquet, D., & Gundelfinger, E. D. (2009). Brain extracellular matrix affects AMPA receptor lateral mobility and short-term synaptic plasticity. Nature Neuroscience (Vol. 12, Issue 7, pp. 897–904). https://doi.org/10.1038/nn.2338

Frost, N. A., Shroff, H., Kong, H., Betzig, E., & Blanpied, T. A. (2010). Single-Molecule Discrimination of Discrete Perisynaptic and Distributed Sites of Actin Filament Assembly within Dendritic Spines. Neuron (Vol. 67, Issue 1, pp. 86–99). https://doi.org/10.1016/j.neuron.2010.05.026

Fuccillo, M. V., Földy, C., Gökce, Ö., Rothwell, P. E., Sun, G. L., Malenka, R. C., & Südhof, T. C. (2015). Single-Cell mRNA Profiling Reveals Cell-Type-Specific Expression of Neurexin Isoforms. Neuron (Vol. 87, Issue 2, pp. 326–340). https://doi.org/10.1016/j.neuron.2015.06.028

Fukata, Y., Chen, X., Chiken, S., Hirano, Y., Yamagata, A., Inahashi, H., Sanbo, M., Sano, H., Goto, T., Hirabayashi, M., Kornau, H.-C., Prüss, H., Nambu, A., Fukai, S., Nicoll, R. A., & Fukata, M. (2021). LGI1–ADAM22–MAGUK configures transsynaptic nanoalignment for synaptic transmission and epilepsy prevention. Proceedings of the National Academy of Sciences (Vol. 118, Issue 3, p. e2022580118). https://doi.org/10.1073/pnas.2022580118

Fukata, Y., Dimitrov, A., Boncompain, G., Vielemeyer, O., Perez, F., & Fukata, M. (2013). Local palmitoylation cycles define activity-regulated postsynaptic subdomains. Journal of Cell Biology (Vol. 202, Issue 1, pp. 145–161). https://doi.org/10.1083/jcb.201302071

Fukata, Y., Hirano, Y., Miyazaki, Y., Yokoi, N., & Fukata, M. (2021). Trans-synaptic LGI1–ADAM22–MAGUK in AMPA and NMDA receptor regulation. Neuropharmacology (Vol. 194, p. 108628). https://doi.org/10.1016/j.neuropharm.2021.108628

Fukumoto, Y., Obata, Y., Ishibashi, K., Tamura, N., Kikuchi, I., Aoyama, K., Hattori, Y., Tsuda, K., Nakayama, Y., & Yamaguchi, N. (2010). Cost-effective gene transfection by DNA compaction at pH 4.0 using acidified, long shelf-life polyethylenimine. Cytotechnology (Vol. 62, Issue 1, pp. 73–82). https://doi.org/10.1007/s10616-010-9259-z

García-Nafría, J., Herguedas, B., Watson, J. F., & Greger, I. H. (2016). The dynamic AMPA receptor extracellular region: a platform for synaptic protein interactions. The Journal of Physiology (Vol. 594, Issue 19, pp. 5449–5458). https://doi.org/10.1113/jp271844

Geppert, M., Goda, Y., Hammer, R. E., Li, C., Rosahl, T. W., Stevens, C. F., & Südhof, T. C. (1994). Synaptotagmin I: A major Ca2+ sensor for transmitter release

at a central synapse. Cell (Vol. 79, Issue 4, pp. 717–727). https://doi.org/10.1016/0092-8674(94)90556-8

Getz, A. M., Ducros, M., Breillat, C., Lampin-Saint-Amaux, A., Daburon, S., François, U., Nowacka, A., Fernández-Monreal, M., Hosy, E., Lanore, F., Zieger, H., Sainlos, M., Humeau, Y., & Choquet, D. (2021). High-resolution imaging and manipulation of endogenous AMPA receptor surface mobility during synaptic plasticity and learning. https://doi.org/10.1101/2021.09.21.461215

Gomez, A. M., Traunmüller, L., & Scheiffele, P. (2021). Neurexins: molecular codes for shaping neuronal synapses. Nature Reviews Neuroscience (Vol. 22, Issue 3, pp. 137–151). https://doi.org/10.1038/s41583-020-00415-7

Goodman, L., Baddeley, D., Ambroziak, W., Waites, C. L., Garner, C. C., Soeller, C., & Montgomery, J. M. (2017). N-terminal SAP97 isoforms differentially regulate synaptic structure and postsynaptic surface pools of AMPA receptors. Hippocampus (Vol. 27, Issue 6, pp. 668–682). https://doi.org/10.1002/hipo.22723

Graf, E. R., Zhang, X., Jin, S.-X., Linhoff, M. W., & Craig, A. M. (2004). Neurexins Induce Differentiation of GABA and Glutamate Postsynaptic Specializations via Neuroligins. Cell (Vol. 119, Issue 7, pp. 1013–1026). https://doi.org/10.1016/j.cell.2004.11.035

Granger, A. J., Shi, Y., Lu, W., Cerpas, M., & Nicoll, R. A. (2012). LTP requires a reserve pool of glutamate receptors independent of subunit type. Nature (Vol. 493, Issue 7433, pp. 495–500). https://doi.org/10.1038/nature11775

Greger, I. H., Watson, J. F., & Cull-Candy, S. G. (2017). Structural and Functional Architecture of AMPA-Type Glutamate Receptors and Their Auxiliary Proteins. Neuron (Vol. 94, Issue 4, pp. 713–730). https://doi.org/10.1016/j.neuron.2017.04.009

Groc, L., & Choquet, D. (2020). Linking glutamate receptor movements and synapse function. Science (Vol. 368, Issue 6496). https://doi.org/10.1126/science.aay4631

Groc, L., Heine, M., Cognet, L., Brickley, K., Stephenson, F. A., Lounis, B., & Choquet, D. (2004). Differential activity-dependent regulation of the lateral mobilities of AMPA and NMDA receptors. Nature Neuroscience (Vol. 7, Issue 7, pp. 695–696). https://doi.org/10.1038/nn1270

Grunwald, C., Schulze, K., Giannone, G., Cognet, L., Lounis, B., Choquet, D., & Tampé, R. (2011). Quantum-Yield-Optimized Fluorophores for Site-Specific Labeling and Super-Resolution Imaging. Journal of the American Chemical Society (Vol. 133, Issue 21, pp. 8090–8093). https://doi.org/10.1021/ja200967z

Guo, CH., Senzel, A., Li, K. et al. De Novo Protein Synthesis of Syntaxin-1 and Dynamin-1 in Long-Term Memory Formation Requires CREB1 Gene Transcription

in Lymnaea stagnalis . Behav Genet 40, 680–693 (2010). https://doi.org/10.1007/s10519-010-9374-9

Haas, K. T., Compans, B., Letellier, M., Bartol, T. M., Grillo-Bosch, D., Sejnowski, T. J., Sainlos, M., Choquet, D., Thoumine, O., & Hosy, E. (2018). Pre-post synaptic alignment through neuroligin-1 tunes synaptic transmission efficiency. eLife (Vol. 7). https://doi.org/10.7554/elife.31755

Han, Y., Kaeser, P. S., Südhof, T. C., & Schneggenburger, R. (2011). RIM Determines Ca2+ Channel Density and Vesicle Docking at the Presynaptic Active Zone. Neuron (Vol. 69, Issue 2, pp. 304–316). https://doi.org/10.1016/j.neuron.2010.12.014

Harlow, M. L., Ress, D., Stoschek, A., Marshall, R. M., & McMahan, U. J. (2001). The architecture of active zone material at the frog's neuromuscular junction. Nature (Vol. 409, Issue 6819, pp. 479–484). https://doi.org/10.1038/35054000

Harris, K. M. (2020). Structural LTP: from synaptogenesis to regulated synapse enlargement and clustering. Current Opinion in Neurobiology (Vol. 63, pp. 189–197). https://doi.org/10.1016/j.conb.2020.04.009

Harris, K., & Stevens, J. (1989). Dendritic spines of CA 1 pyramidal cells in the rat hippocampus: serial electron microscopy with reference to their biophysical characteristics. The Journal of Neuroscience (Vol. 9, Issue 8, pp. 2982–2997). https://doi.org/10.1523/jneurosci.09-08-02982.1989

Hata, Y., Butz, S., & Sudhof, T. (1996). CASK: a novel dlg/PSD95 homolog with an N-terminal calmodulin-dependent protein kinase domain identified by interaction with neurexins. The Journal of Neuroscience (Vol. 16, Issue 8, pp. 2488–2494). https://doi.org/10.1523/jneurosci.16-08-02488.1996

Hayashi, M. K., Tang, C., Verpelli, C., Narayanan, R., Stearns, M. H., Xu, R.-M., Li, H., Sala, C., & Hayashi, Y. (2009). The Postsynaptic Density Proteins Homer and Shank Form a Polymeric network Structure. Cell (Vol. 137, Issue 1, pp. 159–171). https://doi.org/10.1016/j.cell.2009.01.050

Hayer, A., & Bhalla, U. S. (2005). Molecular Switches at the Synapse Emerge from Receptor and Kinase Traffic. PLoS Computational Biology (Vol. 1, Issue 2, p. e20). https://doi.org/10.1371/journal.pcbi.0010020

Heck, J., Parutto, P., Ciuraszkiewicz, A., Bikbaev, A., Freund, R., Mitlöhner, J., Andres-Alonso, M., Fejtova, A., Holcman, D., & Heine, M. (2019). Transient Confinement of CaV2.1 Ca2+-Channel Splice Variants Shapes Synaptic Short-Term Plasticity. Neuron (Vol. 103, Issue 1, pp. 66-79.e12). https://doi.org/10.1016/j.neuron.2019.04.030

Heine, M., & Holcman, D. (2020). Asymmetry Between Pre- and Postsynaptic Transient Nanodomains Shapes Neuronal Communication. Trends in Neurosciences (Vol. 43, Issue 3, pp. 182–196). https://doi.org/10.1016/j.tins.2020.01.005

Heine, M., Groc, L., Frischknecht, R., Béïque, J.-C., Lounis, B., Rumbaugh, G., Huganir, R. L., Cognet, L., & Choquet, D. (2008). Surface Mobility of Postsynaptic AMPARs Tunes Synaptic Transmission. Science (Vol. 320, Issue 5873, pp. 201–205). https://doi.org/10.1126/science.1152089

Heine, M., Thoumine, O., Mondin, M., Tessier, B., Giannone, G., & Choquet, D. (2008). Activity-independent and subunit-specific recruitment of functional AMPA receptors at neurexin/neuroligin contacts. Proceedings of the National Academy of Sciences (Vol. 105, Issue 52, pp. 20947–20952). https://doi.org/10.1073/pnas.0804007106

Hembrook-Short, J. R., Mock, V. L., Usrey, W. M., & Briggs, F. (2018). Attention Enhances the Efficacy of Communication in V1 Local Circuits. The Journal of Neuroscience (Vol. 39, Issue 6, pp. 1066–1076). Society for Neuroscience. https://doi.org/10.1523/jneurosci.2164-18.2018

Herguedas, B., Krieger, J., & Greger, I. H. (2013). Receptor Heteromeric Assembly—How It Works and Why It Matters. Progress in Molecular Biology and Translational Science (pp. 361–386). https://doi.org/10.1016/b978-0-12-386931-9.00013-1

Herguedas, B., Watson, J. F., Ho, H., Cais, O., García-Nafría, J., & Greger, I. H. (2019). Architecture of the heteromeric GluA1/2 AMPA receptor in complex with the auxiliary subunit TARP γ8. Science (Vol. 364, Issue 6438). https://doi.org/10.1126/science.aav9011

Heuser, J. E., & Reese, T. S. (1973). EVIDENCE FOR RECYCLING OF SYNAPTIC VESICLE MEMBRANE DURING TRANSMITTER RELEASE AT THE FROG NEUROMUSCULAR JUNCTION. Journal of Cell Biology (Vol. 57, Issue 2, pp. 315–344). https://doi.org/10.1083/jcb.57.2.315

Hibino, H., Pironkova, R., Onwumere, O., Vologodskaia, M., Hudspeth, A. J., & Lesage, F. (2002). RIM Binding Proteins (RBPs) Couple Rab3-Interacting Molecules (RIMs) to Voltage-Gated Ca2+ Channels. Neuron (Vol. 34, Issue 3, pp. 411–423). https://doi.org/10.1016/s0896-6273(02)00667-0

Hjelmstad, G. O., Nicoll, R. A., & Malenka, R. C. (1997). Synaptic Refractory Period Provides a Measure of Probability of Release in the Hippocampus. Neuron (Vol. 19, Issue 6, pp. 1309–1318). https://doi.org/10.1016/s0896-6273(00)80421-3

Holcman, D., & Schuss, Z. (2014). Time scale of diffusion in molecular and cellular biology. Journal of Physics A: Mathematical and Theoretical (Vol. 47, Issue 17, p. 173001). https://doi.org/10.1088/1751-8113/47/17/173001

Holcman, D., & Yuste, R. (2015). The new nanophysiology: regulation of ionic flow in neuronal subcompartments. Nature Reviews Neuroscience (Vol. 16, Issue 11, pp. 685–692). https://doi.org/10.1038/nrn4022

Hollmann, M., Hartley, M., & Heinemann, S. (1991). Ca2+ permeability of KA-AMPA--gated glutamate receptor channels depends on subunit composition. Science (Vol. 252, Issue 5007, pp. 851–853). https://doi.org/10.1126/science.1709304

Holmes, W. R. (1995). Modeling the effect of glutamate diffusion and uptake on NMDA and non-NMDA receptor saturation. Biophysical Journal (Vol. 69, Issue 5, pp. 1734–1747). https://doi.org/10.1016/s0006-3495(95)80043-3

Hoppa, M. B., Lana, B., Margas, W., Dolphin, A. C., & Ryan, T. A. (2012). α2δ expression sets presynaptic calcium channel abundance and release probability. Nature (Vol. 486, Issue 7401, pp. 122–125). https://doi.org/10.1038/nature11033

Hori, T., & Takahashi, T. (2012). Kinetics of Synaptic Vesicle Refilling with Neurotransmitter Glutamate. Neuron (Vol. 76, Issue 3, pp. 511–517). https://doi.org/10.1016/j.neuron.2012.08.013

Hou, Q., Zhang, D., Jarzylo, L., Huganir, R. L., & Man, H.-Y. (2008). Homeostatic regulation of AMPA receptor expression at single hippocampal synapses. Proceedings of the National Academy of Sciences (Vol. 105, Issue 2, pp. 775–780). https://doi.org/10.1073/pnas.0706447105

Hruska, M., & Dalva, M. B. (2012). Ephrin regulation of synapse formation, function and plasticity. Molecular and Cellular Neuroscience (Vol. 50, Issue 1, pp. 35–44). https://doi.org/10.1016/j.mcn.2012.03.004

Hruska, M., Henderson, N., Le Marchand, S. J., Jafri, H., & Dalva, M. B. (2018). Synaptic nanomodules underlie the organization and plasticity of spine synapses. Nature Neuroscience (Vol. 21, Issue 5, pp. 671–682). https://doi.org/10.1038/s41593-018-0138-9

Hu, Z., Tong, X.-J., & Kaplan, J. M. (2013). UNC-13L, UNC-13S, and Tomosyn form a protein code for fast and slow neurotransmitter release in Caenorhabditis elegans. eLife (Vol. 2). https://doi.org/10.7554/elife.00967

Huang, B., Jones, S. A., Brandenburg, B., & Zhuang, X. (2008). Whole-cell 3D STORM reveals interactions between cellular structures with nanometer-scale resolution. Nature Methods (Vol. 5, Issue 12, pp. 1047–1052). https://doi.org/10.1038/nmeth.1274

Huganir, R. L., & Nicoll, R. A. (2013). AMPARs and Synaptic Plasticity: The Last 25 Years. Neuron (Vol. 80, Issue 3, pp. 704–717). https://doi.org/10.1016/j.neuron.2013.10.025

Ichtchenko, K., Hata, Y., Nguyen, T., Ullrich, B., Missler, M., Moomaw, C., & Südhof, T. C. (1995). Neuroligin 1: A splice site-specific ligand for β-neurexins. Cell (Vol. 81, Issue 3, pp. 435–443). https://doi.org/10.1016/0092-8674(95)90396-8

Ichtchenko, K., Nguyen, T., & Südhof, T. C. (1996). Structures, Alternative Splicing, and Neurexin Binding of Multiple Neuroligins. Journal of Biological Chemistry (Vol. 271, Issue 5, pp. 2676–2682). https://doi.org/10.1074/jbc.271.5.2676

Irie, M. (1997). Binding of Neuroligins to PSD-95. Science (Vol. 277, Issue 5331, pp. 1511–1515). https://doi.org/10.1126/science.277.5331.1511

Isaac, J. T. R., Nicoll, R. A., & Malenka, R. C. (1995). Evidence for silent synapses: Implications for the expression of LTP. Neuron (Vol. 15, Issue 2, pp. 427–434). https://doi.org/10.1016/0896-6273(95)90046-2

Ishikawa, T., Sahara, Y., & Takahashi, T. (2002). A Single Packet of Transmitter Does Not Saturate Postsynaptic Glutamate Receptors. Neuron (Vol. 34, Issue 4, pp. 613–621). https://doi.org/10.1016/s0896-6273(02)00692-x

Jacob, A. L., & Weinberg, R. J. (2015). The organization of AMPA receptor subunits at the postsynaptic membrane. Hippocampus (Vol. 25, Issue 7, pp. 798–812). https://doi.org/10.1002/hipo.22404

Jahn, R., & Scheller, R. H. (2006). SNAREs — engines for membrane fusion. Nature Reviews Molecular Cell Biology (Vol. 7, Issue 9, pp. 631–643). https://doi.org/10.1038/nrm2002

Johansen, J. P., Wolff, S. B. E., Lüthi, A., & LeDoux, J. E. (2012). Controlling the Elements: An Optogenetic Approach to Understanding the Neural Circuits of Fear. Biological Psychiatry (Vol. 71, Issue 12, pp. 1053–1060). Elsevier BV. https://doi.org/10.1016/j.biopsych.2011.10.023

Jonas, P., & Spruston, N. (1994). Mechanisms shaping glutamate-mediated excitatory postsynaptic currents in the CNS. Current Opinion in Neurobiology (Vol. 4, Issue 3, pp. 366–372). https://doi.org/10.1016/0959-4388(94)90098-1

Kaeser, P. S., & Regehr, W. G. (2017). The readily releasable pool of synaptic vesicles. Current Opinion in Neurobiology (Vol. 43, pp. 63–70). https://doi.org/10.1016/j.conb.2016.12.012

Kaeser, P. S., Deng, L., Fan, M., & Sudhof, T. C. (2012). RIM genes differentially contribute to organizing presynaptic release sites. Proceedings of the National Academy of Sciences (Vol. 109, Issue 29, pp. 11830–11835). https://doi.org/10.1073/pnas.1209318109

Kaeser, P. S., Deng, L., Wang, Y., Dulubova, I., Liu, X., Rizo, J., & Südhof, T. C. (2011). RIM Proteins Tether Ca2+ Channels to Presynaptic Active Zones via a Direct PDZ-Domain Interaction. Cell (Vol. 144, Issue 2, pp. 282–295). https://doi.org/10.1016/j.cell.2010.12.029

Karlocai, M. R., Heredi, J., Benedek, T., Holderith, N., Lorincz, A., & Nusser, Z. (2021). Variability in the Munc13-1 content of excitatory release sites. eLife (Vol. 10). https://doi.org/10.7554/elife.67468

Kavalali, E. T. (2014). The mechanisms and functions of spontaneous neurotransmitter release. Nature Reviews Neuroscience (Vol. 16, Issue 1, pp. 5–16). https://doi.org/10.1038/nrn3875

Keinänen, K., Wisden, W., Sommer, B., Werner, P., Herb, A., Verdoorn, T. A., Sakmann, B., & Seeburg, P. H. (1990). A Family of AMPA-Selective Glutamate Receptors. Science (Vol. 249, Issue 4968, pp. 556–560). https://doi.org/10.1126/science.2166337

Kennedy, M. B., & Mastro, T. L. (2017). Liquid Phase Transition in the Postsynaptic Density? Trends in Biochemical Sciences (Vol. 42, Issue 1, pp. 2–4). https://doi.org/10.1016/j.tibs.2016.11.005

Kennedy, M. J., & Ehlers, M. D. (2006). ORGANELLES AND TRAFFICKING MACHINERY FOR POSTSYNAPTIC PLASTICITY. Annual Review of Neuroscience (Vol. 29, Issue 1, pp. 325–362). https://doi.org/10.1146/annurev.neuro.29.051605.112808

Kennedy, M. J., Davison, I. G., Robinson, C. G., & Ehlers, M. D. (2010). Syntaxin-4 Defines a Domain for Activity-Dependent Exocytosis in Dendritic Spines. Cell (Vol. 141, Issue 3, pp. 524–535). https://doi.org/10.1016/j.cell.2010.02.042

Kerr, J. M., & Blanpied, T. A. (2012). Subsynaptic AMPA Receptor Distribution Is Acutely Regulated by Actin-Driven Reorganization of the Postsynaptic Density. Journal of Neuroscience (Vol. 32, Issue 2, pp. 658–673). https://doi.org/10.1523/jneurosci.2927-11.2012

Kessels, H. W., Kopec, C. D., Klein, M. E., & Malinow, R. (2009). Roles of stargazin and phosphorylation in the control of AMPA receptor subcellular distribution. Nature Neuroscience (Vol. 12, Issue 7, pp. 888–896). https://doi.org/10.1038/nn.2340

Kessler, J.-P. (2013). Control of Cleft Glutamate Concentration and Glutamate Spill-Out by Perisynaptic Glia: Uptake and Diffusion Barriers. PLoS ONE (Vol. 8, Issue 8, p. e70791). https://doi.org/10.1371/journal.pone.0070791

Kim, J. J., & Jung, M. W. (2006). Neural circuits and mechanisms involved in Pavlovian fear conditioning: A critical review. Neuroscience & Biobehavioral Reviews (Vol. 30, Issue 2, pp. 188–202). https://doi.org/10.1016/j.neubiorev.2005.06.005

Kinney, J. P., Spacek, J., Bartol, T. M., Bajaj, C. L., Harris, K. M., & Sejnowski, T. J. (2012). Extracellular sheets and tunnels modulate glutamate diffusion in hippocampal neuropil. Journal of Comparative Neurology (Vol. 521, Issue 2, pp. 448–464). https://doi.org/10.1002/cne.23181

Kirkpatrick, L. L., Matzuk, M. M., Dodds, D. C., & Perin, M. S. (2000). Biochemical Interactions of the Neuronal Pentraxins. Journal of Biological Chemistry (Vol. 275, Issue 23, pp. 17786–17792). https://doi.org/10.1074/jbc.m002254200

Kiyonaka, S., Wakamori, M., Miki, T., Uriu, Y., Nonaka, M., Bito, H., Beedle, A. M., Mori, E., Hara, Y., De Waard, M., Kanagawa, M., Itakura, M., Takahashi, M., Campbell, K. P., & Mori, Y. (2007). RIM1 confers sustained activity and neurotransmitter vesicle anchoring to presynaptic Ca2+ channels. Nature Neuroscience (Vol. 10, Issue 6, pp. 691–701). https://doi.org/10.1038/nn1904

Klaassen, R. V., Stroeder, J., Coussen, F., Hafner, A.-S., Petersen, J. D., Renancio, C., Schmitz, L. J. M., Normand, E., Lodder, J. C., Rotaru, D. C., Rao-Ruiz, P., Spijker, S., Mansvelder, H. D., Choquet, D., & Smit, A. B. (2016). Shisa6 traps AMPA receptors at postsynaptic sites and prevents their desensitization during synaptic activity. Nature Communications (Vol. 7, Issue 1). https://doi.org/10.1038/ncomms10682

Klatt, O., Repetto, D., Brockhaus, J., Reissner, C., El khallouqi, A., Rohlmann, A., Heine, M., & Missler, M. (2021). Endogenous β-neurexins on axons and within synapses show regulated dynamic behavior. Cell Reports (Vol. 35, Issue 11, p. 109266). https://doi.org/10.1016/j.celrep.2021.109266

Klueva, J., Gundelfinger, E. D., Frischknecht, R. R., & Heine, M. (2014). Intracellular Ca 2+ and not the extracellular matrix determines surface dynamics of AMPA-type glutamate receptors on aspiny neurons. Philosophical Transactions of the Royal Society B: Biological Sciences (Vol. 369, Issue 1654, p. 20130605). https://doi.org/10.1098/rstb.2013.0605

Ko, J. (2012). The leucine-rich repeat superfamily of synaptic adhesion molecules: LRRTMs and Slitrks. Molecules and Cells (Vol. 34, Issue 4, pp. 335–340). https://doi.org/10.1007/s10059-012-0113-3

Ko, J. S., Pramanik, G., Um, J. W., Shim, J. S., Lee, D., Kim, K. H., Chung, G.-Y., Condomitti, G., Kim, H. M., Kim, H., de Wit, J., Park, K.-S., Tabuchi, K., & Ko, J. (2015). PTPσ functions as a presynaptic receptor for the glypican-4/LRRTM4 complex and is essential for excitatory synaptic transmission. Proceedings of the National Academy of Sciences (Vol. 112, Issue 6, pp. 1874–1879). https://doi.org/10.1073/pnas.1410138112

Ko, J., Fuccillo, M. V., Malenka, R. C., & Südhof, T. C. (2009). LRRTM2 Functions as a Neurexin Ligand in Promoting Excitatory Synapse Formation. Neuron (Vol. 64, Issue 6, pp. 791–798). https://doi.org/10.1016/j.neuron.2009.12.012

Koh, D. S., Burnashev, N., & Jonas, P. (1995). Block of native Ca(2+)-permeable AMPA receptors in rat brain by intracellular polyamines generates double rectification. The Journal of Physiology (Vol. 486, Issue 2, pp. 305–312). https://doi.org/10.1113/jphysiol.1995.sp020813

Kropf, M., Rey, G., Glauser, L., Kulangara, K., Johnsson, K., & Hirling, H. (2008). Subunit-specific surface mobility of differentially labeled AMPA receptor subunits. European Journal of Cell Biology (Vol. 87, Issue 10, pp. 763–778). https://doi.org/10.1016/j.ejcb.2008.02.014

Kullmann, D. M., & Asztely, F. (1998). Extrasynaptic glutamate spillover in the hippocampus: evidence and implications. Trends in Neurosciences (Vol. 21, Issue 1, pp. 8–14). https://doi.org/10.1016/s0166-2236(97)01150-8

Kullmann, D. M., Erdemli, G., & Asztély, F. (1996). LTP of AMPA and NMDA Receptor–Mediated Signals: Evidence for Presynaptic Expression and Extrasynaptic Glutamate Spill-Over. Neuron (Vol. 17, Issue 3, pp. 461–474). https://doi.org/10.1016/s0896-6273(00)80178-6

Laurén, J., Airaksinen, M. S., Saarma, M., & Timmusk, T. õnis. (2003). A novel gene family encoding leucine-rich repeat transmembrane proteins differentially expressed in the nervous system. Genomics (Vol. 81, Issue 4, pp. 411–421). https://doi.org/10.1016/s0888-7543(03)00030-2

Lee, S. H., Jin, C., Cai, E., Ge, P., Ishitsuka, Y., Teng, K. W., de Thomaz, A. A., Nall, D., Baday, M., Jeyifous, O., Demonte, D., Dundas, C. M., Park, S., Delgado, J. Y., Green, W. N., & Selvin, P. R. (2017). Super-resolution imaging of synaptic and Extra-synaptic AMPA receptors with different-sized fluorescent probes. eLife (Vol. 6). https://doi.org/10.7554/elife.27744

Levet, F., Hosy, E., Kechkar, A., Butler, C., Beghin, A., Choquet, D., & Sibarita, J.-B. (2015). SR-Tesseler: a method to segment and quantify localization-based super-resolution microscopy data. Nature Methods (Vol. 12, Issue 11, pp. 1065–1071). https://doi.org/10.1038/nmeth.3579

Li, L.-P., Dustrude, E. T., Haulcomb, M. M., Abreu, A. R., Fitz, S. D., Johnson, P. L., Thakur, G. A., Molosh, A. I., Lai, Y., & Shekhar, A. (2018). PSD95 and nNOS interaction as a novel molecular target to modulate conditioned fear: relevance to PTSD. Translational Psychiatry (Vol. 8, Issue 1). https://doi.org/10.1038/s41398-018-0208-5

Li, S., Raychaudhuri, S., Lee, S. A., Brockmann, M. M., Wang, J., Kusick, G., Prater, C., Syed, S., Falahati, H., Ramos, R., Bartol, T. M., Hosy, E., & Watanabe, S. (2021). Asynchronous release sites align with NMDA receptors in mouse hippocampal synapses. Nature Communications (Vol. 12, Issue 1). https://doi.org/10.1038/s41467-021-21004-x

Li, T. P., Song, Y., MacGillavry, H. D., Blanpied, T. A., & Raghavachari, S. (2016). Protein Crowding within the Postsynaptic Density Can Impede the Escape of Membrane Proteins. The Journal of Neuroscience (Vol. 36, Issue 15, pp. 4276–4295). https://doi.org/10.1523/jneurosci.3154-15.2016

Liao, D., Hessler, N. A., & Malinow, R. (1995). Activation of postsynaptically silent synapses during pairing-induced LTP in CA1 region of hippocampal slice. Nature (Vol. 375, Issue 6530, pp. 400–404). https://doi.org/10.1038/375400a0

Linhoff, M. W., Laurén, J., Cassidy, R. M., Dobie, F. A., Takahashi, H., Nygaard, H. B., Airaksinen, M. S., Strittmatter, S. M., & Craig, A. M. (2009). An Unbiased Expression Screen for Synaptogenic Proteins Identifies the LRRTM Protein Family as Synaptic Organizers. Neuron (Vol. 61, Issue 5, pp. 734–749). https://doi.org/10.1016/j.neuron.2009.01.017

Liouta, K., Chabbert, J., Benquet, S., Tessier, B., Studer, V., Sainlos, M., De Wit, J., Thoumine, O., & Chamma, I. (2021). Role of regulatory C-terminal motifs in synaptic confinement of LRRTM2. Biology of the Cell. https://doi.org/10.1111/boc.202100026

Lisman, J. (2017). Glutamatergic synapses are structurally and biochemically complex because of multiple plasticity processes: long-term potentiation, long-term depression, short-term potentiation and scaling. Philosophical Transactions of the Royal Society B: Biological Sciences (Vol. 372, Issue 1715, p. 20160260). https://doi.org/10.1098/rstb.2016.0260

Liu, G., Choi, S., & Tsien, R. W. (1999). Variability of Neurotransmitter Concentration and Nonsaturation of Postsynaptic AMPA Receptors at Synapses in Hippocampal Cultures and Slices. Neuron (Vol. 22, Issue 2, pp. 395–409). https://doi.org/10.1016/s0896-6273(00)81099-5

Liu, S. J., & Cull-Candy, S. G. (2005). Subunit interaction with PICK and GRIP controls Ca2+ permeability of AMPARs at cerebellar synapses. Nature Neuroscience (Vol. 8, Issue 6, pp. 768–775). https://doi.org/10.1038/nn1468

Longsworth, L. G. (1953). Diffusion Measurements, at 25°, of Aqueous Solutions of Amino Acids, Peptides and Sugars. Journal of the American Chemical Society (Vol. 75, Issue 22, pp. 5705–5709). https://doi.org/10.1021/ja01118a065

López, J. C. (2002). Quantifying synaptic efficacy. Nature Reviews Neuroscience (Vol. 3, Issue 5, pp. 332–332). Springer Science and Business Media LLC. https://doi.org/10.1038/nrn814

Lu, W., Shi, Y., Jackson, A. C., Bjorgan, K., During, M. J., Sprengel, R., Seeburg, P. H., & Nicoll, R. A. (2009). Subunit Composition of Synaptic AMPA Receptors Revealed by a Single-Cell Genetic Approach. Neuron (Vol. 62, Issue 2, pp. 254–268). https://doi.org/10.1016/j.neuron.2009.02.027

Lucic, V., Yang, T., Schweikert, G., Förster, F., & Baumeister, W. (2005). Morphological Characterization of Molecular Complexes Present in the Synaptic Cleft. Structure (Vol. 13, Issue 3, pp. 423–434). https://doi.org/10.1016/j.str.2005.02.005

Lüscher, C., Xia, H., Beattie, E. C., Carroll, R. C., von Zastrow, M., Malenka, R. C., & Nicoll, R. A. (1999). Role of AMPA Receptor Cycling in Synaptic Transmission and Plasticity. Neuron (Vol. 24, Issue 3, pp. 649–658). https://doi.org/10.1016/s0896-6273(00)81119-8

Lüthi, A., & Lüscher, C. (2014). Pathological circuit function underlying addiction and anxiety disorders. Nature Neuroscience (Vol. 17, Issue 12, pp. 1635–1643). https://doi.org/10.1038/nn.3849

Ma, C., Su, L., Seven, A. B., Xu, Y., & Rizo, J. (2012). Reconstitution of the Vital Functions of Munc18 and Munc13 in Neurotransmitter Release. Science (Vol. 339, Issue 6118, pp. 421–425). https://doi.org/10.1126/science.1230473

MacGillavry, H. D., Song, Y., Raghavachari, S., & Blanpied, T. A. (2013). Nanoscale Scaffolding Domains within the Postsynaptic Density Concentrate Synaptic AMPA Receptors. Neuron (Vol. 78, Issue 4, pp. 615–622). https://doi.org/10.1016/j.neuron.2013.03.009

MacGillavry, H. D., Song, Y., Raghavachari, S., & Blanpied, T. A. (2013). Nanoscale Scaffolding Domains within the Postsynaptic Density Concentrate Synaptic AMPA Receptors. Neuron (Vol. 78, Issue 4, pp. 615–622). https://doi.org/10.1016/j.neuron.2013.03.009

Maglione, M., & Sigrist, S. J. (2013). Seeing the forest tree by tree: super-resolution light microscopy meets the neurosciences. Nature Neuroscience (Vol. 16, Issue 7, pp. 790–797). https://doi.org/10.1038/nn.3403

Maio, V. D., Ventriglia, F., & Santillo, S. (2017). Stochastic, structural and functional factors influencing AMPA and NMDA synaptic response variability: a review. Neuronal Signaling (Vol. 1, Issue 3). https://doi.org/10.1042/ns20160051

Makino, H., & Malinow, R. (2009). AMPA Receptor Incorporation into Synapses during LTP: The Role of Lateral Movement and Exocytosis. Neuron (Vol. 64, Issue 3, pp. 381–390). https://doi.org/10.1016/j.neuron.2009.08.035

Makino, H., & Malinow, R. (2009). AMPA Receptor Incorporation into Synapses during LTP: The Role of Lateral Movement and Exocytosis. Neuron (Vol. 64, Issue 3, pp. 381–390). https://doi.org/10.1016/j.neuron.2009.08.035

Malenka, R. C. (2003). The long-term potential of LTP. Nature Reviews Neuroscience (Vol. 4, Issue 11, pp. 923–926). https://doi.org/10.1038/nrn1258

Malenka, R. C., & Bear, M. F. (2004). LTP and LTD. Neuron (Vol. 44, Issue 1, pp. 5–21). https://doi.org/10.1016/j.neuron.2004.09.012

Malinow, R., & Tsien, R. W. (1990). Presynaptic enhancement shown by whole-cell recordings of long-term potentiation in hippocampal slices. Nature (Vol. 346, Issue 6280, pp. 177–180). https://doi.org/10.1038/346177a0

MANDERS, E. M. M., VERBEEK, F. J., & ATEN, J. A. (1993). Measurement of co-localization of objects in dual-colour confocal images. Journal of Microscopy (Vol. 169, Issue 3, pp. 375–382). https://doi.org/10.1111/j.1365-2818.1993.tb03313.x

Maren, S. (2005). Synaptic Mechanisms of Associative Memory in the Amygdala. Neuron (Vol. 47, Issue 6, pp. 783–786). https://doi.org/10.1016/j.neuron.2005.08.009

Martin, S., Henley, J. M., Holman, D., Zhou, M., Wiegert, O., van Spronsen, M., Joëls, M., Hoogenraad, C. C., & Krugers, H. J. (2009). Corticosterone Alters AMPAR Mobility and Facilitates Bidirectional Synaptic Plasticity. PLoS ONE (Vol. 4, Issue 3, p. e4714). https://doi.org/10.1371/journal.pone.0004714

Martineau, M., Guzman, R. E., Fahlke, C., & Klingauf, J. (2017). VGLUT1 functions as a glutamate/proton exchanger with chloride channel activity in hippocampal glutamatergic synapses. Nature Communications (Vol. 8, Issue 1). https://doi.org/10.1038/s41467-017-02367-6

Martinez-Sanchez, A., Laugks, U., Kochovski, Z., Papantoniou, C., Zinzula, L., Baumeister, W., & Lučić, V. (2021). Trans-synaptic assemblies link synaptic vesicles and neuroreceptors. Science Advances (Vol. 7, Issue 10). https://doi.org/10.1126/sciadv.abe6204

Matsui, K. (2004). Differential Control of Synaptic and Ectopic Vesicular Release of Glutamate. Journal of Neuroscience (Vol. 24, Issue 41, pp. 8932–8939). https://doi.org/10.1523/jneurosci.2650-04.2004

Matsuzaki, M., Ellis-Davies, G. C. R., Nemoto, T., Miyashita, Y., Iino, M., & Kasai, H. (2001). Dendritic spine geometry is critical for AMPA receptor expression in hippocampal CA1 pyramidal neurons. Nature Neuroscience (Vol. 4, Issue 11, pp. 1086–1092). https://doi.org/10.1038/nn736

Matsuzaki, M., Honkura, N., Ellis-Davies, G. C. R., & Kasai, H. (2004). Structural basis of long-term potentiation in single dendritic spines. Nature (Vol. 429, Issue 6993, pp. 761–766). https://doi.org/10.1038/nature02617

Matt, L., Kim, K., Hergarden, A. C., Patriarchi, T., Malik, Z. A., Park, D. K., Chowdhury, D., Buonarati, O. R., Henderson, P. B., Gökçek Saraç, Ç., Zhang, Y., Mohapatra, D., Horne, M. C., Ames, J. B., & Hell, J. W. (2018). α-Actinin Anchors PSD-95 at Postsynaptic Sites. Neuron (Vol. 97, Issue 5, pp. 1094-1109.e9). https://doi.org/10.1016/j.neuron.2018.01.036

Maximov, A., Shin, O.-H., Liu, X., & Südhof, T. C. (2006). Synaptotagmin-12, a synaptic vesicle phosphoprotein that modulates spontaneous neurotransmitter release. Journal of Cell Biology (Vol. 176, Issue 1, pp. 113–124). https://doi.org/10.1083/jcb.200607021

Mayer, M. L., & Westbrook, G. L. (1987). The physiology of excitatory amino acids in the vertebrate central nervous system. Progress in Neurobiology (Vol. 28, Issue 3, pp. 197–276). https://doi.org/10.1016/0301-0082(87)90011-6

McAllister, A. K. (2007). Dynamic Aspects of CNS Synapse Formation. Annual Review of Neuroscience (Vol. 30, Issue 1, pp. 425–450). https://doi.org/10.1146/annurev.neuro.29.051605.112830

McAllister, A. K., & Stevens, C. F. (2000). Nonsaturation of AMPA and NMDA receptors at hippocampal synapses. Proceedings of the National Academy of Sciences (Vol. 97, Issue 11, pp. 6173–6178).. https://doi.org/10.1073/pnas.100126497

McKinney, R. A., Capogna, M., Dürr, R., Gähwiler, B. H., & Thompson, and S. M. (1999). Miniature synaptic events maintain dendritic spines via AMPA receptor activation. Nature Neuroscience (Vol. 2, Issue 1, pp. 44–49). https://doi.org/10.1038/4548

Miklósi, Á., & Andrew, R. J. (2006). The Zebrafish as a Model for Behavioral Studies. Zebrafish (Vol. 3, Issue 2, pp. 227–234). Mary Ann Liebert Inc. https://doi.org/10.1089/zeb.2006.3.227

Missler, M., Sudhof, T. C., & Biederer, T. (2012). Synaptic Cell Adhesion. Cold Spring Harbor Perspectives in Biology (Vol. 4, Issue 4, pp. a005694–a005694). https://doi.org/10.1101/cshperspect.a005694

Molnár, G., Rózsa, M., Baka, J., Holderith, N., Barzó, P., Nusser, Z., & Tamás, G. (2016). Human pyramidal to interneuron synapses are mediated by multi-vesicular release and multiple docked vesicles. eLife (Vol. 5). https://doi.org/10.7554/elife.18167

Mondin, M., Labrousse, V., Hosy, E., Heine, M., Tessier, B., Levet, F., Poujol, C., Blanchet, C., Choquet, D., & Thoumine, O. (2011). Neurexin-Neuroligin Adhesions Capture Surface-Diffusing AMPA Receptors through PSD-95 Scaffolds. Journal of Neuroscience (Vol. 31, Issue 38, pp. 13500–13515). https://doi.org/10.1523/jneurosci.6439-10.2011

Mortillo, S., Elste, A., Ge, Y., Patil, S. B., Hsiao, K., Huntley, G. W., Davis, R. L., & Benson, D. L. (2012). Compensatory redistribution of neuroligins and N-cadherin following deletion of synaptic β1-integrin. The Journal of Comparative Neurology (Vol. 520, Issue 9, pp. 2041–2052). https://doi.org/10.1002/cne.23027

Mosbacher, J., Schoepfer, R., Monyer, H., Burnashev, N., Seeburg, P., & Ruppersberg, J. (1994). A molecular determinant for submillisecond desensitization in glutamate receptors. Science (Vol. 266, Issue 5187, pp. 1059–1062). https://doi.org/10.1126/science.7973663

Mrestani, A., Pauli, M., Kollmannsberger, P., Repp, F., Kittel, R. J., Eilers, J., Doose, S., Sauer, M., Sirén, A.-L., Heckmann, M., & Paul, M. M. (2021). Active zone compaction correlates with presynaptic homeostatic potentiation. Cell Reports (Vol. 37, Issue 1, p. 109770). https://doi.org/10.1016/j.celrep.2021.109770

MROZKOVA, P., PALECEK, J., & SPICAROVA, D. (2016). The Role of Protease-Activated Receptor Type 2 in Nociceptive Signaling and Pain. Physiological Research (pp. 357–367). https://doi.org/10.33549/physiolres.933269

Nair, D., Hosy, E., Petersen, J. D., Constals, A., Giannone, G., Choquet, D., & Sibarita, J.-B. (2013). Super-Resolution Imaging Reveals That AMPA Receptors Inside Synapses Are Dynamically Organized in Nanodomains Regulated by PSD95. Journal of Neuroscience (Vol. 33, Issue 32, pp. 13204–13224). https://doi.org/10.1523/jneurosci.2381-12.2013

Nam, C. I., & Chen, L. (2005). Postsynaptic assembly induced by neurexin-neuroligin interaction and neurotransmitter. Proceedings of the National Academy of Sciences (Vol. 102, Issue 17, pp. 6137–6142). https://doi.org/10.1073/pnas.0502038102

Nicoll, R. A. (2006). Auxiliary Subunits Assist AMPA-Type Glutamate Receptors. Science (Vol. 311, Issue 5765, pp. 1253–1256). https://doi.org/10.1126/science.1123339

Nielsen, T. A., DiGregorio, D. A., & Silver, R. A. (2004). Modulation of Glutamate Mobility Reveals the Mechanism Underlying Slow-Rising AMPAR EPSCs and the Diffusion Coefficient in the Synaptic Cleft. Neuron (Vol. 42, Issue 5, pp. 757–771). https://doi.org/10.1016/j.neuron.2004.04.003

Nilsen, S. P., Chan, Y.-B., Huber, R., & Kravitz, E. A. (2004). Gender-selective patterns of aggressive behavior in Drosophila melanogaster. Proceedings of the National Academy of Sciences (Vol. 101, Issue 33, pp. 12342–12347). Proceedings of the National Academy of Sciences. https://doi.org/10.1073/pnas.0404693101

Nishimune, A., Isaac, J. T. R., Molnar, E., Noel, J., Nash, S. R., Tagaya, M., Collingridge, G. L., Nakanishi, S., & Henley, J. M. (1998). NSF Binding to GluR2 Regulates Synaptic Transmission. Neuron (Vol. 21, Issue 1, pp. 87–97). https://doi.org/10.1016/s0896-6273(00)80517-6

Nusser, Z., Lujan, R., Laube, G., Roberts, J. D. B., Molnar, E., & Somogyi, P. (1998). Cell Type and Pathway Dependence of Synaptic AMPA Receptor Number and Variability in the Hippocampus. Neuron (Vol. 21, Issue 3, pp. 545–559). https://doi.org/10.1016/s0896-6273(00)80565-6

O'Brien, R. J., Kamboj, S., Ehlers, M. D., Rosen, K. R., Fischbach, G. D., & Huganir, R. L. (1998). Activity-Dependent Modulation of Synaptic AMPA Receptor Accumulation. Neuron (Vol. 21, Issue 5, pp. 1067–1078). https://doi.org/10.1016/s0896-6273(00)80624-8

O'Brien, R. J., Xu, D., Petralia, R. S., Steward, O., Huganir, R. L., & Worley, P. (1999). Synaptic Clustering of AMPA Receptors by the Extracellular Immediate-Early Gene Product Narp. Neuron (Vol. 23, Issue 2, pp. 309–323). https://doi.org/10.1016/s0896-6273(00)80782-5

Ohtsuka, T., Takao-Rikitsu, E., Inoue, E., Inoue, M., Takeuchi, M., Matsubara, K., Deguchi-Tawarada, M., Satoh, K., Morimoto, K., Nakanishi, H., & Takai, Y. (2002). Cast. Journal of Cell Biology (Vol. 158, Issue 3, pp. 577–590). https://doi.org/10.1083/jcb.200202083

Oliva, C., Escobedo, P., Astorga, C., Molina, C., & Sierralta, J. (2011). Role of the maguk protein family in synapse formation and function. Developmental Neurobiology (Vol. 72, Issue 1, pp. 57–72). https://doi.org/10.1002/dneu.20949

Opazo, P., Sainlos, M., & Choquet, D. (2012). Regulation of AMPA receptor surface diffusion by PSD-95 slots. Current Opinion in Neurobiology (Vol. 22, Issue 3, pp. 453–460). https://doi.org/10.1016/j.conb.2011.10.010

Otis, T., Zhang, S., & Trussell, L. O. (1996). Direct Measurement of AMPA Receptor Desensitization Induced by Glutamatergic Synaptic Transmission. The Journal of Neuroscience (Vol. 16, Issue 23, pp. 7496–7504).. https://doi.org/10.1523/jneurosci.16-23-07496.1996

Paatero, A., Rosti, K., Shkumatov, A. V., Sele, C., Brunello, C., Kysenius, K., Singha, P., Jokinen, V., Huttunen, H., & Kajander, T. (2016). Crystal Structure of an Engineered LRRTM2 Synaptic Adhesion Molecule and a Model for Neurexin Binding. Biochemistry (Vol. 55, Issue 6, pp. 914–926).). https://doi.org/10.1021/acs.biochem.5b00971

Pandya, N. J., Seeger, C., Babai, N., Gonzalez-Lozano, M. A., Mack, V., Lodder, J. C., Gouwenberg, Y., Mansvelder, H. D., Danielson, U. H., Li, K. W., Heine, M., Spijker, S., Frischknecht, R., & Smit, A. B. (2018). Noelin1 Affects Lateral Mobility of Synaptic AMPA Receptors. Cell Reports (Vol. 24, Issue 5, pp. 1218–1230). https://doi.org/10.1016/j.celrep.2018.06.102

Passafaro, M., Piëch, V., & Sheng, M. (2001). Subunit-specific temporal and spatial patterns of AMPA receptor exocytosis in hippocampal neurons. Nature Neuroscience (Vol. 4, Issue 9, pp. 917–926). https://doi.org/10.1038/nn0901-917

Peixoto, R. T., Kunz, P. A., Kwon, H., Mabb, A. M., Sabatini, B. L., Philpot, B. D., & Ehlers, M. D. (2012). Transsynaptic Signaling by Activity-Dependent Cleavage of Neuroligin-1. Neuron (Vol. 76, Issue 2, pp. 396–409). https://doi.org/10.1016/j.neuron.2012.07.006

Peled, E. S., & Isacoff, E. Y. (2011). Optical quantal analysis of synaptic transmission in wild-type and rab3-mutant Drosophila motor axons. Nature Neuroscience (Vol. 14, Issue 4, pp. 519–526). https://doi.org/10.1038/nn.2767

Penn, A. C., Zhang, C. L., Georges, F., Royer, L., Breillat, C., Hosy, E., Petersen, J. D., Humeau, Y., & Choquet, D. (2017). Hippocampal LTP and contextual learning require surface diffusion of AMPA receptors. Nature (Vol. 549, Issue 7672, pp. 384–388). https://doi.org/10.1038/nature23658

Perez de Arce, K., Schrod, N., Metzbower, S. W. R., Allgeyer, E., Kong, G. K.-W., Tang, A.-H., Krupp, A. J., Stein, V., Liu, X., Bewersdorf, J., Blanpied, T. A., Lučić, V., & Biederer, T. (2015). Topographic Mapping of the Synaptic Cleft into Adhesive Nanodomains. Neuron (Vol. 88, Issue 6, pp. 1165–1172). https://doi.org/10.1016/j.neuron.2015.11.011

Petazzi, R. A., Aji, A. K., & Chiantia, S. (2020). Fluorescence microscopy methods for the study of protein oligomerization. Progress in Molecular Biology and Translational Science (pp. 1–41). https://doi.org/10.1016/bs.pmbts.2019.12.001

Petrini, E. M., Lu, J., Cognet, L., Lounis, B., Ehlers, M. D., & Choquet, D. (2009). Endocytic Trafficking and Recycling Maintain a Pool of Mobile Surface AMPA Receptors Required for Synaptic Potentiation. Neuron (Vol. 63, Issue 1, pp. 92–105). https://doi.org/10.1016/j.neuron.2009.05.025

Prieto, M. L., & Wollmuth, L. P. (2010). Gating Modes in AMPA Receptors. Journal of Neuroscience (Vol. 30, Issue 12, pp. 4449–4459). https://doi.org/10.1523/jneurosci.5613-09.2010

Purkey, A. M., Woolfrey, K. M., Crosby, K. C., Stich, D. G., Chick, W. S., Aoto, J., & Dell'Acqua, M. L. (2018). AKAP150 Palmitoylation Regulates Synaptic Incorporation of Ca2+-Permeable AMPA Receptors to Control LTP. Cell Reports (Vol. 25, Issue 4, pp. 974-987.e4). https://doi.org/10.1016/j.celrep.2018.09.085

Raghavachari, S., & Lisman, J. E. (2004). Properties of Quantal Transmission at CA1 Synapses. Journal of Neurophysiology (Vol. 92, Issue 4, pp. 2456–2467). https://doi.org/10.1152/jn.00258.2004

Ramirez, D. M., & Kavalali, E. T. (2011). Differential regulation of spontaneous and evoked neurotransmitter release at central synapses. Current Opinion in Neurobiology (Vol. 21, Issue 2, pp. 275–282). https://doi.org/10.1016/j.conb.2011.01.007

Renner, M., Lacor, P. N., Velasco, P. T., Xu, J., Contractor, A., Klein, W. L., & Triller, A. (2010). Deleterious Effects of Amyloid β Oligomers Acting as an Extracellular Scaffold for mGluR5. Neuron (Vol. 66, Issue 5, pp. 739–754). https://doi.org/10.1016/j.neuron.2010.04.029

Ribrault, C., Reingruber, J., Petkovic, M., Galli, T., Ziv, N. E., Holcman, D., & Triller, A. (2011). Syntaxin1A Lateral Diffusion Reveals Transient and Local SNARE Interactions. Journal of Neuroscience (Vol. 31, Issue 48, pp. 17590–17602). https://doi.org/10.1523/jneurosci.4065-11.2011

Richmond, J. E., Weimer, R. M., & Jorgensen, E. M. (2001). An open form of syntaxin bypasses the requirement for UNC-13 in vesicle priming. Nature (Vol. 412, Issue 6844, pp. 338–341). https://doi.org/10.1038/35085583

Roppongi, R. T., Dhume, S. H., Padmanabhan, N., Silwal, P., Zahra, N., Karimi, B., Bomkamp, C., Patil, C. S., Champagne-Jorgensen, K., Twilley, R. E., Zhang, P., Jackson, M. F., & Siddiqui, T. J. (2020). LRRTMs Organize Synapses through Differential Engagement of Neurexin and PTPσ. Neuron (Vol. 106, Issue 1, pp. 108-125.e12). https://doi.org/10.1016/j.neuron.2020.01.003

Rosenmund, C. (2003). Molecular mechanisms of active zone function. Current Opinion in Neurobiology (Vol. 13, Issue 5, pp. 509–519). https://doi.org/10.1016/j.conb.2003.09.011

Rouach, N., Byrd, K., Petralia, R. S., Elias, G. M., Adesnik, H., Tomita, S., Karimzadegan, S., Kealey, C., Bredt, D. S., & Nicoll, R. A. (2005). TARP γ-8 controls hippocampal AMPA receptor number, distribution and synaptic plasticity. Nature Neuroscience (Vol. 8, Issue 11, pp. 1525–1533). https://doi.org/10.1038/nn1551

Rowen, L., Young, J., Birditt, B., Kaur, A., Madan, A., Philipps, D. L., Qin, S., Minx, P., Wilson, R. K., Hood, L., & Graveley, B. R. (2002). Analysis of the Human Neurexin Genes: Alternative Splicing and the Generation of Protein Diversity. Genomics (Vol. 79, Issue 4, pp. 587–597). https://doi.org/10.1006/geno.2002.6734

Rozov, A., Bolshakov, A. P., & Valiullina-Rakhmatullina, F. (2019). The Ever-Growing Puzzle of Asynchronous Release. Frontiers in Cellular Neuroscience (Vol. 13). https://doi.org/10.3389/fncel.2019.00028

Rusakov, D. A., & Kullmann, D. M. (1998). Extrasynaptic Glutamate Diffusion in the Hippocampus: Ultrastructural Constraints, Uptake, and Receptor Activation. The Journal of Neuroscience (Vol. 18, Issue 9, pp. 3158–3170). https://doi.org/10.1523/jneurosci.18-09-03158.1998

Rusakov, D. A., & Kullmann, D. M. (1998). Geometric and viscous components of the tortuosity of the extracellular space in the brain. Proceedings of the National Academy of Sciences (Vol. 95, Issue 15, pp. 8975–8980). https://doi.org/10.1073/pnas.95.15.8975

Rusakov, D. A., & Stewart, M. G. (2021). Synaptic environment and extrasynaptic glutamate signals: The quest continues. Neuropharmacology (Vol. 195, p. 108688). https://doi.org/10.1016/j.neuropharm.2021.108688

Rust, M. J., Bates, M., & Zhuang, X. (2006). Sub-diffraction-limit imaging by stochastic optical reconstruction microscopy (STORM). Nature Methods (Vol. 3, Issue 10, pp. 793–796). https://doi.org/10.1038/nmeth929

Sainlos, M., Tigaret, C., Poujol, C., Olivier, N. B., Bard, L., Breillat, C., Thiolon, K., Choquet, D., & Imperiali, B. (2010). Biomimetic divalent ligands for the acute disruption of synaptic AMPAR stabilization. Nature Chemical Biology (Vol. 7, Issue 2, pp. 81–91). https://doi.org/10.1038/nchembio.498

Sainlos, M., Tigaret, C., Poujol, C., Olivier, N. B., Bard, L., Breillat, C., Thiolon, K., Choquet, D., & Imperiali, B. (2010). Biomimetic divalent ligands for the acute disruption of synaptic AMPAR stabilization. Nature Chemical Biology (Vol. 7, Issue 2, pp. 81–91). https://doi.org/10.1038/nchembio.498

Sakamoto, H., Ariyoshi, T., Kimpara, N., Sugao, K., Taiko, I., Takikawa, K., Asanuma, D., Namiki, S., & Hirose, K. (2017). Synaptic weight set by Munc13-1

supramolecular assemblies. Nature Neuroscience (Vol. 21, Issue 1, pp. 41–49). https://doi.org/10.1038/s41593-017-0041-9

Sando, R., Jiang, X., & Südhof, T. C. (2019). Latrophilin GPCRs direct synapse specificity by coincident binding of FLRTs and teneurins. Science (Vol. 363, Issue 6429, p. eaav7969). https://doi.org/10.1126/science.aav7969

Santos, M. S., Li, H., & Voglmaier, S. M. (2009). Synaptic vesicle protein trafficking at the glutamate synapse. Neuroscience (Vol. 158, Issue 1, pp. 189–203). https://doi.org/10.1016/j.neuroscience.2008.03.029

Sara, Y., Bal, M., Adachi, M., Monteggia, L. M., & Kavalali, E. T. (2011). Use-Dependent AMPA Receptor Block Reveals Segregation of Spontaneous and Evoked Glutamatergic Neurotransmission. Journal of Neuroscience (Vol. 31, Issue 14, pp. 5378–5382). https://doi.org/10.1523/jneurosci.5234-10.2011

Sara, Y., Virmani, T., Deák, F., Liu, X., & Kavalali, E. T. (2005). An Isolated Pool of Vesicles Recycles at Rest and Drives Spontaneous Neurotransmission. Neuron (Vol. 45, Issue 4, pp. 563–573). https://doi.org/10.1016/j.neuron.2004.12.056

Savtchenko, L. P., & Rusakov, D. A. (2005). Extracellular diffusivity determines contribution of high-versus low-affinity receptors to neural signaling. NeuroImage (Vol. 25, Issue 1, pp. 101–111). https://doi.org/10.1016/j.neuroimage.2004.11.020

Savtchenko, L. P., Sylantyev, S., & Rusakov, D. A. (2012). Central synapses release a resource-efficient amount of glutamate. Nature Neuroscience (Vol. 16, Issue 1, pp. 10–12). https://doi.org/10.1038/nn.3285

Schluter, O. M. (2006). Rab3 Superprimes Synaptic Vesicles for Release: Implications for Short-Term Synaptic Plasticity. Journal of Neuroscience (Vol. 26, Issue 4, pp. 1239–1246). https://doi.org/10.1523/jneurosci.3553-05.2006

Schnell, E., Bensen, A. L., Washburn, E. K., & Westbrook, G. L. (2012). Neuroligin-1 Overexpression in Newborn Granule Cells In Vivo. PLoS ONE (Vol. 7, Issue 10, p. e48045). https://doi.org/10.1371/journal.pone.0048045

Schroeder, A., Vanderlinden, J., Vints, K., Ribeiro, L. F., Vennekens, K. M., Gounko, N. V., Wierda, K. D., & de Wit, J. (2018). A Modular Organization of LRR Protein-Mediated Synaptic Adhesion Defines Synapse Identity. Neuron (Vol. 99, Issue 2, pp. 329-344.e7). https://doi.org/10.1016/j.neuron.2018.06.026

Schwenk, J., & Fakler, B. (2020). Building of AMPA-type glutamate receptors in the endoplasmic reticulum and its implication for excitatory neurotransmission. The Journal of Physiology (Vol. 599, Issue 10, pp. 2639–2653). https://doi.org/10.1113/jp279025

Schwenk, J., Baehrens, D., Haupt, A., Bildl, W., Boudkkazi, S., Roeper, J., Fakler, B., & Schulte, U. (2014). Regional Diversity and Developmental Dynamics of the AMPA-Receptor Proteome in the Mammalian Brain. Neuron (Vol. 84, Issue 1, pp. 41–54). https://doi.org/10.1016/j.neuron.2014.08.044

Schwenk, J., Harmel, N., Brechet, A., Zolles, G., Berkefeld, H., Müller, C. S., Bildl, W., Baehrens, D., Hüber, B., Kulik, A., Klöcker, N., Schulte, U., & Fakler, B. (2012). High-Resolution Proteomics Unravel Architecture and Molecular Diversity of Native AMPA Receptor Complexes. Neuron (Vol. 74, Issue 4, pp. 621–633). https://doi.org/10.1016/j.neuron.2012.03.034

Sekine-Aizawa, Y., & Huganir, R. L. (2004). Imaging of receptor trafficking by using -bungarotoxin-binding-site-tagged receptors. Proceedings of the National Academy of Sciences (Vol. 101, Issue 49, pp. 17114–17119). https://doi.org/10.1073/pnas.0407563101

Shi, Y., Suh, Y. H., Milstein, A. D., Isozaki, K., Schmid, S. M., Roche, K. W., & Nicoll, R. A. (2010). Functional comparison of the effects of TARPs and cornichons on AMPA receptor trafficking and gating. Proceedings of the National Academy of Sciences (Vol. 107, Issue 37, pp. 16315–16319). https://doi.org/10.1073/pnas.1011706107

Shipman, S. L., Schnell, E., Hirai, T., Chen, B.-S., Roche, K. W., & Nicoll, R. A. (2011). Functional dependence of neuroligin on a new non-PDZ intracellular domain. Nature Neuroscience (Vol. 14, Issue 6, pp. 718–726). https://doi.org/10.1038/nn.2825

Siddiqui, T. J., Pancaroglu, R., Kang, Y., Rooyakkers, A., & Craig, A. M. (2010). LRRTMs and Neuroligins Bind Neurexins with a Differential Code to Cooperate in Glutamate Synapse Development. Journal of Neuroscience (Vol. 30, Issue 22, pp. 7495–7506). https://doi.org/10.1523/jneurosci.0470-10.2010

Siddiqui, T. J., Tari, P. K., Connor, S. A., Zhang, P., Dobie, F. A., She, K., Kawabe, H., Wang, Y. T., Brose, N., & Craig, A. M. (2013). An LRRTM4-HSPG Complex Mediates Excitatory Synapse Development on Dentate Gyrus Granule Cells. Neuron (Vol. 79, Issue 4, pp. 680–695). https://doi.org/10.1016/j.neuron.2013.06.029

Sinha, R., Ahmed, S., Jahn, R., & Klingauf, J. (2011). Two synaptobrevin molecules are sufficient for vesicle fusion in central nervous system synapses. Proceedings of the National Academy of Sciences (Vol. 108, Issue 34, pp. 14318–14323). https://doi.org/10.1073/pnas.1101818108

Smith KS, Graybiel AM. Habit formation. Dialogues Clin Neurosci. 2016 Mar;18(1):33-43. doi: 10.31887/DCNS.2016.18.1/ksmith. PMID: 27069378; PMCID: PMC4826769.

Smith, K. R., Jones, K. A., Kopeikina, K. J., Burette, A. C., Copits, B. A., Yoon, S., Forrest, M. P., Fawcett-Patel, J. M., Hanley, J. G., Weinberg, R. J., Swanson, G. T., & Penzes, P. (2017). Cadherin-10 Maintains Excitatory/Inhibitory Ratio through Interactions with Synaptic Proteins. The Journal of Neuroscience (Vol. 37, Issue 46, pp. 11127–11139). https://doi.org/10.1523/jneurosci.1153-17.2017

Sobolevsky, A. I., Rosconi, M. P., & Gouaux, E. (2009). X-ray structure, symmetry and mechanism of an AMPA-subtype glutamate receptor. Nature (Vol. 462, Issue 7274, pp. 745–756). https://doi.org/10.1038/nature08624

Soler-Llavina, G. J., Arstikaitis, P., Morishita, W., Ahmad, M., Südhof, T. C., & Malenka, R. C. (2013). Leucine-Rich Repeat Transmembrane Proteins Are Essential for Maintenance of Long-Term Potentiation. Neuron (Vol. 79, Issue 3, pp. 439–446). https://doi.org/10.1016/j.neuron.2013.06.007

Soler-Llavina, G. J., Fuccillo, M. V., Ko, J., Sudhof, T. C., & Malenka, R. C. (2011). The neurexin ligands, neuroligins and leucine-rich repeat transmembrane proteins, perform convergent and divergent synaptic functions in vivo. Proceedings of the National Academy of Sciences (Vol. 108, Issue 40, pp. 16502–16509). https://doi.org/10.1073/pnas.1114028108

Söllner, T., & Rothman, J. E. (1994). Neurotransmission: harnessing fusion machinery at the synapse. Trends in Neurosciences (Vol. 17, Issue 8, pp. 344–348). https://doi.org/10.1016/0166-2236(94)90178-3

Song, J.-Y., Ichtchenko, K., Sudhof, T. C., & Brose, N. (1999). Neuroligin 1 is a postsynaptic cell-adhesion molecule of excitatory synapses. Proceedings of the National Academy of Sciences (Vol. 96, Issue 3, pp. 1100–1105). https://doi.org/10.1073/pnas.96.3.1100

Stern-Bach, Y., Russo, S., Neuman, M., & Rosenmund, C. (1998). A Point Mutation in the Glutamate Binding Site Blocks Desensitization of AMPA Receptors. Neuron (Vol. 21, Issue 4, pp. 907–918). https://doi.org/10.1016/s0896-6273(00)80605-4

Stevens, B., Allen, N. J., Vazquez, L. E., Howell, G. R., Christopherson, K. S., Nouri, N., Micheva, K. D., Mehalow, A. K., Huberman, A. D., Stafford, B., Sher, A., Litke, A. M., Lambris, J. D., Smith, S. J., John, S. W. M., & Barres, B. A. (2007). The Classical Complement Cascade Mediates CNS Synapse Elimination. Cell (Vol. 131, Issue 6, pp. 1164–1178). https://doi.org/10.1016/j.cell.2007.10.036

Stevens, C. F., & Wang, Y. (1995). Facilitation and depression at single central synapses. Neuron (Vol. 14, Issue 4, pp. 795–802). https://doi.org/10.1016/0896-6273(95)90223-6

Südhof, T. C. (2004). THE SYNAPTIC VESICLE CYCLE. Annual Review of Neuroscience (Vol. 27, Issue 1, pp. 509–547). https://doi.org/10.1146/annurev.neuro.26.041002.131412

Südhof, T. C. (2013). Neurotransmitter Release: The Last Millisecond in the Life of a Synaptic Vesicle. Neuron (Vol. 80, Issue 3, pp. 675–690). https://doi.org/10.1016/j.neuron.2013.10.022

Sumioka, A., Yan, D., & Tomita, S. (2010). TARP Phosphorylation Regulates Synaptic AMPA Receptors through Lipid Bilayers. Neuron (Vol. 66, Issue 5, pp. 755–767). https://doi.org/10.1016/j.neuron.2010.04.035

Sutton, M. A., Ito, H. T., Cressy, P., Kempf, C., Woo, J. C., & Schuman, E. M. (2006). Miniature Neurotransmission Stabilizes Synaptic Function via Tonic Suppression of Local Dendritic Protein Synthesis. Cell (Vol. 125, Issue 4, pp. 785–799). https://doi.org/10.1016/j.cell.2006.03.040

Szepesi, Z., Hosy, E., Ruszczycki, B., Bijata, M., Pyskaty, M., Bikbaev, A., Heine, M., Choquet, D., Kaczmarek, L., & Wlodarczyk, J. (2014). Synaptically Released Matrix Metalloproteinase Activity in Control of Structural Plasticity and the Cell Surface Distribution of GluA1-AMPA Receptors. PLoS ONE (Vol. 9, Issue 5, p. e98274). https://doi.org/10.1371/journal.pone.0098274

Tabuchi, K., Biederer, T., Butz, S., & Südhof, T. C. (2002). CASK Participates in Alternative Tripartite Complexes in which Mint 1 Competes for Binding with Caskin 1, a Novel CASK-Binding Protein. The Journal of Neuroscience (Vol. 22, Issue 11, pp. 4264–4273). https://doi.org/10.1523/jneurosci.22-11-04264.2002

Takamori, S., Holt, M., Stenius, K., Lemke, E. A., Grønborg, M., Riedel, D., Urlaub, H., Schenck, S., Brügger, B., Ringler, P., Müller, S. A., Rammner, B., Gräter, F., Hub, J. S., De Groot, B. L., Mieskes, G., Moriyama, Y., Klingauf, J., Grubmüller, H., … Jahn, R. (2006). Molecular Anatomy of a Trafficking Organelle. Cell (Vol. 127, Issue 4, pp. 831–846). https://doi.org/10.1016/j.cell.2006.10.030

Tanaka, J. -i. (2005). Number and Density of AMPA Receptors in Single Synapses in Immature Cerebellum. Journal of Neuroscience (Vol. 25, Issue 4, pp. 799–807). https://doi.org/10.1523/jneurosci.4256-04.2005

Tang, A.-H., Chen, H., Li, T. P., Metzbower, S. R., MacGillavry, H. D., & Blanpied, T. A. (2016). A trans-synaptic nanocolumn aligns neurotransmitter release to receptors. Nature (Vol. 536, Issue 7615, pp. 210–214). https://doi.org/10.1038/nature19058

Tardin, C. (2003). Direct imaging of lateral movements of AMPA receptors inside synapses. The EMBO Journal (Vol. 22, Issue 18, pp. 4656–4665). https://doi.org/10.1093/emboj/cdg463

Tomita, S., Chen, L., Kawasaki, Y., Petralia, R. S., Wenthold, R. J., Nicoll, R. A., & Bredt, D. S. (2003). Functional studies and distribution define a family of transmembrane AMPA receptor regulatory proteins. In Journal of Cell Biology (Vol. 161, Issue 4, pp. 805–816). Rockefeller University Press. https://doi.org/10.1083/jcb.200212116

Tomita, S., Fukata, M., Nicoll, R. A., & Bredt, D. S. (2004). Dynamic Interaction of Stargazin-like TARPs with Cycling AMPA Receptors at Synapses. Science (Vol. 303, Issue 5663, pp. 1508–1511). https://doi.org/10.1126/science.1090262

Topinka, J. R., & Bredt, D. S. (1998). N-Terminal Palmitoylation of PSD-95 Regulates Association with Cell Membranes and Interaction with K+ Channel Kv1.4. Neuron (Vol. 20, Issue 1, pp. 125–134). https://doi.org/10.1016/s0896-6273(00)80440-7

Torri-Tarelli, F., Grohovaz, F., Fesce, R., & Ceccarelli, B. (1985). Temporal coincidence between synaptic vesicle fusion and quantal secretion of acetylcholine. The Journal of Cell Biology (Vol. 101, Issue 4, pp. 1386–1399). https://doi.org/10.1083/jcb.101.4.1386

Traynelis, S. F., Wollmuth, L. P., McBain, C. J., Menniti, F. S., Vance, K. M., Ogden, K. K., Hansen, K. B., Yuan, H., Myers, S. J., & Dingledine, R. (2010). Glutamate Receptor Ion Channels: Structure, Regulation, and Function. Pharmacological Reviews (Vol. 62, Issue 3, pp. 405–496). https://doi.org/10.1124/pr.109.002451

Trotter, J. H., Dargaei, Z., Sclip, A., Essayan-Perez, S., Liakath-Ali, K., Raju, K., Nabet, A., Liu, X., Wöhr, M., & Südhof, T. C. (2020). Compartment-Specific Neurexin Nanodomains Orchestrate Tripartite Synapse Assembly. https://doi.org/10.1101/2020.08.21.262097

Trotter, J. H., Hao, J., Maxeiner, S., Tsetsenis, T., Liu, Z., Zhuang, X., & Südhof, T. C. (2019). Synaptic neurexin-1 assembles into dynamically regulated active zone nanoclusters. Journal of Cell Biology (Vol. 218, Issue 8, pp. 2677–2698). https://doi.org/10.1083/jcb.201812076

Trussell, L. O., & Fischbach, G. D. (1989). Glutamate receptor desensitization and its role in synaptic transmission. Neuron (Vol. 3, Issue 2, pp. 209–218). https://doi.org/10.1016/0896-6273(89)90034-2

Turrigiano, G. G., Leslie, K. R., Desai, N. S., Rutherford, L. C., & Nelson, S. B. (1998). Activity-dependent scaling of quantal amplitude in neocortical neurons. Nature (Vol. 391, Issue 6670, pp. 892–896). https://doi.org/10.1038/36103

Twomey, E. C., & Sobolevsky, A. I. (2017). Structural Mechanisms of Gating in Ionotropic Glutamate Receptors. Biochemistry (Vol. 57, Issue 3, pp. 267–276). https://doi.org/10.1021/acs.biochem.7b00891

Tzingounis, A. V., & Wadiche, J. I. (2007). Glutamate transporters: confining runaway excitation by shaping synaptic transmission. Nature Reviews Neuroscience (Vol. 8, Issue 12, pp. 935–947). https://doi.org/10.1038/nrn2274

Um, J. W., Kim, K. H., Park, B. S., Choi, Y., Kim, D., Kim, C. Y., Kim, S. J., Kim, M., Ko, J. S., Lee, S.-G., Choii, G., Nam, J., Heo, W. D., Kim, E., Lee, J.-O., Ko, J., & Kim, H. M. (2014). Structural basis for LAR-RPTP/Slitrk complex-mediated synaptic adhesion. Nature Communications (Vol. 5, Issue 1). https://doi.org/10.1038/ncomms6423

Uteshev, V. V., & Pennefather, P. S. (1996). A mathematical description of miniature postsynaptic current generation at central nervous system synapses. Biophysical Journal (Vol. 71, Issue 3, pp. 1256–1266). https://doi.org/10.1016/s0006-3495(96)79325-6

van de Linde, S., Endesfelder, U., Mukherjee, A., Schüttpelz, M., Wiebusch, G., Wolter, S., Heilemann, M., & Sauer, M. (2009). Multicolor photoswitching microscopy for subdiffraction-resolution fluorescence imaging. Photochemical & Photobiological Sciences (Vol. 8, Issue 4, p. 465). https://doi.org/10.1039/b822533h

van den Bogaart, G., Holt, M. G., Bunt, G., Riedel, D., Wouters, F. S., & Jahn, R. (2010). One SNARE complex is sufficient for membrane fusion. Nature Structural & Molecular Biology (Vol. 17, Issue 3, pp. 358–364). https://doi.org/10.1038/nsmb.1748

Ventriglia, F., & Di Maio, V. (2000). A Brownian model of glutamate diffusion in excitatory synapses of hippocampus. Biosystems (Vol. 58, Issues 1–3, pp. 67–74). https://doi.org/10.1016/s0303-2647(00)00108-8

Voronin, L. L., & Cherubini, E. (2004). 'Deaf, mute and whispering' silent synapses: their role in synaptic plasticity. The Journal of Physiology (Vol. 557, Issue 1, pp. 3–12). https://doi.org/10.1113/jphysiol.2003.058966

Wahl, P., Madsen, U., Banke, T., Krogsgaard-Larsen, P., & Schousboe, A. (1996). Different characteristics of AMPA receptor agonists acting at AMPA receptors expressed in Xenopus oocytes. European Journal of Pharmacology (Vol. 308, Issue 2, pp. 211–218). https://doi.org/10.1016/0014-2999(96)00292-0

Waites, C. L., Craig, A. M., & Garner, C. C. (2005). MECHANISMS OF VERTEBRATE SYNAPTOGENESIS. Annual Review of Neuroscience (Vol. 28, Issue 1, pp. 251–274). https://doi.org/10.1146/annurev.neuro.27.070203.144336

Walkup, W. G., IV, Mastro, T. L., Schenker, L. T., Vielmetter, J., Hu, R., Iancu, A., Reghunathan, M., Bannon, B. D., & Kennedy, M. B. (2016). A model for regulation by SynGAP-α1 of binding of synaptic proteins to PDZ-domain "Slots" in the postsynaptic density. eLife (Vol. 5). https://doi.org/10.7554/elife.16813

Wang, Y., Liu, X., Biederer, T., & Sudhof, T. C. (2002). A family of RIM-binding proteins regulated by alternative splicing: Implications for the genesis of synaptic active zones. Proceedings of the National Academy of Sciences (Vol. 99, Issue 22, pp. 14464–14469). https://doi.org/10.1073/pnas.182532999

Wang, Y., Okamoto, M., Schmitz, F., Hofmann, K., & Südhof, T. C. (1997). Rim is a putative Rab3 effector in regulating synaptic-vesicle fusion. Nature (Vol. 388, Issue 6642, pp. 593–598). https://doi.org/10.1038/41580

Wang, Y., Sugita, S., & Südhof, T. C. (2000). The RIM/NIM Family of Neuronal C2 Domain Proteins. Journal of Biological Chemistry (Vol. 275, Issue 26, pp. 20033–20044). https://doi.org/10.1074/jbc.m909008199

Washburn, H. R., Xia, N. L., Zhou, W., Mao, Y.-T., & Dalva, M. B. (2020). Positive surface charge of GluN1 N-terminus mediates the direct interaction with EphB2 and NMDAR mobility. Nature Communications (Vol. 11, Issue 1). https://doi.org/10.1038/s41467-020-14345-6

Watanabe, S. (2016). Flash-and-Freeze: Coordinating Optogenetic Stimulation with Rapid Freezing to Visualize Membrane Dynamics at Synapses with Millisecond Resolution. Frontiers in Synaptic Neuroscience (Vol. 8). https://doi.org/10.3389/fnsyn.2016.00024

Watanabe, S., Rost, B. R., Camacho-Pérez, M., Davis, M. W., Söhl-Kielczynski, B., Rosenmund, C., & Jorgensen, E. M. (2013). Ultrafast endocytosis at mouse hippocampal synapses. Nature (Vol. 504, Issue 7479, pp. 242–247). https://doi.org/10.1038/nature12809

Watson, D. J., Ostroff, L., Cao, G., Parker, P. H., Smith, H., & Harris, K. M. (2015). LTP enhances synaptogenesis in the developing hippocampus. Hippocampus (Vol. 26, Issue 5, pp. 560–576). https://doi.org/10.1002/hipo.22536

Watson, J. F., Ho, H., & Greger, I. H. (2017). Synaptic transmission and plasticity require AMPA receptor anchoring via its N-terminal domain. eLife (Vol. 6). https://doi.org/10.7554/elife.23024

Watson, J. F., Pinggera, A., Ho, H., & Greger, I. H. (2021). AMPA receptor anchoring at CA1 synapses is determined by N-terminal domain and TARP γ8 interactions. Nature Communications (Vol. 12, Issue 1). https://doi.org/10.1038/s41467-021-25281-4

Weiss, S. (2000). Shattering the diffraction limit of light: A revolution in fluorescence microscopy? Proceedings of the National Academy of Sciences (Vol. 97, Issue 16, pp. 8747–8749). https://doi.org/10.1073/pnas.97.16.8747

Wenthold, R., Petralia, R., Blahos J, I., & Niedzielski, A. (1996). Evidence for multiple AMPA receptor complexes in hippocampal CA1/CA2 neurons. The Journal of Neuroscience (Vol. 16, Issue 6, pp. 1982–1989). https://doi.org/10.1523/jneurosci.16-06-01982.1996

Weston, M. C., Gertler, C., Mayer, M. L., & Rosenmund, C. (2006). Interdomain Interactions in AMPA and Kainate Receptors Regulate Affinity for Glutamate. Journal of Neuroscience (Vol. 26, Issue 29, pp. 7650–7658). https://doi.org/10.1523/jneurosci.1519-06.2006

Wheeler, D. B., Randall, A., & Tsien, R. W. (1994). Roles of N-Type and Q-Type Ca 2+ Channels in Supporting Hippocampal Synaptic Transmission. Science (Vol. 264, Issue 5155, pp. 107–111). https://doi.org/10.1126/science.7832825

Willems, J., de Jong, A. P. H., Scheefhals, N., Mertens, E., Catsburg, L. A. E., Poorthuis, R. B., de Winter, F., Verhaagen, J., Meye, F. J., & MacGillavry, H. D. (2020). ORANGE: A CRISPR/Cas9-based genome editing toolbox for epitope tagging of endogenous proteins in neurons. PLOS Biology (Vol. 18, Issue 4, p. e3000665). https://doi.org/10.1371/journal.pbio.3000665

Wilson, N. R. (2005). Presynaptic Regulation of Quantal Size by the Vesicular Glutamate Transporter VGLUT1. Journal of Neuroscience (Vol. 25, Issue 26, pp. 6221–6234). https://doi.org/10.1523/jneurosci.3003-04.2005

Winter, S. (2005). G o2 Regulates Vesicular Glutamate Transporter Activity by Changing Its Chloride Dependence. Journal of Neuroscience (Vol. 25, Issue 18, pp. 4672–4680). https://doi.org/10.1523/jneurosci.0549-05.2005

Wojcik, S. M., Rhee, J. S., Herzog, E., Sigler, A., Jahn, R., Takamori, S., Brose, N., & Rosenmund, C. (2004). An essential role for vesicular glutamate transporter 1 (VGLUT1) in postnatal development and control of quantal size. Proceedings of the National Academy of Sciences (Vol. 101, Issue 18, pp. 7158–7163). https://doi.org/10.1073/pnas.0401764101

Wolff, S. B., & Ölveczky, B. P. (2018). The promise and perils of causal circuit manipulations. Current Opinion in Neurobiology (Vol. 49, pp. 84–94). Elsevier BV. https://doi.org/10.1016/j.conb.2018.01.004

Wu, L.-G., Borst, J. G. G., & Sakmann, B. (1998). R-type Ca2+ currents evoke transmitter release at a rat central synapse. Proceedings of the National Academy of Sciences (Vol. 95, Issue 8, pp. 4720–4725). https://doi.org/10.1073/pnas.95.8.4720

Xie, X., Liaw, J.-S., Baudry, M., & Berger, T. W. (1997). Novel expression mechanism for synaptic potentiation: Alignment of presynaptic release site and postsynaptic receptor. Proceedings of the National Academy of Sciences (Vol. 94, Issue 13, pp. 6983–6988). https://doi.org/10.1073/pnas.94.13.6983

Xu, D., Hopf, C., Reddy, R., Cho, R. W., Guo, L., Lanahan, A., Petralia, R. S., Wenthold, R. J., O'Brien, R. J., & Worley, P. (2003). Narp and NP1 Form Heterocomplexes that Function in Developmental and Activity-Dependent Synaptic Plasticity. Neuron (Vol. 39, Issue 3, pp. 513–528). https://doi.org/10.1016/s0896-6273(03)00463-x

Yamagata, A., Goto-Ito, S., Sato, Y., Shiroshima, T., Maeda, A., Watanabe, M., Saitoh, T., Maenaka, K., Terada, T., Yoshida, T., Uemura, T., & Fukai, S. (2018). Structural insights into modulation and selectivity of transsynaptic neurexin–LRRTM interaction. Nature Communications (Vol. 9, Issue 1). https://doi.org/10.1038/s41467-018-06333-8

Yan, D., & Tomita, S. (2011). Defined criteria for auxiliary subunits of glutamate receptors. The Journal of Physiology (Vol. 590, Issue 1, pp. 21–31). https://doi.org/10.1113/jphysiol.2011.213868

Yan, D., & Tomita, S. (2011). Defined criteria for auxiliary subunits of glutamate receptors. The Journal of Physiology (Vol. 590, Issue 1, pp. 21–31). https://doi.org/10.1113/jphysiol.2011.213868

Yang, X., Le Corronc, H., Legendre, P., Triller, A., & Specht, C. G. (2021). Differential regulation of glycinergic and GABAergic nanocolumns at mixed inhibitory synapses. EMBO reports (Vol. 22, Issue 7). https://doi.org/10.15252/embr.202052154

Yudowski, G. A., Olsen, O., Adesnik, H., Marek, K. W., & Bredt, D. S. (2013). Acute Inactivation of PSD-95 Destabilizes AMPA Receptors at Hippocampal Synapses. PLoS ONE (Vol. 8, Issue 1, p. e53965). https://doi.org/10.1371/journal.pone.0053965

Zeng, M., Díaz-Alonso, J., Ye, F., Chen, X., Xu, J., Ji, Z., Nicoll, R. A., & Zhang, M. (2019). Phase Separation-Mediated TARP/MAGUK Complex Condensation and AMPA Receptor Synaptic Transmission. Neuron (Vol. 104, Issue 3, pp. 529-543.e6). https://doi.org/10.1016/j.neuron.2019.08.001

Zhang, P., Lu, H., Peixoto, R. T., Pines, M. K., Ge, Y., Oku, S., Siddiqui, T. J., Xie, Y., Wu, W., Archer-Hartmann, S., Yoshida, K., Tanaka, K. F., Aricescu, A. R., Azadi, P., Gordon, M. D., Sabatini, B. L., Wong, R. O. L., & Craig, A. M. (2018). Heparan Sulfate Organizes Neuronal Synapses through Neurexin Partnerships. Cell (Vol. 174, Issue 6, pp. 1450-1464.e23). https://doi.org/10.1016/j.cell.2018.07.002

Zhao, Y., Chen, S., Swensen, A. C., Qian, W.-J., & Gouaux, E. (2019). Architecture and subunit arrangement of native AMPA receptors elucidated by cryo-EM. Science (Vol. 364, Issue 6438, pp. 355–362). https://doi.org/10.1126/science.aaw8250

Zhao, Y., Chen, S., Swensen, A. C., Qian, W.-J., & Gouaux, E. (2019). Architecture and subunit arrangement of native AMPA receptors elucidated by cryo-EM. Science (Vol. 364, Issue 6438, pp. 355–362). https://doi.org/10.1126/science.aaw8250

Zhou, K., Stawicki, T. M., Goncharov, A., & Jin, Y. (2013). Position of UNC-13 in the active zone regulates synaptic vesicle release probability and release kinetics. eLife (Vol. 2). https://doi.org/10.7554/elife.01180

Zhou, Y., & Danbolt, N. C. (2014). Glutamate as a neurotransmitter in the healthy brain. Journal of Neural Transmission (Vol. 121, Issue 8, pp. 799–817). https://doi.org/10.1007/s00702-014-1180-8

Zhu, J., Shang, Y., & Zhang, M. (2016). Mechanistic basis of MAGUK-organized complexes in synaptic development and signaling. Nature Reviews Neuroscience (Vol. 17, Issue 4, pp. 209–223). https://doi.org/10.1038/nrn.2016.18

Zucker, R. S. (2005). Minis: Whence and Wherefore? Neuron (Vol. 45, Issue 4, pp. 482–484). https://doi.org/10.1016/j.neuron.2005.02.003